Current Ground Motions in Montgomery, Western Liberty, and Northern Harris Counties Derived from Continuous GPS Observations (1994-2018)

A Thesis Presented to

the Faculty of the Department of Earth and Atmospheric Sciences

University of Houston

In Partial Fulfillment

of the Requirements for the Degree

Master of Science

by

Jennifer C. Welch

December, 2018

Current Ground Motions in Montgomery, Western Liberty, and Northern Harris Counties Derived from Continuous GPS Observations (1994-2018)

Jennifer C. Welch

APPROVED:

Dr. Guoquan Wang, Chairperson

Dr. Shuhab D. Khan

Dr. Ramesh Shretha

Dean, College of Natural Sciences and Mathematics

ACKNOWLEDGEMENTS

I would like to thank my committee for their patience and continued involvement in my project. This project has certainly taught me to ask more questions, to ask for help more often, and to better communicate ideas and thoughts in my personal and professional life.

As the HoustonNet GPS network installations were coming to an end, Guoquan Wang, his students, and I spent a large amount of time performing station reconnaissance, collecting data, installing new instrumentation, and repairing existing receiver issues as they arose. It has been an intense time of learning both the technical and relevant parts of the work being done in the Houston and surrounding areas. I am also grateful to the many employees within the Subsidence Districts for use of their time, thoughts, ideas, and for being my sounding board when I needed it most. A special thank you to all of my colleagues, both past and present, for continuing to explore and conquer the new (and old) ideas being presented in all fields of research. May you keep asking the questions that help and influence the future practices of others.

Finally, I would like to deeply thank my family and friends for their continued love and support. Ultimately, I dedicate this work to my children Emily and Andrew, who encouraged me to do things I never would have done for myself. You both are the loves of my life. Life at times has not been easy for the three of us. The mama drama is almost over! I hope I have always shown you that you can accomplish anything if you work hard. Never let anyone tell you that you can’t do it. Strive to reach the unreachable no matter what. Dream big! Love you Chips-Ahoy-Boy and Baby Penguin!

Current Ground Motions in Montgomery, Western Liberty, and Northern Harris Counties Derived from Continuous GPS Observations (1994-2018)

An Abstract of a Thesis

Presented to

the Faculty of the Department of Earth and Atmospheric Sciences

University of Houston

In Partial Fulfillment

of the Requirements for the Degree

Master of Science

by

Jennifer C. Welch

December, 2018

ABSTRACT

The greater Houston area has been adversely affected by land subsidence possibly more than any other area in the United States. Houston and its surrounding areas have been suffering frequent infrastructure damage associated with faulting and land subsidence for almost a century. Currently, land subsidence in downtown Houston and the southeastern region of the Houston metropolitan area has nearly ceased (< 3 mm/ year) as a result of enforced groundwater regulations. Slight land rebound has been observed along the Houston Ship Channel area since 2005. However, GPS observations indicate that subsidence rates over about 2 cm/year are occurring in the southern part of Montgomery county and the northwest and central northern part of Harris County. Montgomery County is one of the areas that is suffering from severe damage resulting from land subsidence and local faulting.

This study investigated the on-going vertical ground motions recorded by GPS and ground water level changes recorded by wells within Montgomery County, northern Harris County, and west Liberty County. The U.S. Geological Survey (USGS), Lone Star Groundwater Conservation District (LSGCD), Harris Galveston Subsidence District (HGSD), University of Houston (UH), and other local agents have been continuously monitoring ground water and land subsidence in this area for over 10 years. Through the use of USGS ground water monitoring wells and permanent GPS stations, this study explored the long-term interaction between fluctuation of groundwater and land subsidence. GPS stations recorded subsidence rates that range from 0.082 cm/year to -2.739 cm/year and provides fundamental information for predicting future land

subsidence, which is critical for properly implementing a plan for adjusting the ground water regulations within the foreseeable future.

Table of Contents

1 Introduction 1
2 Study Area 7
2.1 Location 7
2.2 Deformation Monitoring Network 11
2.3 Regional Geology 13
2.4 Hydrostratigraphy 17
3 Groundwater 21
3.1 Movement of Water in the Gulf Coast Aquifer System 21
3.2 History of Subsidence in the Houston Area 25
3.3 Monitoring Aquifer Levels 28
4 GPS Positioning 31
4.1 GPS as a Surveying Tool 33
4.2 GPS Data Processing 35
4.3 Sources of Error and Accuracy 39
4.4 Reference Frame 42
5 Interaction of Subsidence and Groundwater Level Change 50
5.1 Groundwater Withdrawal 50
5.2 Groundwater Levels 52
5.3 GPS Measured Surface Deformation 57
5.4 Subsidence in Response to Groundwater Levels 65
6 Conclusions 76
7 References 78
8 Appendix I: Groundwater Levels 87
9 Appendix II: GPS Timeseries 190

List of Figures

Figure 1-1 Texas 2015 Groundwater Withdrawals 3

Figure 2-1 Regulatory Area for Harris and Galveston Counties 10

Figure 2-2 Locations of Permanent GPS Monitoring Stations 12

Figure 2-3 Regional Fault Lines and Salt Domes 12

Figure 2-4 Hydrogeologic Section of the Gulf Coast Aquifer System 19

Figure 3-1 Principal Stresses within the Aquifer 24

Figure 3-2 USGS Groundwater Monitoring Wells 30

Figure 4-1 HoustonNet Stations installed by University of Houston 32

Figure 4-2 PAM Station Setup 35

Figure 4-3 15 Reference Stations for Realizing Houston16 45

Figure 4-4 TXL1 Displacement Time-series in Three Reference Frames 49

Figure 5-1 Groundwater Withdrawal History for Regulatory Area 3 50

Figure 5-1-2 Groundwater Withdrawal History for Montgomery County By Use 51

Figure 5-2-1 USGS Chicot Groundwater Monitoring Wells 54

Figure 5-2-2 USGS Evangeline Groundwater Monitoring Wells 55

Figure 5-2-3 USGS Jasper Groundwater Monitoring Wells 56

Figure 5-3-1 GPS Station Locations for TXLI, UHWL, LKHU. 60

Figure 5-3-2 GPS Data for Stations TXLI, UHWL, LKHU. 61

Figure 5-3-3 GPS Station Locations for PA02, PA07, PA08, PA46. 60

Figure 5-3-4 GPS Data for Stations PA02, PA07, PA08, PA46 64

Figure 5-4-1 GPS Station Locations for PAM 02, PAM 08, etc. with USGS Wells 66

Figure 5-4-2 GPS Stations PAM 02, PAM 08, etc. with USGS Well Data..... 67

Figure 5-4-3 GPS Station Locations for PAM 07, PAM 46, etc. with USGS Wells..... 69

Figure 5-4-4 GPS Stations PAM 07, PAM 46, etc. with USGS Well Data..... 70

Figure 5-4-5 GPS Stations Locations for PAM 69, WHCR, etc. with USGS Wells..... 72

Figure 5-4-6 GPS Stations PAM 69, WHCR, etc. with USGS Well Data 73

Figure 5-4-7 GPS Stations Locations for CLVD, TXLI, UHWL with USGS Wells 74

Figure 5-4-8 GPS Stations CLVD, TXLI, UHWL with USGS Well Data..... 75

List of Tables

Table 2-3 Hydrostratigraphic Column 18

Table 4-4 Seven Parameters for Transforming XYZ Coordinates 48

Table 5-3 GPS Station Average Vertical Displacement Over Recorded History..... 58

1 Introduction

Montgomery County is located north of Houston, an historic area of land surface subsidence due to fluid (oil, gas, or water) withdrawal. In developed areas, land subsidence can severely damage property and infrastructure. The first documented case of subsidence and faulting occurred at Goose Creek Oil field, an area north of Galveston Bay (Pratt and Johnson, 1926). Yerkes and Castle (1969) studied differential subsidence, horizontal displacements and faulting associated with oil and gas extractions from shallow fields. Oil and gas production target older, Oligocene aged sediments are found in Montgomery, western Liberty, and northern Harris counties and are therefore disregarded for this shallow subsidence study.

Land surface subsidence typically occurs naturally over long geologic timescale as sediments compact and dewater with burial. This process can be expedited by anthropogenic activities such as oil and gas extraction, groundwater withdrawal, and mining (Galloway and Burbey, 2011; Gabrysch and Bonnet, 1975). Subsidence within and around Houston occur due primarily to groundwater withdrawal. This type of subsidence is a known problem in several places around the world. Dry, arid parts of America that rely on groundwater for irrigation like the San Joaquin Valley, California and south-central Arizona, or densely populated metropolitan areas like Houston, Texas and Las Vegas, Nevada are significantly affected.

The Gulf Coast aquifer system, comprised of three aquifers, the Chicot, Evangeline, and the Jasper, has an abundant supply of potable groundwater (Kasmarek and Strom, 2002), purified over hundreds to thousands of years by filtering through

alternating layers of sand and clay (Fogg, 1986). In the early 1900's, the Gulf Coast aquifer system was under artesian conditions (Wesselman, 1972) where wells would flow freely without being pumped because the potentiometric water level was greater than land surface elevation. By the mid 1940's, these wells ceased to flow due to increased pumping within the aquifers (Loskot et al., 1982).

Montgomery, west Liberty, and north Harris counties all were once a sparsely populated agricultural community prior to the 1900's and has become a booming center for residential and economic development over the past two centuries. Harris county is estimated to be the fourth fastest growing county in the United States from 2016 to 2017 (U.S. Census Bureau, 2018). Groundwater was initially developed in Montgomery and northern Harris counties for agricultural irrigation from the 19th to 20th century, and more recently for municipal and industrial supply. The large volumes being extracted since 1990 to meet water demands in both counties have caused major declines in the potentiometric surface in and around Houston. There is a corresponding, regional deepening of the potentiometric surface on the southern half of Montgomery county and northern half of Harris county that can be attributed to both the increased rate of withdrawal and population in Montgomery and northern Harris counties.

The rate of groundwater withdrawal is almost five times greater in Harris County, than in Montgomery county when comparing the Harris-Galveston Subsidence Districts (HGSD) 2017 annual groundwater report to that of Montgomery counties Lone Star Groundwater Conservation Districts 2017 Annual report. Montgomery county consumes about 48.4 MG (million gallons) per day while Harris County Regulatory Area 3

consumes an astonishing 183.4 MG per day according to each district's respective annual report. The 2015 Groundwater withdraw levels reported by county to the Texas Water Development Board are shown in Figure 1. As population increases, conservation districts across the state are tasked with regulating sustainable development of the groundwater resources (Theis, 1940).

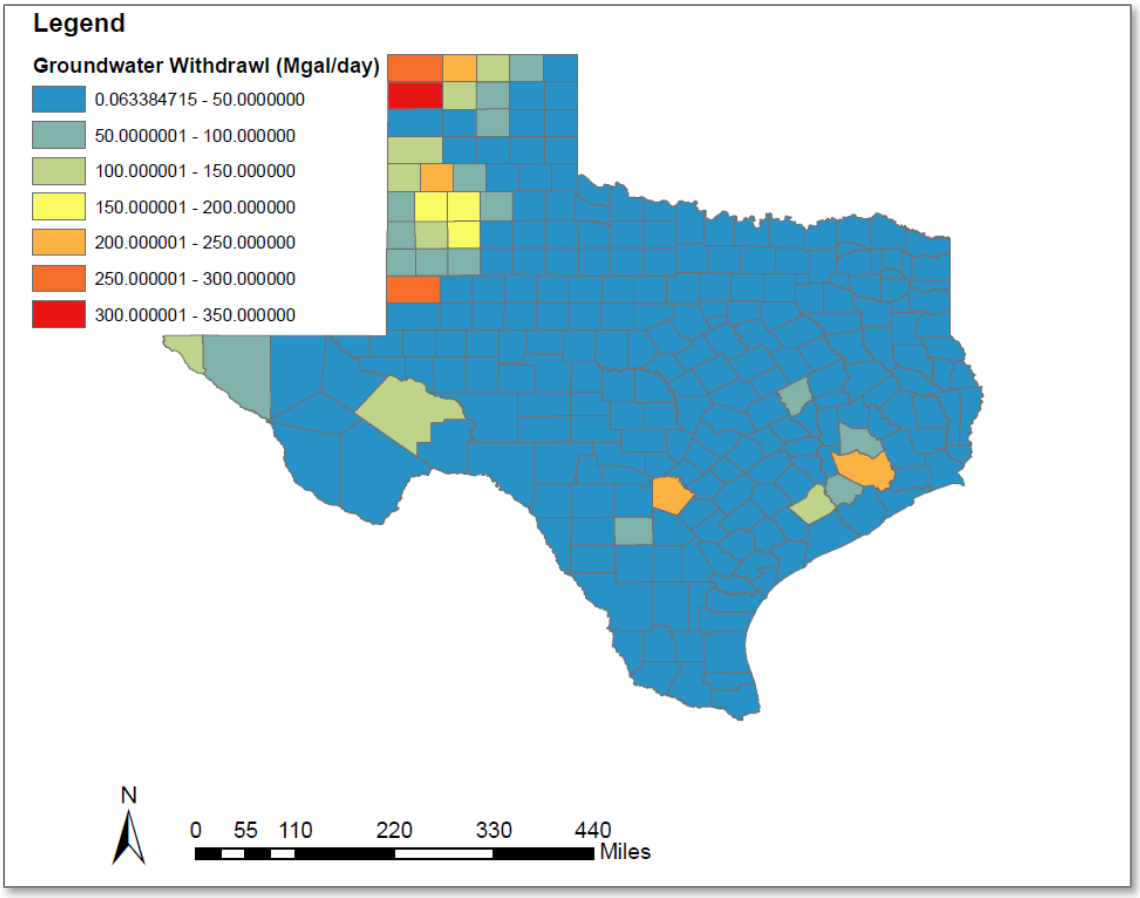

Figure 1-1 Texas 2015 Groundwater Withdrawals.
The map shows groundwater withdrawal rates across Texas, by county. Montgomery County extracts 46.6 million gallons per day (Mgal/day), while Harris County extracts 226.4 Mgal/day. Data sources: Groundwater Levels (Texas Water Development Board, 2017).

Groundwater is extracted from Miocene and younger units to supply water for municipal, industrial, commercial and agricultural purposes in both Montgomery and northern Harris counties. Groundwater resources are relied on more heavily to water lawns or maintain crops in times of drought, a pertinent issue to recognize as both counties try to decrease consumption and the associated negative effects of surface deformation.

Surface deformation is a function of the soil moisture content, which includes clays with strong shrink and swell properties (Kasmarek et al., 2014). As the ground slowly shifts it adversely affects infrastructure in developed areas causing structural instability and damage to buildings, roadways, and pipelines. Subsurface pipelines burst during the 2011 drought causing the loss of 18 billion gallons of water from June through October of 2011 (Houston Chronicle, 2011).

Development of surface and groundwater supplies can manipulate coastal processes through starving the sediment supply (dams), controlling flooding which would recharge aquifers over a broad area and deposit clay rich organic sediments to fields. Subsidence induced by groundwater withdrawal significantly impacts the gulf coast through flooding and the degradation of infrastructure (shifting foundations, road and pipelines). Subsidence in coastal areas has resulted in land being inundated by bay waters (Galloway, 2001), while episodic rainfalls or hurricanes significantly affect and flood more inland locations.

In 2001, Tropical Storm Allison stalled over Houston dropping about 90 centimeters (36 inches) of rain in four days (Grant and Rodriguez, 2006). In 2015 the

Memorial Day floods dumped almost 12 inches of rain in 10 hours. In 2016 Houston had the Tax Day flood which dumped almost 17 inches of rain in parts of Houston in 24 hours. In September 2017, Hurricane Harvey poured over 40 inches of rain over parts of eastern Texas within the course of 4 days. Each storm caused significant flooding and damage as the bayous overflowed in and around downtown Houston and the medical center. Highways become a secondary source for runoff as the flooding continues. The problem of subsidence within Houston and its surrounding areas is continuously affecting a larger geographic area as population and development increases to the north and west of Houston. Jersey Village, in northwest Houston has subsided 3 meters (~9.8 feet) in elevation due to fluid withdrawal (Kasmarek et al., 2014).

Montgomery and northern Harris counties offer a unique opportunity to study the changing aquifer stress patterns in these areas that were historically considered stable. This report analyzes groundwater and GPS data from 1994 through 2017 focusing on time periods of significant change.

There is a reliable, existing network of GPS stations currently in place with sufficient data history to conduct this study. There are 14 permanent GPS stations, including 8 PAMs operated by HGSD, 1 NGS CORS, and 5 UH HoustonNet stations. To minimize the influence of seasonal signals on velocity patterns within a time-series, only GPS stations with equal to three years of data or more were used.

The goal of this study is to determine if there is a regional control on subsidence and to quantify one-dimensional deformation in Montgomery and northern Harris counties as the aquifers are subjected to an increase in demand as development in these

areas continue to grow. The history and characteristics of the aquifer will be examined, including current monitoring efforts aided by the USGS. Surface deformation data will be analyzed for spatial and temporal trends. Correlations and anomalies between the two datasets will be discussed to describe potential mechanisms driving compaction within the aquifer. This report confirms that subsidence is not just an historical issue in Houston and its surrounding areas, but is and will continue to affect these rapidly growing areas provided that water conserving measure are not taken and alternative water sources are not utilized.

2 Study Area

The study area is contained within three counties, Montgomery, west Liberty, and northern Harris County. Groundwater use in Montgomery County is regulated by the Lone Star Groundwater Conservation District while groundwater use in Harris County is regulated by the Harris Galveston Subsidence District. Liberty County does not have a groundwater conservation district as it has not gone before legislation to create one. Population is this area is just starting to increase with the expansion of the West Park Tollway. The Houston metropolitan area and Gulf Coast aquifer system extends far beyond the border of these counties, making this study a detailed analysis of only a small part of a much larger system.

2.1 Location

Montgomery County is located 40 miles north of downtown Houston in the East Texas Timberlands region. The 2010 census showed a population of 455,746 residents within the county. Estimated population by 2020 is around 627,921 residents. Montgomery County covers an area of 1,077 square miles with 1,042 square miles being land and the remaining 35 square miles being water. The topography consists of flat to gently rolling terrain with the land being sued in commercial, industrial, agriculture, and residential use.

Harris county, whose county seat is Houston, Texas, encompasses many smaller cities within its boundaries. Harris counties population in 2010 was 4,092,459 residents and is estimated to be 4,729,102 residents by 2020. Harris county has a total area of 1,777

square miles of which 1,703 square miles is land and the remaining 74 square miles is in water. The topography is generally flat with land use primarily in commercial, industrial, and residential use.

Liberty County was created in 1831 as a municipality and became a county in 1837. The 2010 census showed a population of 75,653 residents. The county has a total land mass of 1,176 square miles of which 1,158 square miles is land and the remaining 18 square miles is water. In the 1990s, the economy of Liberty Country was primarily in agriculture and the oil industry. In recent years, the county has established four correctional facilities that contribute about 22 million in the county's annual payroll. The area is flat with land use primarily in agriculture.

Many new neighborhoods are built on drained wetlands and include a retention pond to offset lost drainage area. Flooding in Harris and Montgomery counties are mitigated through groundwater regulations, Harris County Flood Control, United States Army Core of Engineers, Municipal utility districts, and the cities. Large stretches of coastal prairie and farmland are quickly being developed into sprawling suburban communities with high demand for groundwater resources. Groundwater is considered a private property right within the state of Texas, whereas surface water (lakes, rivers, reservoirs, and streams) are state owned and regulated.

In 2001 the Texas State Legislature created the Lone Star Ground Water Conservation District (LSGCD) with the purpose of preserving, conserving, and protecting Montgomery Counties water supply. The regulations apply across the entire county and are not separated by areas such as those set by HGSD.

The Texas State Legislature created the Harris Galveston Subsidence District (HGSD) in 1975 with the intent to regulate groundwater usage contributing to subsidence and flooding (HGSD, 2018). The district is subdivided into three regulatory "areas" (Figure 2-1) with unique regulations and groundwater reduction plans, addressing the past and future potential of subsidence, present and forecasted population growth, and surface water availability to help meet total demand in each respective area. This study was conducted in the northern part of Harris County and will only focus on Area 3.

The HGSD Groundwater Regulatory Plan (HGBSD, 2013) aims to reduce countywide reliance on groundwater through conversion to surface water resources. The District is divided into three regulatory areas. HGSD Area 1 groundwater withdraw for each permittee cannot exceed 10% of their total water demand. Regulatory Area 2 requires that groundwater withdrawals for each permittee use no more than 20% of the permittee's annual total water demand. Area three requires groundwater withdraw not exceed 20% of the permittee's total water demand unless they are operating under a certified Groundwater Reduction Plan (GRP). A permittee operating under a certified GRP must maintain their groundwater withdraws to no more than 70% of the permittee's total water demand. All percentages indicate the portion of total water demand to be replaced with surface water. A permittee may be exempted from a regulatory Area's groundwater reduction requirements and disincentive fees if they do not have an available alternative water supply, are not located in a service area of any regional water supplier, or present an acceptable groundwater conservation plan to the District.

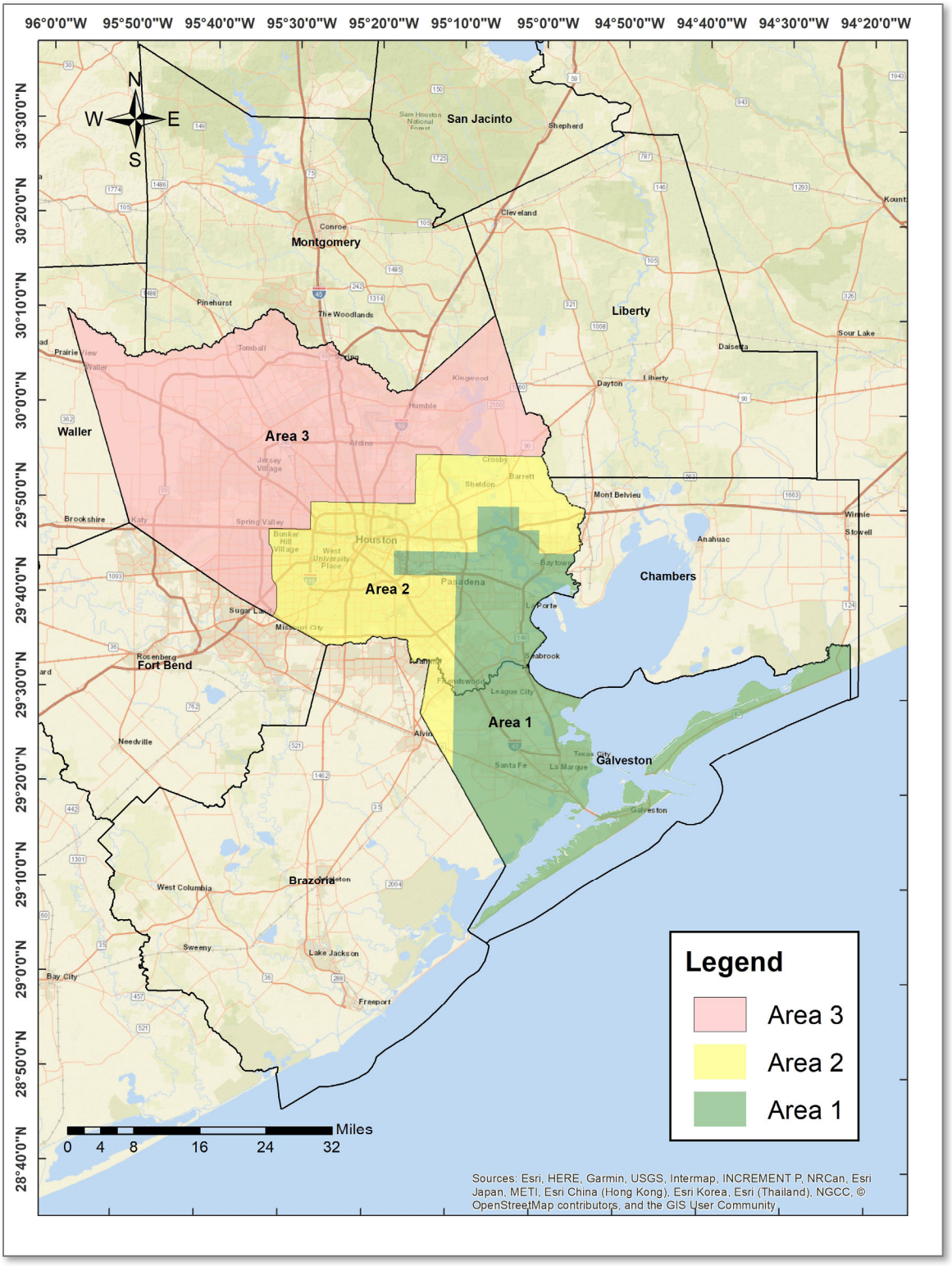

Figure 2-1 Regulatory Areas for Harris and Galveston Counties

2.2 Deformation Monitoring Network

At present, there are eight Continuously Operating Reference Station (CORS) within the study area (Fig. 2-2). HoustonNet is a dense network of GPS stations provided by the University of Houston. All GPS stations are permanent and collect GPS data on a continuous basis. This study uses five HoustonNet stations in Montgomery county, four in northern Harris county, and one in Liberty county. There are twenty-one Port-A-Measure Stations (PAMS) used in this study. Each station is mounted onto a pole at specific locations. On average each station collects about a week of data. The rotation schedules vary between HGSD and LSGCD. HGSD collects a week of data every 6 to 8 weeks or almost 2 months, while LSGCD collects a week of data every 4 weeks or 1 month. At the end of each week, only the receiver and the antenna are moved to the next location. Temporal resolution at older sites has decreased with the addition of new PAMS with the intent of increasing spatial data density. PAMS sites were installed at different time intervals, so historical data varies across the network. The oldest station (PA04) dates back to 1994. Blewitt and Lavalée (2002) determined that three years of data is necessary for reliable results.

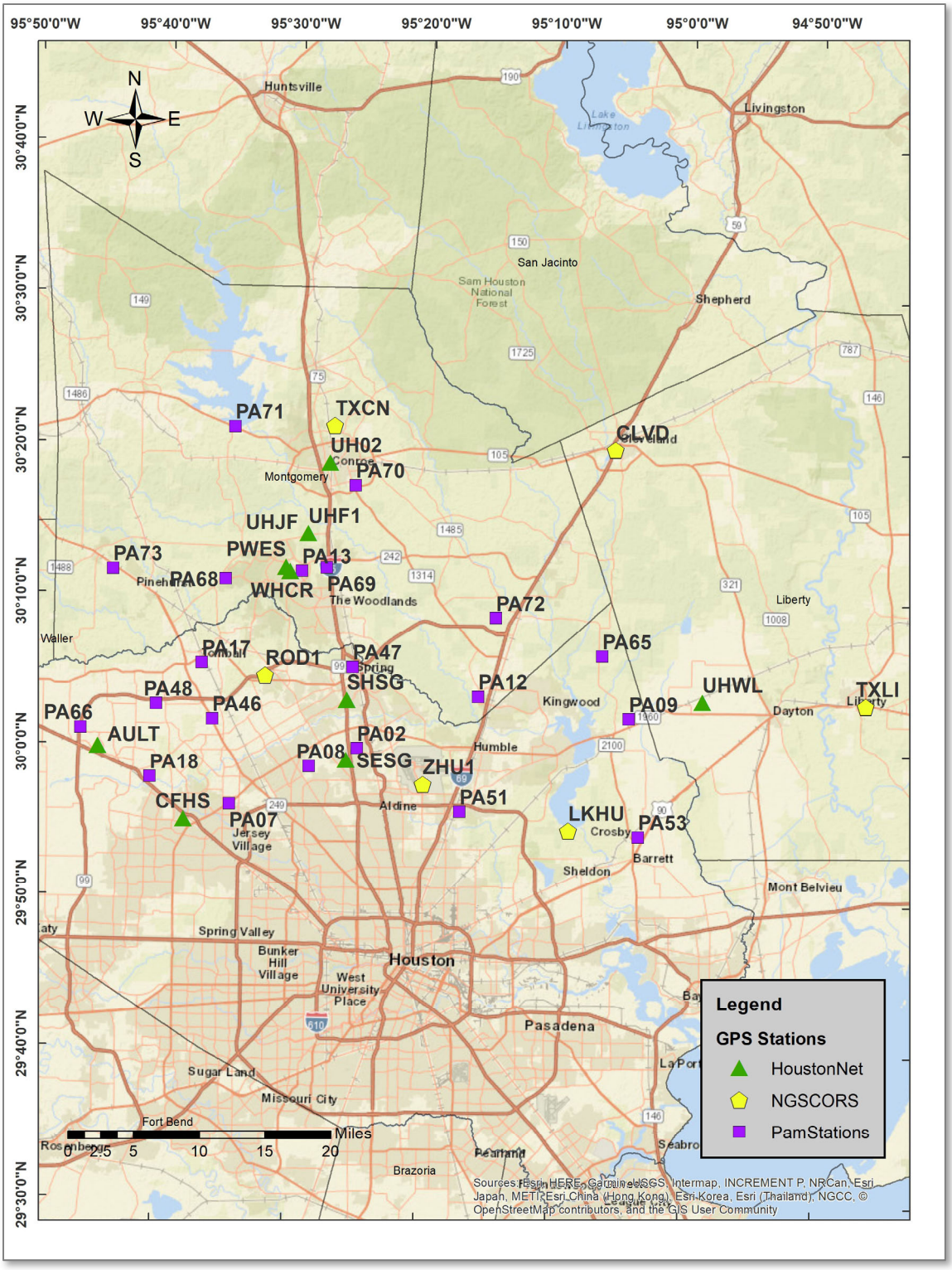

Figure 2-2 Locations of Permanent GPS Monitoring Stations

2.3 Regional Geology

The Gulf Coastal Plains is an area that is composed of thousands of meters of Cenozoic sedimentary deposits (Baker, 1979). The Texas gulf coast stretches about seventy to ninety miles in width and is comprised of sedimentary deposits including sand, silt, gravel, and clay. The coastal plain itself stretches from Florida in the east to Mexico in the southwest (Kasmarek and Strom, 2002). The Texas Coastal Plain consists of sediments deposited during relatively high sea levels by successive repetitions of fluvial to shallow marine depositional systems (Engelkemeir et al., 2010). The Texas Gulf Plain's geology is complex and is attributed to several factors; the spatial and temporal variability of the sediments that makeup the Texas coast, the motion of ancient Jurassic salt, and the presence of growth faults that parallel the coast. As Pangea began drifting apart during the Late Triassic, the earliest sediments of sand silt, gravel and clay in the Gulf of Mexico were first deposited (Chowdhury and Turco, 2006). The development of the Gulf of Mexico basin during the Middle Jurassic allowed for the deposition of the Louann salt, the most influential layer of the Gulf of Mexico, and clastic, non-marine sediments (Salvador, 1991). While the Gulf of Mexico basin had restrictive seawater flow during the middle Jurassic, the resulting rotation of the Yucatan during the late Jurassic allowed for intermittent seawater influx, producing massive salt deposition (Bird et al., 2005).

Sediment deposits within the Gulf of Mexico region are characterized primarily by the composition of clays, silts, sands, and gravel. Grain size is dependent on depositional facies (i.e. depositional environment) (Kreitler et al., 1977; Kasmarek et al.,

2014). Sea level rise and fall is a direct function of the Gulf of Mexico's depositional environment. As polar ice sheets melt we see a rise in global sea level and when polar ice sheets increase in size we see a fall in global see level. The most recent glaciation, from approximately 22,000 to 16,000 years ago, dominated the planet's climate (Anderson and Rodriguez, 2001). The lowering of sea level also allowed saline waters to be flushed out of the aquifers to considerable depths (Fetter, 2001). During this time massive ice sheets covered the continents lowering sea level to approximately 120 meters below its current position. This allowed for sediments to be carried by rivers to approximately 100 kilometers beyond the present shoreline (Burkett et al., 2002; Anderson and Rodriguez, 2001). As the glaciers melted, sea level rose quickly at a rate of approximately five centimeters per year (Burkett et al., 2002). During this time of slow sea level rise, the modern Gulf of Mexico coast line formed. Multiple rivers cut perpendicular to the coastline, carrying sediment directly to the Gulf of Mexico. A network of barrier islands developed from the interaction of sediment supply and longshore currents. The sediments that were deposited along the coastline are interpreted to represent varying degrees of fluvial to shallow marine environments (Chowdhury and Turco, 2006). The sedimentary deposits that developed the Texas coast are interpreted to represent the varying influence of fluvial-deltaic to shallow marine depositional environments. Sediment deposits characteristics vary in response to climate, eustatic sea level, and sediment supply (Chowdhury and Turco, 2006).

Both subsidence and faulting are forms of surface motion that can induce slow, imperceptible damage to buildings and roads (Holzer and Gabrysch, 1987). Pratt and

Johnson (1926) documented the first occurrence of human-induced faulting in the region, where oil and gas withdrawal accompanied localized subsidence. In general, Gulf Coast regional faults parallel the coastline (Ewing, 1991). In contrast, localized faulting related to collapsed salt domes or oil and gas fields (Pratt and Johnson, 1926) may exhibit arced to radial patterns (Van Siclen, 1968).

Many active faults that are aseismic, meaning there is no sudden release of stress, underly the Houston metropolitan area. (Khan et al., 2013). The Hockley Fault system is located in northwest Harris county. The Hackley fault system is considered to be one of the fastest moving faults in the region yet very little is known about its subsurface character. (Khan et al., 2013). Almost 80% of the Houston area faults are located directly above known salt domes. (Khan et al., 2014; Norman and Howe, 2011). Geophysical studies including gravity, magnetic, conductivity, and resistivity have since been completed to gain a better understanding of the impacts of deformation from the system. Regional faults have offset of about one to three centimeters per year (Holzer and Gabrysch, 1987; Buckley et al., 2003; Shah and Lanning-Rush, 2005), making them difficult to identify since erosion will conceal the scarp. LiDAR of structural damage observations are the most effective methods of identifying scarps in an urbanized area (Engelkemeir and Khan, 2008).

The Gulf Coast region was deformed through salt diapirism and growth faulting (Engelkemeir et al., 2010) as the accumulated Cenozoic overburden began to mobilize the Louann salt, a ductile material that can deform and rise due to density differences

(Ewing, 1983). A salt diapir can have little or no surface expression whether it is shallow or buried thousands of meters below the surface.

Regional faults are listric growth faults; *listric* means displacement increases with depth as the fault angle shallows and *growth* indicates offset is caused by rapid sedimentation along a failure plane coeval with deposition (Ewing, 1991). Kreitler (1977) found that growth faults around Houston could act as hydraulic barriers, compartmentalizing (at least partially) the lateral effects of drawdown within the aquifer. Offset along faults within the study area do not demonstrate great enough displacement to completely isolate sand-rich units within the aquifer (Jorgensen, 1975; Kasmarek and Strom, 2002).

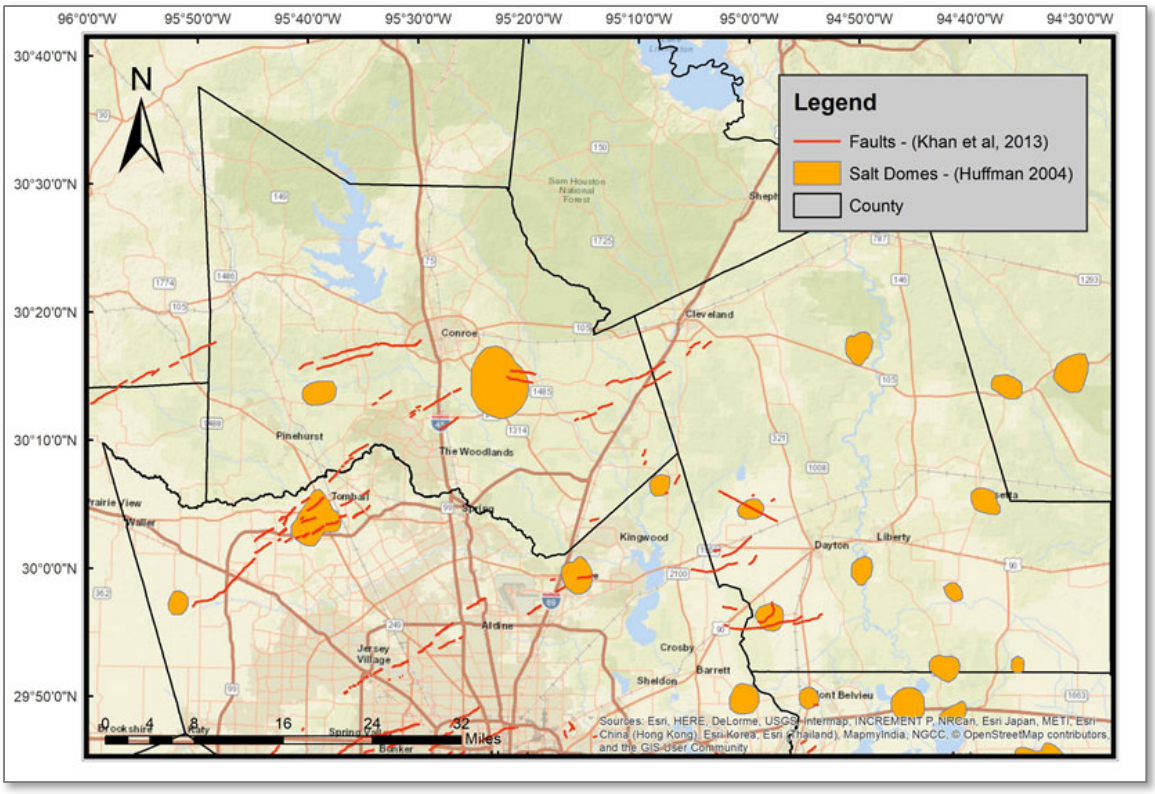

Figure 2-3: Regional Fault Lines and Salt Domes

According to Ewing (1983), shelf-margin growth faults developed before the modern configuration of salt domes existed. Faulting within Tertiary deposits along the Gulf of Mexico is due to unstable depositional surfaces and differing sediment types (Ewing, 1991). The continental shelf break indicates a change in depositional environment, moving from coarser materials deposited on the gently dipping shelf to fine grained materials deposited on the continental slope. Montgomery and Harris County are situated above the Oligocene shelf margin break (Winker, 1982; Ewing, 1991).

2.4 Hydrostratigraphy

This section focuses on the hydrologic units supplying water for most of the industrial, municipal, agricultural and commercial demand in Montgomery, west Liberty, and northern Harris counties. The Gulf Coast aquifer system extends across the coastal plains from Mexico to Florida. Units dip (slightly more than the land surface gradient) and thicken towards the coast, ranging from 600 to 800 meters in thickness (Wesselman, 1972).

Regionally, the aquifer system includes units from the surface to the Oligocene-aged Frio Formation, but is locally limited to the depth of fresh water (Baker, 1979). This study follows the naming scheme proposed by Baker (1979) for the hydrologic units, which are comprised of geologic formations. Table 2-1 shows the relationship between stratigraphic and hydrogeologic units in the study area.

Table 2-3 Hydrostratigraphic Column (after Baker, 1979)

<table>
<tr><th>Period</th><th>Epoch</th><th colspan="2">Stratigraphic Unit</th><th colspan="2">Hydrologic Unit (Baker, 1979)</th></tr>
<tr><td rowspan="5">Quaternary</td><td>Holocene</td><td colspan="2">Alluvium</td><td rowspan="4">Chicot Aquifer</td><td rowspan="7">Gulf Coast aquifer system</td></tr>
<tr><td rowspan="4">Pleistocene</td><td colspan="2">Beaumont Clay</td></tr>
<tr><td rowspan="2">Lissie Formation</td><td>Montgomery Formation</td></tr>
<tr><td>Bentley Formation</td></tr>
<tr><td colspan="2">Willis Sand</td></tr>
<tr><td rowspan="3">Neogene</td><td>Pliocene</td><td colspan="2">Goliad Sand</td><td>Evangeline Aquifer</td></tr>
<tr><td rowspan="2">Miocene</td><td colspan="2">Fleming Formation</td><td>Burkeville confining unit</td></tr>
<tr><td colspan="2">Oakville Sandstone</td><td>Jasper Aquifer</td></tr>
</table>

The primary hydrogeologic units within the study area are, from oldest to youngest, the: Jasper aquifer, Burkeville aquiclude, Evangeline aquifer, and Chicot aquifer. The Jasper aquifer is potable mostly in the upper part of the aquifer where there is more sand. The lower parts of the Jasper aquifer have interbedded sand and clay where only a little freshwater can be found. The Burkeville confining unit, is a regionally extensive, clay-dominated layer (Jorgenson, 1975). Kasmarek and Strom (2002) defined the freshwater limit to be at or near the base of Miocene aged sediments, and Pliocene aged sediments to the south. For this study, the base of the aquifer system in both Montgomery and northern Harris counties will be defined as the Jasper Aquifer.

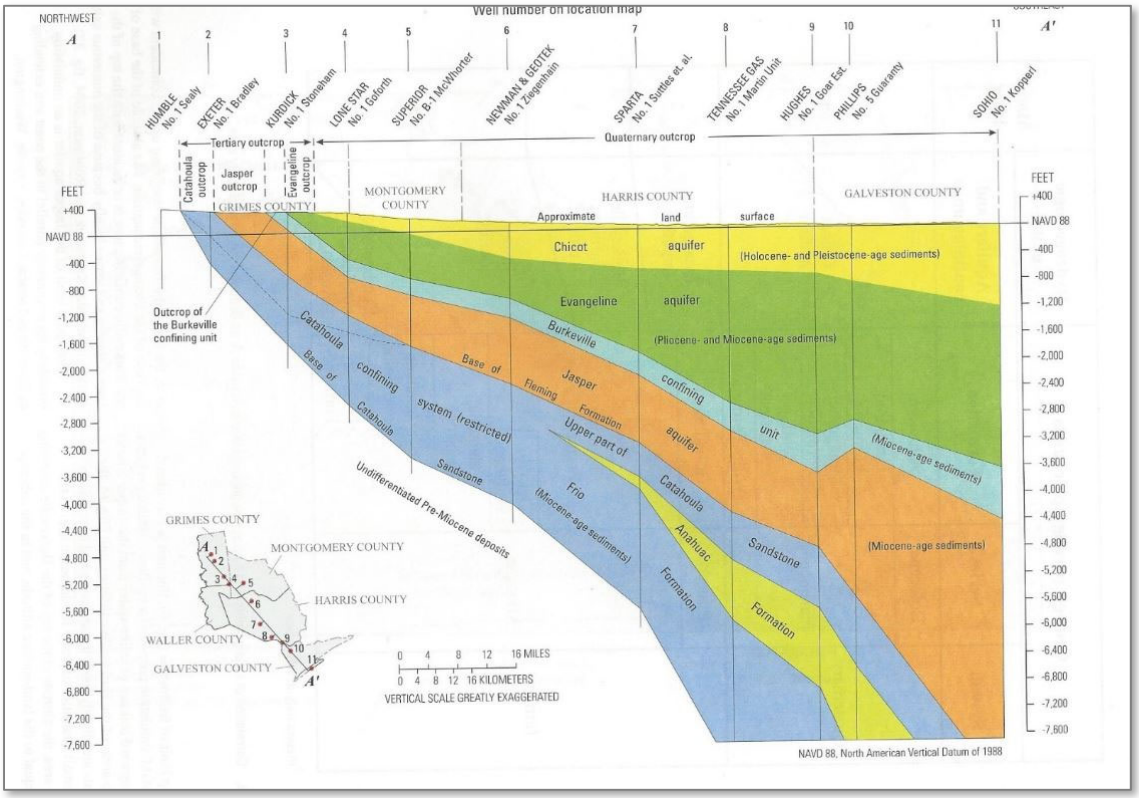

Figure 2-4: Hydrogeologic Section of the Gulf Coast Aquifer System in Montgomery county, Harris county, and adjacent counties, Texas (Kasmarek, 2012).

The Evangeline aquifer is an important source of water in the Houston area and is composed of a sequence of alternating sands and clays in Goliad Sands (Wesselman, 1972). The top of the Evangeline aquifer is defined by a single flooding surface, ranging from 120 to 230 meters below sea level (Wesselman, 1972). The Chicot and Evangeline aquifers are hydraulically connected, meaning that changes in the hydraulic head of one will affect the other (Jorgenson, 1975).

The shallower Chicot aquifer is composed of Holocene to Pleistocene aged Willis Sand, Montgomery and Bentley Formations, and younger deposits. Remints of these formations can also be found in the Evangeline aquifer in the northern part of Montgomery county. Groundwater wells are intentionally screened in and produce from these thick, sand-rich intervals. Laterally discontinuous interbeds make up the remaining seventy to twenty-five percent of the section. Leake and Prudic (1991) defined an interbed as having (1) a significantly lower hydraulic conductivity than the surrounding units, (2) sufficient permeability and porosity to permit fluid flow, (3) lateral discontinuity, i.e. is not a regional confining layer, and (4) a larger horizontal extent compared to the vertical thickness. The abundance of interbeds is integral to explaining the mechanism driving inelastic compaction.

3 Groundwater

3.1 Movement of Water in the Gulf Coast Aquifer System

The rate and direction of regional groundwater flow is controlled by the depositional pattern, lithology, and potentiometric surface within an aquifer (Kreitler et al., 1977). Most precipitation entering the ground flows into the saturation zone. From there the water travels a short distance through the shallow saturation zone and discharges into nearby streams, bayous, reservoirs, and lakes. The remainder of the water in the ground moves southeastward into intermediate and deeper zones of the aquifer system where it can later be withdrawn by groundwater wells.

3.2 Aquifer Mechanics

The Gulf Coast aquifer system is an unconsolidated accretionary wedge of interbedded sands, silts, and clay particularly predisposed to compaction due to shallow fluid withdraw. Either high pumping rates at a single location or multiple closely spaced wells can cause drastic pressure declines within the aquifer and a subsequent drop of the potentiometric surface (Kasmarek and Strom, 2002). The combined weight of overlying sediments, interstitial fluids and the atmosphere at any depth within the aquifer is referred to as overburden. The force exerted by the aquifer to counterbalance the overburden comes from both the aquifer matrix and the pressure exerted by pore fluids (Bawden et al., 2012).

Sandstone aquifers generally consist of discontinuous sand lenses, which are complexly distributed in a matrix of less permeable materials, i.e. clay and silt (Fogg, 1986). Each material has a unique hydraulic conductivity, which is the measure of a rock's ability to transmit water (Fetter, 2001). Clays for example can have rather large pore spaces, but they are not well connected, making it less transmissive than sand. Fogg (1986) found that flow within the aquifer is controlled not by the hydraulic conductivity, but rather the interconnectedness and continuity of the sand bodies.

Groundwater withdrawal can cause both elastic and inelastic compaction within the aquifer, depending on the lithology. Elastic compaction happens near the surface, especially over the summer months when the clay compacts due to shrink swell. Inelastic compaction occurs at depth when the dewatering of clay matrix occurs. The clay reorients its matrix perpendicular to the overbearing vertical stress. No amount of energy can be put back into the system to reverse the matrix. Inelastic compaction is permeant. Extraction of groundwater from sand rich intervals can cause compaction that reverses as water levels recover (Kasmarek et al., 2014). Rebound was observed at the Baytown and Clear Lake extensometers in response to the increase in potentiometric water levels due to regulated reduction of groundwater use. Kasmarek et al. (2014) suggest the land surface rebound was driven by recovering water levels in Southeast Harris County.

Water contained within an aquifer is considered to be "in storage." This can refer to water in the deep, sand-rich, regional system or the tight pore spaces of clays. Compaction of the clay and silt layers reduces the porosity and groundwater storage capacity of the clay layers (Kasmarek et al., 2014). The storage and compressibility of an

aquifer depends on the stress history, transmutability, and permeability of materials within the aquifer.

In a closed aquifer system, groundwater extraction will cause aquifer pressure to decrease. As the interstitial fluid pressure decreases, the aquifer will experience an equal increase in effective stress (Galloway et al., 1999). The removal of water from storage within interbedded clay can be induced if the hydraulic gradient is favorable between fast draining (high transmissivity) sands and low permeability (low transmissivity) clays (Fetter, 2001).

As water releases from storage in the clay matrix, the overburden stress causes the clay matrix to collapse. Clay grains preferentially realign perpendicular to the overburden stress, resulting in irreversible or inelastic compaction (Figure 3-1). Even if groundwater levels are reestablished, much of the porosity has been lost and the land surface level can only partially rebound. Gabrysch and Bonnet (1975) estimated that only ten percent of the height lost to permanent compaction would be restored with the theoretical re-establishment of artesian conditions within the aquifer.

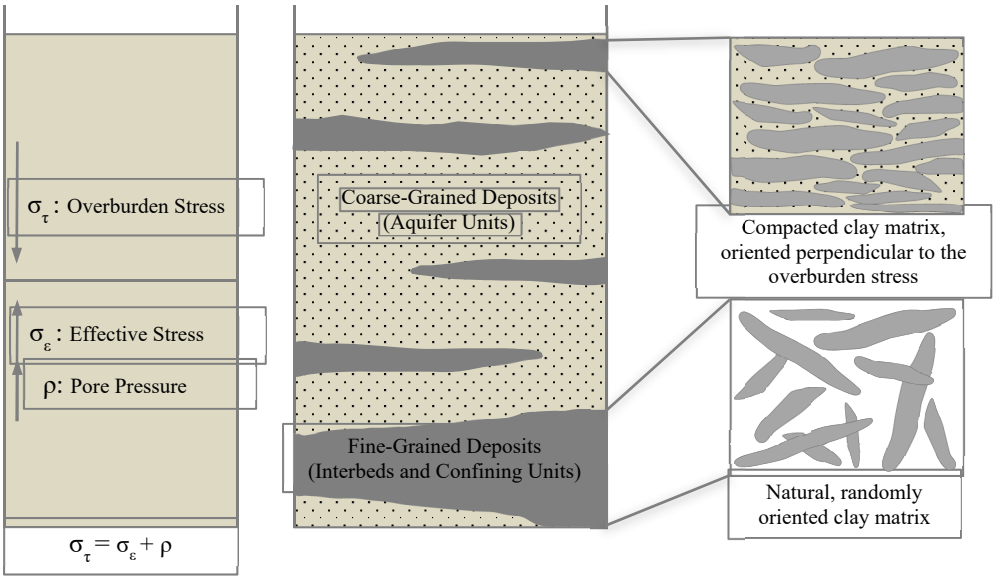

Figure 3-1 Principal Stresses within the Aquifer System
This figure shows the relationship between compaction and changes in the subsurface stress regime in response to fluid withdrawal. The weight of overlying sediment (σ_τ) is equal to the force exerted by the sediment matrix (σ_ε) and interstitial fluids (ρ) below. In a confined aquifer, groundwater withdrawal causes a uniform decrease in pore pressure and an equal increase in the effective stress (Leake and Prudic, 1991). The change in pressure, and increased effective stress, causes water to be expelled from storage (in the fine-grained layers) and the clay matrix to collapse. Figure modeled after Galloway et al. (1999).

Factors such as the age of the sediment, clay content, and previous drawdown level will affect the amount of subsidence observed at a given location. Kasmarek et al. (2014) suggests that subsidence is a localized phenomenon, meaning rates of compaction cannot be extrapolated or inferred across an area because groundwater withdrawal rates, local lithology and compressibility of sediments are unique at each location.

As reported by Jorgenson (1975) and Baker (1979), the Chicot aquifer can be distinguished from the Evangeline aquifer by a clear increase in hydraulic conductivity, which is a function of increasing sand content (Young et al, 2014). The two aquifers are

hydraulically connected, meaning that changes in the hydraulic head of one will affect the other (Jorgenson, 1975). Vertical head gradients have increased as a result of pumping, inducing downward flow from shallow zones into the deeper regional flow systems, capturing in storage groundwater that would have discharged naturally (Gabrysch, 1969).

Additionally, the rate at which groundwater is extracted, the porosity, and permeability of the unit will affect the rate of dewatering (Galloway and Burbey, 2011). Previous studies (e.g., Burbey et al., 2006; Warner, 2003) address three-dimensional strain within an unconsolidated aquifer. The dewatering process changes stress patterns on the sediment matrix, as each material has a unique transmissivity. Gulf Coast aquifer units are more transmissive in the horizontal direction than vertical causing the transmissivity to be dampened by abrupt changes in lithology (Fetter, 2001).

3.2 History of Subsidence in the Houston Area

Subsidence is a negative vertical deformation of the land surface. Subsidence naturally occurs very slowly but can be dramatically accelerated due to anthropogenic depressurization of the aquifer. Natural subsidence along the Gulf Coast can be attributed to three main processes:

1) Consolidation and compaction of sediments. Younger sediments are more susceptible to compaction as they have been exposed to less overburden stress and subsequent dewatering. Older sediments are still susceptible, but at lower rates. Marshy sediments, rich in organic materials, will also compact rapidly when drained for development

(agricultural or urban). Carbon-rich soils will oxidize as the sediments desiccate, releasing CO_2 into the atmosphere with associated mass and volume loss to the soil (Dixon and Dokka, 2008). This process tends to vary spatially in association with clay to sand ratios, organic content, burial depth and groundwater withdrawal.

2) Subsidence due to mass loading or isostacy. Flexure of the continental crust has been attributed to the increasing sediment load in the Gulf of Mexico basin (Jurkowski and Brown, 1987), while González and Tornqvist (2006) suggest that the crust is still rebounding in response to the Larentide Ice Sheet melting.

3) Tectonic subsidence in the form of gravity sliding. Gulfward, or down dip, movement of deltaic sediments due to gravitational loading is thought to connect to actively deforming subsurface salt (Dokka et al., 2006). Engelkemeir and Khan (2008) have identified hundreds of surface faults in the Houston Metropolitan Area using LiDAR, implying that neotectonics are still actively deforming the region.

Traditional methods for quantifying rates of compaction were based on the stratigraphic record. Until the latter half of the 20th century, subsidence estimates assumed relative coastal stability and were reported on millennial scale or time-averaged rates referenced to chronostratigraphic data. Paine (1993) calculated long-term, natural rates of subsidence for the Texas Gulf Coast to be, on average, 0.05 millimeters per year.

Rapid subsidence was first observed in the Houston area at Goose Creek Oil Field, where oil and gas withdrawal caused localized faulting and a rapid drop in ground level (Pratt and Johnson, 1926). Various early workers (e.g., Winslow and Doyle, 1954; Holzer and Johnson, 1985) found a strong correlation between groundwater withdrawal

and aquifer compaction. The United States Geological Survey (USGS) correlated artesian pressure declines within the aquifer system to pronounced regional subsidence (Kasmarek et al., 2014). Gabrysch (1969) postulated that the recovery of water levels would decrease the rate of subsidence and possibly allow for rebound to occur.

The USGS then began to install a network of extensometers in the Houston area to monitor aquifer compaction, and implement regulations limiting groundwater withdrawal. There was a corresponding effort by the City of Houston in the 1950's and 1970's to increase surface water supplies by creating local reservoirs (e.g., Lakes Livingston, Conroe and Houston) to serve the greater Houston metropolitan area.

It is difficult to discern between the various processes without a deep-seated monument to constrain the interval of compaction and the controlling mechanism. Previous studies by Ortega (2013) and Burrough (2013) utilized the Addicks and Southwest Extensometers in Harris County to study subsidence related to groundwater withdrawal. Results indicated that surface deformation recorded at GPS stations corresponded with the aquifer compaction rates recorded by nearby extensometers. Therefore, this paper assumes that the observed surface deformation is representative of aquifer compaction and *subsidence* will refer to compaction of aquifer sediments due to groundwater withdrawal.

Modern measuring techniques include leveling, GPS, InSAR and LiDAR; each of which can be referenced to a localized or geocentric datum. Many parts of Houston experience five to ten millimeters of vertical motion every year, whereas the Addicks site is sinking fifty millimeters per year (Bawden et al., 2012), a rate two to three orders of

magnitude greater than the historic rate from the rock record. Such a pronounced acceleration of geologic processes has been attributed to fluid extraction from young sediments in the Gulf Coast region (Kasmarek et al., 2014).

3.3 Monitoring Aquifer Levels

An aquifer is primarily monitored through measuring groundwater levels and maintained through pumping regulations. In the Gulf Coast Aquifer system, the groundwater levels and pumping rates are closely related. Groundwater levels indicate the health of an aquifer, which is controlled by groundwater extraction rates.

The primary source for groundwater level measurements used in this study is the USGS Groundwater Watch website. All groundwater monitoring wells in the Chicot, Evangeline, and Jasper aquifers were used in this study as shown in Figure 3-2. Groundwater levels were measured by USGS within municipal supply wells after the methods described by Kasmarek et al. (2014). The hydraulic head, or potentiometric surface, is the elevation in a sealed borehole to which water will rise, representing the pressure within the aquifer at the screened depth.

Aquifers are dynamic and constantly changing to maintain equilibrium with flow patterns changing in response to pumping. Water level monitoring can either be continuous or periodic measurements. Continuous monitoring provides the highest level of resolution of water-level fluctuations. Hydrographs constructed from frequent water-level measurements collected with continuous monitoring equipment can be used to

accurately identify the effects of various stresses on the aquifer system and to provide the most accurate estimates of maximum and minimum water-level fluctuations in aquifers. Periodic ground-water-level measurements are those made at scheduled intervals, either weekly, monthly, or yearly. These measurements are generally used for water-table or potentiometric surface mapping and to reduce the costs of long-term monitoring (Taylor and Alley, 2001).

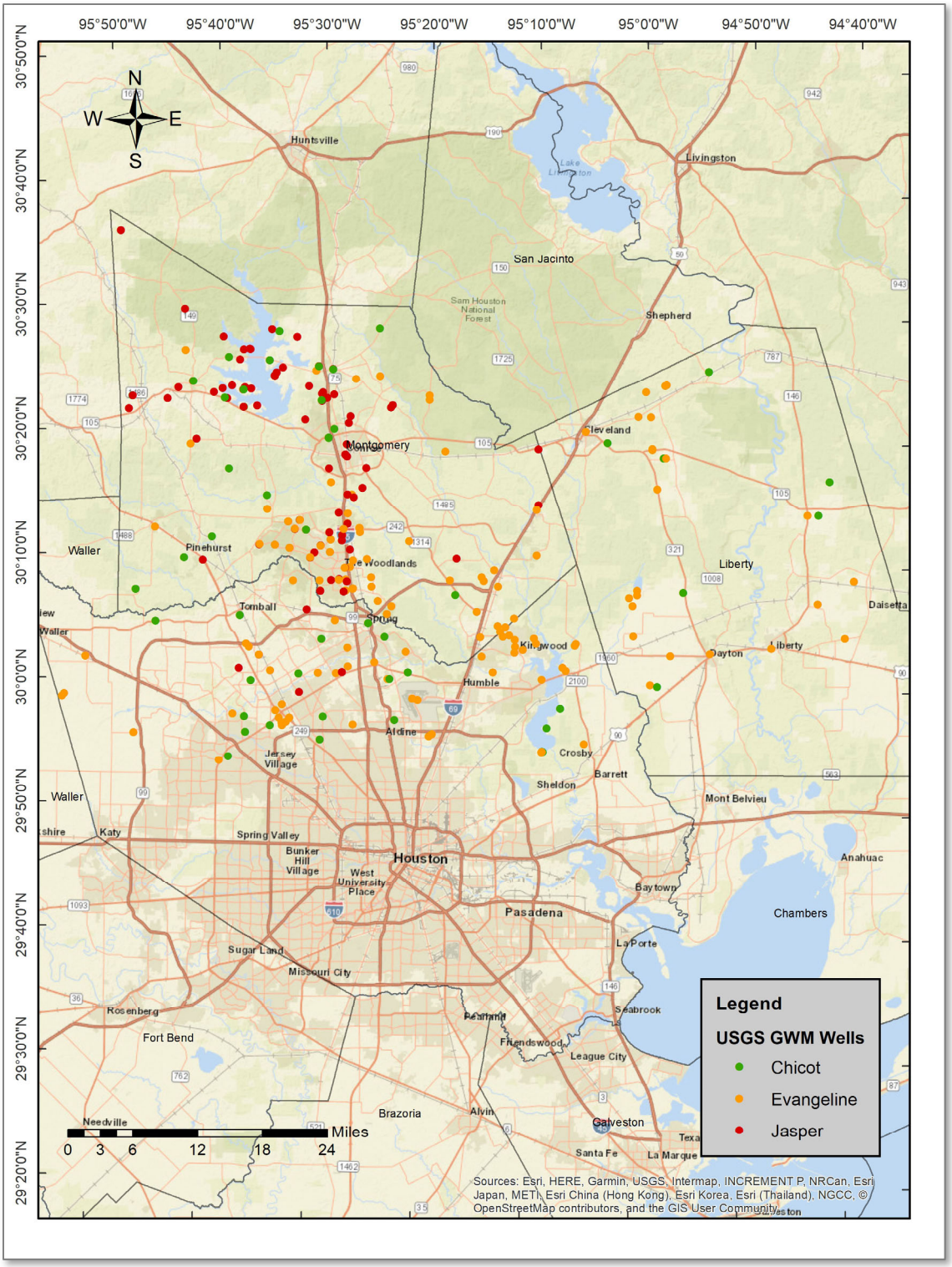

Figure 3-2 USGS Groundwater Water Level Network within the study area.

4 GPS Positioning

GPS technology has been applied to surveying and scientific applications since its advent in the early 90's. This study utilizes GPS data collected by both the University of Houston and the Harris-Galveston Subsidence District (HGSD). The raw GPS data was then processed to create time-series dating back to 1994.

In further support of this effort, the National Science Foundation awarded the University of Houston a grant to establish a dense, real-time GPS network known as HoustonNet. The HoustonNet stations are being used to monitor hazards relating to natural processes such as land surface subsidence, active faulting, as well as human induced subsidence such as fluid withdraw. Figure 4-1 shows three of the HoustonNet stations within the study area paid for under the NSF grant. These three stations were installed in 2014 at the Woodlands High School, Jones Forest Park, and at Liberty airport by students at the University of Houston.

Figure 4-1 HoustonNet stations installed by graduate students at the University of Houston. The upper left is station WHCR located at the Woodlands High school, the bottom left is station UHJF located at Jones Forest State Park, and station on the right is TXLI located at Liberty airport.

All data was uniformly post-processed using the Jet Propulsion Laboratory's GIPSY-OASIS software ver. 6.4. This software employs the Precise Point Positioning (PPP) method, yielding sub-centimeter accuracy results. Accuracy and data outliers were determined and eliminated if greater than two times the standard deviation (2σ). Initial results from GIPSY are provided within the Earth-Centered, Earth-Fixed International GNSS Service (IGS08) reference frame.

A local reference frame, Houston16, was established using GPS observations (> 5 years) through 2016 using 15 Continuous Operating Reference Stations (CORS) located outside of the greater Houston area. The results were then translated from IGS08 to

Houston16 using a 7-parameter Helmert transformation. The Houston16 sites surrounding the study area were selected using criteria outlined in this chapter. The stable reference frame highlights intra-regional processes by eliminating dominant and consistent signals attributed to crustal motion. All positions are reported within Houston16 and the complete time-series are available in Appendix II.

4.1 GPS as a Surveying Tool

The United States Department of Defense began developing GPS technology in the early seventies (El-Rabbany, 2006). Diverse and unique arrays of industries have since found applications for using GPS technology ranging from real time navigation of cars, aircraft, and ships to measuring the soil moisture content of crops and determining property line boundaries for new and existing road construction. Other scientific applications include monitoring geological activity including earth tremors, earthquakes, and volcanic rumblings.

In the early nineties, GPS became an accurate and economically feasible alternative to campaign style re-leveling surveys (Zilkoski et al., 2001). GPS instruments are able to measure ground surface motions much more frequently than traditional land surveying techniques, and maintain a comparable range of error. The spatial and temporal variability of surface deformation can be constrained by installing multiple permanent or campaign style GPS stations over an area.

Harris Galveston Subsidence District (HGSD) and Lone Star Water Conservation District (LSCD) in Montgomery county have a network of permanent GPS stations that utilize a rotating set of equipment. Permanent monumentation at each site includes a concrete pad with a pole anchored 6 m into the ground. An opening at the center of the pad allows the pole to slip freely. This helps avoid any superficial shrink-swell motions associated with fluctuating soil-moisture content and highly expansive clays.

A GPS antenna is fixed on top of the pole three meters above the land surface to avoid the effects of multipath from surrounding objects. The rotating set of equipment includes a Trimble antenna, pictured in figure 4-1, and is paired with a Trimble NetR9 receiver within the receiver enclosure. The rotating GPS instrumentation, referred to as Port-A-Measure Stations (PAMS), collects data at each location for seven to ten days before being moved to the next station. An antenna is collecting data at a single site for six to seven weeks out of the year, or about twelve percent of the time. A general understanding of how the instrument works, and the associated processing method, is necessary to understand and interpret GPS data.

Figure 4-2 PAM Station Setup
This photo shows PAM47 in Spring. The battery and GPS receiver are attached inside the receiver enclosure, while the GPS antenna and solar panel are mounted on the top and middle of the pole respectively. (Photo Credit to Eloy Gonzalez from HGSD)

4.2 GPS Data Processing

Obtaining an accurate position using the Global Positioning System (GPS) requires a processing method to account for meaningful variables affecting the accuracy of a position. Results can either compromise on accuracy and be produced in real-time (rapid), or post-processed to obtain high accuracy results. To utilize either method correctly, one must understand the technical aspects of how to get a position using GPS.

Global Positioning System (GPS) defines a position through triangulation. The orbit and position of each satellite is geocentric, or referenced to the center of the earth. By measuring the travel time of radio signals, a pseudo-range from satellite to receiver is calculated within a few seconds. An actual distance is derived from the pseudo-range by multiplying travel time by the speed of light ($c=3.0 \times 10^8$ m/s). The range is then used to determine the position at the intersection of all four spheres, resulting in one unique point on the surface of the earth. This method relies on an accurate travel time and knowing exactly when the satellite sent the radio signal, which is dependent on synchronous clocks. GPS satellites are equipped with incredibly precise clocks made of cesium, resonating at a known and uniform frequency.

According to Trimble (2010), each satellite sends out its signal on two carrier frequencies. The L1 carrier transmits a pseudo-random code and status message, while L2 carries more precise coding that is specifically for military use. Any discrepancies between the clocks in orbit and on earth will introduce error. These errors are monitored by the Department of Defense and corrections are communicated back to satellites.

Since 2005, satellites have been equipped to transmit a second signal (L2C) that is available to civilians, thereby improving the accuracy of measurements. The L2C signal created the ability to directly measure and remove errors related to ionospheric delay. Accuracy is further increased through post-processing the data, which utilizes satellite paths and eliminates several sources of noise and errors.

Raw GPS data is provided in a binary format and must be processed to produce meaningful results. Converting data from the receiver specific format to the standardized

Receiver **In**dependent **Ex**change (RINEX) file format is necessary prior to processing. Observation files (*.12o) include time, satellite, C1 (distance), P2 (distance), L1 (cycles), and L2 (cycles). RINEX was developed for the easy exchange of GPS data and archiving.

Two main methods have been established for post-processing raw data to produce a positional time-series differential (relative positioning) and precise point positioning, or PPP (absolute positioning). Differential GPS measures the relative distance between a pair of stations with a short baseline on the scale of 100's of kilometers (Eckl et al., 2001). The relative positioning method measures single-frequency pseudo-range numbers, yielding sub-meter accuracy positions at best (Rizos et al., 2012).

Networks of reference receiver stations, such as the Continuously Operating Reference Stations (CORS), were established to facilitate more accurate positioning using the differential technique. The two stations will have a set of shared errors in their signals that can be canceled using the differential method, except multipath.

Precise Point Positioning (PPP) is a processing method that has been developed over the past two decades for the measurement of individual GPS station motions. The Global Navigation Satellite System's (GNSS) PPP method requires a single receiver, removing the need for another station nearby. This is advantageous in remote locations that lack infrastructure because it does not require the same dense and costly infrastructure as differential GPS. Though, according to Rizos et al. (2012), if CORS are present they could be used to enhance PPP, especially regarding real-time applications.

There is a dense GPS network already in place within the Houston Metropolitan area. Localized phenomena near the reference station, like subsidence, can bias results

when using the differential method. Determining the position of a station utilizing the PPP method eliminates the possibility of this kind of anomaly. This study employs the PPP method to study land subsidence; reasoning and methodology are described below.

GPS data was initially formatted specifically to the receiver type and converted to a standard Receiver Independent Exchange (RINEX) format. Receivers collect a data sample every 30 seconds. The PPP method averages the 2,880 positions collected over a 24-hour period to produce a daily solution. Averaging is an effective way to minimize any minor noise in the signal due to atmospheric conditions or multipath since GPS orbits are designed to circumnavigate the globe twice a day (Blewitt and Lavallée, 2002).

Data was then post-processed using GIPSY/OASIS ver. 6.4, a software package developed by NASA's Jet Propulsion Laboratory (JPL). GIPSY data processing method employs PPP, which compares the L1/L2 bands at a single receiver to eliminate differences in carrier phase velocity (Wang, et. al., 2017). The absolute positioning method allows users to get a position from a single receiver with dual-frequency (L1 and L2) P code processing capabilities (Rizos et al., 2012). This method uses the difference between the L1 and L2 band to eliminate atmospheric noise.

Minute horizontal and vertical motions are discernible using high-resolution GPS receivers. This sensitivity is associated with more noise, which requires a longer time-series to define a trend. The positional time-series was only analyzed if it had an observation period of three or more years to minimize the influence of seasonal signals on interpretation (Blewitt and Lavallée, 2002).

4.3 Sources of Error and Accuracy

Generally, the main sources of error for a GPS system stem from an inaccurate satellite clock (time) or ephemeris (satellite position), phase ambiguity bias, or signal delay from traveling through earth's atmosphere. These errors may be estimated, corrected or reduced using the detailed processing techniques discussed in this study.

Finalized station positions are highly dependent upon the travel time of a signal. When inaccuracies are introduced into this fundamental function, error will result. Travel time in turn depends on the accuracy of satellite clocks. GPS satellites have atomic clocks made of cesium, which are accurate to the nanosecond. Multipath is caused by signals reflecting off surfaces near the antenna resulting in a longer travel time; clocks that are out of synch will introduce errors into the signal travel time as well. Noise from the receiver and pseudo-random number can also reduce accuracy.

Ephemeris error is introduced when the actual position of a satellite strays from the predicted or modeled path. Though the ephemeris error is a fixed distance between the predicted and true positions, the effects vary depending on the viewing angle of each individual receiver. Short-baseline observations can be very useful in this particular situation (El-Rabbany, 2006). As distance between stations decreased, accuracy of the ephemeris estimation was found to improve as the distance decreased between monitoring stations. Producing accurate positions are therefore dependent on precise ephemeris data, which was obtained from the International GNSS Service (IGS).

In order to process carrier phase data for a GPS station, one must estimate the number of wavelengths between a transmitter and receiver (Remondi, 1985). Remondi

(1985) explains that satellites transmit carrier signals, which are then stripped of modulations so that the waveform may be isolated and used to calculate distances. In theory, the number of cycles or wavelengths transmitted and received will increase with time in a linear fashion. In other words, signal propagation proceeds at a constant rate, but since the GPS system is in motion, it does not behave in linear manner. The process of estimating an accurate number of phase cycles was termed bias-optimization by Blewitt (1989), who suggested that the reliability of data could be improved through large GPS networks with differing baselines.

The ionosphere, ranging from 50 to 500 km in altitude, creates the most significant source of error. Radio signals can travel from the satellite to receiver at varying speeds due to atmospheric conditions, referring to both the different atmospheric layers and weather events. Corrections must consider the properties of the troposphere and ionosphere, and estimate how long the signal takes to pass through each.

Tropospheric (0 – 50 km altitude) delays result from both hydrostatic and wet parameters (Davis et al., 1985). Hydrostatic delay occurs when dry gases and the non-dipole component of water vapor are present. It is strongly correlated to surface pressure and accounts for about ninety percent of the observed delay (Bar-Sever et al., 1998). On the other hand, wet delay, a product of dipole water vapor, is much more variable (Bar-Sever et al., 1998; Davis et al., 1985).

As the signal continues traveling, it will encounter ionospheric delays, which have been organized into first and second order delays. The larger first-order delays depend upon factors such as satellite elevation, solar activity, local season and time of day (Kedar

et al., 2003). Minor second-order delays are on the scale of millimeter to centimeter errors, but as the accuracy of GPS solutions improve, these small errors can become significant. Correcting for second-order ionospheric delays can reduce movements associated with seasonal variability, and thereby improve the precision of results (Kedar et al., 2003).

Since station positions are initially reported within the geocentric IGS08 reference frame, any force periodically displacing the Earth's center of mass must be accounted for. Solar and lunar tides can cause displacement of both the ocean and solid earth. Earth's tidal pattern is regular and predictable; large enough volumes of water are displaced from one side of the Earth to the other that it causes a minute shift in the earth's center of mass, affecting the accuracy of satellite positions.

When a source of noise cannot be modeled or corrected for, it results in an anomalous position that must be systematically removed. GIPSY outputs a sigma value for each daily position coordinate produced through the program. The sigma value indicates the average amount of noise in each direction (NEU) and every position (2880 positions per day). Sigma is therefore an effective measurement for removing outliers from within the context of the entire dataset. Averaging the daily results will eliminate some minor errors, but if an anomalous noise source is present for an extended amount of time, high frequency measurements will exhibit more variability.

Outliers were systematically identified and removed through an approach modified from previous studies (Firuzabidi and King, 2012; Wang, 2013). Firuzabidi and King (2012) implemented a study in central Italy to understand the relationship between

each position's precision, observational timespan and reference station location. Within their local reference frame, any position coordinate with a sigma value greater than two times the average sigma value was considered to be an outlier. Similarly, the data for each directional component was de-trended, the standard deviation calculated, and any position value greater than two times the standard deviation were removed.

4.4 Reference Frame

A position is, by definition, reported relative to an established point or frame of reference. A reference frame may be celestial or terrestrial (global, regional, national or local) (Matsuzaka, 2012). A reference frame can aid the understanding of how changes to the Earth's surface relate to the underlying geologic processes (Bawden et al., 2012). In order to produce meaningful results when working with GPS data, it is essential to choose a stable reference frame appropriate to the scale of the project.

For example, if plate tectonics are being studied, a global reference frame should be chosen. In such a case, one plate will be "fixed" and all other plate motions are described relative to the fixed plate. The North American Datum of 1983 (NAD83) (Schwarz, 1989; Soler and Snay, 2004) is a regional or continental-scale reference frame that fixes the North American tectonic plate motion, highlighting intra-continental processes. Subsidence is a localized to regional scale phenomenon, commonly linked to localized groundwater withdrawal practices unique to the climate and urbanization of a given area (Galloway and Burbey, 2011).

GPS velocity vectors and surface positions in the Houston Metropolitan Area have historically been reported relative to CORS mounted on stable, deep-seated extensometers. An alternative to the baseline-pair method involves the use of multiple stable sites to establish a local reference frame. Observations from stable sites in the region can be used to determine the orientation, origin, scale and time-derivatives of these parameters (Kearns et al., 2018). Any observation within this reference frame will more readily display internal, or localized, deformation.

GPS data processing using GIPSY-OASIS ver. 6.4 yields solutions referred to the geocentric International GNSS Service (IGS) reference frame of 2008 (IGS08). The most current version offered at the time of data processing, IGS08 was used for this study. Subsequent revisions, or realizations to the IGS reference frame are GPS based, using fifty well-established stations around the world (Soler and Snay, 2004). Modern GPS coordinate frames provide very accurate and reliable solutions achieved by the precise orbits (ephemerides) distributed by IGS (Soler and Snay, 2004). High-precision GPS relies on GNSS satellites and International Terrestrial Reference Frame (ITRF) solutions. The IGS began using ITRF precision products in 1994 (Kouba, 2002).

As ITRF coordinates improve with time, and subsequent realizations are released, updated IGS products are also released. This ensures that precise orbit and clock corrections are in step with any changes to ITRF. Since 2000, IGS began defining their own global reference frame, which is still based on the most recent realization of the ITRF (Ray et al., 2011). For example, IGS replaced the IGS05 reference frame in 2011 with IGS08, which is referenced to ITRF08.

Positions are actualized as X, Y, and Z components in a geocentric reference frame. Solutions are then converted to latitude, longitude and ellipsoid height. Ellipsoid height is defined as the distance to a point measured perpendicular to the ellipsoid surface (Wang and Soler, 2014). All results (Appendix II) are reported as displacement in the Northing, Easting and Up (NEU) direction. When no displacement occurs, or it is within the calculated error of the instrument, the station is considered to be stable in that direction. If a significant change in position was observed, then the velocity (speed and direction) can be derived from the time-series. This study of subsidence encompasses three counties and only the vertical components were considered.

Global positions were transformed into a localized reference frame, Houston16. Houston16 (Wang, et al., 2017) that was realized using fifteen CORS outside the Houston area that have a long and stable history of greater than five years. Each station's coordinates were transformed into the localized reference frame, displacement values were calculated with respect to the initial position, and a time-series was created for analysis. Solutions within Houston16 are able to achieve +-0.4 mm/year horizontal accuracy and +-0.8 mm/year vertical accuracy (Kearns, et al., 2018).

Utilizing the precise point position (PPP) method within this stable reference frame eliminated the possibility of losing data due to site-specific motion. Instead, each point was referenced to a stable reference frame for the Houston area, which effectively averages and fixed the localized motion in three dimensions.

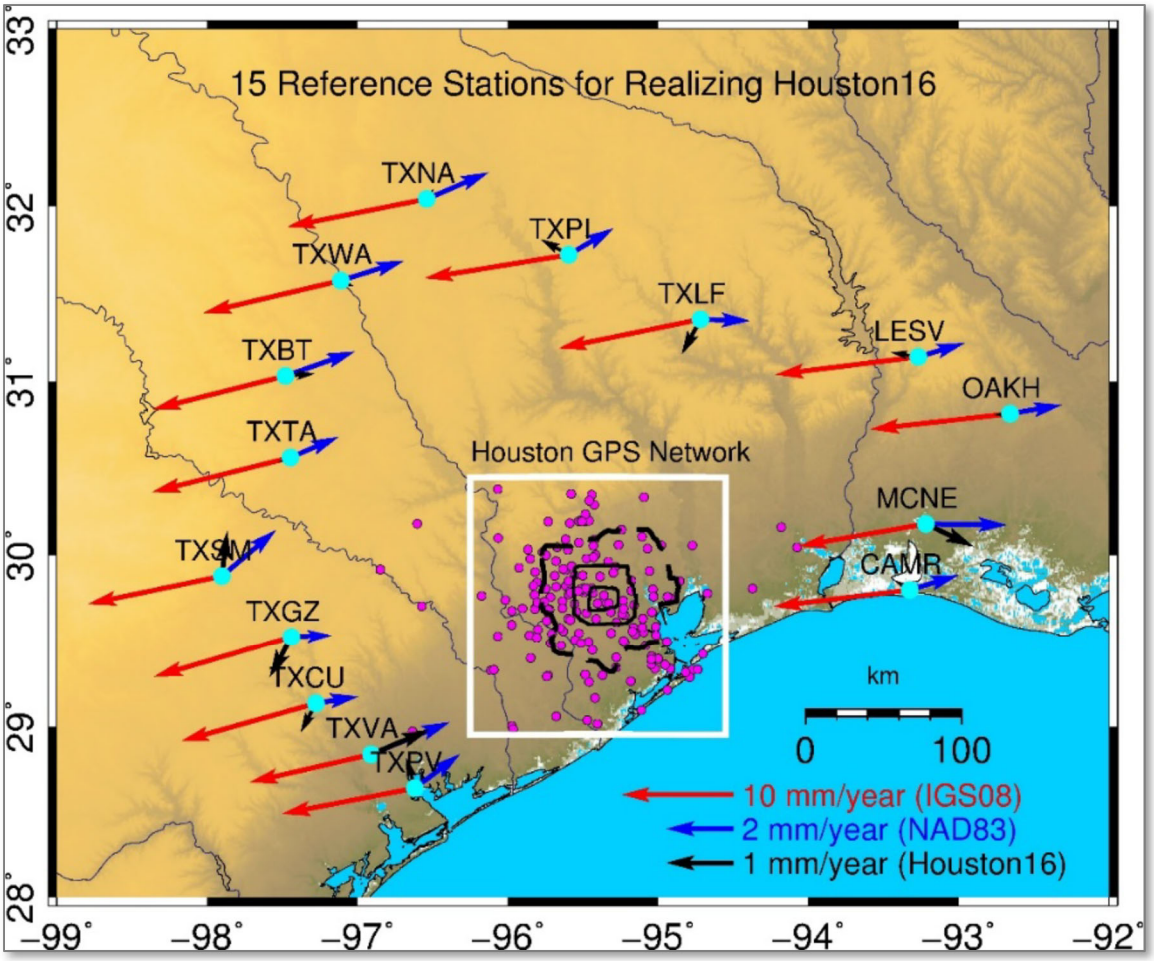

Figure 4-3 Map showing the locations of 15 reference GPS stations used to establish the Stable Houston Reference Frame of 2016 (Houston16). The vectors represent the horizontal velocity vectors with respect to IGS08 (red), NAD83 (blue), and the regional reference frame Houston16 (dark). The white box represents the Houston metropolitan area (Kearns et al. 2018).

A reference frame's most important mathematical and physical parameters are the origin, scale, orientation and the change of these properties over time (Wang et al., 2013). A 7-parameter Helmert Transformation, which accounts for each parameter, was used to translate coordinates from an IGS08 reference frame into Houston16 following the

methodology of previous studies (e.g. Soler and Snay, 2004; Pearson et. al., 2010; Kearns et al., 2018). Two types of transformations exist that consist of a daily 7-parameter transformation and a similarity 14-parameter transformation.

The 7-parameter similarity transformation, which includes 3 translations, 3 rotations, 1 scale and the respective rates, was utilized in this study. Parameters (Table 3-1) are defined with respect to time, and can be solved for using a set of unique, individual points with known coordinates in each reference system preceding and following the transformation. Since there are seven parameters that need to be determined, at least one coordinate and two points must be known. This enables a system of seven linear equations with seven unknowns to be solved.

Three common points will fulfill the minimum requirements mathematically, but observational errors at each point make it almost impossible to satisfy the parameters. In practice, adding additional points will increase the solution accuracy. Known IGS08 coordinates of a GPS site are related to their corresponding SHRF coordinates by a similarity transformation that is determined using the following equations (Kearns et al,. 2018):

$$
\begin{aligned}
X(t)_{Houston16} &= X(t)_{IGS08} + T'_x \cdot (t - t_0) + R'_z \cdot (t - t_0) \cdot Y(t)_{IGS08} - R'_y \cdot (t - t_0) \cdot Z(t)_{IGS08} \\
Y(t)_{Houston16} &= Y(t)_{IGS08} + T'_y \cdot (t - t_0) - R'_z \cdot (t - t_0) \cdot X(t)_{IGS08} + R'_x \cdot (t - t_0) \cdot Z(t)_{IGS08} \qquad (1) \\
Z(t)_{Houston16} &= Z(t)_{IGS08} + T'_z \cdot (t - t_0) + R'_y \cdot (t - t_0) \cdot X(t)_{IGS08} - R'_x \cdot (t - t_0) \cdot Y(t)_{IGS08}
\end{aligned}
$$

These equations show $X(t)_{Houston16}$, $Y(t)_{Houston16}$, and $Z(t)_{Houston16}$ indicating the X, Y, and Z position coordinates, at time t, for the ground station within Houston16. Similarly,

$X(t)_{IGS08}$, $Y(t)_{IGS08}$, and $Z(t)_{IGS08}$ represent the respective position coordinates, of the same station, within the IGS08 reference frame.

Equation 1 (Kearns et al., 2018; Soler and Snay 2004) demonstrates X, Y, and Z position coordinates in IGS08 being transformed into Houston16 as a function of time using:

$T_x(t)$, $T_y(t)$, $T_z(t)$	*translation* along the x-, y-, and z-axis respectively, at time *t*;
$R_x(t)$, $R_y(t)$, $R_z(t)$	counterclockwise, positive *rotation* about respective axes, at time *t*;
to	the epoch alibiing two reference frames (IGS08 and Houston16)

Approximated equations are sufficient due to the small magnitudes of the three rotations. Note that each of the seven parameters is represented as a function of time. These time-related functions are assumed to be linear, as expressed by Pearson and Snay (2013):

Table 4-4 shows the values used for the parameters used to transform the IGS08 coordinates into the NAD83 reference frame, and IGS08 to the SHRF. The long data history available in the vicinity of the Houston metropolitan area allowed the SHRF transformation to account for all seven parameters and their respective time derivatives. The results of transformations are visible in the time-series for station TXL1 (Figure 4-4-2).

Table 4-4: Seven Parameters for Transforming XYZ Coordinates from IGS08 to Houston16

Parameters	Unit	**IGS08 to Houston16**
T'_x	m/year	1.1427832E-002
T'_y	m/year	-2.4771197E-003
T'_z	m/year	5.8795944E-004
R'_x	radian/year	2.0734184E-010
R'_y	radian/year	-2.0205941E-009
R'_z	radian/year	1.0549129E-009
t_0	year	2012.0

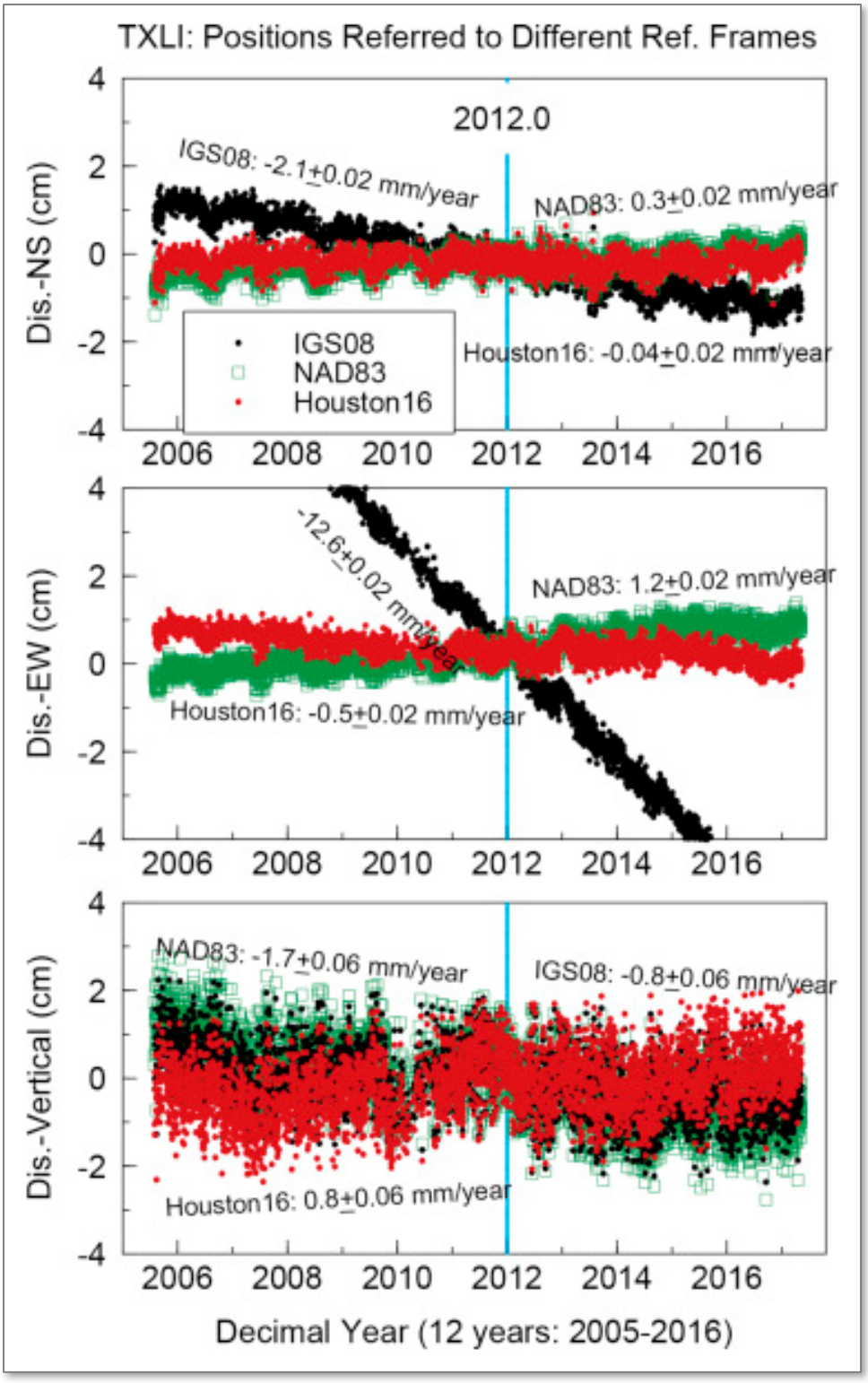

Figure 4-4 TXL1 Displacement Time-series in Three Reference Frames

5 Interaction of Subsidence and Groundwater Level Change

5.1 Groundwater Withdrawal

Population continues to grow as development increases in Montgomery and northern Harris counties. Stress and strain occur on the aquifer system as demand increases. The Harris Galveston Subsidence District (HGSD) regulations required a 30% conversion to surface water supplies by 2010 for Areas 3 in an effort to mitigate subsidence and ensure ample water supplies for future generations. Groundwater pumping history across regulatory Area 3 are shown in Figure 5-1 (HGSD, 2018). In 2009, Montgomery county put regulations in place for large volume water to reduce their amount of groundwater use by 30% in 2016. Figure 5-1-2 (LSWCD, 2018) shows the amount of groundwater withdraw by use from 2007 to 2017.

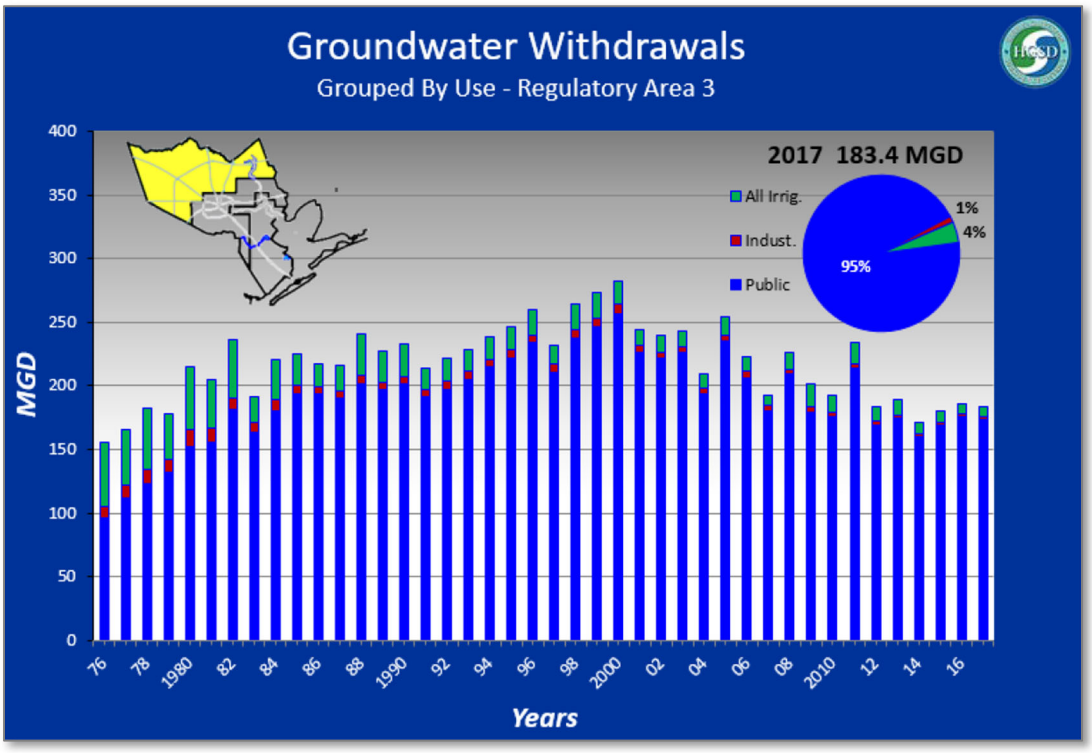

Figure 5-1 Groundwater Withdrawal History for Regulatory Area 3

Data comes from the 2017 HGSD Annual Report.

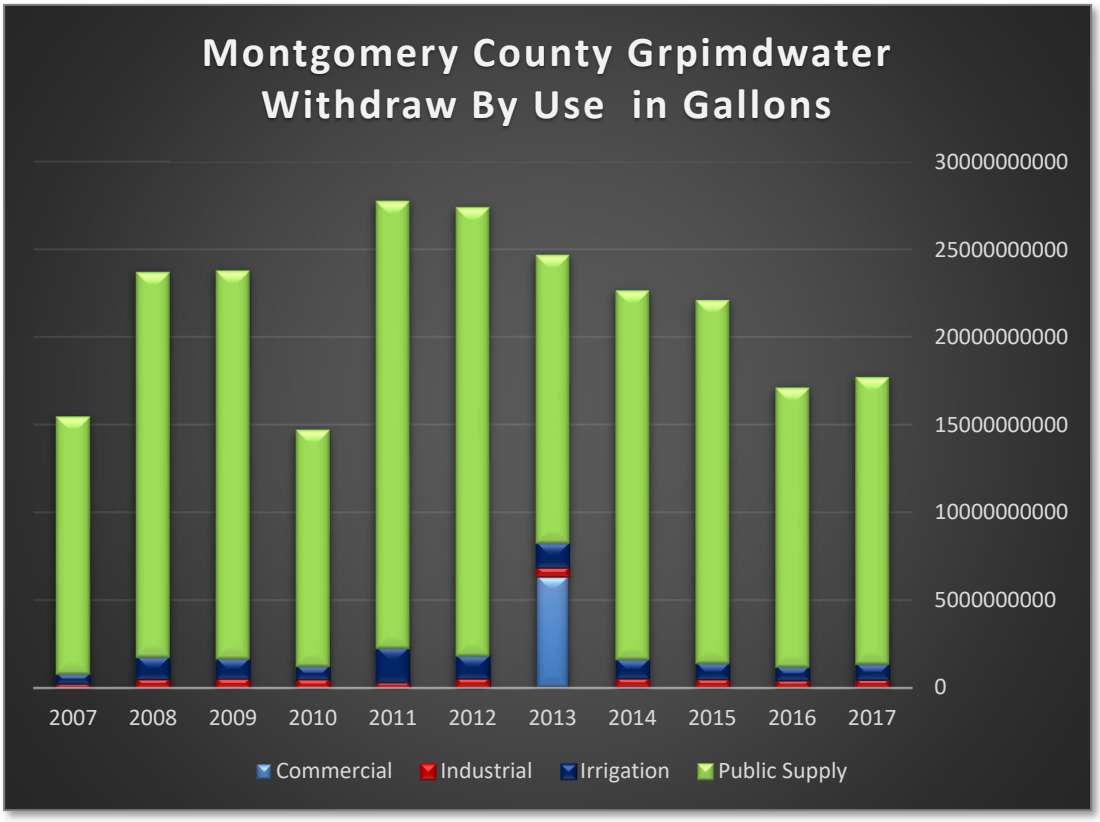

Figure 5-1-2 Groundwater Withdrawal History for Montgomery County By Use
Data comes from the Montgomery County Annual Reports (2007-2017).

Public water supplies clearly dominate by use in Montgomery county and in Area 3 of Harris county. Irrigation, industrial, and commercial use for both Montgomery county and Area 3 are fractional compared to the public water supply. Overall both counties groundwater water use levels rise and fall as population increases and local climate conditions such as droughts occur.

5.2 Groundwater Levels

The U.S. Geological Survey provided groundwater level observations for Montgomery county and northern Harris county through the Groundwater Watch program. A map of the monitoring wells within the Chicot, Evangeline, and Jasper aquifers are shown in Figure 3-2. Monitoring wells within each individual aquifer are shown below and a list of each well by its corresponding number is shown in Appendix 1. Measurements were originally reported in feet below land surface but have been converted to meters to maintain consistency.

Figure 5-2-1 shows the groundwater wells monitored at the Chicot aquifer within the study area. There are 51 Chicot groundwater monitoring wells within the study area. Four of these wells have water level changes of less than 2 cm/year indicating that there is little to no recovery nor drawdowns at these locations. Fourteen of the wells have positive velocities over the monitoring time, indicating that these wells have higher recovery rates. Nine of the wells with positive velocities are located in Harris county, one is located in the northeast corner of Montgomery county, and the remaining three are in Liberty county. The remaining 37 monitoring wells in the Chicot aquifer all have negative velocities ranging from -1.29 cm/year to -269.28 cm/year in the negative direction. These negative velocities indicated small to severe drawdowns within the Chicot aquifer. The fastest drawdowns are located at well sites TS-60-37-718, TS-60-36-615, and TS-60-36-710 in Montgomery county.

The Evangeline aquafer within the study area has 141 monitoring wells within the study area. Figure 5-2-2 depicts a map of each of these wells. Velocities range from

+188.09 cm/year to -255.92 cm/year. 57 of these wells have positive velocities ranging from +4.33 cm/year to +188.09 cm/year indicating that these wells have strong to weak recovery levels. 34 of these wells are in Harris county, 15 are in Liberty county, and 8 are in Montgomery county. 4 Evangeline wells have velocities less than 2 cm/year indicating that water levels at these locations remain stable. The remaining 80 wells have velocities that range from -2.25 cm/year to -255.92 cm/year. The well with the fastest drawdown is well site TS-60-52-212 and is located in Montgomery county.

The Jasper aquifer has 86 monitoring wells within the study area. Figure 5-2-3 depicts the monitoring wells in this study. Five wells all located in Montgomery county have a positive velocity while the remaining 81 wells have negative velocities. The fastest drawdown is located at well site LJ-60-60-306.

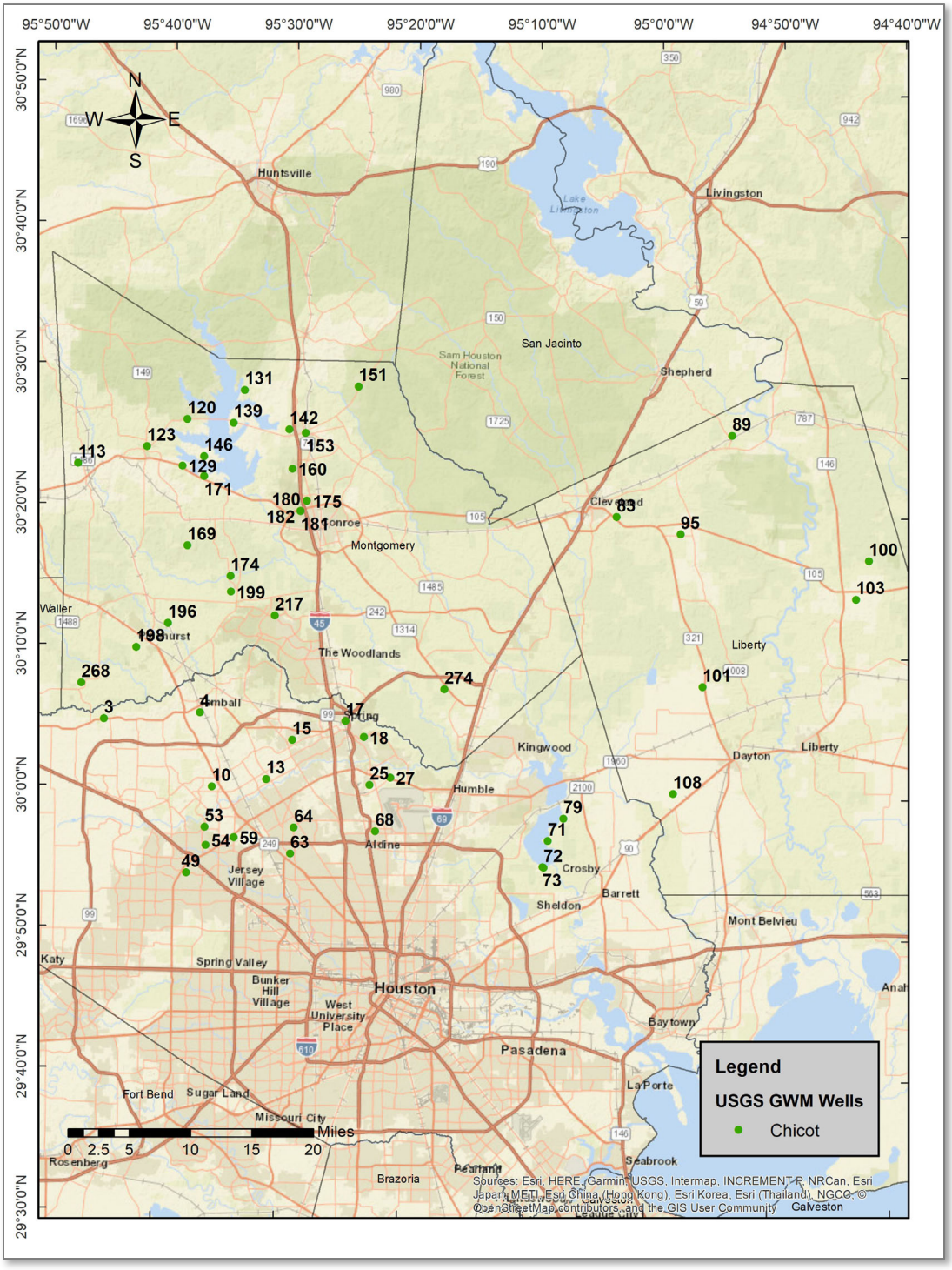

Figure 5-2-1 USGS Chicot Groundwater Monitoring Wells. Each number references an ID that can be found in Appendix I where well names and site numbers are provided.

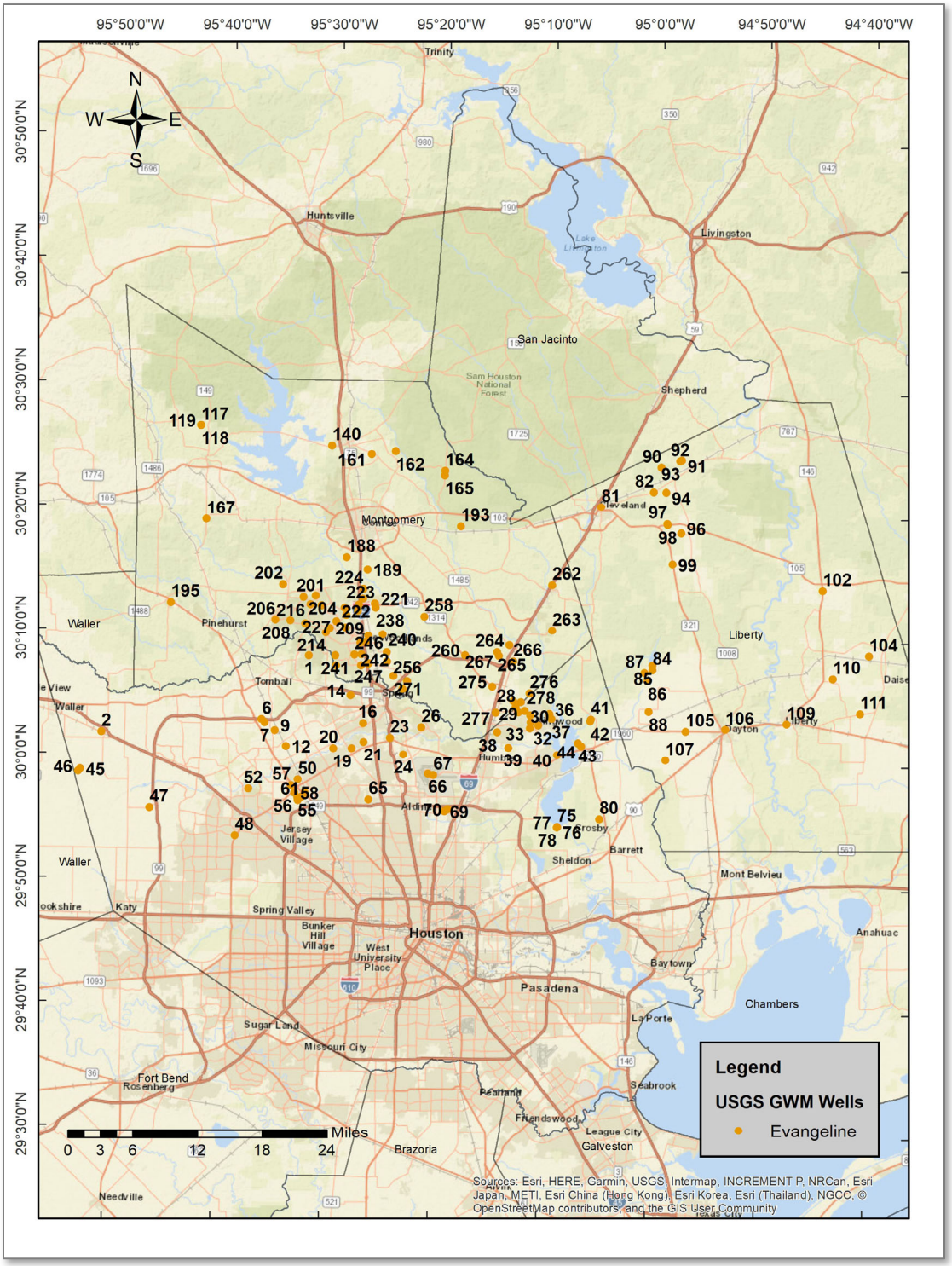

Figure 5-2-2 USGS Evangeline Groundwater Monitoring Wells. Each number references an ID that can be found in Appendix I where well names and site numbers are provided.

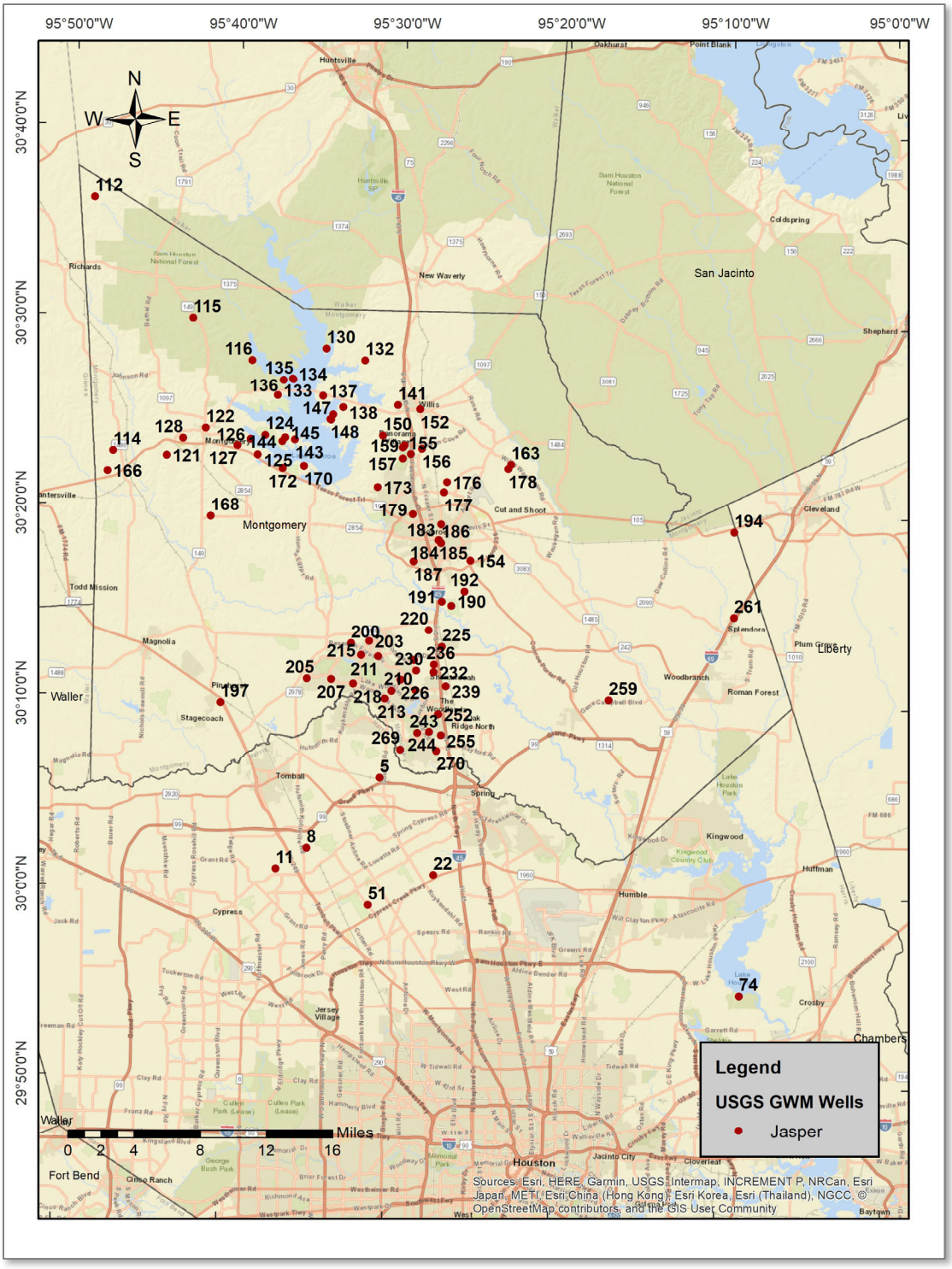

Figure 5-2-3 USGS Jasper Groundwater Monitoring Wells. Each number references an ID that can be found in Appendix I where well names and site numbers are provided.

The preconsolidation head for the northern part of the Gulf Cost aquifer system was set at 70 ft (21.336 m) in the Houston Area Groundwater Model (HAGM) used by Kasmarek in 2009. Kasmarek, M. C. (2012) states that if the preconsolidation head falls below 70 ft that an inelastic response occurs. In Appendix1 graphs of individual groundwater monitoring wells and their respective water levels are show. Currently the Chicot aquifer sits above 21.336 m in most of Montgomery county and northern Harris county. The Evangeline and Jasper aquifers vary with some being above the 21.336 m indicating an elastic response to changes in water levels. Some approach the 21.336 m threshold indicating that wells int these area experience both elastic and inelastic responses depending on the water levels. The remaining wells have water levels below the 21.336 m threshold, indicating an inelastic response or permanent compaction is occurring.

5.3 GPS Measured Surface Deformation

GPS data collected by UH, HGSD, and NGS CORS was processed through July 2018 using Houston16 to provide the vertical displacement from each station's respective beginning recording date. A complete collection of the GPS time-series analyzed in this study is included in Appendix II. An RMS accuracy of 8 mm was achieved for the vertical component direction for solutions within the Houston16 reference frame (Kearns et al., 2018).

GPS station displacement in the downward or negative vertical direction is termed as subsidence, while upward or positive displacement is referred to as rebound. Total observed vertical displacement velocities for the 37 GPS stations varying in operational time from 1994-2018 is listed in Table 5-3.

Station	StationType	Latitude	Longitude	RefFrame	FirstReadDate	LastReadDate	Subsidence Rate (cm/year)
AULT	HoustonNet	29.9981	-95.7447	HRF16	2015.5565	2018.4120	-0.974301916
CFHS	HoustonNet	29.9188	-95.6344	HRF16	2015.5948	2018.4586	-1.432937909
CLVD	NGSCORS	30.3350	-95.0940	HRF16	2012.6653	2017.1472	-0.320659070
LKHU	NGSCORS	29.9135	-95.1457	HRF16	1996.3395	2018.5708	0.014665315
PA02	PamStations	30.0006	-95.4159	HRF16	1994.3151	2018.5562	-2.664713110
PA07	PamStations	29.9363	-95.5766	HRF16	1999.1123	2018.4959	-2.739174416
PA08	PamStations	29.9797	-95.4763	HRF16	1999.6082	2018.5781	-2.245242555
PA09	PamStations	30.0381	-95.0715	HRF16	1999.3425	2018.5397	-0.482542152
PA12	PamStations	30.0597	-95.2631	HRF16	2000.8907	2018.5616	-0.586084203
PA13	PamStations	30.1948	-95.4900	HRF16	2000.9098	2018.5425	-1.676469083
PA17	PamStations	30.0912	-95.6153	HRF16	2000.8907	2018.5397	-1.731556178
PA18	PamStations	29.9649	-95.6782	HRF16	2000.8579	2018.5205	-1.999763205
PA46	PamStations	30.0300	-95.6000	HRF16	2007.3178	2018.5397	-2.052986916
PA47	PamStations	30.0895	-95.4235	HRF16	2007.3342	2018.5589	-1.969514250
PA48	PamStations	30.0454	-95.6717	HRF16	2007.3178	2018.5589	-1.536493222
PA51	PamStations	29.9325	-95.2842	HRF16	2007.3370	2018.5973	-0.555754404
PA53	PamStations	29.9080	-95.0573	HRF16	2007.3370	2018.5151	-0.219759918
PA65	PamStations	30.1064	-95.1067	HRF16	2012.4290	2018.5397	-1.185078932
PA66	PamStations	30.0178	-95.7673	HRF16	2011.1644	2018.5589	-1.460716696
PA68	PamStations	30.1848	-95.5868	HRF16	2011.7973	2018.6027	-1.187467448
PA69	PamStations	30.1990	-95.4590	HRF16	2011.7452	2018.5425	-1.308166750
PA70	PamStations	30.2911	-95.4244	HRF16	2011.7589	2018.5753	-0.751747084
PA71	PamStations	30.3531	-95.5789	HRF16	2011.7808	2018.5808	-0.678375231
PA72	PamStations	30.1470	-95.2425	HRF16	2011.9918	2018.4685	-0.246068620
PA73	PamStations	30.1934	-95.7302	HRF16	2012.0492	2018.5973	-0.976358513
PWES	HoustonNet	30.1990	-95.5106	HRF16	2015.2225	2018.5708	-0.728322205
ROD1	NGSCORS	30.0786	-95.5344	HRF16	2007.0034	2018.5708	-1.212753807
SESG	HoustonNet	29.9875	-95.4296	HRF16	2014.6776	2018.5708	-0.899265592
SHSG	HoustonNet	30.0536	-95.4301	HRF16	2014.7214	2018.4394	-1.094723290
TXCN	NGSCORS	30.3563	-95.4520	HRF16	2005.5797	2018.5708	-1.246774610
TXLI	NGSCORS	30.0558	-94.7708	HRF16	2005.5797	2018.5708	0.082179585
UH02	HoustonNet	30.3152	-95.4571	HRF16	2015.0034	2018.5708	-0.546801884
UHF1	HoustonNet	30.2363	-95.4831	HRF16	2014.3901	2018.3792	-0.556084221
UHJF	HoustonNet	30.2363	-95.4831	HRF16	2014.3901	2018.3792	-0.277575675
UHWL	HoustonNet	30.0577	-94.9784	HRF16	2014.3573	2018.5708	-0.048341634
WHCR	HoustonNet	30.1943	-95.5054	HRF16	2014.7789	2018.5708	-0.406261937
ZHU1	NGSCORS	29.9619	-95.3314	HRF16	2003.0418	2018.5708	-0.792238004

Table 5-3 GPS Station Vertical Displacement Over Recorded History.

Some GPS stations display a wavy pattern indicating seasonal variability. These stations include AULT, CFHS, PWES, SHSG, UH02, UHF1, UHJF, and WHCR. For

example, UHJF, a station installed by the University of Houston in the summer of 2014, displays this wave pattern with the average decline in the negative direction. Seasonal variability exists where there is upward movement in the GPS station during spring when the Houston and surrounding areas see more rainfall, followed by downward movement during the summer when temperatures are higher and precipitation is low. Overall, each of these stations have been recoding data between 3 and 4 years. Because of the shorter recording periods we can see the seasonal variability more clearly in in of these graphs.

Two GPS stations TXLI and LKHU remain stationary in the vertical direction during past 10 years. Station UHWL has a vertical velocity rate of less than a cm/year. The horizonal components showing movement in the north, south, east, and west directions are plotted in Figure 5-3-1. These stations are considered vertically stable as the velocities are less than 1 mm/year. (Figure 5-3-1). While these three stations do show slight increase and decreased changes in velocities, the velocities still need to consider the uncertainty of GPS positioning and the seasonal ground motions, thus making each of these stations show a stable vertical velocity of 0 cm/year.

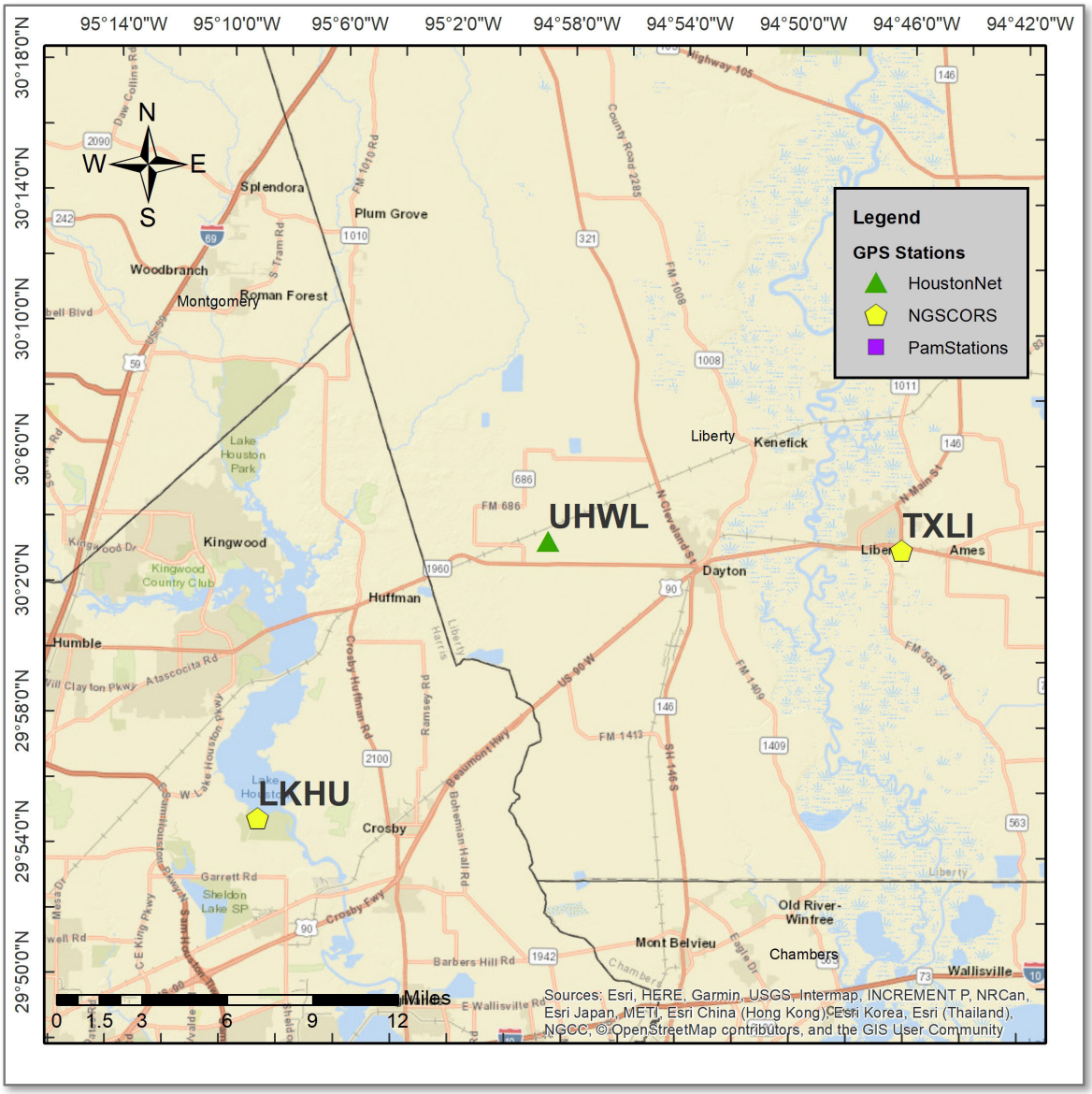

Figure 5-3-1 GPS Station Locations for TXL1, UHWL, and LKHU.

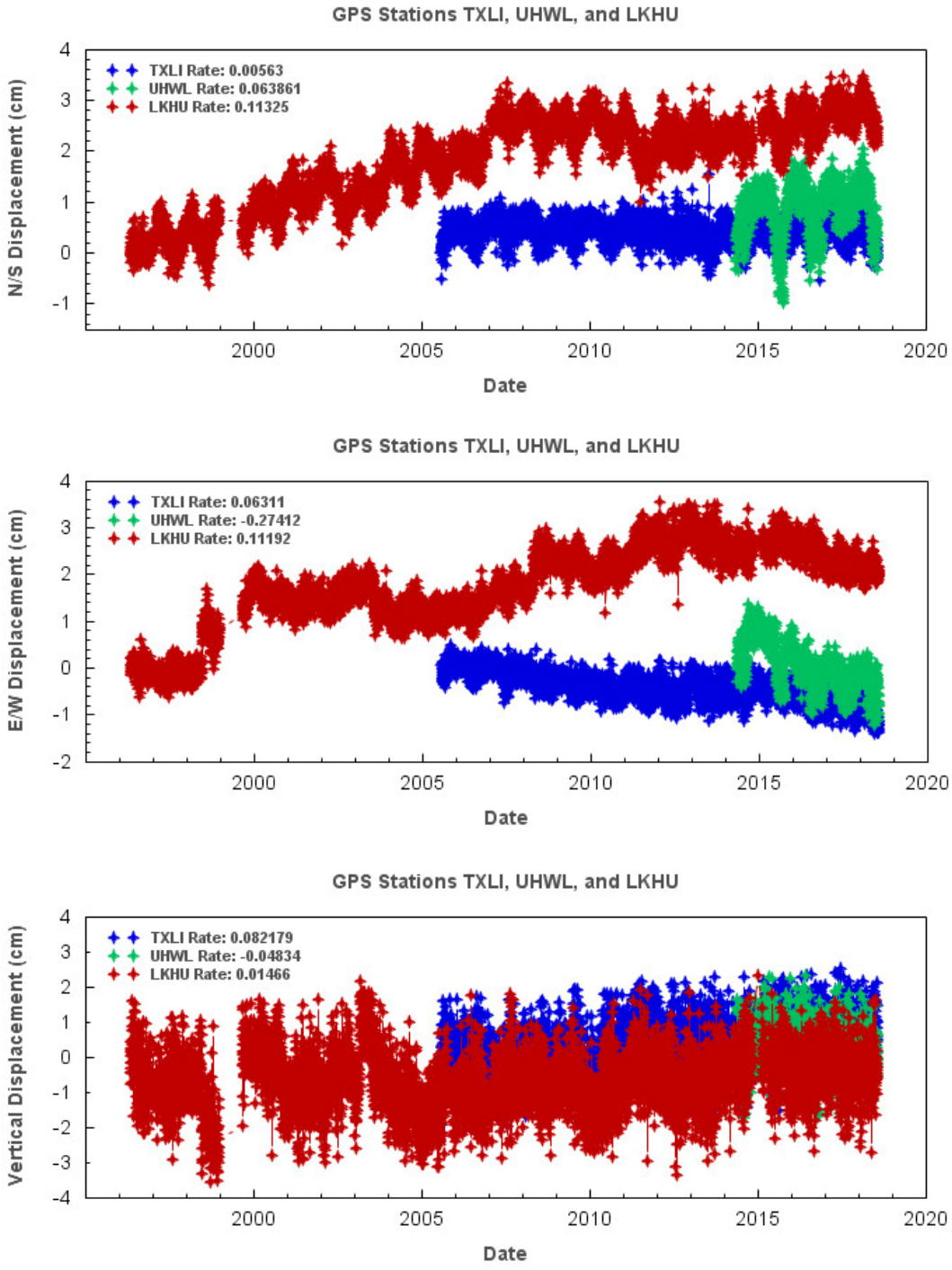

Figure 5-3-2 GPS data for TXL1, UHWL, and LKHU. The upper graph shows the north south component, the middle graph shows the east west component, and the lower graph shows the vertical component for each station.

The remaining stations gradually subside over a time period greater than 4 years. These stations include CLVD, PA02, PA07, PA08, PA09, PA12, PA13, PA17, PA18, PA46, PA47, PA48, PA51, PA55, PA65, PA66, PA68, PA69, PA70, PA71, PA72, PA73, ROD1, SESG, TXCN, and ZHUL. The velocities range in the negative direction from -0.219 cm/year to -2.739 cm/year. Four stations, PA02, PA 07, PA08, and PA46, have the fastest subsidence rates with downward vertical displacements of greeter than 2 cm/year. (Figure 5-3-2.) The north/south and east/west horizontal components are also plotted in Figure 5-3-2.

There is one station, PA12, where the velocity reading drops significantly between 2007 and 2011. This station is located in Humble at a pump station. The data at times looked a little noisy and this was due to the pump on the well. This problem was resolved in 2012 when a choke ring was installed. In addition, there was significant overgrowth and overhang of trees over the station. The city of Houston removed this brush in 2012 (Chrismer, 2018).

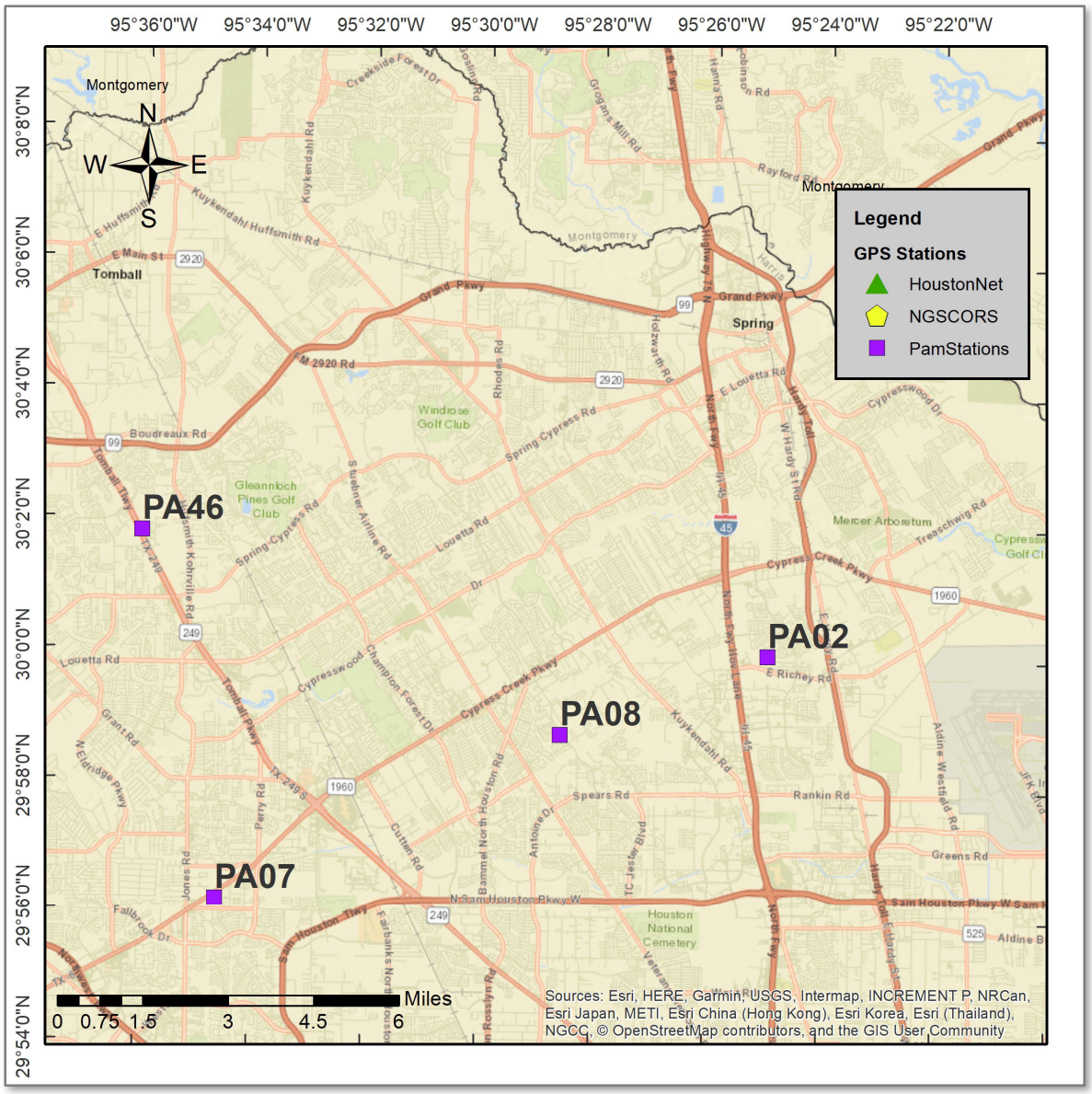

Figure 5-3-3 GPS Station Locations for PA02, PA07, PA08, PA46.

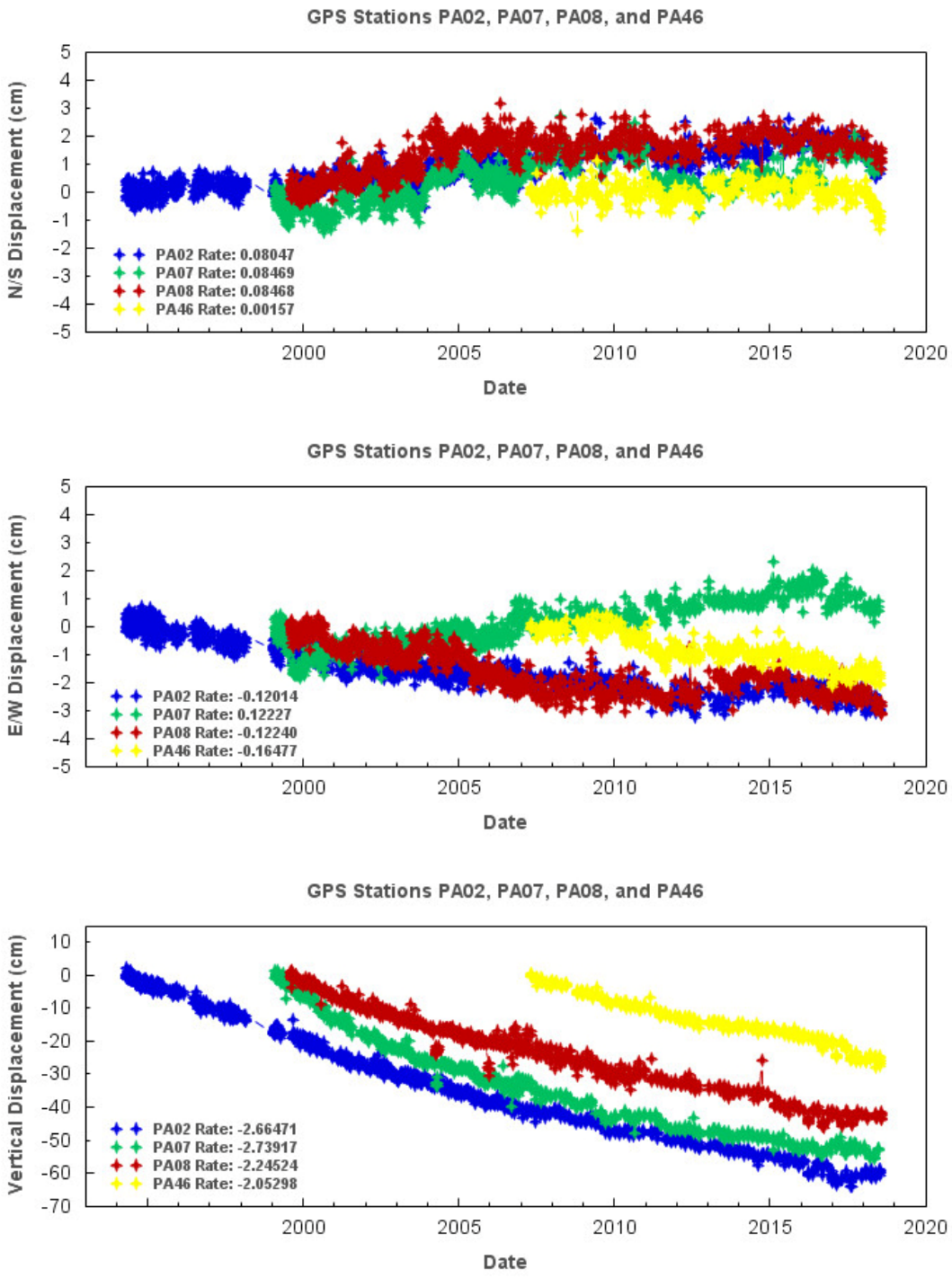

Figure 5-3-4 GPS data for PA02, PA07, PA08, and PA46. The upper graph shows the north south component, the middle graph shows the east west component, and the lower graph shows the vertical component for each station.

5.4 Subsidence in Response to Groundwater Levels

Water levels within several monitoring wells within the study areas were collected. GPS station data measuring the vertical component near these groundwater wells were analyzed in three serpate locations within the study area. A closer look into the Chicot, Evangeline, and Jasper water levels and the GPS station closest to those wells are described below.

GPS stations located near in the central part of north Harris county shown in Figure 5-4-1 were analyzed. Monitoring wells in the Chicot aquifer, LS-65-05-425, LS-65-05-414, and LS-60-61-919 are the closest groundwater monitoring wells near these GPS stations. There are water level declines and recovery from 2004 to 2018 within the Chicot aquifer at this location. There are 4 Evangeline wells near these GPS stations: LJ-60-61-626, LJ-60-61-905, LJ-60-61-914, and LJ-60-61-713. There are water level declines between 1992 to 2007, followed by water level increases up to current date. The GPS stations have two Jasper monitoring wells closest to them. These two monitoring wells show significant declines in the water levels for almost as much as 40 m since 2004. Results indicates that the negative vertical movement or subsidence in the area is caused by water level declines within the Jasper aquifer.

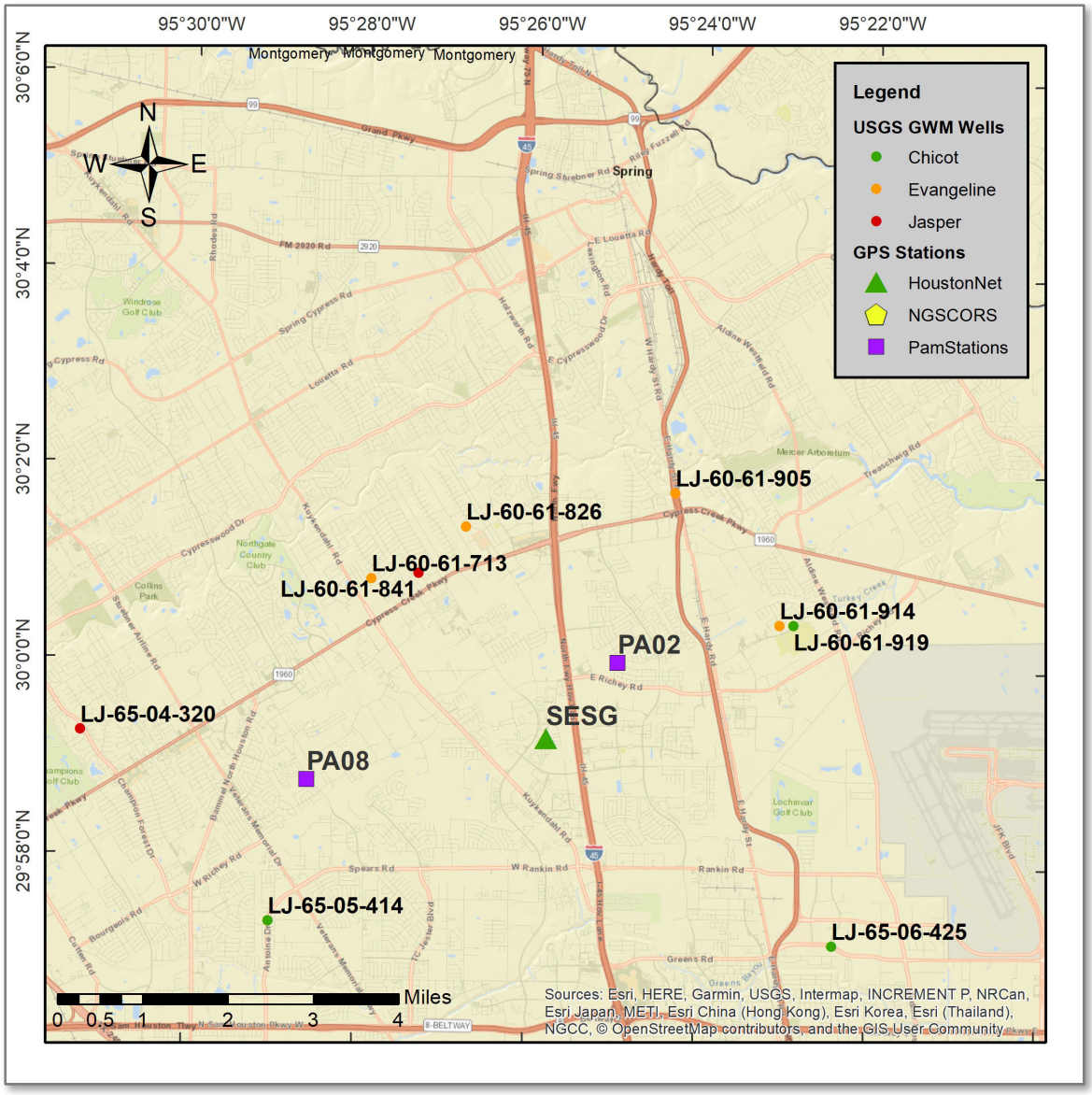

Figure 5-4-1 GPS Station Locations for PAM 02, PAM 08, and SESG with USGS monitoring wells near GPS stations.

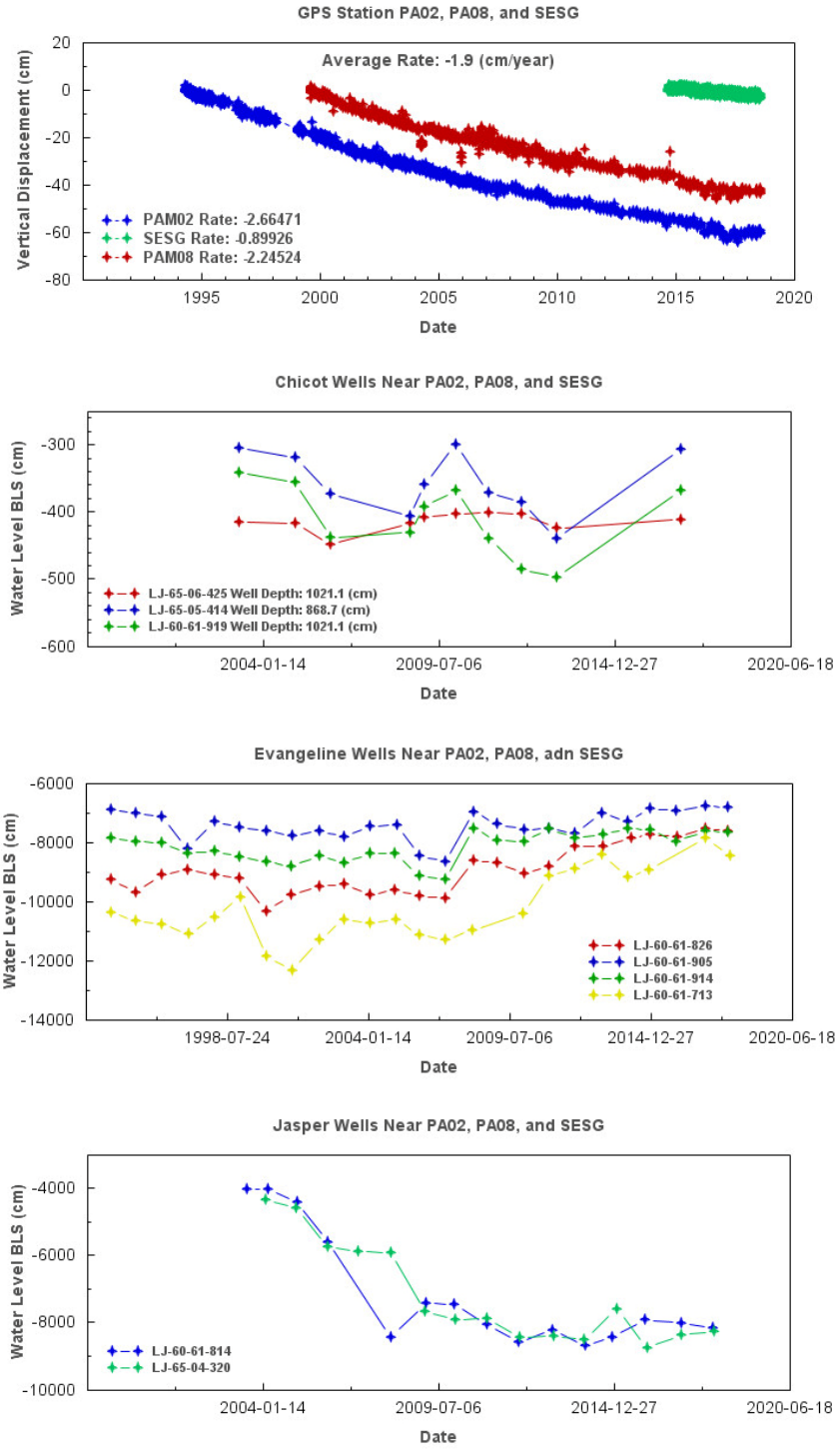

Figure 5-4-2 GPS Stations PAM 02, PAM 08, and SESG with USGS Well Data. Chicot aquifer monitoring wells near PAM 02, Evangeline monitoring wells near PAM 02, and Jasper monitoring wells near PAM 02.

GPS stations located on the north-west side of in Harris county shown in Figure 5-4-2 were evaluated along with the closest monitoring wells with in the Chicot, Evangeline, and Jasper aquifers. GPS stations PAM 07, PAM 46, CFHS, PAM 08, and PAM 18 are close proximity to each other. Each of these stations shows significant subsidence is occurring in this area with the vertical velocity rate at PAM 07 being the fastest of all other GPS stations within this study. Chicot aquifer monitoring wells near these stations are showing only a slight movement in water level. Evangeline monitoring wells near these stations show signs of increased water level recovery within the area. The Jasper monitoring wells near these stations show significant water level declines since 2004 for as much as 50 m indicating that the water level declines seen in the Jasper are the primary cause for subsidence at this location.

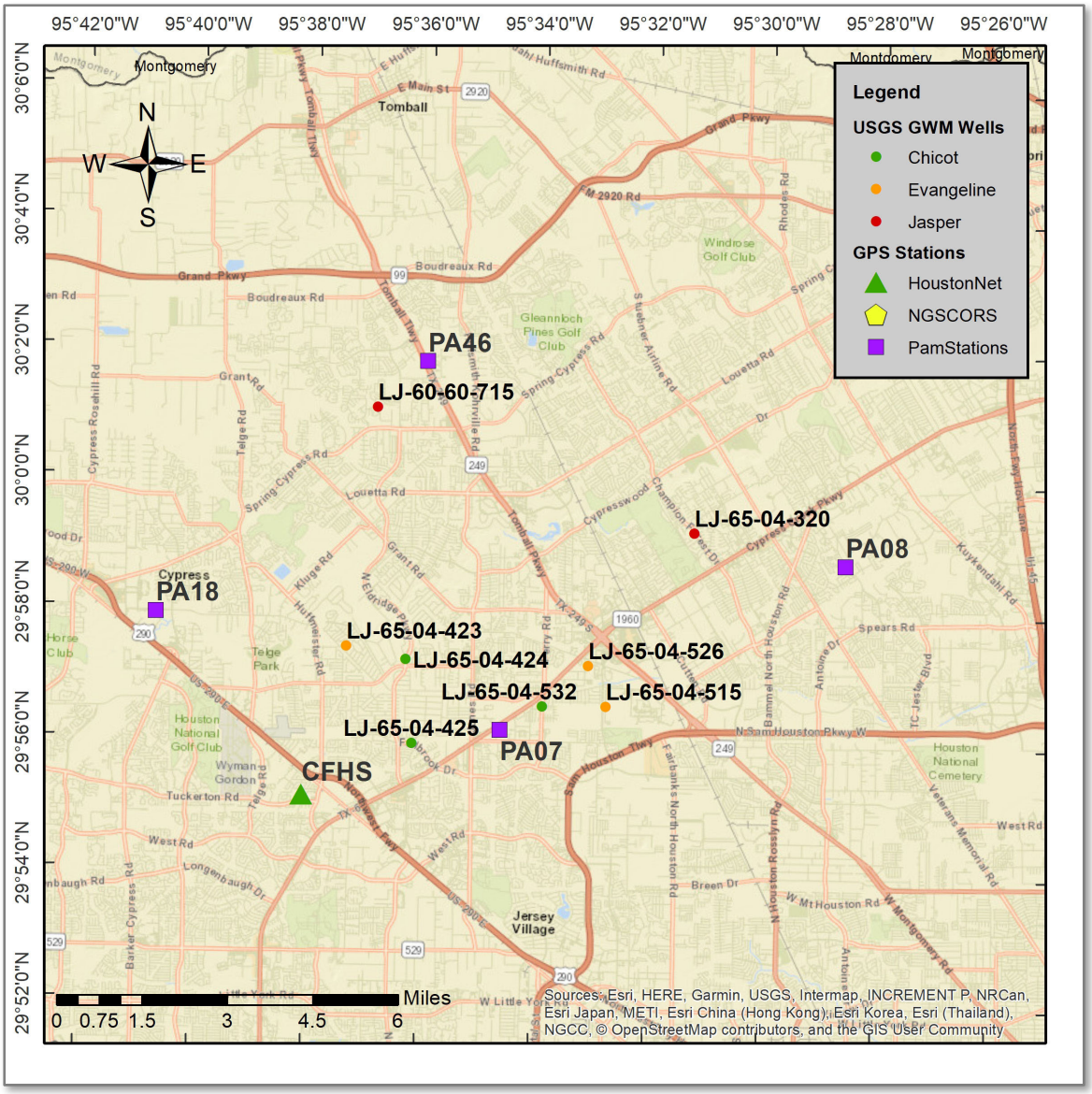

Figure 5-4-3 GPS Station Locations for PAM 07, PAM 46, CFHS, PAM 08, and PAM 18 with USGS monitoring wells near GPS stations.

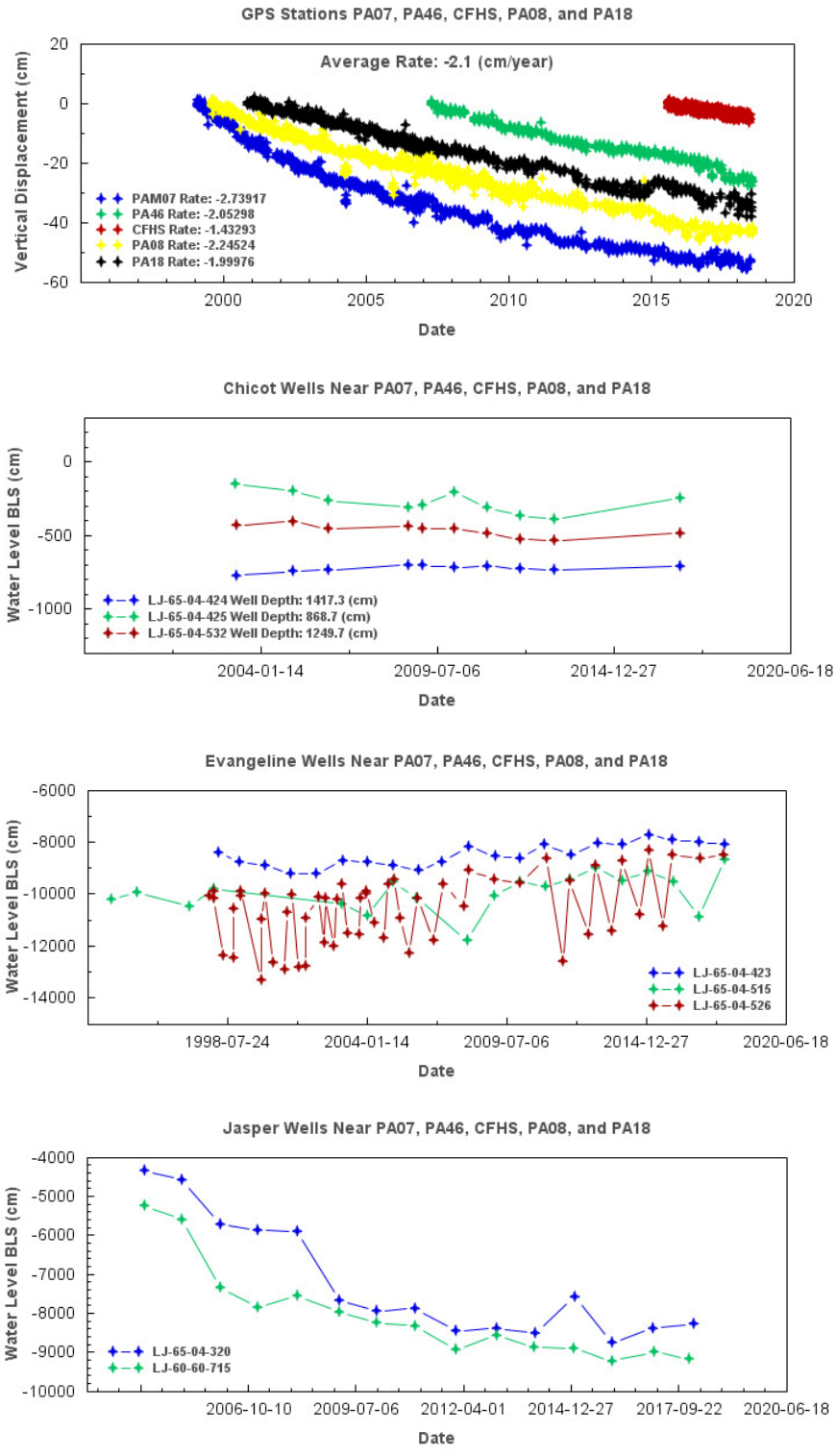

Figure 5-4-4 GPS Stations PAM 07, PAM 46, CFHS, PAM 08, and PAM 18 with USGS Well Data. Chicot aquifer monitoring wells near PAM 07, Evangeline monitoring wells near PAM 07, and Jasper monitoring wells near PAM 07.

GPS stations in Montgomery county near The Woodlands shown in Figure 5-4-3 were analyzed along with the closest groundwater monitoring wells in the Chicot, Evangeline, and Jasper aquifers. GPS results show subsidence within The Woodlands area. Groundwater monitoring wells within the Chicot aquifer show that the water levels are mostly at equilibrium. The Evangeline aquifers show slight decreases in the water levels since 1999. On average, the water level declines over time around 20m to 30m. The Jasper monitoring wells near these GPS stations have severe declines since 1994 in the amount of about 100m over time. Results indicate that subsidence in this area are due to declines in both the Evangeline and Jasper aquifers.

GPS stations in Liberty county are plotted in figure 5-4-4s. These three GPS stations, CLVD, TXLI, and UHWL show very little to no subsidence occurring at these stations. 3 wells screened in the Chicot near these stations were plotted in Figure 5-4-4. These wells show very little change in the water levels overt time indicating that no compaction is occurring at these locations. 3 Evangeline wells were screen near these three GPS stations. Two of these wells have very little data, while the third is still being monitored. The water level has had little change over time indicating that subsidence is not occluding in this area because the water levels remain steady. There are no wells screened in the Jasper aquifer in Liberty county.

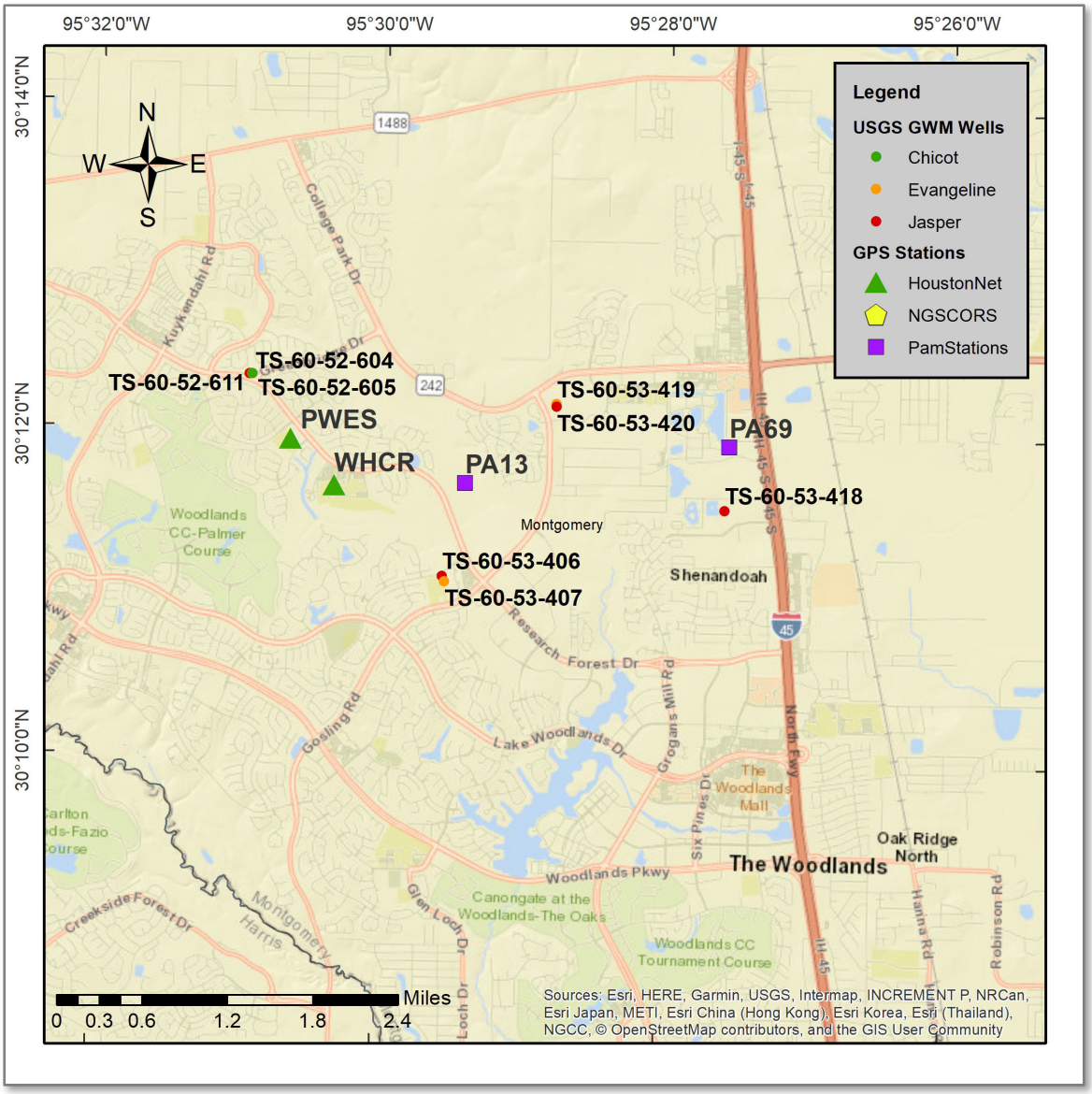

Figure 5-4-5 GPS Station Locations for PAM 69, WHCR, PAM 13, and PWES with USGS monitoring wells near GPS stations.

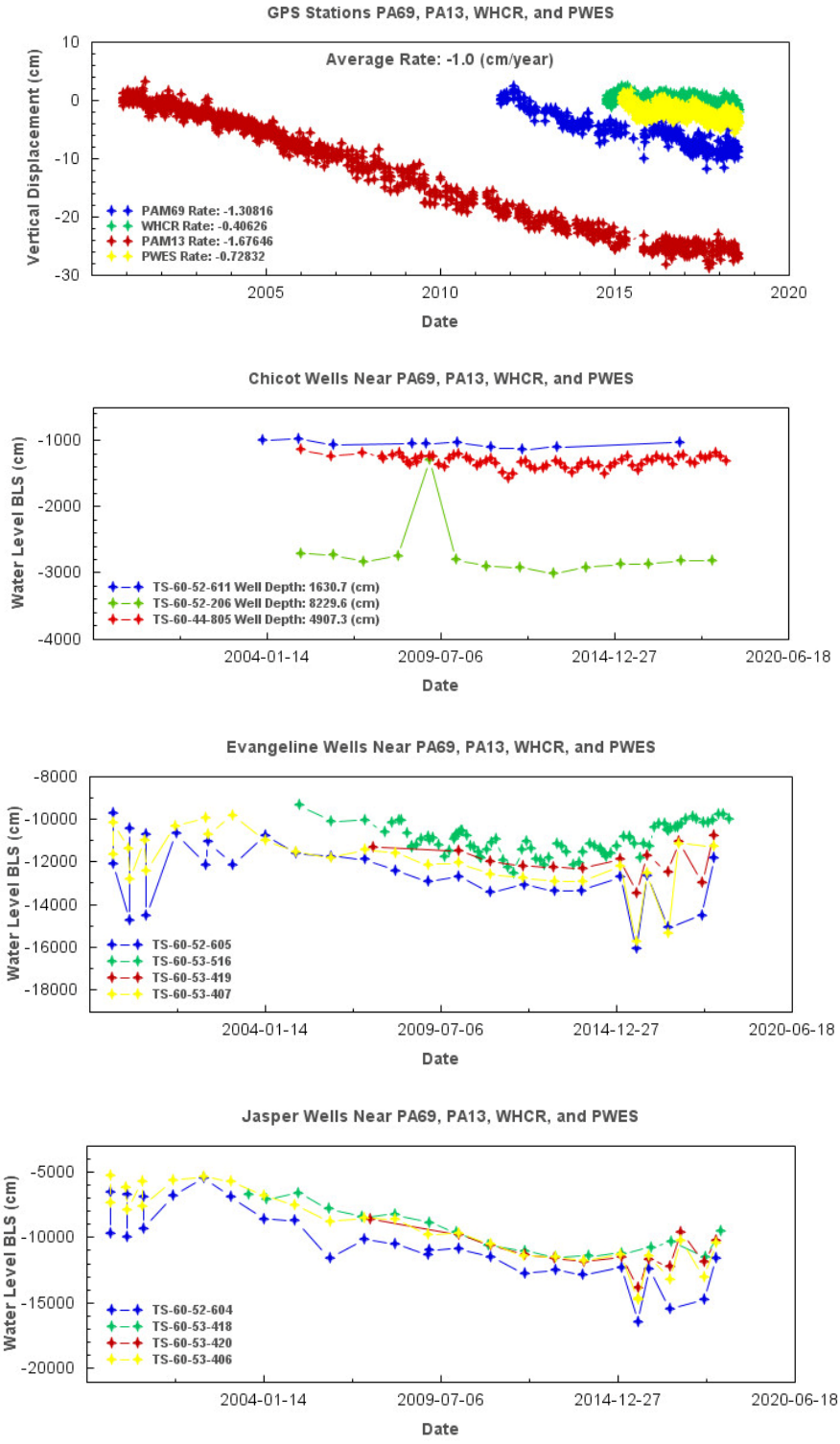

Figure 5-4-6 GPS Stations PAM 69, WHCR, PAM 13, and PWES with USGS Well Data. Chicot aquifer monitoring wells near PAM 69, Evangeline monitoring wells near PAM 69, and Jasper monitoring wells near PAM 69.

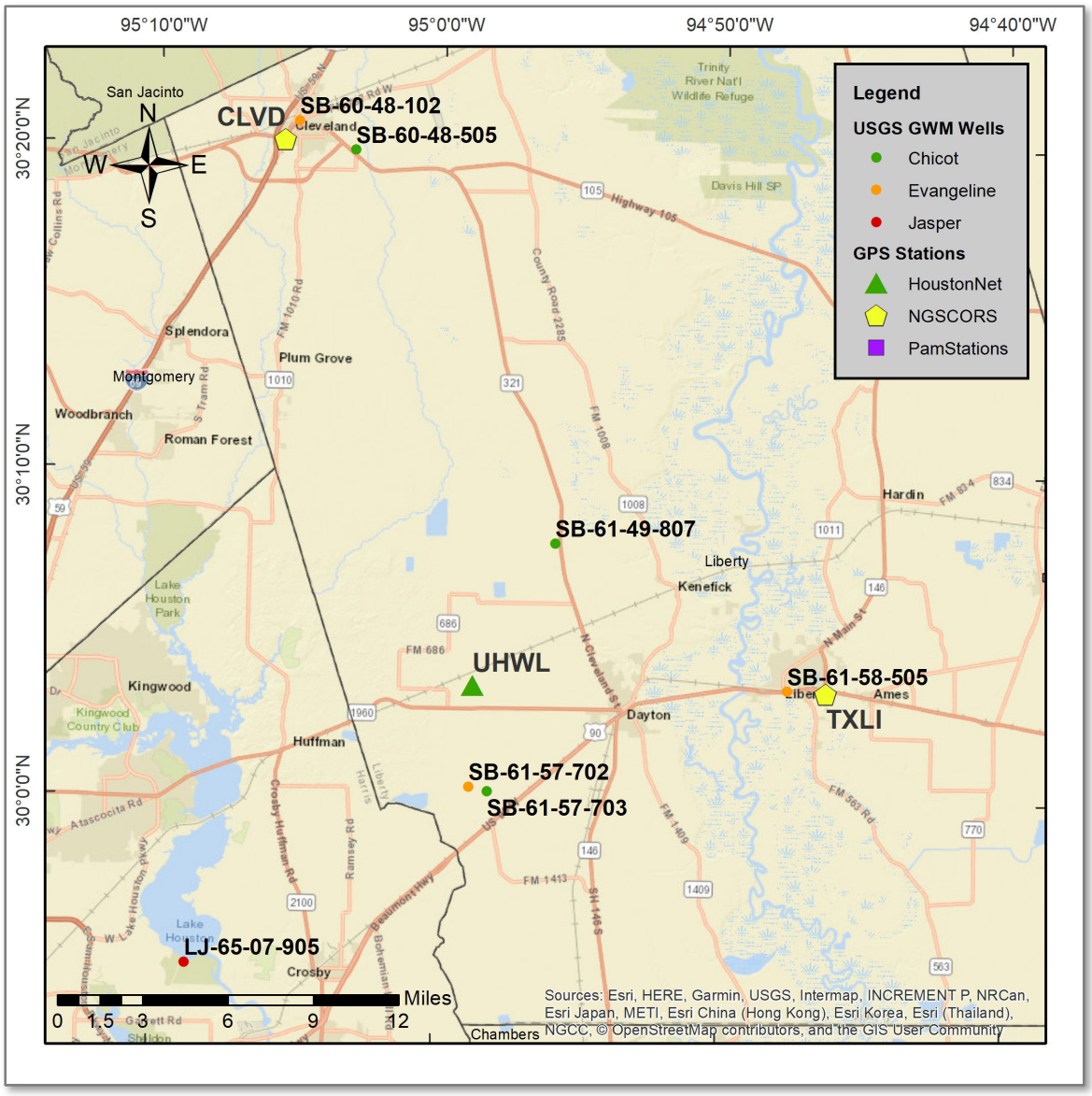

Figure 5-4-7 GPS Station Locations for CLVD, TXLI, and UHWL with USGS monitoring wells near GPS stations.

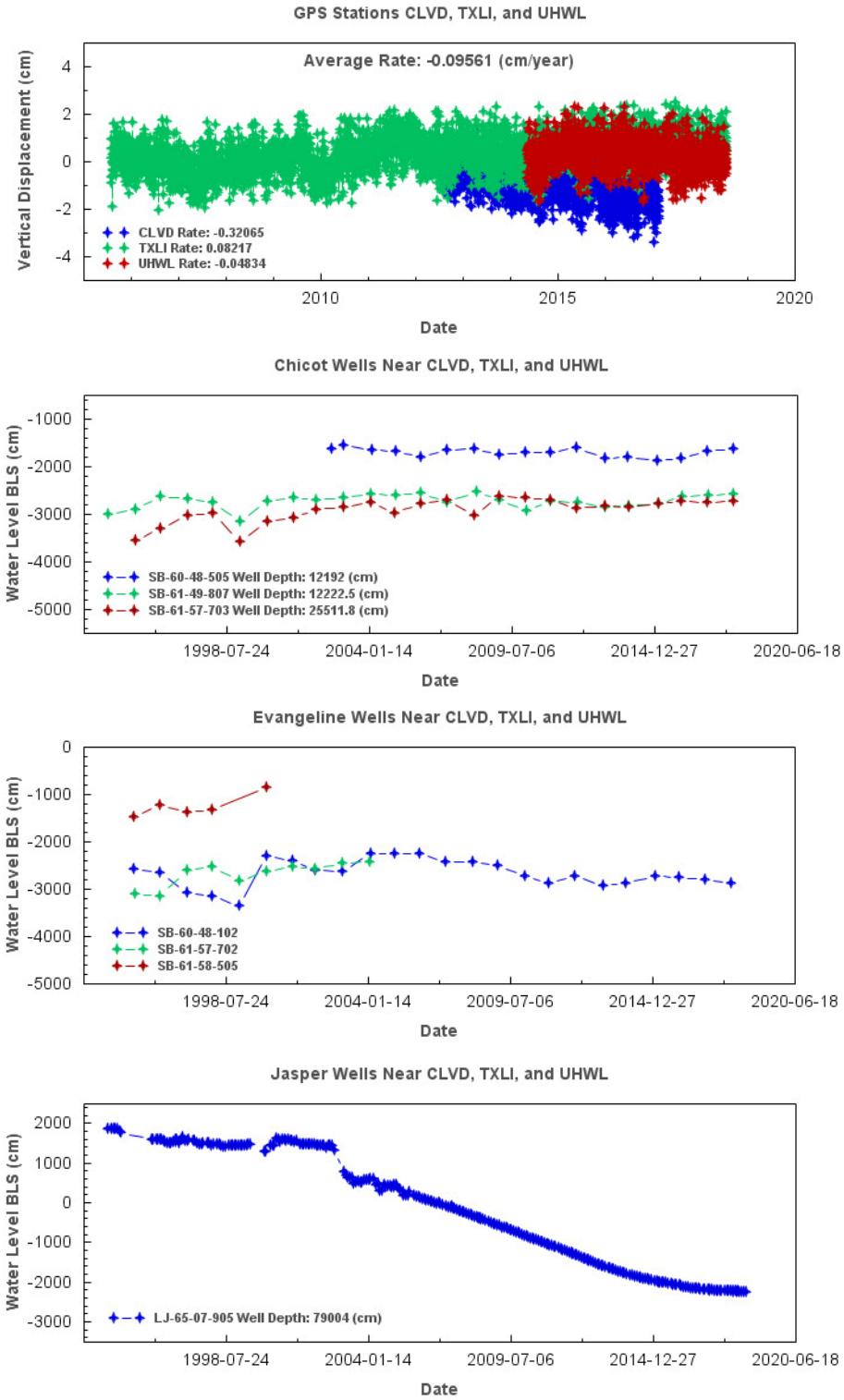

Figure 5-4-4 GPS Stations CLVD, TXLI, and UHWL with USGS Well Data. Chicot aquifer monitoring wells near CLVD, TXLI, and UHWL. Evangeline monitoring wells near CLVD, TXLI, and UHWL.

6 Conclusions

This study investigated land surface deformation related to groundwater withdrawal in Montgomery County, north Harris County, and Liberty County in Texas. GPS observations were processed and analyzed within Houston16 reference frame from 1994 through July 2018. There is spatial consistency in the results within areas near The Woodlands, Spring, and northwest Harris County. These areas are subsiding with a steady rate of approximately 2 cm/year. Groundwater levels with the Jasper aquifer mirror this trend with the hydraulic gradient decreasing over time.

Analysis of GPS observations, localized groundwater pumping patterns, and hydraulic head measurements were used to develop the following conclusions. Regional subsidence trends are driven by drawdown primarily within the Jasper aquifer followed by the Evangeline aquifer. Subsidence trends appear to be driven by increased groundwater pumping rates. As more water is needed for increased population growth in the area, more groundwater was pumped prior to regulations being put in place by both LSGCD and HGSD.

The results of this research would benefit from further testing of the horizontal components of the GPS stations data. The hydraulic characteristic of faulting in the Montgomery county area is still an area of academic debate; the author suggests further GPS studies are necessary to conclusively determine hydraulic characteristics and deformation trends across faults in the area. The results of this research can be used in managing regional groundwater use in relation to subsidence and can be extended to

understanding ground surface deformation of the Gulf Coast Aquifer System in other regions.

As population increases and the demand for water increases, the demand for groundwater also increases. The preconsolidation head for the HAGM model used in 2009 by Kasmarek were set to 70 ft. As the groundwater levels decline as a response to the increases in demand, the preconsolidation head will fall below 70 ft causing further subsidence in both counties. Local utility districts and cities have been and continue to work towards providing alternate water sources in order to prevent further subsidence. Water conservation education to the public is critical if everyone is to do their part in conserving the water resources we have and preventing further subsidence in our communities.

7 References

Anderson, J. B., and Rodriguez, A. B. (2001). The Episodic Evolution of Galveston Bay; Implications for Future Response to Global Change. *State of the Bay Symposium V* (pp. 125-131). Galveston, TX: Galveston Estuary Program.

Baker Jr, E. (1979). Stratigraphic and Hydrogeologic Framework of Part of the Coastal Plain of Texas. *USGS Open-File Report 77-712*.

Bar-Sever, Y. E., Kroger, P. M., and Borjesson, J. A. (1998). Estimating Horizontal Gradients of Tropospheric Path Delay with a Single GPS Receiver. *Journal of Geophysical Research*, 103(B3), 5019–5035.

Bawden, G. W., Johnson, M. R., Kasmarek, M. C., Brandt, J., and Middleton, C. S. (2012). Investigation of Land Subsidence in the Houston-Galveston Region of Texas by Using the Global Positioning System and Interferometric Synthetic Aperture Radar, 1993–2000. Denver, CO: *U.S. Geological Survey Scientific Investigations Report 2012–5211*.

Bird, D. E., K. Burke, S. A. Hall, and J. F. Casey. (2005). Gulf of Mexico tectonic history: Hotspot tracks, crustal boundaries, and early salt distribution. *AAPG bulletin*, 89.3, 311-328.

Blewitt, G. (1989). Carrier phase ambiguity resolution for the Global Positioning System applied to geodetic baselines up to 2000 km. *Journal of Geophysical Research: Solid Earth (1978–2012)*, *94*(B8), 10187-10203.

Blewitt, G., and Lavallée, D. (2002). Effect of annual signals on geodetic velocity. *Journal of Geophysical Research: Solid Earth*, 107(B7), ETG-9.

Buckley, S. M., Rosen, P., Hensley, S., and Taplay, B. D. (2003). Land subsidence in Houston, Texas, measured by radar interferometry and constrained by extensometers. *Geophysics Research*, 108(B11). doi:10.1029/2002JB001848

Burbey, T. J., Warner, S. M., Blewitt, G., Bell, J. W., and Hill, E. (2006). Three-dimensional deformation and strain induced by municipal pumping, part 1: Analysis of field data. *Journal of Hydrology*, *319*(1), 123-142.

Burrough, T. M. (2013). Spatial and Temporal Variability in Vertical Deformation in Willowbend, TX Derived from Long-Term GPS and Extensometer Observations. *Master's thesis*, University of Houston.

Burkett, V. R., Zilkoski, D. B., and Hart, D. A. (2002). Sea-Level Rise and Subsidence: Implications for Flooding in New Orleans, Louisiana. *Subsidence Interest Group Conference: Proceedings of the Technical Meeting. Galveston, TX*: U.S. Geological Survey.

Chrismer, M. (2018) Personal communication, September 7, 2018. Email correspondence.

Chowdhury, A. H., and Turco, M. J. (2006). Geology of the Gulf Coast aquifer, Texas. Texas Water Development Board Report 365. Retrieved 08 25 2018, from http://www.twdb.texas.gov/publications/reports/numbered_reports/doc/R365/ch02-Geology.pdf

Davis, J. L., Herring, T. A., Shapiro, I., Rogers, A., and Elgered, G. (1985). Geodesy by radio interferometry: Effects of Atmospheric Modeling Errors on Estimates of Baseline Length. *Radio Science*, 20(6), 1593-1607.

Dixon, T. H., and R. K. Dokka (2008), Earth Scientists and Public Policy: Have We Failed New Orleans?, *Eos Trans. AGU*, 89(10), 96–96.

Dokka, R. K., G. F. Sella, and T. H. Dixon. (2006). Tectonic control of subsidence and southward displacement of southeast Louisiana with respect to stable North America, *Geophysical Research Letters*, 33.

Eckl, M. C., Snay, R. A., Soler, T., Cline, M. W., and Mader, G. L. (2001). Accuracy of GPS-derived relative positions as a function of interstation distance and observing-session duration. *Journal of Geodesy*, 75(12), 633-640.

El-Rabbany, A. (2006). Introduction to GPS: The Global Positioning System 2nd Edition. Norwood: Artech House.

Engelkemeir, R. M., and Khan, S. D. (2008). Lidar Mapping of Faults in Houston, Texas, USA. *Geosphere*, 4(1), 170-182.

Engelkemeir, R., Khan, S. D., and Burke, K. (2010). Surface Deformation in Houston, Texas Using GPS. *Tectonophysics*, 490(1-2), 47-54.

Ewing, T. E. (1983). Growth Faults and Salt Tectonics in the Houston Diapir Province—Relation, Timing and Exploration Significance." *Gulf Coast Association of Geologists Society Transactions*, 33, 83-90.

Ewing, T. E. (1991). Structural framework. *The Gulf of Mexico Basin: Geological Society of America, The Geology of North America*, J, 31-52.

Fetter, C.W. (2001), Applied Hydrogeology. 4th Edition. Prentice-Hall, Upper Saddle Creek, NJ.

Fogg, G. E. (1986). Groundwater Flow and Sand Body Interconnectedness in a Thick, Multiple-Aquifer System, *Water Resources Research*, 22(5), 679–694.

Gabrysch, R. K. (1969). Land Surface Subsidence in the Houston-Galveston Region, Texas. Tokyo, Japan: *International Symposium on Land Subsidence*.

Gabrysch, R. K., and Bonnet, C. W. (1975). Land Surface Subsidence in the Houston-Galveston Region, Texas. Austin, TX: *Texas Water Development Board Report 188*.

Galloway, W. E. (2001). Cenozoic evolution of sediment accumulation in deltaic and shore-zone depositional systems, northern Gulf of Mexico Basin. *Marine and Petroleum Geology*, 18(10), 1031-1040.

Galloway, D. L., and Burbey, T. J. (2011). Review: Regional Land Subsidence Accompanying Groundwater Extraction. *Hydrogeology Journal*, 19, 1459 - 1486. doi:10.1007/s10040-011-0775-5

Galloway, D., Jones, D., and Ingebritsen, S. (1999). Land Subsidence in the United States. Denver, CO: U.S. Geological Survey Circular 1182.

González, J. L., and Tornqvist, T. E. (2006). Coastal Louisiana in Crisis: Subsidence or Sea Level Rise?. EOS, Transactions American Geophysical Union, 87(45), 493-498.

Grant, A. and Rodriguez, L. (2006). 5 years after Allison, is city safer from flooding?. Houston Chronicle, June 4, 2006. Accessed 04 21 2015 from http://www.chron.com /news/houston-texas/article/5-years-after-Allison-is-city-safer-from-1851965.php

HGSD (2013). Harris Galveston Subsidence District Regulatory Plan, accessed 10 13 2018 from: https://hgsubsidence.org/wp-content/uploads/2013/07/HGSD-2013-Regulatory-Plan-with-Amendment.pdf

HGSD (2018). Harris Galveston Subsidence District 2017 Annual Groundwater Report, accessed 10 13 2018 from: https://hgsubsidence.org/wp-content/uploads/2018/06/HG-GW-Report-2017-Board-Final.pdf

Holzer, T. L. (1984) Ground Failure Induced by Ground-water Withdrawal from Unconsolidated Sediments. *Reviews in Engineering Geology*, 6, 67-106.

Holzer, T. L., and R. K. Gabrysch. (1987). Effect of Water-Level Recoveries on Fault Creep, Houston, Texas. *Groundwater*, 25(4), 392-397.

Holzer, T. L., and A. I. Johnson. (1985). Land subsidence caused by ground water withdrawal in urban areas. *GeoJournal*, 11(3), 245-255.

Jorgensen, D. G. (1975). Analog-Model Studies of Groundwater Hydrology in the Houston District, Texas. Austin, TX: U.S. Geological Survey and the Texas Water Development Board.

Jurkowski, G., Ni, J., and Brown, L. (1984). Modern uparching of the Gulf coastal plain. Journal of Geophysical Research: Solid Earth (1978–2012), 89(B7), 6247-6255.

Kasmarek, M. C. (2012). Hydrogeology and Simulation of Groundwater Flow and Land-Surface Subsidence in the Northern Part of the Gulf Coast Aquifer System, Texas, 1891-2009. Denver, CO: U.S. Geological Survey Scientific Investigations Report 2012–5154.

Kasmarek, M. C., Johnson, M. R., and Ramage, J. K. (2014). Water-Level Altitudes 2013 and Water-Level Changes in the Chicot, Evangeline, and Jasper Aquifers and Compaction 1973–2013 in the Chicot and Evangeline Aquifers, Houston–Galveston Region, Texas. Denver, CO: *U.S. Geological Survey Scientific Investigations Map 3308*.

Kasmarek, M. C., and Strom, E. W. (2002). Hydrogeology and Simulation of Ground-Water Flow and Land-Surface Subsidence in the Chicot and Evangeline Aquifers, Houston Area, Texas. Austin, TX: U.S. Geological Survey Water-Resources Investigations Report 02–4022.

Kearns, T. J., Wang G., Turco M., Welch J., Tsibanos V., and Hanlin, L. (2018). Houston16: A stable geodetic reference frame for subsidence and faulting study in the Houston metropolitan area, Texas, U.S. *Geodesy &Geodynamics*

Kedar, S., Hajj, G. A., Wilson, B. D., and Heflin, M. B. (2003). The Effect of the Second Order GPS Ionospheric Correction on Receiver Positions. *Geophysical Research Letters*, 30(16), 1829. doi:10.1029/2003GL017639

Khan, S., Stewart, R., Otoum, M., Chang, L. (2013). A Geophysical Investigation of the active Hockley Fault System near Houston, Texas. Geophysics. Vol. 78(4):B177-B185.

Khan, S. D., Huang, Z., Karacay, A., 2014. Study of ground subsidence in northwest Harris county using GPS, LiDAR, and InSAR techniques. Natural Hazards, 73:1143-1173.

Kouba, J. (2002). The GPS Toolbox - ITRF Transformations. *GPS Solutions*, 5(3), 88-90.

Kreitler, C. W. (1977). Fault Control of Subsidence, Houston, Texas. *Groundwater*, 15.3, 203-214.

Kreitler, C. W., Guevera, E., Granata, G., and McKalips, D. (1977). Hydrogeology of Gulf Coast aquifers, Houston-Galveston area, Texas. *Gulf Coast Association of Geological Societies Transactions*, 27, 72-89.

Leake, S., and Prudic, D. (1991). Documentation of a Computer Program to Simulate Aquifer System Compaction using the Modular Finite-Difference Ground-Water Flow Model. Denver, CO: U.S. Geological Survey Techniques of Water-Resources Investigations Book 6 Chapter A2.

Loskot, C.L., Sandean, W., and Follert, C.R. (1982). Groundwater resources of Colorado, Lavaca, and Whatron counties, Texas: Texas Department of Water resources Report, 270. p. 33.

Matsuzaka, S. (2012, 05 24-25). Geodesy and Geodetic Reference Frame. Retrieved 10 14, 2018, from http://ggim.un.org/meetings/2012-Hangzhou/documents/session%203/Geodesy%20and%20Geodetic%20reference%20system.pdf.

Norman C, Howe RG (2011) Impact of active faults on land-based engineered structures in the gulf coastal zone. AAPG Annual Convention and Exhibition, Houston.

Ortega, J. A. (2013). Groundwater Withdrawal and Aquifer Compaction: A Case Study in Addicks, Texas. *Master's thesis*, University of Houston.

Paine, J. G. (1993). Subsidence of the Texas coast: inferences from historical and late Pleistocene sea levels. *Tectonophysics*. 222.3, 445-458.

Pearson, C., McCaffrey, R., Elliott, J. L., and Snay, R. (2010). HTDP 3.0: Software for Coping with the Coordinate Changes Associated with Crustal Motion. *Journal of Surveying Engineering*, 136(2), 80-90.

Pearson, C., and Snay, R. (2013). Introducing HTDP 3.1 to transform coordinates across time and spatial reference frames. *GPS solutions*, *17*(1), 1-15.

Pratt, W. E., and Johnson, D.W. (1926). Local subsidence of the Goose Creek oil field. *The Journal of Geology,* 577-590.

Ray, J., Rebischung, P., and Schmid, R. (2011). Dependence of IGS Products on the ITRF Datum. *Proceedings of IAG Commission 1 Symposium on Reference Frames for Applications in Geosciences*. Marne-la-Vallée, France.

Remondi, B. W. (1985). Global Positioning System Carrier Phase: Description and Use. *Bulletin of Geodesy*, 59, 361-377.

Rizos, C., Janssen, V., Roberts, C., and Grinter, T. (2012). Precise Point Positioning: Is the era of differential GNSS positioning drawing to an end? In: *Proceedings of FIG Working Week 2012*, 6-10 May 2012, Rome, Italy.

Shah, S. D., and Lanning-Rush, J. (2005). Principal Faults in the Houston Metropolitan Area. Denver, CO: *U.S. Geological Survey Scientific Investigations Map 2874*. Retrieved from http://pubs.usgs.gov/sim/2005/2874/

Soler, T., and Snay, R. A. (2004). Transforming Positions and Velocities between the International Terrestrial Reference Frame of 2000 and North American Datum of 1983. *Journal of Surveying Engineering*, 130(2), 49-55.

Taylor, C. J., and Alley, W. M.. (2001) Groundwater-Water Level Monitoring and the Importance of Long Term Water-Level Data. Denver, CO: U.S. Geological Survey Circular 1217.

Theis, C.V. (1940). The source for water derived from wells. *Civil Engineering, 10* (5), 277-280.

Trimble. (2010). NetR9 (version 4.15) GNSS Reference Receiver User Guide. Dayton, Ohio: *Trimble Navigation.*

U.S. Census Bureau. (2018). Texas Keeps Getting Bigger. Retrieved 08 26, 2018, from https://www.census.gov/library/visualizations/2018/comm/popest-texas.html

Van Siclen, D. C. (1968). The Houston Fault Problem. Dallas, TX: American Institute of Professional Geologists, Texas Section.

Verbeek, E. R., and Clanton, U. S. (1981). Historically active faults in the Houston metropolitan area, Texas. *Houston Area Environmental Geology: Surface Faulting, Ground Subsidence, Hazard Liability*, p 28-68.

Wang, G. Q. (2013). Millimeter-accuracy GPS landslide monitoring using Precise Point Positioning with Single Receiver Phase Ambiguity (PPP-SRPA) resolution: a case study in Puerto Rico. *Journal of Geodetic Science,* 3(1), 22-31.

Wang, G., Yu, J., Ortega, J. Saenz, G., Burrough, T., and Neill, R. (2013). A Stable Reference Frame for Ground Deformation Study in the Houston Metropolitan Area, TX. *Journal of Geodetic Science. 3(3).* DOI: 10.2478/jogs-2013-0021

Wang, G. and Soler, T. (2013). Using OPUS for measuring vertical displacements in Houston, Texas. *Journal of Surveying Engineering.* 139(3), 126-134.

Wang, G. and Soler, T. (2014). Measuring Land Subsidence Using GPS: Ellipsoid Height versus Orthometric Height. Journal of Surveying Engineering, 05014004.

Wang, G. Turco M., Soler T., Kearns T., and Welch, J. (2017). Comparisons of OPUS and PPP solutions for subsidence monitoring in the greater Houston area. Surv. Eng. 143(4), 05017005

Wesselman, J. B. (1972). Ground-water resources of Fort Bend County, Texas. *Texas Water Development Board Report 155*.

Winker, Charles D. (1982). Cenozoic Shelf Margins, Northwestern Gulf of Mexico. *Gulf Coast Association of Geological Societies Transactions*, 32, 427-448.

Winslow, A.G., and W.W. Doyle. (1954). Land-surface subsidence and its relation to the withdrawal of ground water in the Houston-Galveston region, Texas. *Economic Geology*, 49(4), 413-422.

Yerkes, R.F., Castle, R.O., 1969. Surface deformation associated with oil and gas field operation in the United States. In: Tison, L.J. (Ed.), Land Subsidence 1, Vol. 88. 1st International Association of Scientific Hydrology Publication, Wallingford, pp. 55–64.

Young. S. C., J. Pinkard, R. L. Basset, and Chowdhury, A. (2014) Hydrochemical evaluation of the Texas Gulf Coast Aquifer System and implication for developing groundwater availability model: Report prepared by *INTERA, Inc. for the Texas Water Development Board*, Austin.

Zilkoski, D. B., Hall, L. W., Mitchell, G. J., Kammula, V., Singh, A., Chrismer, W. M., and Neighbors, R. J. (2001). The Harris-Galveston Coastal Subsidence District/ National Geodetic Survey Automated GPS Subsidence Monitoring Project. Galveston: *U.S. Geological Survey Subsidence Interest Group Conference*.

8 Appendix I: Groundwater Levels

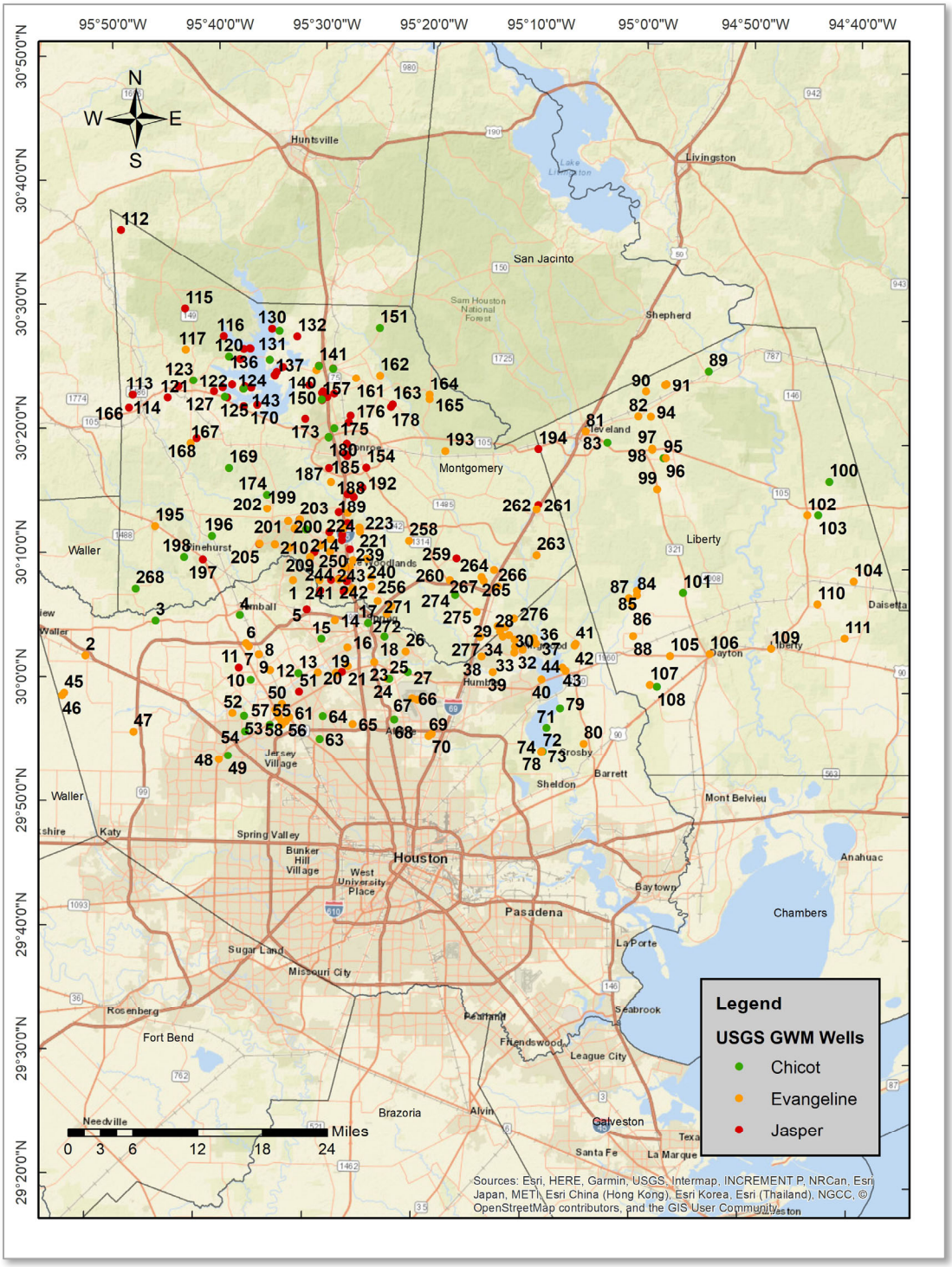

USGS Ground Water Monitoring Wells in Harris, Montgomery, and Liberty Counties - Chicot, Evangeline, and Jasper Aquifers

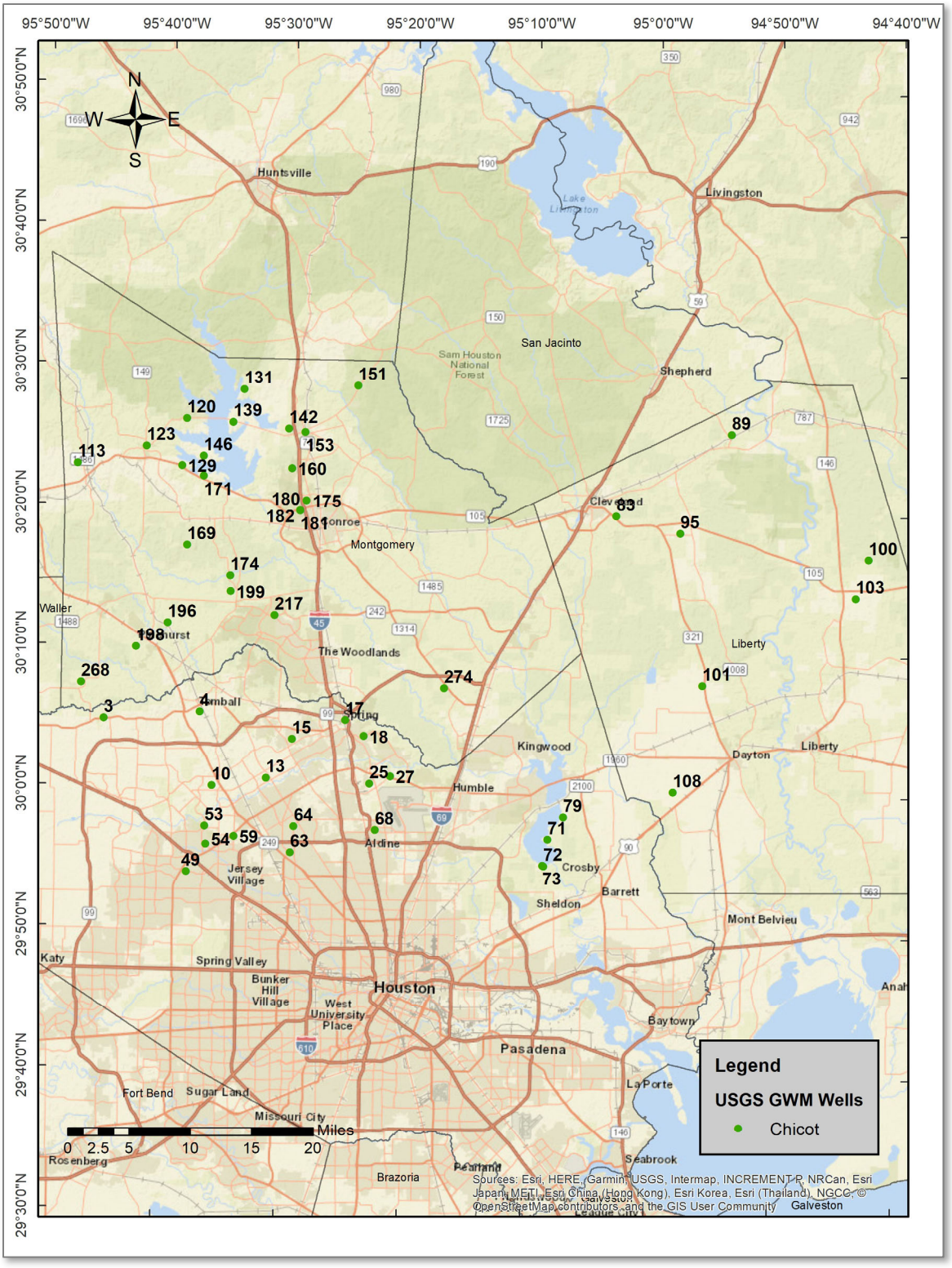

USGS Ground Water Monitoring Wells - Chicot Aquifer

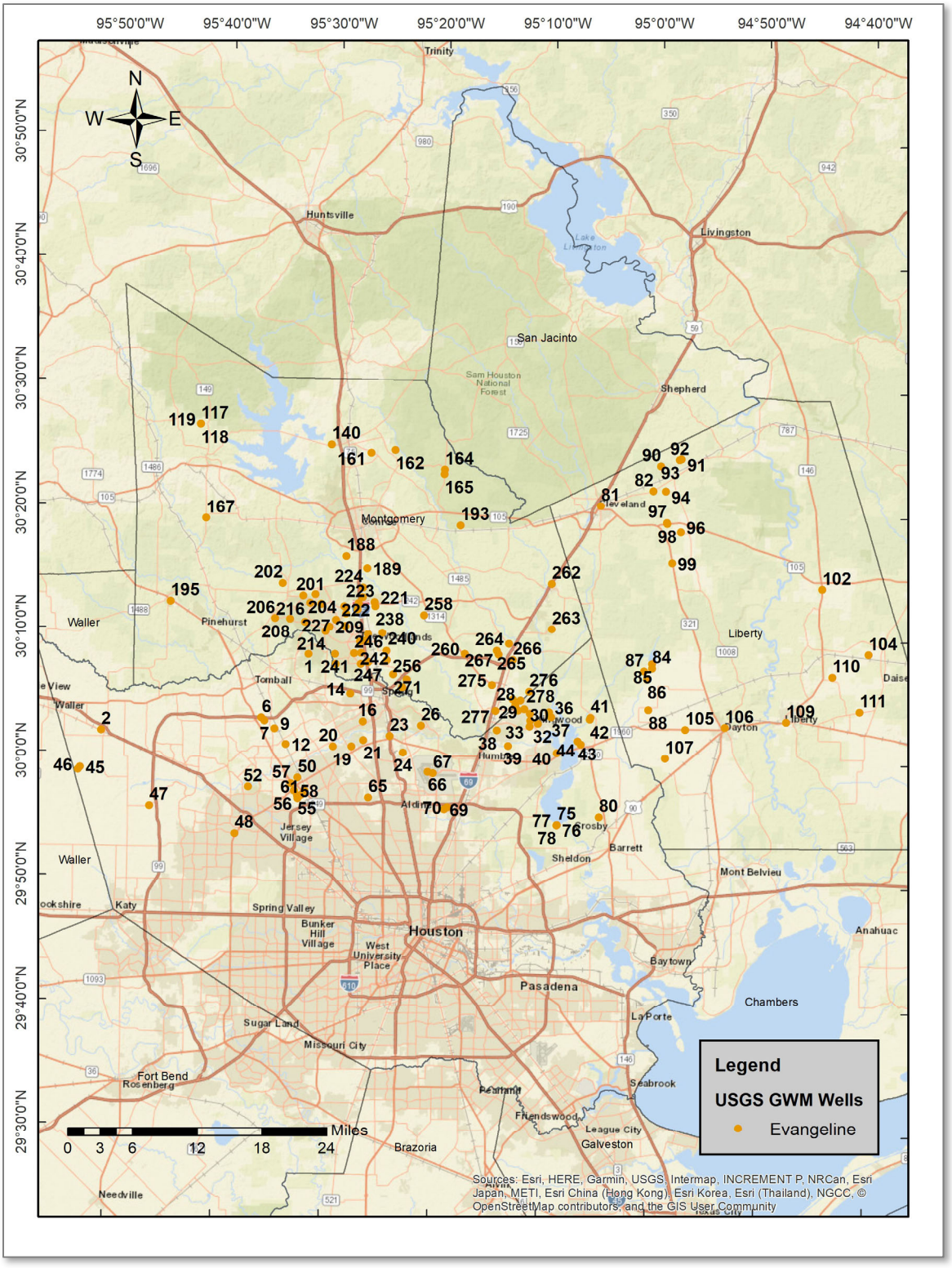

USGS Ground Water Monitoring Wells - Evangeline Aquifer

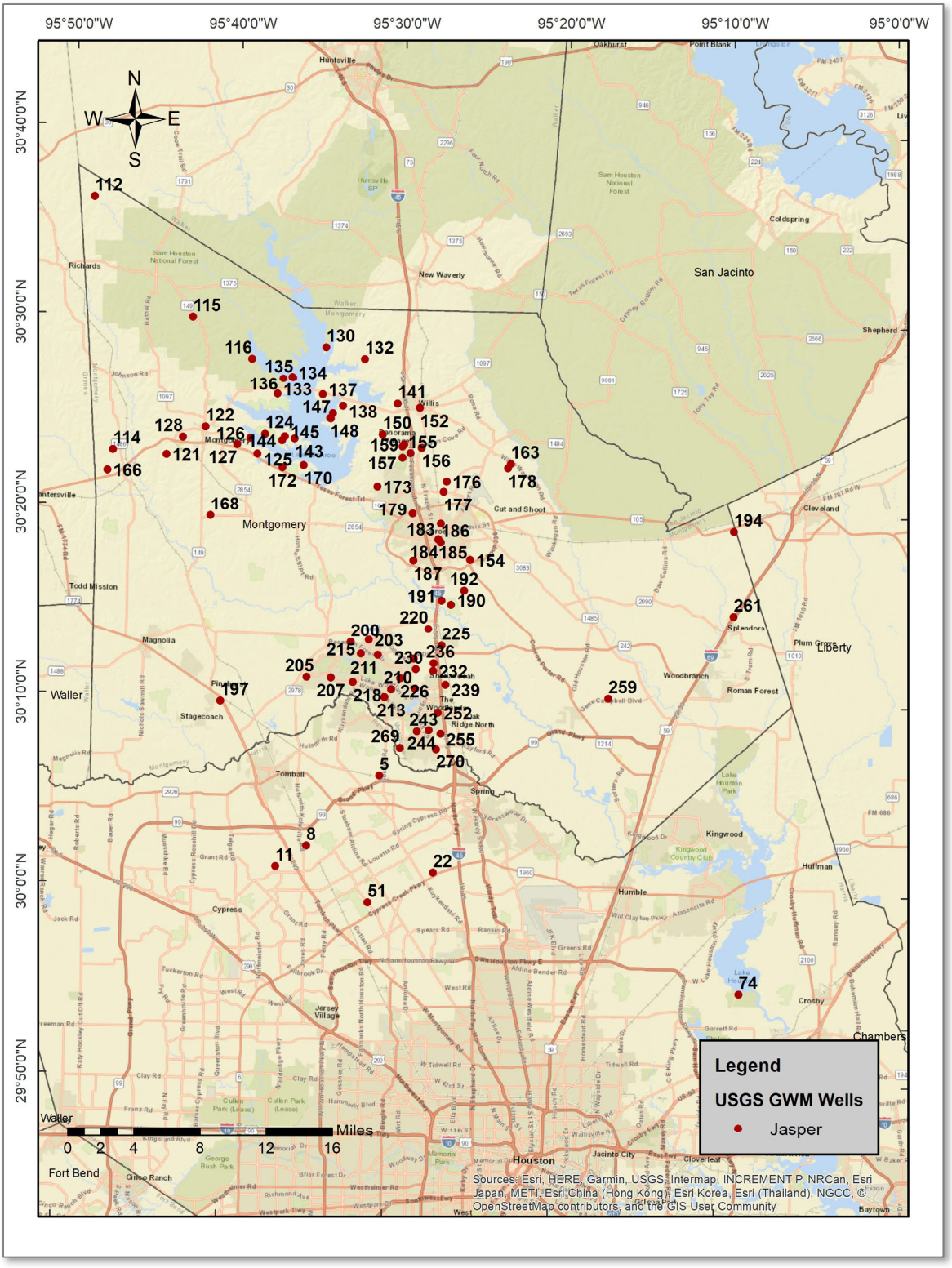

USGS Ground Water Monitoring Wells - Jasper Aquifer

USGS Ground Water Monitoring Well List (Page 1 of 5)

ID	SiteID	SiteName	GeoLat	GeoLong	County	Aquifer	Well Depth (cm)	Water Level Rate (cm/year)
1	300819095315501	LJ-60-52-903	30.13750	-95.53333	Harris	Evangeline	28803.6	29.13
2	300146095510402	LJ-60-58-711	30.02972	-95.85139	Harris	Evangeline	10119.4	-11.90
3	300447095444101	LJ-60-59-405	30.07972	-95.74472	Harris	Chicot	9205.0	-4.09
4	300521095365101	LJ-60-60-103	30.08944	-95.61444	Harris	Chicot	12557.8	-29.03
5	300556095304102	LJ-60-60-306	30.09917	-95.51167	Harris	Jasper	49133.8	-403.00
6	300301095361301	LJ-60-60-406	30.05083	-95.60417	Harris	Evangeline	16154.4	-63.52
7	300249095355701	LJ-60-60-407	30.04694	-95.59944	Harris	Evangeline	16764.0	132.92
8	300211095350101	LJ-60-60-408	30.03667	-95.58361	Harris	Jasper	55961.3	-313.99
9	300211095350102	LJ-60-60-409	30.03667	-95.58361	Harris	Evangeline	18288.0	-106.09
10	300007095354701	LJ-60-60-712	30.00194	-95.59583	Harris	Chicot	9296.4	-2.87
11	300104095365101	LJ-60-60-715	30.01806	-95.61444	Harris	Jasper	55534.6	-241.19
12	300056095335601	LJ-60-60-804	30.01583	-95.56583	Harris	Evangeline	29321.8	98.18
13	300044095312001	LJ-60-60-925	30.01222	-95.52222	Harris	Chicot	2017.8	-6.19
14	300507095280201	LJ-60-61-101	30.08556	-95.46750	Harris	Evangeline	30480.0	17.26
15	300333095291701	LJ-60-61-417	30.05917	-95.48806	Harris	Chicot	2545.1	-19.36
16	300251095265401	LJ-60-61-528	30.04861	-95.44750	Harris	Evangeline	32735.5	-65.10
17	300457095245801	LJ-60-61-601	30.08278	-95.41639	Harris	Chicot	6858.0	-7.81
18	300351095232601	LJ-60-61-621	30.06417	-95.39056	Harris	Chicot	1173.5	-16.63
19	300050095275301	LJ-60-61-713	30.01417	-95.46444	Harris	Evangeline	35509.2	115.40
20	300053095292601	LJ-60-61-728	30.01389	-95.49250	Harris	Evangeline	35966.4	161.03
21	300123095264501	LJ-60-61-826	30.02333	-95.44611	Harris	Evangeline	31394.4	83.62
22	300054095271801	LJ-60-61-841	30.01528	-95.45528	Harris	Jasper	66934.1	-295.25
23	300146095241801	LJ-60-61-905	30.02972	-95.40528	Harris	Evangeline	17068.8	18.36
24	300018095225701	LJ-60-61-914	30.00750	-95.38444	Harris	Evangeline	30175.2	32.43
25	300026095225401	LJ-60-61-919	30.00750	-95.38167	Harris	Chicot	1021.1	-5.21
26	300239095212601	LJ-60-62-401	30.04444	-95.35750	Harris	Evangeline	22098.0	11.89
27	300101095211301	LJ-60-62-716	30.01694	-95.35361	Harris	Chicot	10546.1	13.99
28	300426095123902	LJ-60-63-407	30.07389	-95.21250	Harris	Evangeline	25207.0	-16.17
29	300403095125402	LJ-60-63-502	30.08222	-95.21639	Harris	Evangeline	25572.7	-22.57
30	300408095115201	LJ-60-63-503	30.06917	-95.19833	Harris	Evangeline	32308.8	19.12
31	300334095113401	LJ-60-63-504	30.06306	-95.18944	Harris	Evangeline	33528.0	-37.97
32	300248095105301	LJ-60-63-505	30.05000	-95.17694	Harris	Evangeline	34625.3	10.66
33	300231095113701	LJ-60-63-508	30.04583	-95.18972	Harris	Evangeline	27980.6	-8.79
34	300359095122902	LJ-60-63-510	30.06694	-95.20806	Harris	Evangeline	25359.4	-17.20
35	300302095113301	LJ-60-63-511	30.05389	-95.18861	Harris	Evangeline	31821.1	12.04
36	300355095093501	LJ-60-63-602	30.06556	-95.16000	Harris	Evangeline	35356.8	-94.83
37	300331095092201	LJ-60-63-603	30.05889	-95.15639	Harris	Evangeline	27432.0	-104.05
38	300223095143001	LJ-60-63-712	30.03972	-95.24000	Harris	Evangeline	30845.8	-2.83
39	300111095132302	LJ-60-63-714	30.01917	-95.22250	Harris	Evangeline	20299.7	-22.78
40	300037095084802	LJ-60-63-904	30.01056	-95.14694	Harris	Evangeline	36728.4	-17.91
41	300332095054301	LJ-60-64-406	30.05917	-95.09556	Harris	Evangeline	31455.4	-11.34
42	300321095060201	LJ-60-64-407	30.05667	-95.09667	Harris	Evangeline	30906.7	-29.12
43	300133095065101	LJ-60-64-713	30.02694	-95.11500	Harris	Evangeline	30784.8	-53.54
44	300122095063601	LJ-60-64-715	30.02278	-95.11000	Harris	Evangeline	32918.4	-15.37
45	295840095525901	LJ-65-01-301	29.97861	-95.88250	Harris	Evangeline	20726.4	-2.25
46	295831095530801	LJ-65-01-302	29.97556	-95.88583	Harris	Evangeline	30693.4	8.71
47	295544095462401	LJ-65-02-603	29.92889	-95.77417	Harris	Evangeline	29504.6	-6.99
48	295339095383201	LJ-65-03-907	29.89417	-95.64194	Harris	Evangeline	30175.2	84.97
49	295358095374101	LJ-65-03-919	29.89944	-95.62806	Harris	Chicot	1021.1	0.84
50	295754095324901	LJ-65-04-218	29.97056	-95.54667	Harris	Evangeline	25115.5	77.76
51	295915095311501	LJ-65-04-320	29.98750	-95.52083	Harris	Jasper	63276.5	-291.41
52	295722095372001	LJ-65-04-423	29.95694	-95.62222	Harris	Evangeline	27279.6	55.99
53	295714095361701	LJ-65-04-424	29.95389	-95.60472	Harris	Chicot	1417.3	3.27
54	295557095360901	LJ-65-04-425	29.93250	-95.60250	Harris	Chicot	868.7	-10.50
55	295646095324601	LJ-65-04-514	29.94639	-95.54639	Harris	Evangeline	23530.6	27.92
56	295633095324401	LJ-65-04-515	29.94278	-95.54583	Harris	Evangeline	21427.4	35.36
57	295723095340201	LJ-65-04-522	29.96278	-95.55667	Harris	Evangeline	31089.6	67.76
58	295711095330201	LJ-65-04-526	29.95306	-95.55111	Harris	Evangeline	22250.4	96.61
59	295633095335201	LJ-65-04-532	29.94250	-95.56444	Harris	Chicot	1249.7	-7.38
60	295650095322301	LJ-65-04-612	29.94750	-95.54028	Harris	Evangeline	20513.0	63.62
61	295704095320301	LJ-65-04-614	29.95250	-95.53500	Harris	Evangeline	24231.6	77.71
62	295705095320201	LJ-65-04-615	29.95306	-95.53500	Harris	Evangeline	23896.3	104.68
63	295522095291902	LJ-65-05-404	29.92472	-95.48750	Harris	Chicot	13898.9	42.59

USGS Ground Water Monitoring Well List (Page 2 of 5)

ID	SiteID	SiteName	GeoLat	GeoLong	County	Aquifer	Well Depth (cm)	Water Level Rate (cm/year)
64	295720095290001	LJ-65-05-414	29.95556	-95.48333	Harris	Chicot	868.7	-2.48
65	295644095261001	LJ-65-05-517	29.94583	-95.43667	Harris	Evangeline	32004.0	105.04
66	295855095204301	LJ-65-06-102	29.98194	-95.34556	Harris	Evangeline	46939.2	60.21
67	295850095201301	LJ-65-06-103	29.98028	-95.33750	Harris	Evangeline	47091.6	43.10
68	295711095222301	LJ-65-06-425	29.95306	-95.37306	Harris	Chicot	1021.1	1.15
69	295553095191201	LJ-65-06-528	29.93194	-95.31944	Harris	Evangeline	51206.4	88.93
70	295605095184701	LJ-65-06-530	29.93472	-95.31444	Harris	Evangeline	33771.8	68.77
71	295651095083501	LJ-65-07-601	29.94556	-95.13806	Harris	Chicot	15605.8	55.28
72	295449095083401	LJ-65-07-902	29.91389	-95.14306	Harris	Chicot	5974.1	19.40
73	295451095083901	LJ-65-07-904	29.91444	-95.14444	Harris	Chicot	16459.2	28.73
74	295449095084101	LJ-65-07-905	29.91389	-95.14500	Harris	Jasper	79004.2	-200.50
75	295449095084102	LJ-65-07-906	29.91389	-95.14500	Harris	Evangeline	45811.4	43.36
76	295449095084103	LJ-65-07-907	29.91389	-95.14500	Harris	Evangeline	21305.5	63.25
77	295449095084104	LJ-65-07-908	29.91389	-95.14500	Harris	Evangeline	31943.0	55.53
78	295449095084105	LJ-65-07-909	29.91322	-95.14553	Harris	Evangeline	59131.2	5.50
79	295817095065501	LJ-65-08-103	29.97222	-95.11750	Harris	Chicot	16916.4	19.28
80	295529095043501	LJ-65-08-506	29.92506	-95.08019	Harris	Evangeline	29748.5	44.02
81	302040095050701	SB-60-48-102	30.34472	-95.08556	Liberty	Evangeline	25755.6	-2.81
82	302156095001501	SB-60-48-302	30.36611	-95.00444	Liberty	Evangeline	13777.0	-5.97
83	301948095030701	SB-60-48-505	30.33028	-95.05222	Liberty	Chicot	12192.0	-8.44
84	300736095000701	SB-60-56-901	30.12667	-95.00194	Liberty	Evangeline	30937.2	8.68
85	300756095000601	SB-60-56-902	30.13250	-95.00194	Liberty	Evangeline	31699.2	-1.07
86	300641095003101	SB-60-64-301	30.11194	-95.00889	Liberty	Evangeline	30662.9	10.93
87	300720095005201	SB-60-64-303	30.12250	-95.01417	Liberty	Evangeline	17678.4	16.95
88	300413095002201	SB-60-64-602	30.07083	-95.00667	Liberty	Evangeline	30998.2	15.23
89	302542094534701	SB-61-33-601	30.42861	-94.89667	Liberty	Chicot	4267.2	22.32
90	302353094593701	SB-61-33-701	30.39944	-94.99361	Liberty	Evangeline	25450.8	6.02
91	302434094574101	SB-61-33-710	30.40944	-94.96167	Liberty	Evangeline	11125.2	46.47
92	302429094575101	SB-61-33-712	30.40833	-94.96417	Liberty	Evangeline	8747.8	42.44
93	302422094563403	SB-61-33-806	30.40833	-94.96417	Liberty	Evangeline	11277.6	48.81
94	302154094590701	SB-61-41-101	30.36583	-94.98528	Liberty	Evangeline	15301.0	5.63
95	301839094575201	SB-61-41-407	30.31111	-94.96472	Liberty	Chicot	10576.6	-13.97
96	301840094574501	SB-61-41-409	30.31111	-94.96111	Liberty	Evangeline	14295.1	-8.63
97	301924094585601	SB-61-41-410	30.32361	-94.98250	Liberty	Evangeline	15941.0	-10.44
98	301938094585501	SB-61-41-411	30.32194	-94.98222	Liberty	Evangeline	16154.4	-0.93
99	301608094582401	SB-61-41-701	30.26917	-94.97361	Liberty	Evangeline	19111.0	28.73
100	301658094493001	SB-61-43-801	30.28306	-94.70722	Liberty	Chicot	3048.0	1.69
101	300748094554501	SB-61-49-807	30.13083	-94.93111	Liberty	Chicot	12222.5	5.74
102	301408094442201	SB-61-51-101	30.23694	-94.74056	Liberty	Evangeline	35052.0	-0.74
103	301411094432601	SB-61-51-102	30.23722	-94.72417	Liberty	Chicot	20116.8	-2.43
104	300857094400101	SB-61-51-806	30.14944	-94.66722	Liberty	Evangeline	19019.5	-10.92
105	300242094565701	SB-61-57-506	30.04500	-94.94917	Liberty	Evangeline	28651.2	14.28
106	300254094531801	SB-61-57-611	30.04861	-94.88806	Liberty	Evangeline	40050.7	-9.44
107	300020094584601	SB-61-57-702	30.00583	-94.97972	Liberty	Evangeline	24384.0	68.82
108	300013094580901	SB-61-57-703	30.00361	-94.96889	Liberty	Chicot	25511.8	26.33
109	300324094473501	SB-61-58-505	30.05694	-94.79333	Liberty	Evangeline	19842.5	99.74
110	300705094432101	SB-61-59-106	30.11833	-94.72278	Liberty	Evangeline	14782.8	127.48
111	300417094404801	SB-61-59-501	30.07222	-94.68000	Liberty	Evangeline	35966.4	23.40
112	303610095484501	TS-60-26-208	30.60278	-95.81306	Montgomery	Jasper	5242.6	-13.40
113	302251095471801	TS-60-34-905	30.38089	-95.78838	Montgomery	Chicot	79461.4	-127.50
114	302252095471701	TS-60-34-906	30.38102	-95.78815	Montgomery	Jasper	0.0	40.76
115	302948095422501	TS-60-35-202	30.49883	-95.71061	Montgomery	Jasper	3261.4	-7.80
116	302747095385901	TS-60-35-303	30.46306	-95.64972	Montgomery	Jasper	10607.0	-27.45
117	302636095422801	TS-60-35-503	30.44361	-95.70806	Montgomery	Evangeline	3596.6	-2.76
118	302636095422802	TS-60-35-504	30.44361	-95.70806	Montgomery	Evangeline	2529.8	-5.78
119	302636095422803	TS-60-35-505	30.44361	-95.70806	Montgomery	Evangeline	1828.8	-2.55
120	302609095382601	TS-60-35-604	30.43583	-95.64056	Montgomery	Chicot	75377.0	-155.38
121	302240095440101	TS-60-35-703	30.37806	-95.73389	Montgomery	Jasper	23256.2	-147.33
122	302409095414301	TS-60-35-813	30.40250	-95.69528	Montgomery	Jasper	20269.2	-22.52
123	302409095414201	TS-60-35-814	30.40250	-95.69500	Montgomery	Chicot	0.0	-9.41
124	302350095380401	TS-60-35-908	30.39750	-95.63472	Montgomery	Jasper	15087.6	-155.40
125	302247095383001	TS-60-35-909	30.38000	-95.64194	Montgomery	Jasper	19751.0	-91.38
126	302339095384501	TS-60-35-910	30.39361	-95.64944	Montgomery	Jasper	19507.2	-152.90

USGS Ground Water Monitoring Well List (Page 3 of 5)

ID	SiteID	SiteName	GeoLat	GeoLong	County	Aquifer	Well Depth (cm)	Water Level Rate (cm/year)
127	302309095393301	TS-60-35-911	30.38806	-95.66278	Montgomery	Jasper	22616.2	-197.39
128	302324095391201	TS-60-35-912	30.39333	-95.71778	Montgomery	Jasper	17526.0	-122.15
129	302251095384501	TS-60-35-915	30.38083	-95.64583	Montgomery	Chicot	81716.9	-168.71
130	302828095342801	TS-60-36-207	30.47472	-95.57472	Montgomery	Jasper	14325.6	-128.07
131	302818095334801	TS-60-36-211	30.47179	-95.56331	Montgomery	Chicot	64373.8	-109.97
132	302753095320601	TS-60-36-305	30.46500	-95.53528	Montgomery	Jasper	14569.4	-138.01
133	302557095372201	TS-60-36-409	30.43278	-95.62306	Montgomery	Jasper	18440.4	-117.84
134	302651095362901	TS-60-36-410	30.44778	-95.60833	Montgomery	Jasper	14234.2	-130.16
135	302650095362701	TS-60-36-412	30.44722	-95.60750	Montgomery	Jasper	20787.4	-102.01
136	302647095370301	TS-60-36-413	30.44639	-95.61750	Montgomery	Jasper	13746.5	-97.58
137	302558095343701	TS-60-36-505	30.43306	-95.57722	Montgomery	Jasper	19507.2	-74.64
138	302523095332301	TS-60-36-509	30.42333	-95.55667	Montgomery	Jasper	19873.0	-114.81
139	302558095343801	TS-60-36-514	30.43281	-95.57717	Montgomery	Chicot	53279.0	-145.33
140	302511095300001	TS-60-36-611	30.42028	-95.50472	Montgomery	Evangeline	10241.3	-23.43
141	302535095300401	TS-60-36-612	30.42639	-95.50111	Montgomery	Jasper	29992.3	-152.55
142	302534095300401	TS-60-36-615	30.42611	-95.50111	Montgomery	Chicot	81838.8	-238.01
143	302338095361601	TS-60-36-705	30.39417	-95.60472	Montgomery	Jasper	22860.0	-209.93
144	302331095370201	TS-60-36-706	30.39222	-95.61750	Montgomery	Jasper	22860.0	-104.67
145	302344095365301	TS-60-36-709	30.39556	-95.61472	Montgomery	Jasper	23012.4	-22.40
146	302332095370001	TS-60-36-710	30.39222	-95.61667	Montgomery	Chicot	81686.4	-222.71
147	302444095340501	TS-60-36-809	30.41222	-95.56861	Montgomery	Jasper	22555.2	-162.89
148	302444095340802	TS-60-36-810	30.41250	-95.56917	Montgomery	Jasper	22372.3	-174.74
149	302459095335801	TS-60-36-812	30.41667	-95.56639	Montgomery	Jasper	17708.9	-153.85
150	302356095305501	TS-60-36-908	30.39917	-95.51556	Montgomery	Jasper	32766.0	53.94
151	302844095242901	TS-60-37-315	30.47889	-95.40806	Montgomery	Chicot	69342.0	26.60
152	302522095284202	TS-60-37-402	30.42306	-95.47861	Montgomery	Jasper	27797.8	-114.58
153	302522095284301	TS-60-37-418	30.42278	-95.47861	Montgomery	Chicot	89611.2	-208.19
154	302608095234301	TS-60-37-603	30.29083	-95.42444	Montgomery	Jasper	45720.0	-312.25
155	302320095294201	TS-60-37-711	30.38917	-95.49528	Montgomery	Jasper	33314.6	-193.48
156	302318095283401	TS-60-37-714	30.38833	-95.47611	Montgomery	Jasper	34503.4	-218.79
157	302221095294201	TS-60-37-715	30.37944	-95.49528	Montgomery	Jasper	33619.4	-104.23
158	302300095291301	TS-60-37-716	30.38361	-95.48722	Montgomery	Jasper	26883.4	-318.51
159	302327095293601	TS-60-37-717	30.39111	-95.49361	Montgomery	Jasper	33223.2	-170.12
160	302248095294401	TS-60-37-718	30.38000	-95.49556	Montgomery	Chicot	86380.3	-269.28
161	302436095263501	TS-60-37-806	30.41000	-95.44306	Montgomery	Evangeline	10668.0	188.09
162	302452095242001	TS-60-37-909	30.41472	-95.40583	Montgomery	Evangeline	15697.2	-18.11
163	302233095230701	TS-60-37-911	30.37583	-95.38528	Montgomery	Jasper	32186.9	-101.40
164	302323095194201	TS-60-38-806	30.38972	-95.32833	Montgomery	Evangeline	18288.0	-179.08
165	302301095194301	TS-60-38-807	30.38361	-95.32861	Montgomery	Evangeline	17373.6	-58.46
166	302145095473901	TS-60-42-206	30.36333	-95.79361	Montgomery	Jasper	23164.8	-153.87
167	301904095414801	TS-60-43-511	30.31806	-95.69667	Montgomery	Evangeline	11856.7	-55.01
168	301917095413101	TS-60-43-514	30.32500	-95.68806	Montgomery	Jasper	32004.0	-194.04
169	301711095381201	TS-60-43-902	30.28639	-95.63667	Montgomery	Chicot	3657.6	-1.29
170	302216095354201	TS-60-44-122	30.37111	-95.59500	Montgomery	Jasper	26578.6	-78.30
171	302208095365702	TS-60-44-124	30.36889	-95.61583	Montgomery	Chicot	79461.4	-121.91
172	302208095365901	TS-60-44-125	30.36875	-95.61628	Montgomery	Jasper	31485.8	119.95
173	302111095311101	TS-60-44-318	30.35389	-95.52000	Montgomery	Jasper	36088.3	-227.38
174	301505095343702	TS-60-44-805	30.25139	-95.57694	Montgomery	Chicot	4907.3	-5.50
175	302032095283001	TS-60-45-122	30.34222	-95.47500	Montgomery	Chicot	78821.3	-67.64
176	302138095265501	TS-60-45-213	30.35944	-95.45000	Montgomery	Jasper	38404.8	-144.62
177	302102095271001	TS-60-45-214	30.35056	-95.45278	Montgomery	Jasper	39319.2	420.74
178	302220095231701	TS-60-45-304	30.37222	-95.38806	Montgomery	Jasper	32613.6	-99.27
179	301948095290101	TS-60-45-402	30.33028	-95.48361	Montgomery	Jasper	42458.6	-289.04
180	301948095290002	TS-60-45-412	30.33028	-95.48361	Montgomery	Chicot	7955.3	-9.96
181	301948095290003	TS-60-45-413	30.33000	-95.48361	Montgomery	Chicot	3337.6	-5.08
182	301948095290004	TS-60-45-414	30.33028	-95.48361	Montgomery	Chicot	2438.4	-5.37
183	301918095271901	TS-60-45-501	30.32194	-95.45500	Montgomery	Jasper	39014.4	-307.21
184	301829095272401	TS-60-45-503	30.30833	-95.45694	Montgomery	Jasper	40599.4	-376.53
185	301828095272404	TS-60-45-504	30.30806	-95.45694	Montgomery	Jasper	37216.1	-206.00
186	301819095271501	TS-60-45-507	30.30556	-95.45444	Montgomery	Jasper	39014.4	-336.71
187	301720095285601	TS-60-45-712	30.28917	-95.48194	Montgomery	Jasper	37947.6	-280.55
188	301614095284201	TS-60-45-716	30.27056	-95.47833	Montgomery	Evangeline	21640.8	-93.41
189	301516095264301	TS-60-45-805	30.25472	-95.44556	Montgomery	Evangeline	21397.0	-201.15

USGS Ground Water Monitoring Well List (Page 4 of 5)

ID	SiteID	SiteName	GeoLat	GeoLong	County	Aquifer	Well Depth (cm)	Water Level Rate (cm/year)
190	301503095263301	TS-60-45-812	30.25111	-95.44278	Montgomery	Jasper	38404.8	-288.45
191	301516095270801	TS-60-45-813	30.25472	-95.45250	Montgomery	Jasper	39928.8	-378.08
192	301550095254701	TS-60-45-814	30.26389	-95.42972	Montgomery	Jasper	38892.5	-272.22
193	301853095180701	TS-60-46-505	30.31500	-95.30222	Montgomery	Evangeline	10515.6	-0.99
194	301911095092901	TS-60-47-602	30.32000	-95.15833	Montgomery	Jasper	37002.7	-165.55
195	301218095445401	TS-60-51-409	30.20528	-95.74861	Montgomery	Evangeline	20177.8	-126.18
196	301139095393801	TS-60-51-603	30.19417	-95.66056	Montgomery	Chicot	6705.6	-8.66
197	300943095402501	TS-60-51-815	30.16222	-95.67389	Montgomery	Jasper	50109.1	-259.33
198	300954095421101	TS-60-51-816	30.16500	-95.70306	Montgomery	Chicot	6400.8	-17.87
199	301358095343301	TS-60-52-206	30.23278	-95.57583	Montgomery	Chicot	8229.6	-26.02
200	301258095323501	TS-60-52-209	30.21639	-95.54333	Montgomery	Jasper	50535.8	-389.36
201	301258095323502	TS-60-52-210	30.21639	-95.54333	Montgomery	Evangeline	29748.5	-159.47
202	301358095343302	TS-60-52-212	30.23278	-95.57583	Montgomery	Evangeline	30601.9	-255.92
203	301309095313101	TS-60-52-306	30.21861	-95.52528	Montgomery	Jasper	48585.1	-298.32
204	301309095313001	TS-60-52-307	30.21889	-95.52472	Montgomery	Evangeline	27127.2	-173.68
205	301105095351401	TS-60-52-409	30.18472	-95.58722	Montgomery	Jasper	46512.5	-216.98
206	301106095351101	TS-60-52-410	30.18500	-95.58639	Montgomery	Evangeline	27889.2	-101.02
207	301103095334301	TS-60-52-501	30.18472	-95.56278	Montgomery	Jasper	49682.4	-352.20
208	301103095334302	TS-60-52-502	30.18472	-95.56306	Montgomery	Evangeline	27614.9	-170.70
209	301033095300602	TS-60-52-602	30.17528	-95.50194	Montgomery	Evangeline	31394.4	-65.10
210	301033095300601	TS-60-52-603	30.17556	-95.50167	Montgomery	Jasper	50292.0	-268.36
211	301220095305501	TS-60-52-604	30.20556	-95.51556	Montgomery	Jasper	49682.4	-375.72
212	301220095305502	TS-60-52-605	30.20556	-95.51528	Montgomery	Evangeline	32430.7	-133.33
213	301008095303001	TS-60-52-606	30.16861	-95.50806	Montgomery	Jasper	51206.4	-329.06
214	301007095303001	TS-60-52-607	30.16889	-95.50806	Montgomery	Evangeline	32065.0	-65.26
215	301225095315901	TS-60-52-608	30.20639	-95.53278	Montgomery	Jasper	51023.5	-230.94
216	301225095315902	TS-60-52-609	30.20667	-95.53278	Montgomery	Evangeline	34137.6	-183.17
217	301220095305503	TS-60-52-611	30.20556	-95.51528	Montgomery	Chicot	1630.7	-6.40
218	301051095322401	TS-60-52-612	30.18111	-95.54028	Montgomery	Jasper	47670.7	-376.58
219	301051095322402	TS-60-52-613	30.18083	-95.54000	Montgomery	Evangeline	29291.3	-112.52
220	301346095275401	TS-60-53-111	30.22944	-95.46528	Montgomery	Jasper	47914.6	-149.89
221	301234095255801	TS-60-53-208	30.20944	-95.43306	Montgomery	Evangeline	24993.6	-108.62
222	301256095270401	TS-60-53-209	30.21583	-95.45139	Montgomery	Evangeline	30480.0	-227.61
223	301234095255802	TS-60-53-215	30.20944	-95.43278	Montgomery	Evangeline	7802.9	-101.09
224	301345095270501	TS-60-53-216	30.22917	-95.45139	Montgomery	Evangeline	0.0	-160.28
225	301254095270301	TS-60-53-217	30.21500	-95.45139	Montgomery	Jasper	48310.8	-268.52
226	301107095293001	TS-60-53-406	30.18528	-95.49250	Montgomery	Jasper	49377.6	-377.88
227	301108095293201	TS-60-53-407	30.18472	-95.49222	Montgomery	Evangeline	30632.4	-121.11
228	301034095283801	TS-60-53-408	30.17639	-95.47722	Montgomery	Jasper	49987.2	-339.46
229	301034095283802	TS-60-53-409	30.17639	-95.47722	Montgomery	Evangeline	30480.0	-70.13
230	301135095290101	TS-60-53-416	30.19361	-95.47694	Montgomery	Jasper	50474.9	-391.67
231	301135095290102	TS-60-53-417	30.19361	-95.47667	Montgomery	Evangeline	33345.1	-121.90
232	301133095273401	TS-60-53-418	30.19250	-95.45944	Montgomery	Jasper	51511.2	-306.04
233	301211095284601	TS-60-53-419	30.20306	-95.47944	Montgomery	Evangeline	29047.4	-38.24
234	301210095284601	TS-60-53-420	30.20278	-95.47944	Montgomery	Jasper	49621.4	-209.75
235	301157095273301	TS-60-53-421	30.19944	-95.45917	Montgomery	Evangeline	29199.8	-124.01
236	301157095273302	TS-60-53-422	30.19917	-95.45917	Montgomery	Jasper	51267.4	-173.59
237	301228095272501	TS-60-53-516	30.20778	-95.45750	Montgomery	Evangeline	24597.4	44.17
238	301215095255401	TS-60-53-517	30.20417	-95.43167	Montgomery	Evangeline	8077.2	-6.33
239	301050095264801	TS-60-53-519	30.18056	-95.44667	Montgomery	Jasper	50627.3	-84.74
240	301002095251401	TS-60-53-520	30.16806	-95.42028	Montgomery	Evangeline	10972.8	-20.29
241	300811095291702	TS-60-53-708	30.13822	-95.49244	Montgomery	Evangeline	35966.4	-216.16
242	300816095274701	TS-60-53-709	30.14000	-95.46278	Montgomery	Evangeline	28773.1	-64.39
243	300820095282801	TS-60-53-712	30.13917	-95.47472	Montgomery	Jasper	51450.2	-236.03
244	300823095275001	TS-60-53-713	30.14056	-95.46278	Montgomery	Jasper	52120.8	-349.31
245	300732095292101	TS-60-53-715	30.12481	-95.49133	Montgomery	Evangeline	26517.6	-101.91
246	300824095274701	TS-60-53-718	30.14000	-95.46306	Montgomery	Evangeline	7498.1	34.80
247	300740095262701	TS-60-53-813	30.12806	-95.44111	Montgomery	Evangeline	30358.1	-52.82
248	300925095264501	TS-60-53-814	30.15722	-95.44611	Montgomery	Evangeline	30784.8	-103.86
249	300741095262601	TS-60-53-820	30.12833	-95.44083	Montgomery	Evangeline	15240.0	43.72
250	300956095263001	TS-60-53-826	30.16583	-95.44194	Montgomery	Evangeline	30906.7	-170.04
251	300826095270801	TS-60-53-827	30.14056	-95.45222	Montgomery	Evangeline	17373.6	4.33
252	300920095271401	TS-60-53-829	30.15583	-95.45389	Montgomery	Jasper	51389.3	-307.29

USGS Ground Water Monitoring Well List (Page 5 of 5)

ID	SiteID	SiteName	GeoLat	GeoLong	County	Aquifer	Well Depth (cm)	Water Level Rate (cm/year)
253	300920095271402	TS-60-53-830	30.15611	-95.45417	Montgomery	Evangeline	31242.0	-98.78
254	300731095270701	TS-60-53-831	30.12556	-95.45222	Montgomery	Evangeline	27736.8	-88.97
255	300815095270301	TS-60-53-832	30.13750	-95.45083	Montgomery	Jasper	52364.6	-382.26
256	300742095244301	TS-60-53-902	30.13139	-95.41222	Montgomery	Evangeline	12954.0	21.29
257	300838095244701	TS-60-53-903	30.14389	-95.41306	Montgomery	Evangeline	17007.8	-47.41
258	301136095212101	TS-60-54-406	30.19333	-95.35583	Montgomery	Evangeline	14081.8	-34.62
259	301016095165501	TS-60-54-613	30.17111	-95.28194	Montgomery	Jasper	52943.8	-341.48
260	300831095173401	TS-60-54-804	30.14222	-95.29167	Montgomery	Evangeline	17068.8	-10.22
261	301443095091801	TS-60-55-313	30.24536	-95.15706	Montgomery	Jasper	49956.7	-276.95
262	301420095093201	TS-60-55-315	30.23889	-95.15944	Montgomery	Evangeline	13411.2	-70.25
263	301039095092901	TS-60-55-605	30.17750	-95.15806	Montgomery	Evangeline	40081.2	-198.77
264	300925095132501	TS-60-55-708	30.15694	-95.22361	Montgomery	Evangeline	18897.6	-79.50
265	300849095143301	TS-60-55-710	30.14694	-95.24250	Montgomery	Evangeline	18288.0	-19.46
266	300806095130201	TS-60-55-712	30.13500	-95.21722	Montgomery	Evangeline	20116.8	-108.24
267	300831095142101	TS-60-55-714	30.14194	-95.23944	Montgomery	Evangeline	0.0	-140.12
268	300717095463601	TS-60-58-303	30.12139	-95.77667	Montgomery	Chicot	6217.9	-18.17
269	300728095292901	TS-60-61-104	30.12444	-95.49139	Montgomery	Jasper	53675.3	-395.26
270	300726095271801	TS-60-61-214	30.12389	-95.45500	Montgomery	Jasper	18958.6	155.54
271	300637095240801	TS-60-61-307	30.11222	-95.40194	Montgomery	Evangeline	15422.9	33.87
272	300544095231501	TS-60-61-308	30.09556	-95.38750	Montgomery	Evangeline	36027.4	-235.46
273	300621095225201	TS-60-61-309	30.10583	-95.38111	Montgomery	Evangeline	32491.7	-241.05
274	300720095165701	TS-60-62-305	30.12250	-95.28278	Montgomery	Chicot	8686.8	-4.81
275	300602095145501	TS-60-63-109	30.10083	-95.24889	Montgomery	Evangeline	23469.6	-21.52
276	300534095112801	TS-60-63-205	30.09278	-95.19111	Montgomery	Evangeline	27432.0	-32.11
277	300258095145301	TS-60-63-404	30.06611	-95.24278	Montgomery	Evangeline	31882.1	-11.42
278	300446095121901	TS-60-63-507	30.08083	-95.20444	Montgomery	Evangeline	36271.2	18.74

USGS Ground Water Monitoring Wells Harris County

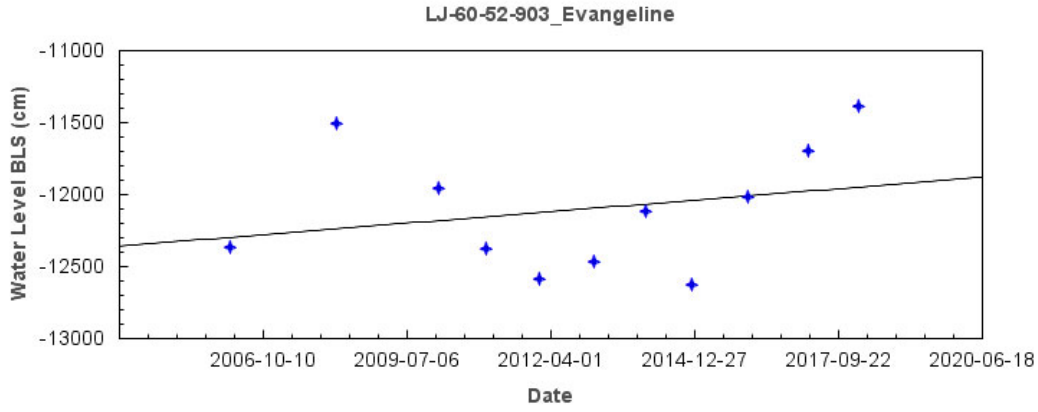

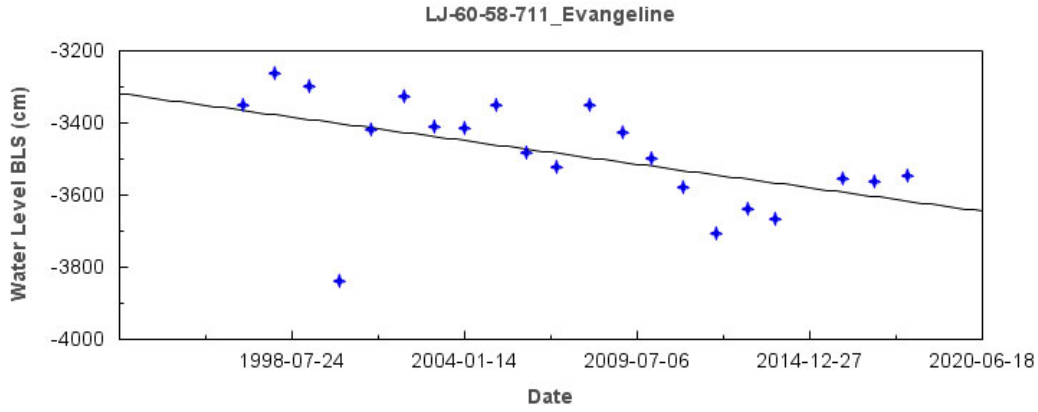

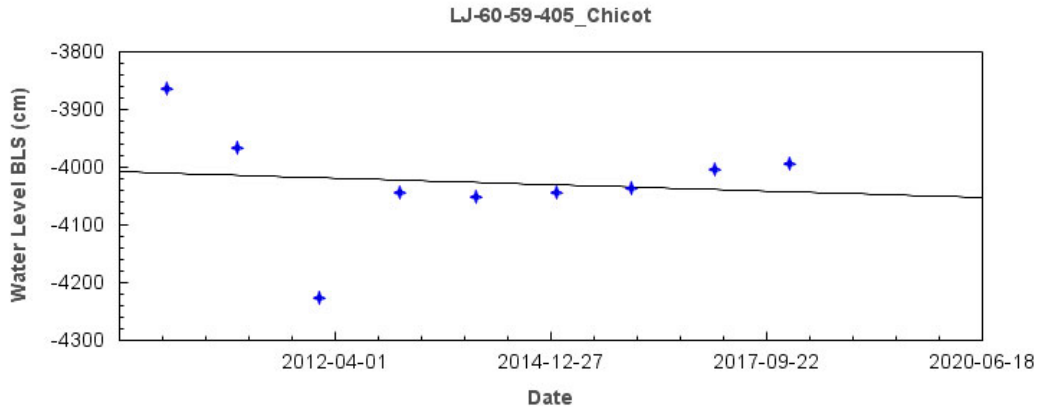

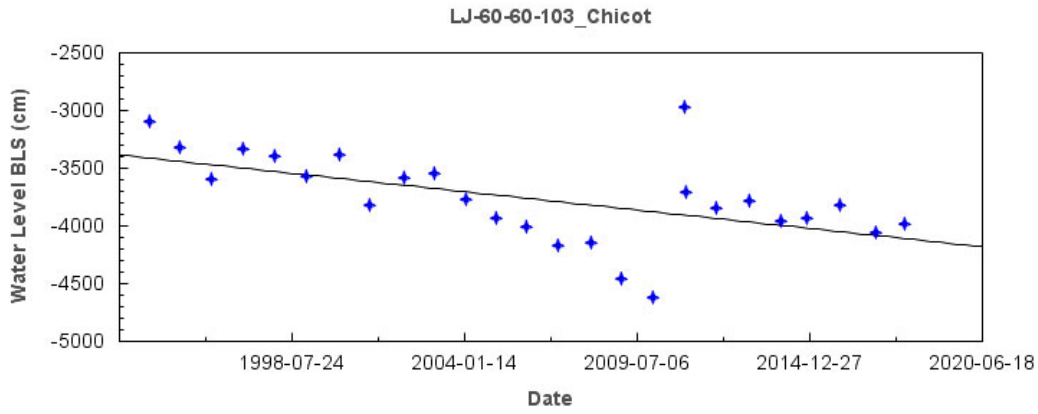
LJ-60-60-103_Chicot
Water Level BLS (cm)
-2500
-3000
-3500
-4000
-4500
-5000
1998-07-24
2004-01-14
2009-07-06
2014-12-27
2020-06-18
Date

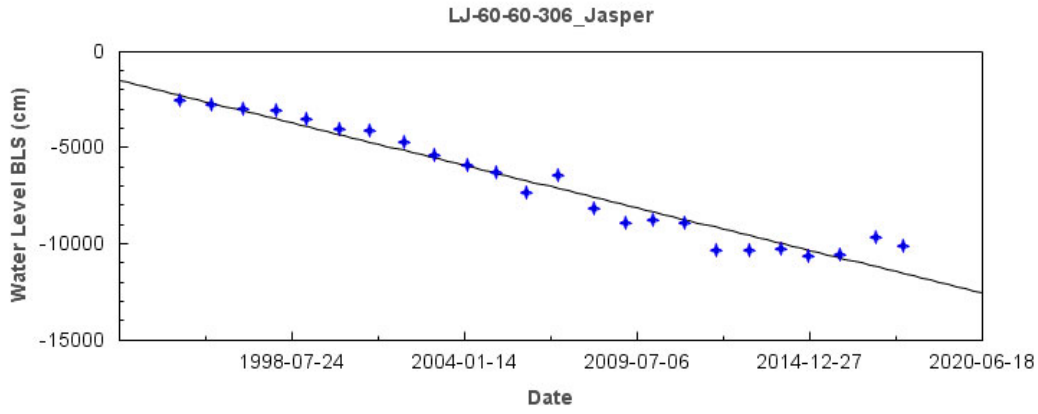
LJ-60-60-306_Jasper
Water Level BLS (cm)
0
-5000
-10000
-15000
1998-07-24
2004-01-14
2009-07-06
2014-12-27
2020-06-18
Date

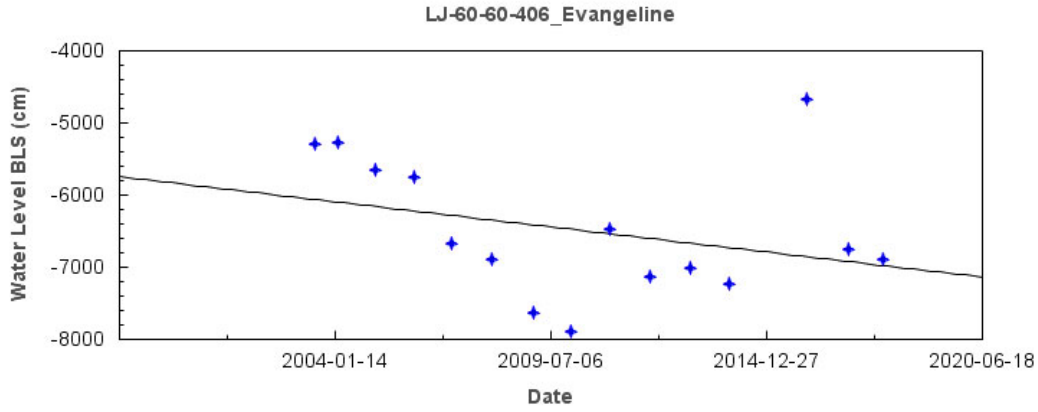
LJ-60-60-406_Evangeline
Water Level BLS (cm)
-4000
-5000
-6000
-7000
-8000
2004-01-14
2009-07-06
2014-12-27
2020-06-18
Date

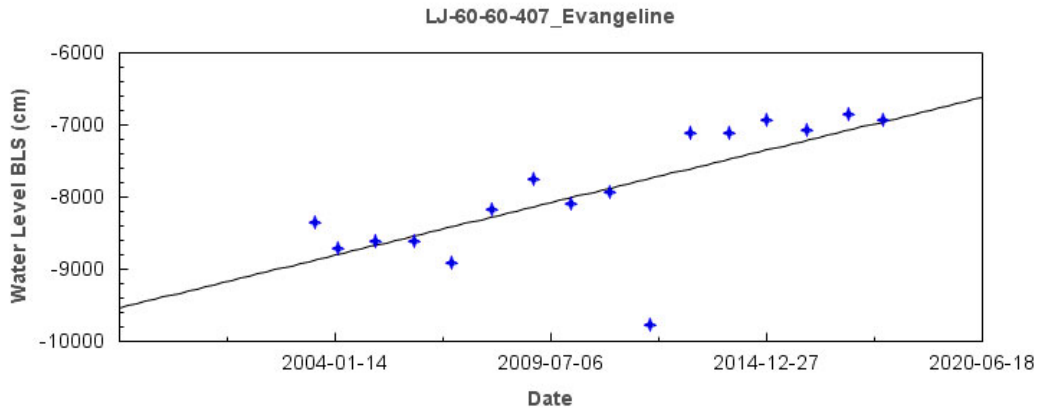
LJ-60-60-407_Evangeline
Water Level BLS (cm)
-6000
-7000
-8000
-9000
-10000
2004-01-14
2009-07-06
2014-12-27
2020-06-18
Date

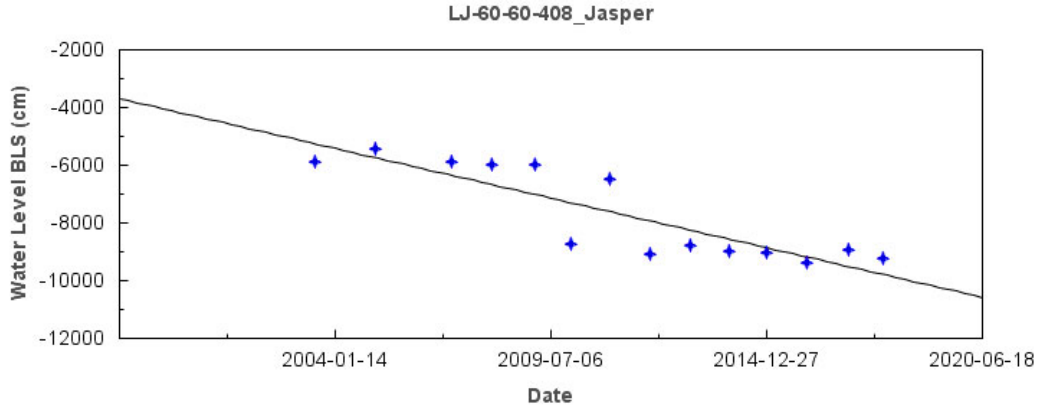
LJ-60-60-408_Jasper
Water Level BLS (cm)
-2000
-4000
-6000
-8000
-10000
-12000
2004-01-14
2009-07-06
2014-12-27
2020-06-18
Date

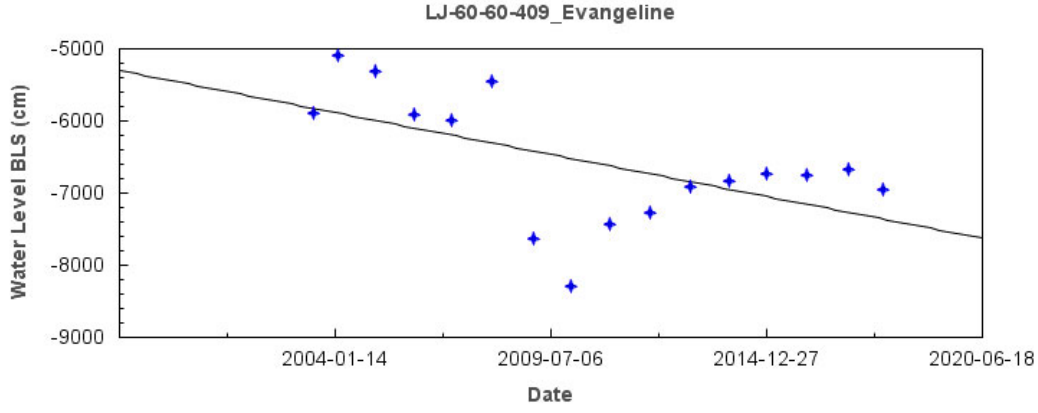
LJ-60-60-409_Evangeline
Water Level BLS (cm)
-5000
-6000
-7000
-8000
-9000
2004-01-14
2009-07-06
2014-12-27
2020-06-18
Date

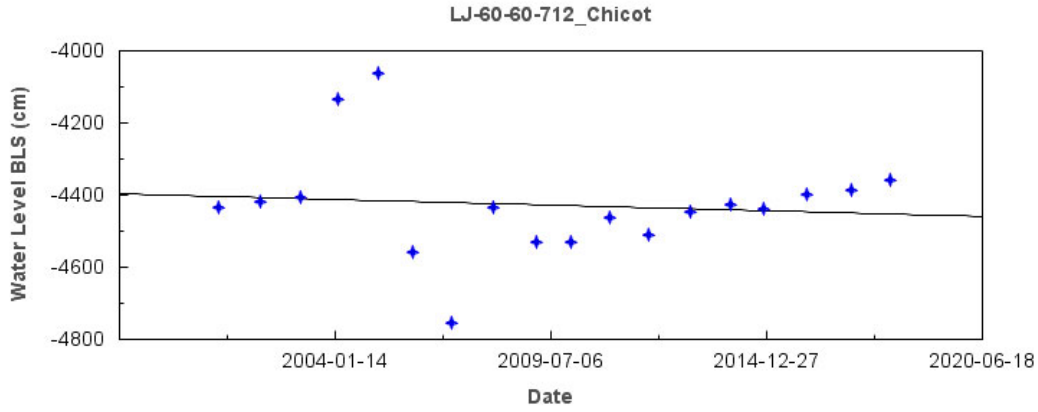
LJ-60-60-712_Chicot
Water Level BLS (cm)
-4000
-4200
-4400
-4600
-4800
2004-01-14
2009-07-06
2014-12-27
2020-06-18
Date

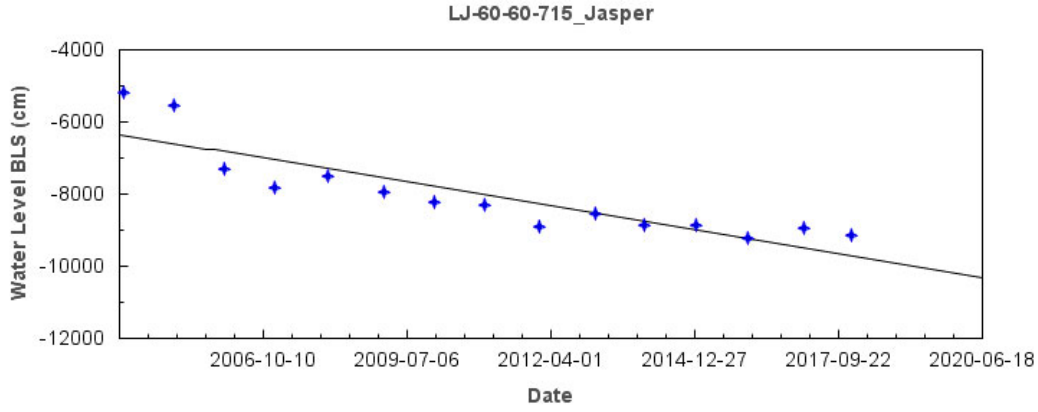
LJ-60-60-715_Jasper
Water Level BLS (cm)
-4000
-6000
-8000
-10000
-12000
2006-10-10
2009-07-06
2012-04-01
2014-12-27
2017-09-22
2020-06-18
Date

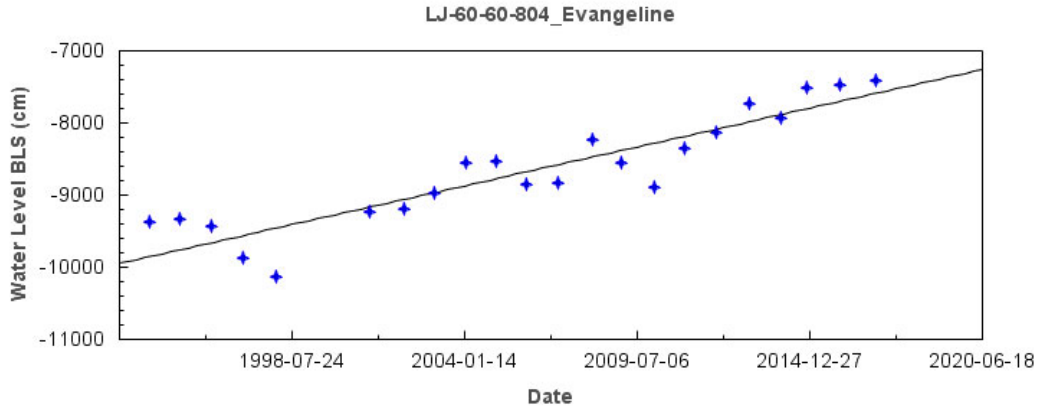
LJ-60-60-804_Evangeline
Water Level BLS (cm)
-7000
-8000
-9000
-10000
-11000
1998-07-24
2004-01-14
2009-07-06
2014-12-27
2020-06-18
Date

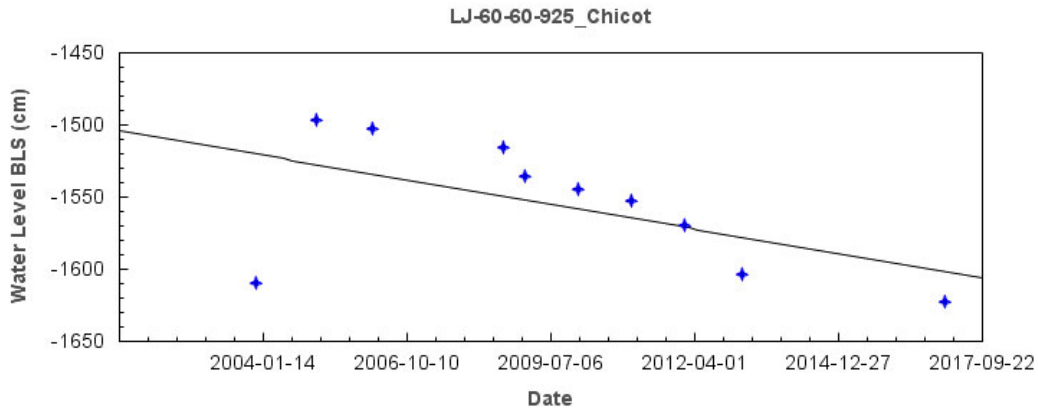
LJ-60-60-925_Chicot
Water Level BLS (cm)
-1450
-1500
-1550
-1600
-1650
2004-01-14
2006-10-10
2009-07-06
2012-04-01
2014-12-27
2017-09-22
Date

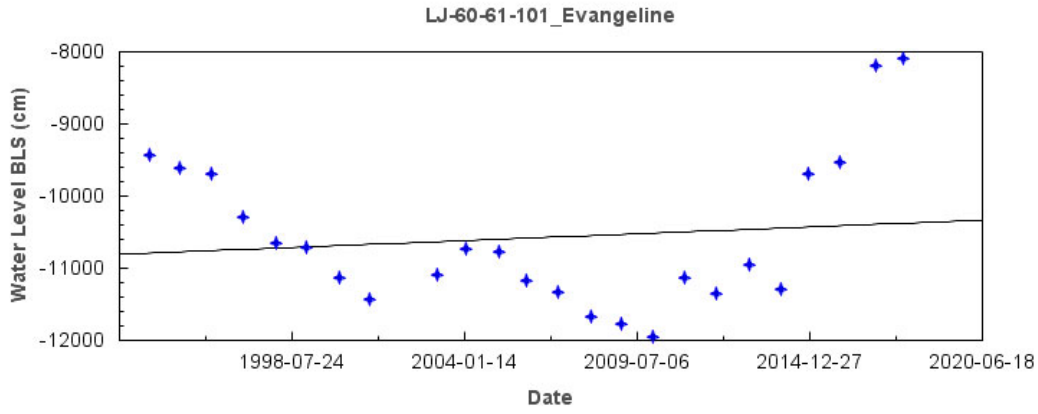
LJ-60-61-101_Evangeline
Water Level BLS (cm)
-8000
-9000
-10000
-11000
-12000
1998-07-24
2004-01-14
2009-07-06
2014-12-27
2020-06-18
Date

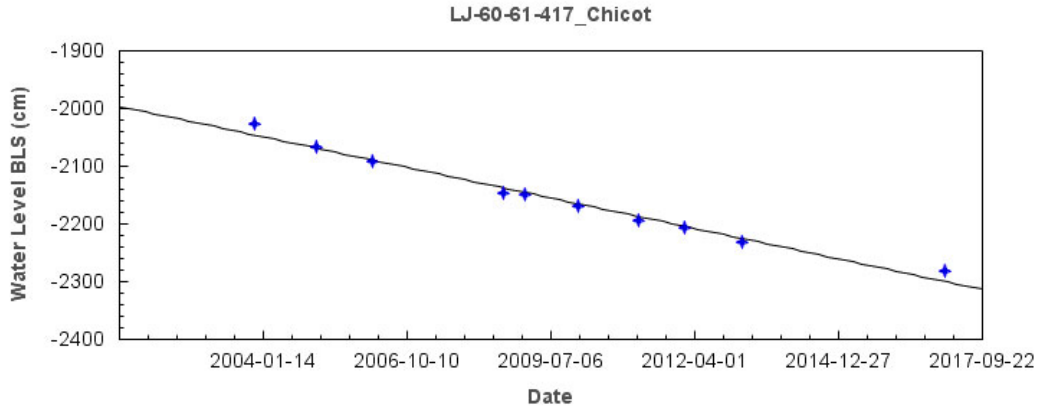
LJ-60-61-417_Chicot
Water Level BLS (cm)
-1900
-2000
-2100
-2200
-2300
-2400
2004-01-14
2006-10-10
2009-07-06
2012-04-01
2014-12-27
2017-09-22
Date

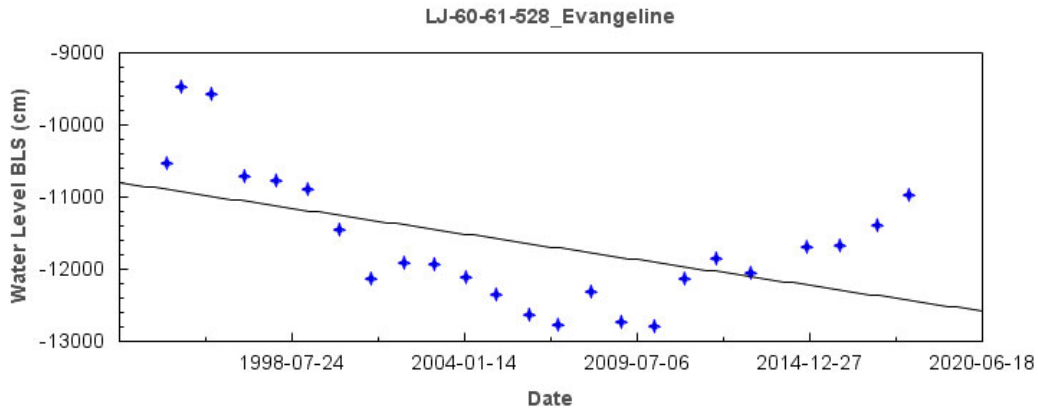
LJ-60-61-528_Evangeline
Water Level BLS (cm)
-9000
-10000
-11000
-12000
-13000
1998-07-24
2004-01-14
2009-07-06
2014-12-27
2020-06-18
Date

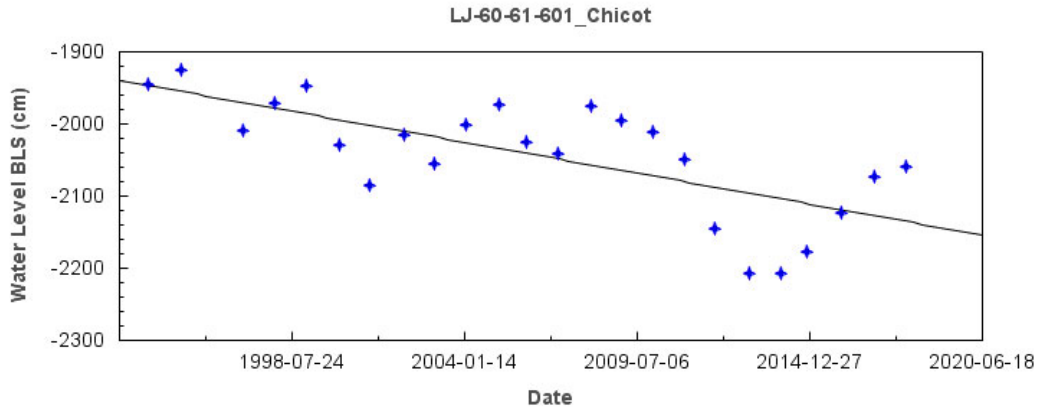
LJ-60-61-601_Chicot
Water Level BLS (cm)
-1900
-2000
-2100
-2200
-2300
1998-07-24
2004-01-14
2009-07-06
2014-12-27
2020-06-18
Date

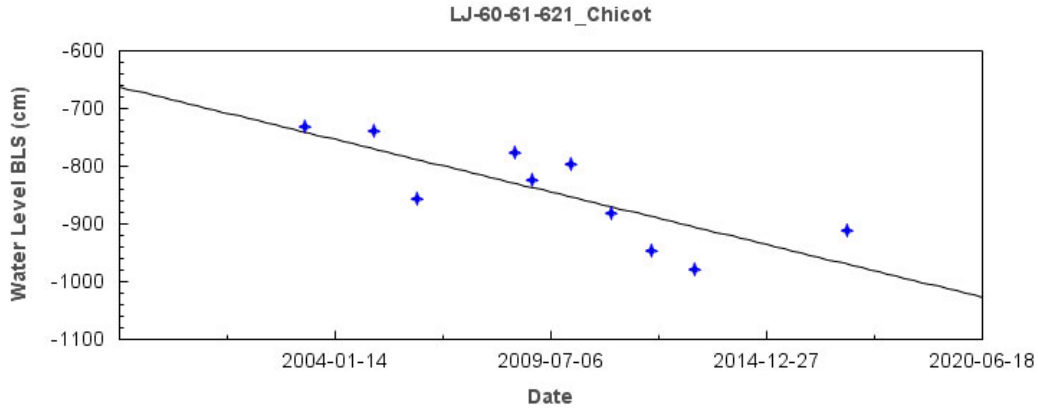
LJ-60-61-621_Chicot
Water Level BLS (cm)
-600
-700
-800
-900
-1000
-1100
2004-01-14
2009-07-06
2014-12-27
2020-06-18
Date

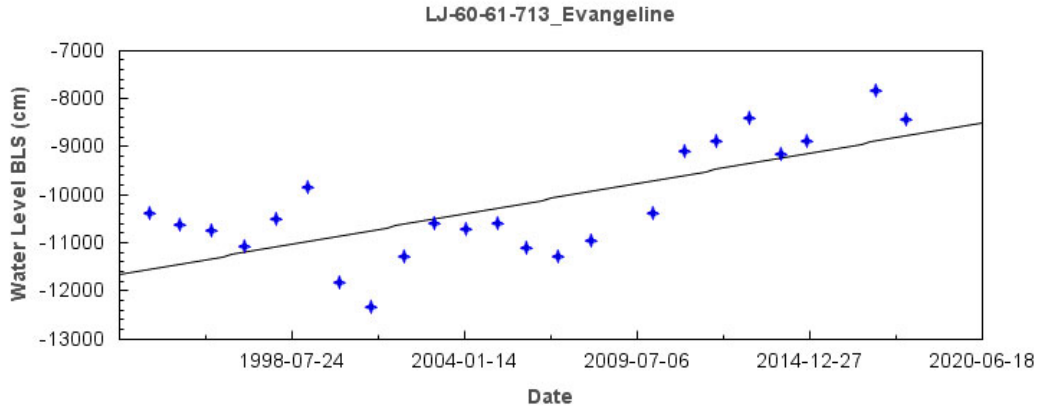
LJ-60-61-713_Evangeline
Water Level BLS (cm)
-7000
-8000
-9000
-10000
-11000
-12000
-13000
1998-07-24
2004-01-14
2009-07-06
2014-12-27
2020-06-18
Date

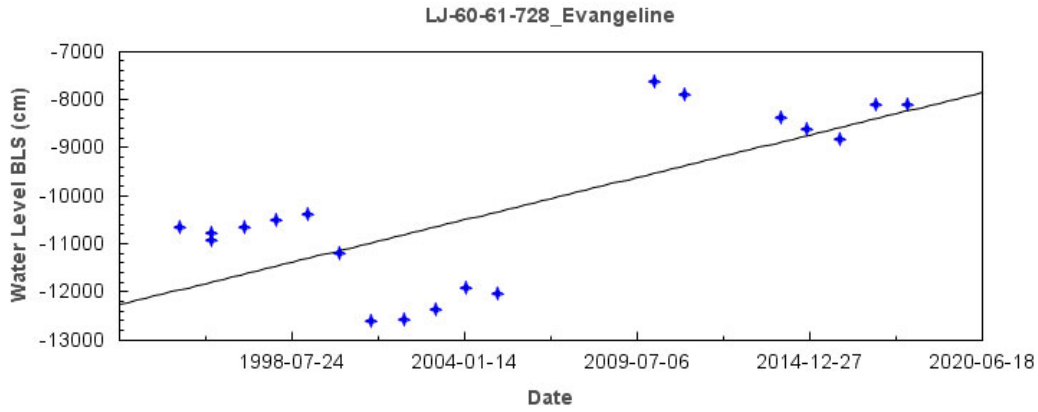
LJ-60-61-728_Evangeline
Water Level BLS (cm)
-7000
-8000
-9000
-10000
-11000
-12000
-13000
1998-07-24
2004-01-14
2009-07-06
2014-12-27
2020-06-18
Date

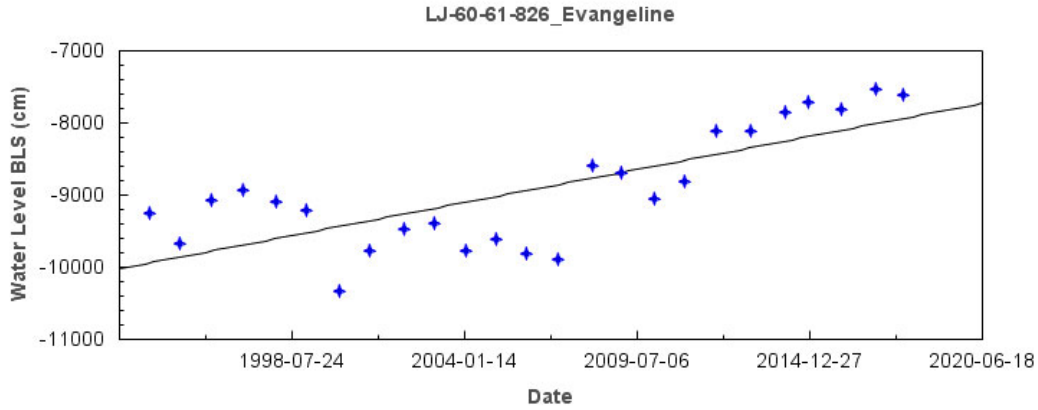
LJ-60-61-826_Evangeline
Water Level BLS (cm)
-7000
-8000
-9000
-10000
-11000
1998-07-24
2004-01-14
2009-07-06
2014-12-27
2020-06-18
Date

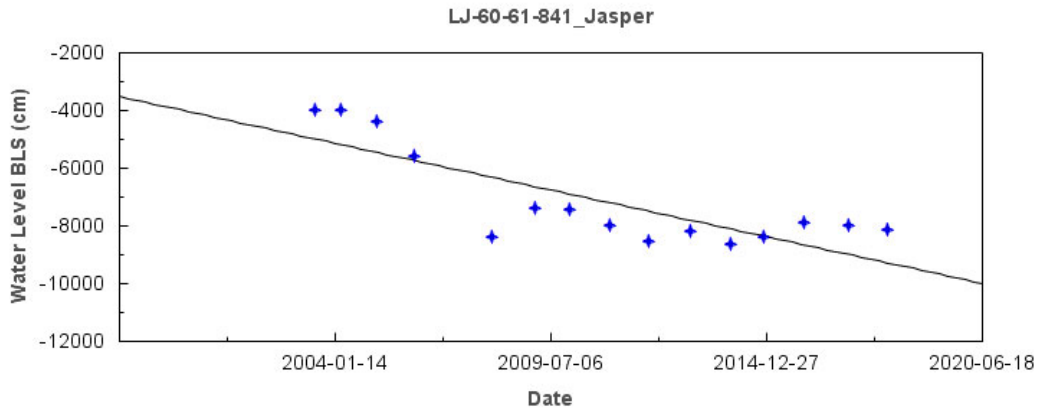
LJ-60-61-841_Jasper
Water Level BLS (cm)
-2000
-4000
-6000
-8000
-10000
-12000
2004-01-14
2009-07-06
2014-12-27
2020-06-18
Date

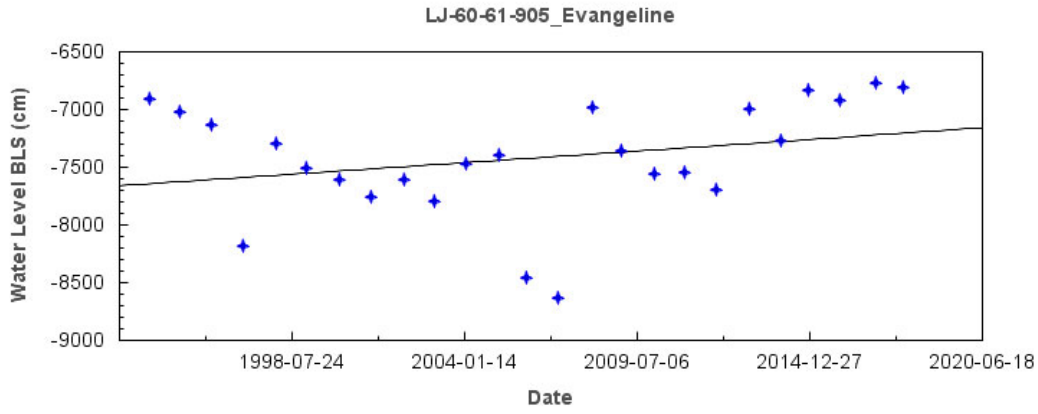
LJ-60-61-905_Evangeline
Water Level BLS (cm)
-6500
-7000
-7500
-8000
-8500
-9000
1998-07-24
2004-01-14
2009-07-06
2014-12-27
2020-06-18
Date

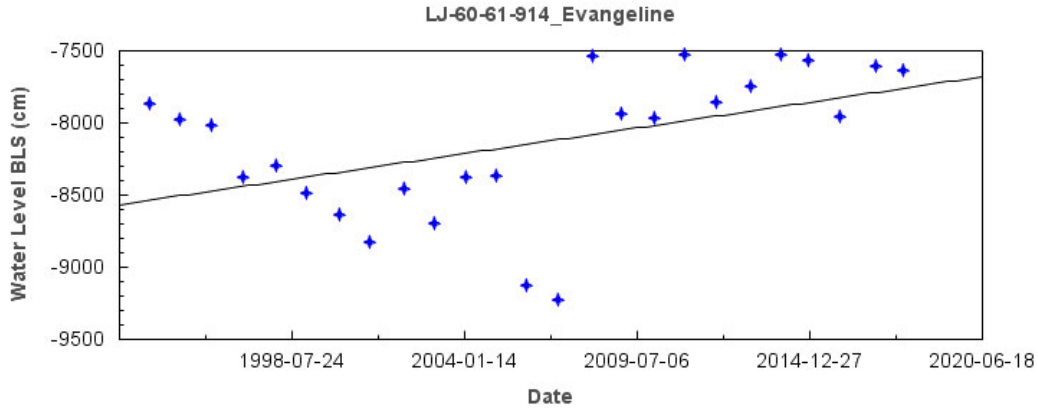
LJ-60-61-914_Evangeline
Water Level BLS (cm)
-7500
-8000
-8500
-9000
-9500
1998-07-24
2004-01-14
2009-07-06
2014-12-27
2020-06-18
Date

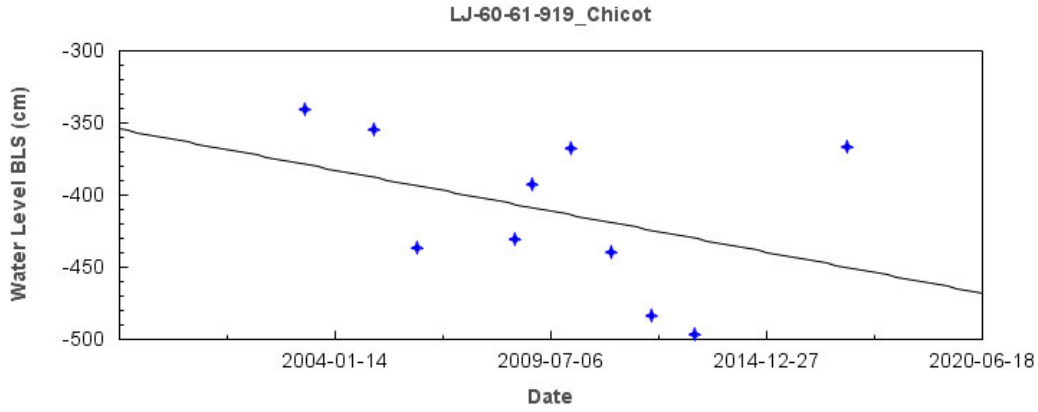
LJ-60-61-919_Chicot
Water Level BLS (cm)
-300
-350
-400
-450
-500
2004-01-14
2009-07-06
2014-12-27
2020-06-18
Date

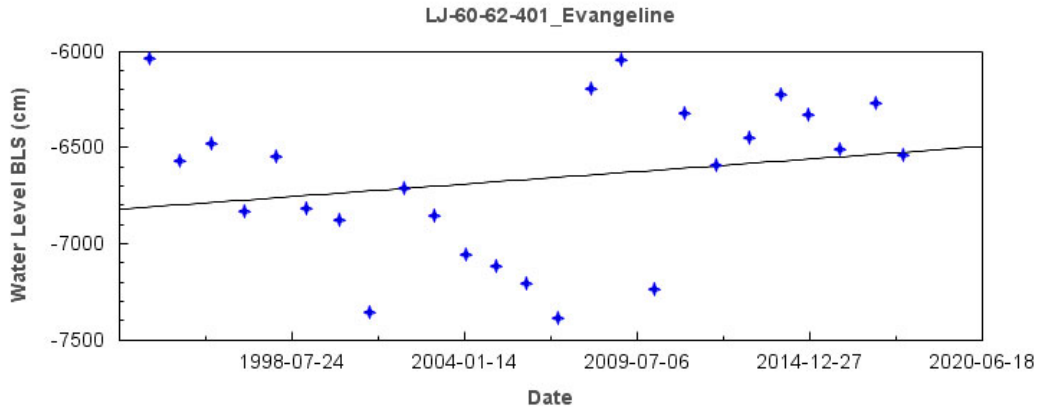
LJ-60-62-401_Evangeline
Water Level BLS (cm)
-6000
-6500
-7000
-7500
1998-07-24
2004-01-14
2009-07-06
2014-12-27
2020-06-18
Date

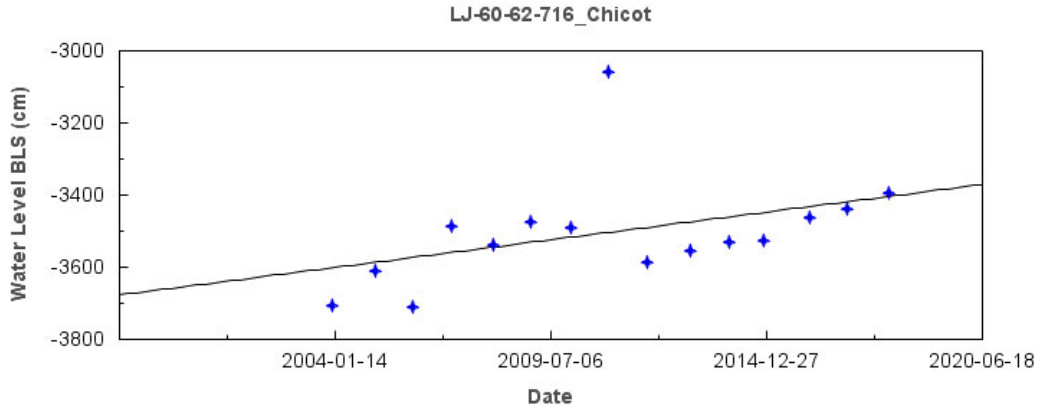
LJ-60-62-716_Chicot
Water Level BLS (cm)
-3000
-3200
-3400
-3600
-3800
2004-01-14
2009-07-06
2014-12-27
2020-06-18
Date

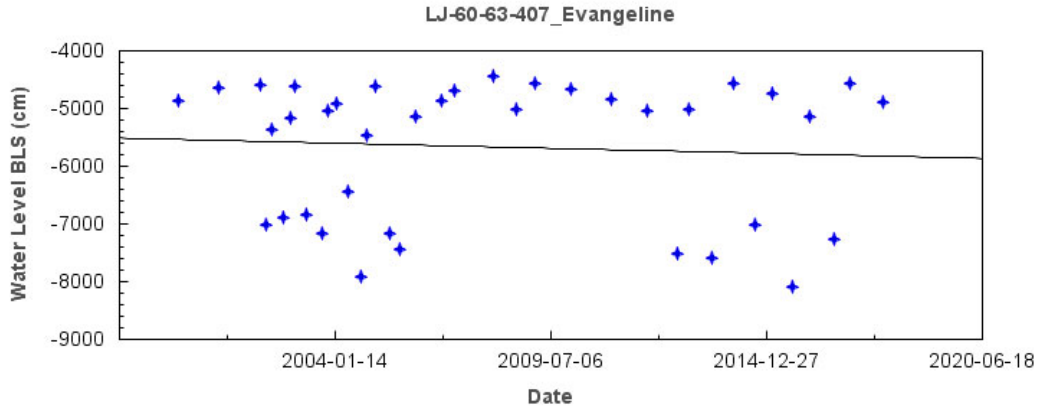
LJ-60-63-407_Evangeline
Water Level BLS (cm)
-4000
-5000
-6000
-7000
-8000
-9000
2004-01-14
2009-07-06
2014-12-27
2020-06-18
Date

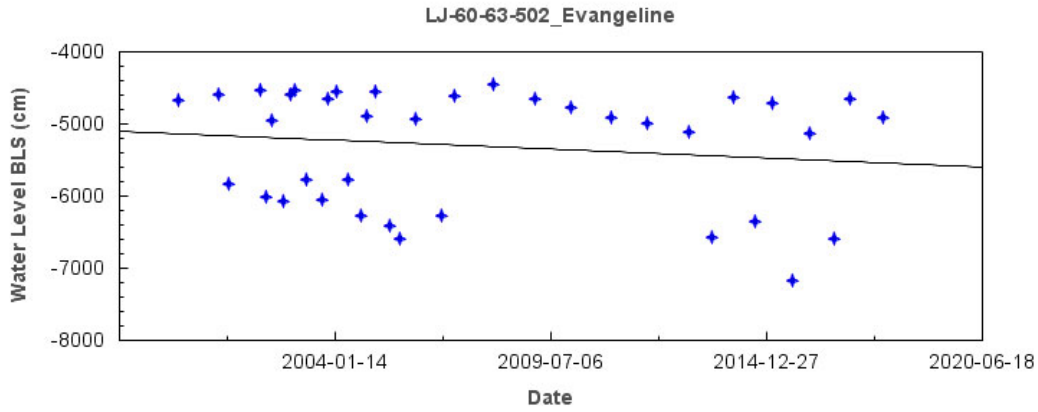
LJ-60-63-502_Evangeline
Water Level BLS (cm)
-4000
-5000
-6000
-7000
-8000
2004-01-14
2009-07-06
2014-12-27
2020-06-18
Date

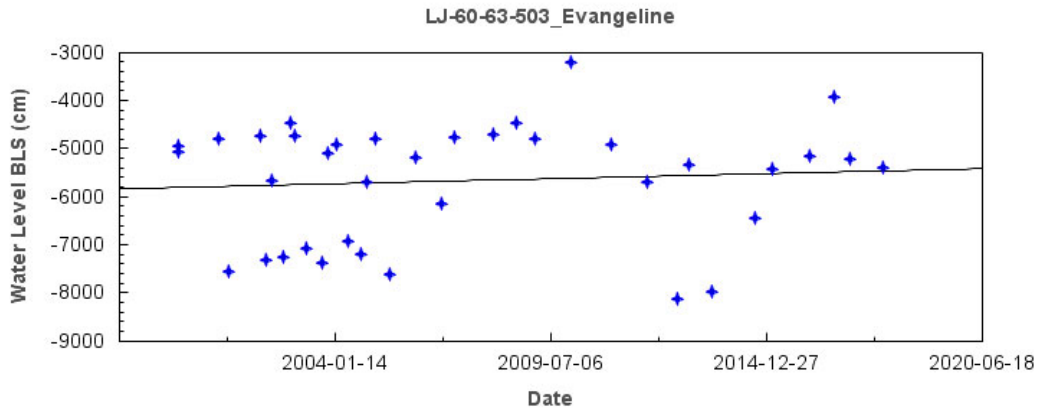
LJ-60-63-503_Evangeline
Water Level BLS (cm)
-3000
-4000
-5000
-6000
-7000
-8000
-9000
2004-01-14
2009-07-06
2014-12-27
2020-06-18
Date

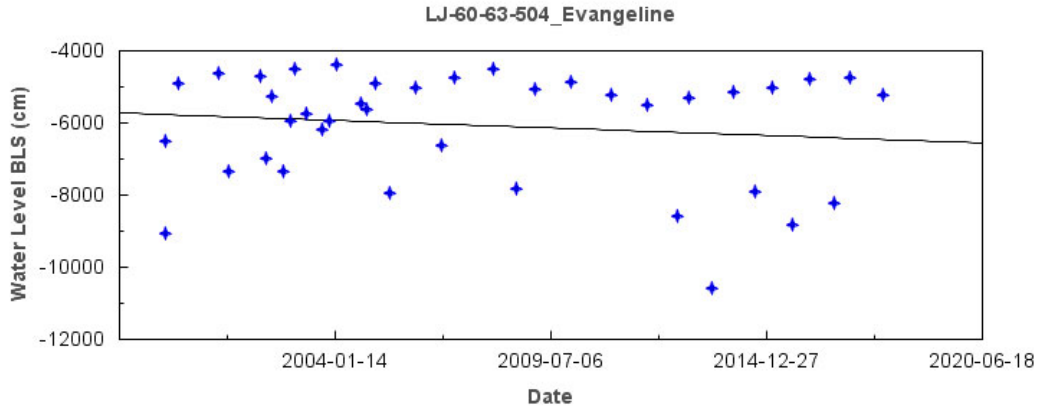
LJ-60-63-504_Evangeline
Water Level BLS (cm)
-4000
-6000
-8000
-10000
-12000
2004-01-14
2009-07-06
2014-12-27
2020-06-18
Date

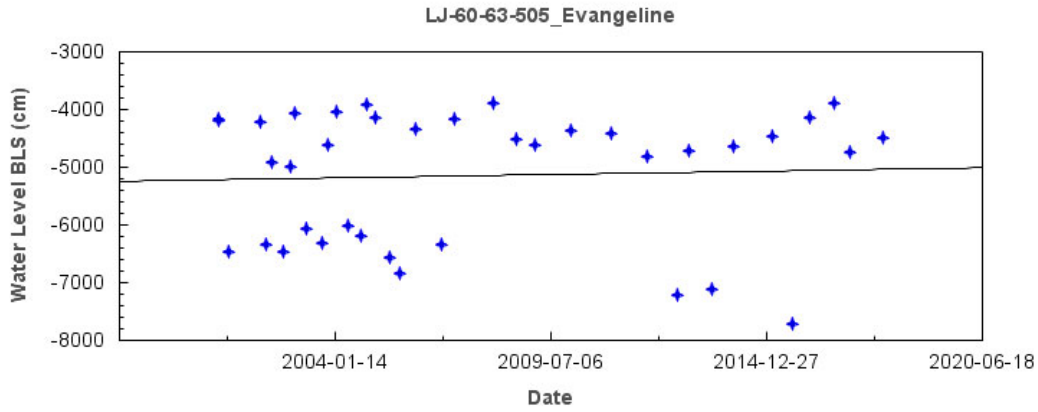
LJ-60-63-505_Evangeline
Water Level BLS (cm)
-3000
-4000
-5000
-6000
-7000
-8000
2004-01-14
2009-07-06
2014-12-27
2020-06-18
Date

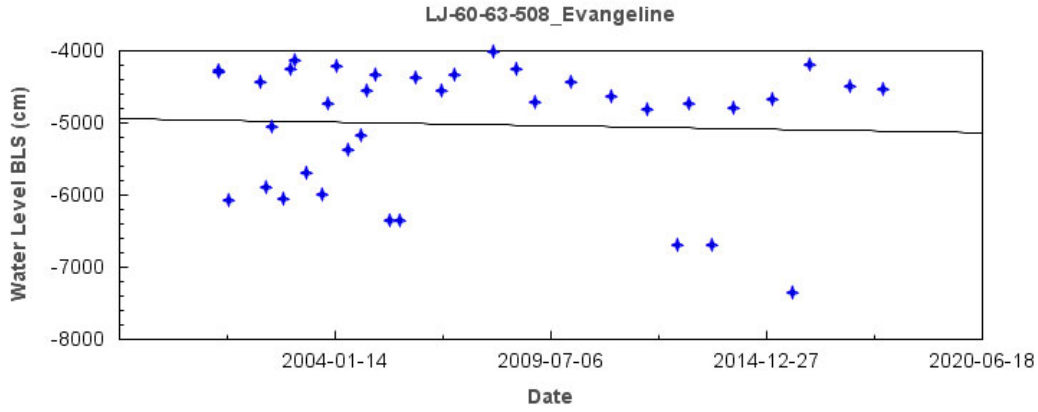
LJ-60-63-508_Evangeline
Water Level BLS (cm)
-4000
-5000
-6000
-7000
-8000
2004-01-14
2009-07-06
2014-12-27
2020-06-18
Date

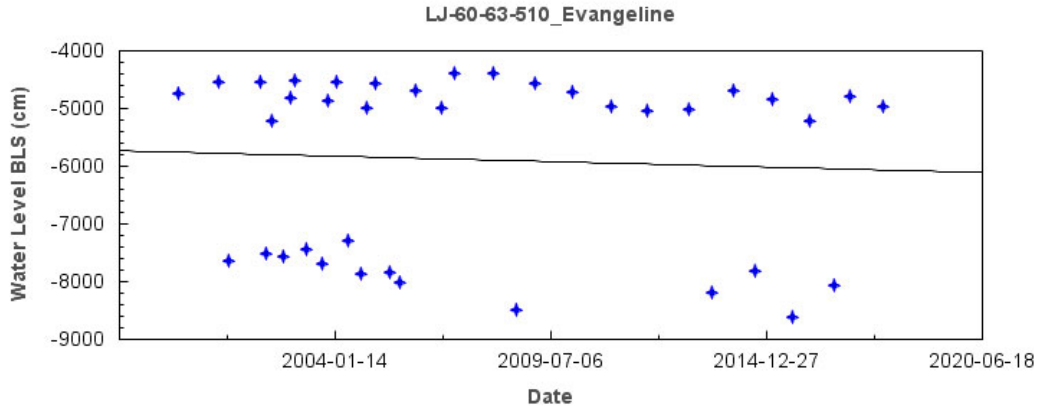
LJ-60-63-510_Evangeline
Water Level BLS (cm)
-4000
-5000
-6000
-7000
-8000
-9000
2004-01-14
2009-07-06
2014-12-27
2020-06-18
Date

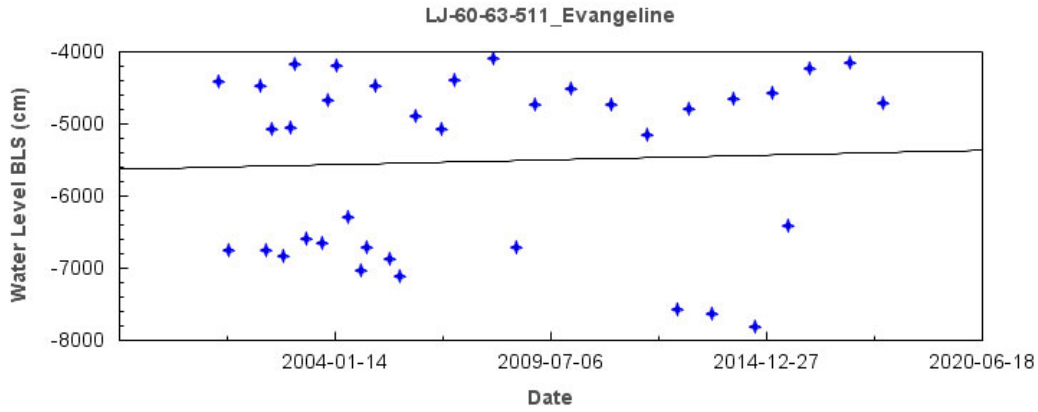
LJ-60-63-511_Evangeline
Water Level BLS (cm)
-4000
-5000
-6000
-7000
-8000
2004-01-14
2009-07-06
2014-12-27
2020-06-18
Date

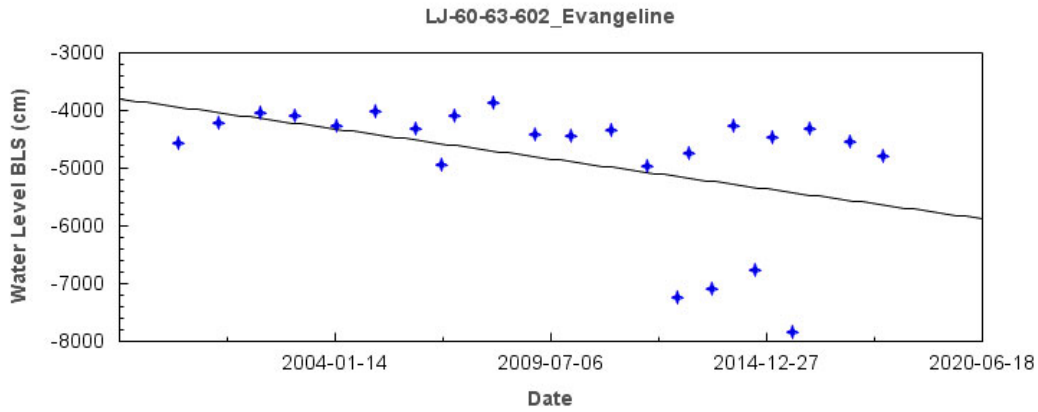
LJ-60-63-602_Evangeline
Water Level BLS (cm)
-3000
-4000
-5000
-6000
-7000
-8000
2004-01-14
2009-07-06
2014-12-27
2020-06-18
Date

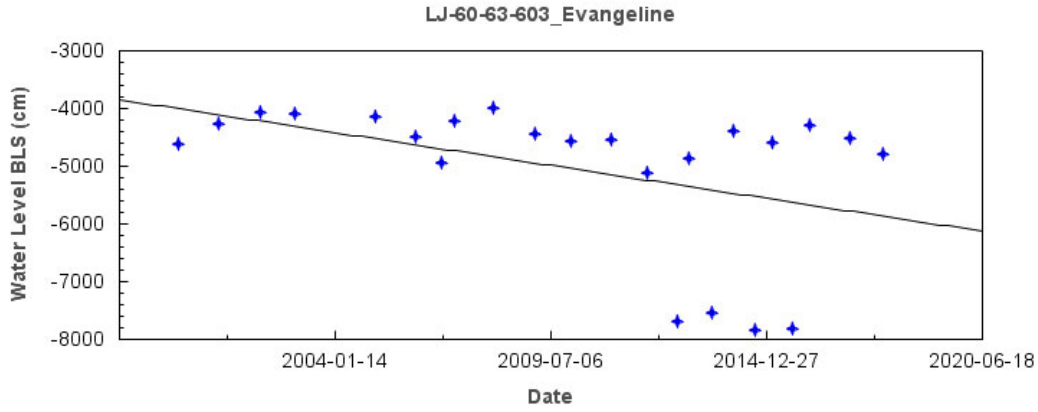
LJ-60-63-603_Evangeline
Water Level BLS (cm)
-3000
-4000
-5000
-6000
-7000
-8000
2004-01-14
2009-07-06
2014-12-27
2020-06-18
Date

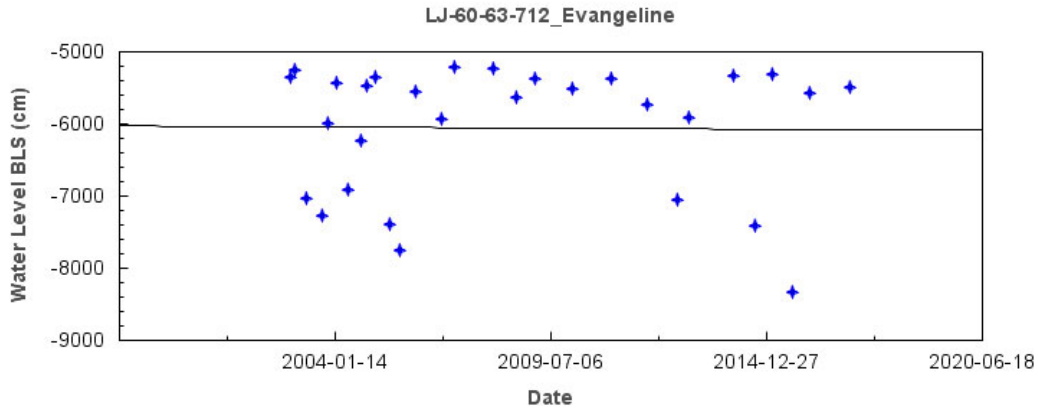
LJ-60-63-712_Evangeline
Water Level BLS (cm)
-5000
-6000
-7000
-8000
-9000
2004-01-14
2009-07-06
2014-12-27
2020-06-18
Date

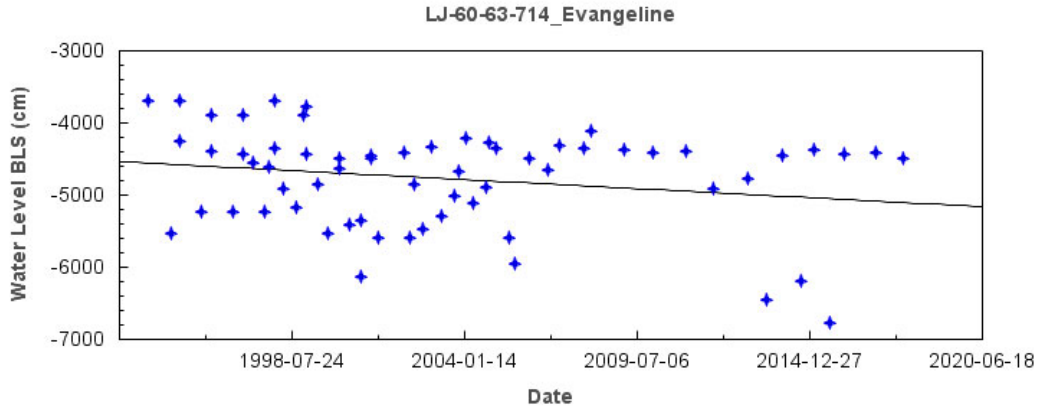
LJ-60-63-714_Evangeline
Water Level BLS (cm)
-3000
-4000
-5000
-6000
-7000
1998-07-24
2004-01-14
2009-07-06
2014-12-27
2020-06-18
Date

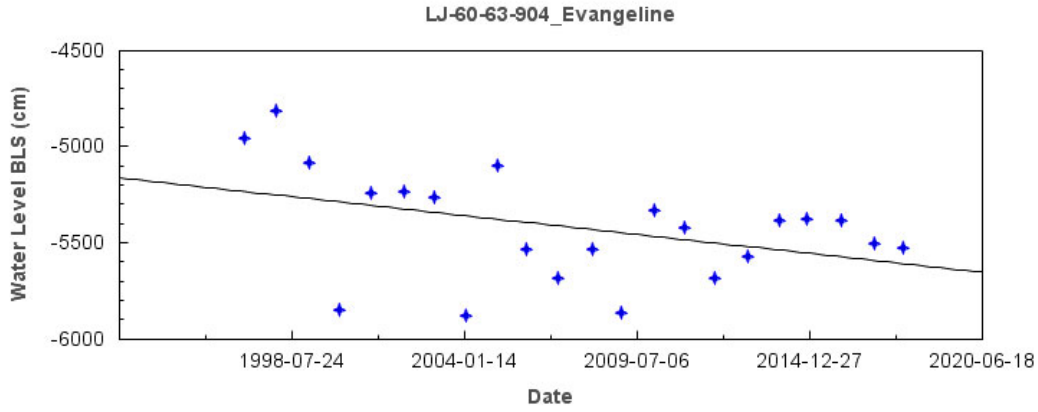
LJ-60-63-904_Evangeline
Water Level BLS (cm)
-4500
-5000
-5500
-6000
1998-07-24
2004-01-14
2009-07-06
2014-12-27
2020-06-18
Date

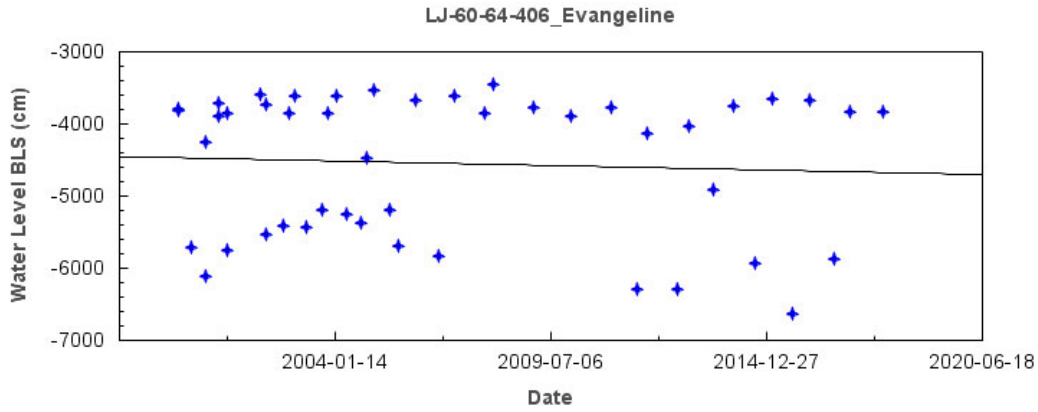
LJ-60-64-406_Evangeline
Water Level BLS (cm)
-3000
-4000
-5000
-6000
-7000
2004-01-14
2009-07-06
2014-12-27
2020-06-18
Date

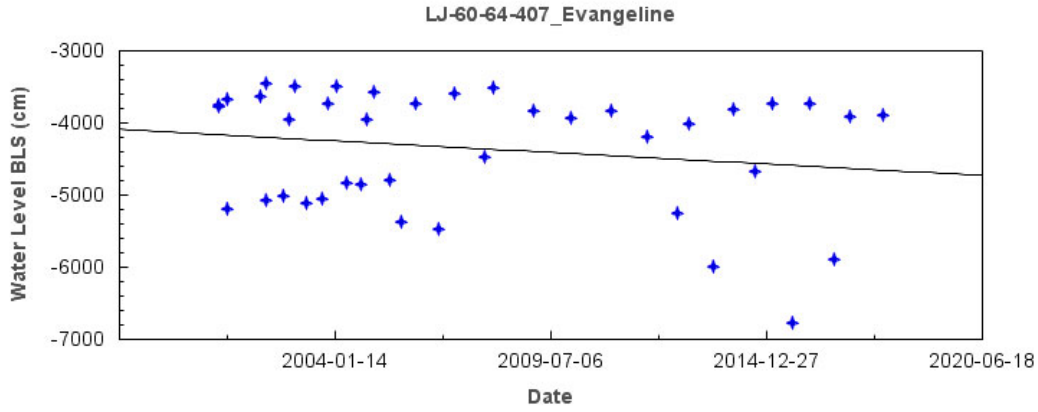
LJ-60-64-407_Evangeline
Water Level BLS (cm)
-3000
-4000
-5000
-6000
-7000
2004-01-14
2009-07-06
2014-12-27
2020-06-18
Date

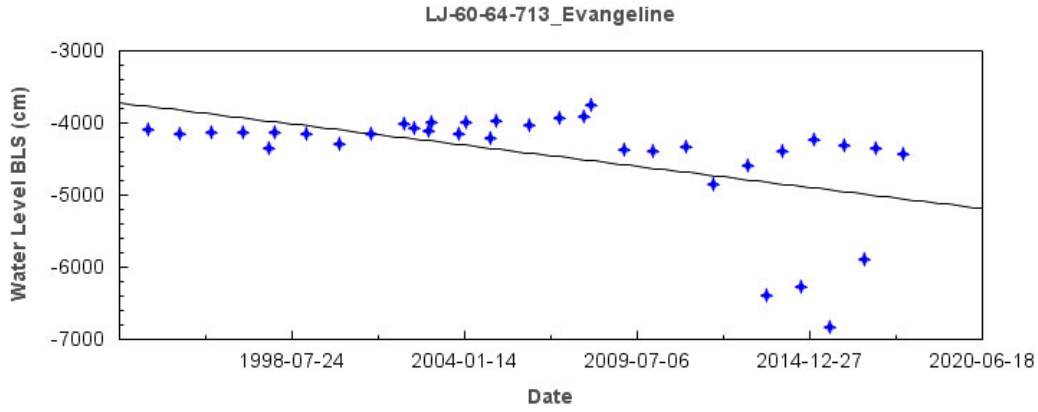
LJ-60-64-713_Evangeline
Water Level BLS (cm)
-3000
-4000
-5000
-6000
-7000
1998-07-24
2004-01-14
2009-07-06
2014-12-27
2020-06-18
Date

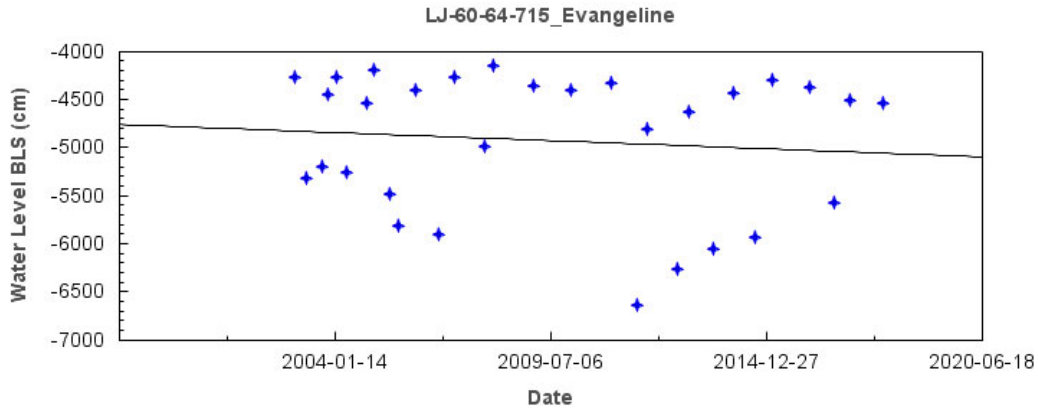
LJ-60-64-715_Evangeline
Water Level BLS (cm)
-4000
-4500
-5000
-5500
-6000
-6500
-7000
2004-01-14
2009-07-06
2014-12-27
2020-06-18
Date

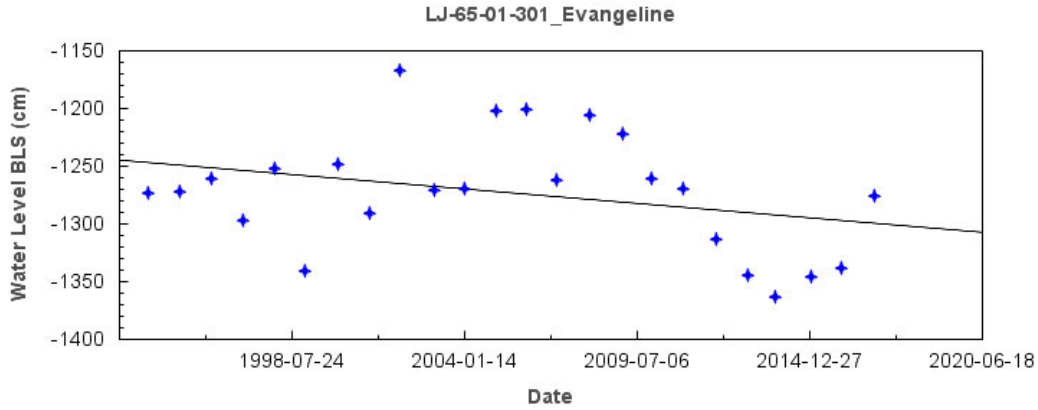
LJ-65-01-301_Evangeline
Water Level BLS (cm)
-1150
-1200
-1250
-1300
-1350
-1400
1998-07-24
2004-01-14
2009-07-06
2014-12-27
2020-06-18
Date

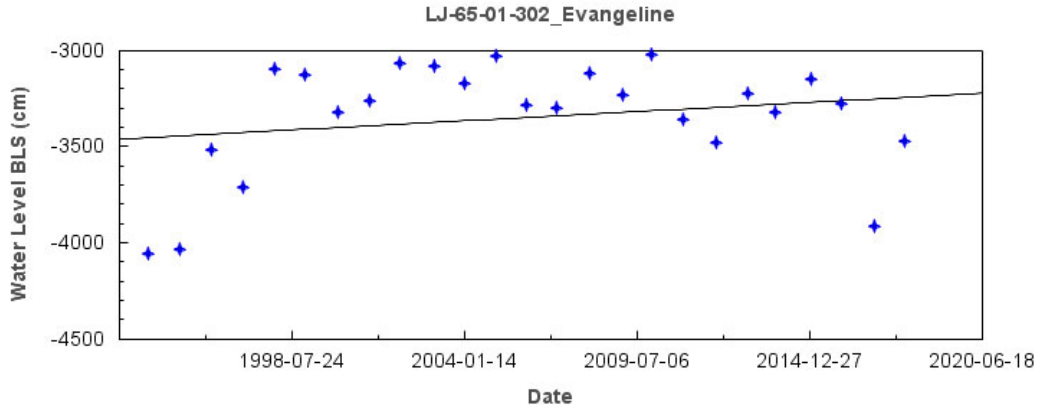
LJ-65-01-302_Evangeline
Water Level BLS (cm)
-3000
-3500
-4000
-4500
1998-07-24
2004-01-14
2009-07-06
2014-12-27
2020-06-18
Date

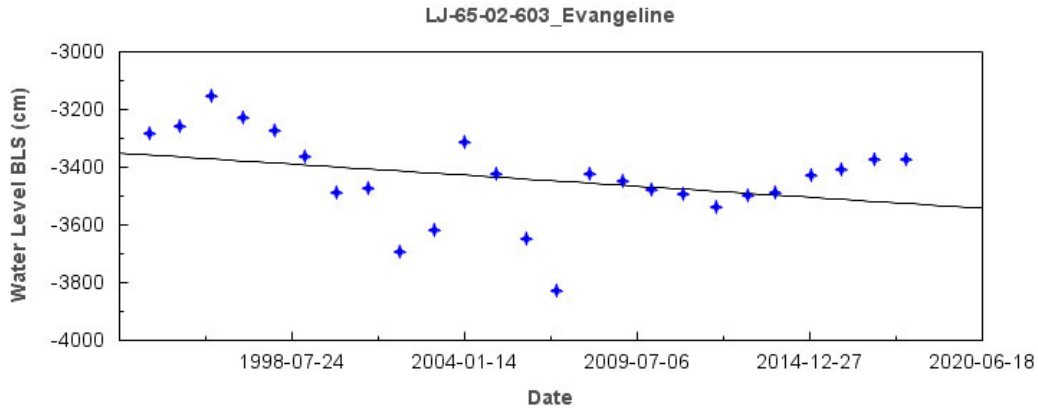
LJ-65-02-603_Evangeline
Water Level BLS (cm)
-3000
-3200
-3400
-3600
-3800
-4000
1998-07-24
2004-01-14
2009-07-06
2014-12-27
2020-06-18
Date

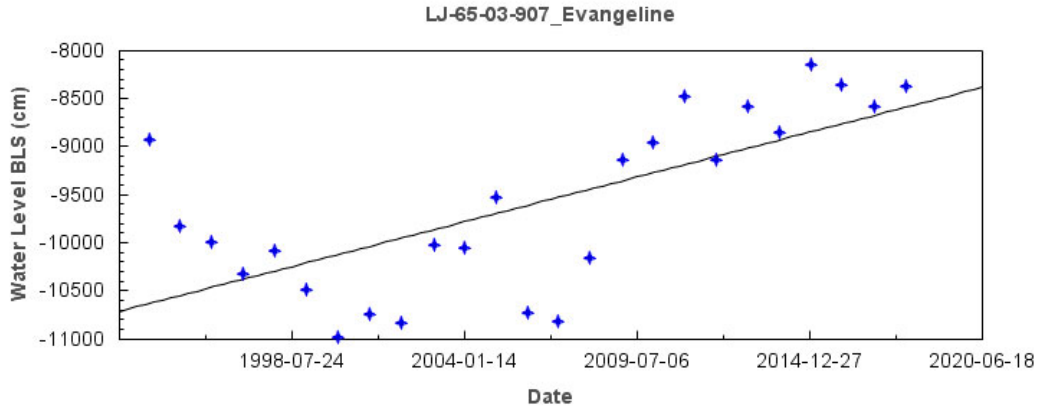
LJ-65-03-907_Evangeline
Water Level BLS (cm)
-8000
-8500
-9000
-9500
-10000
-10500
-11000
1998-07-24
2004-01-14
2009-07-06
2014-12-27
2020-06-18
Date

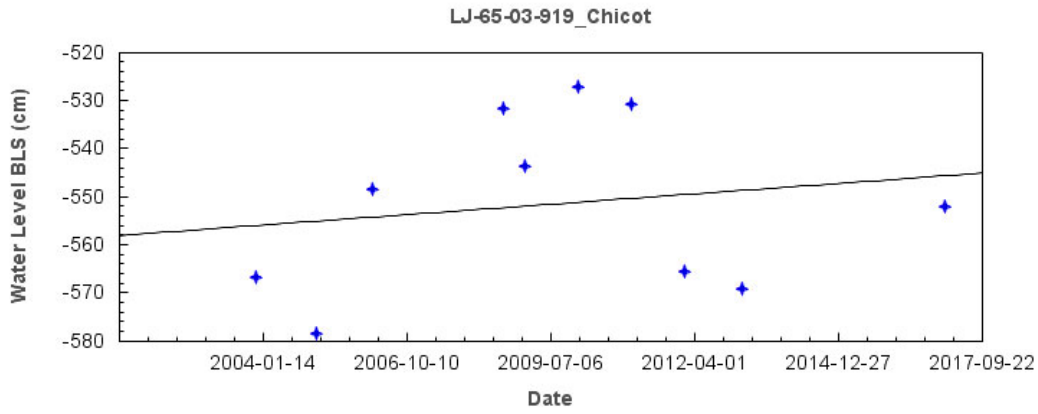
LJ-65-03-919_Chicot
Water Level BLS (cm)
-520
-530
-540
-550
-560
-570
-580
2004-01-14
2006-10-10
2009-07-06
2012-04-01
2014-12-27
2017-09-22
Date

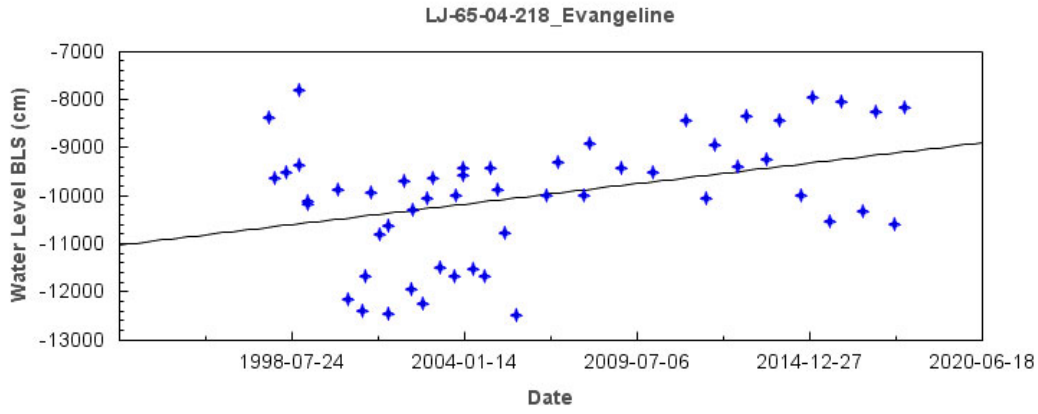
LJ-65-04-218_Evangeline
Water Level BLS (cm)
-7000
-8000
-9000
-10000
-11000
-12000
-13000
1998-07-24
2004-01-14
2009-07-06
2014-12-27
2020-06-18
Date

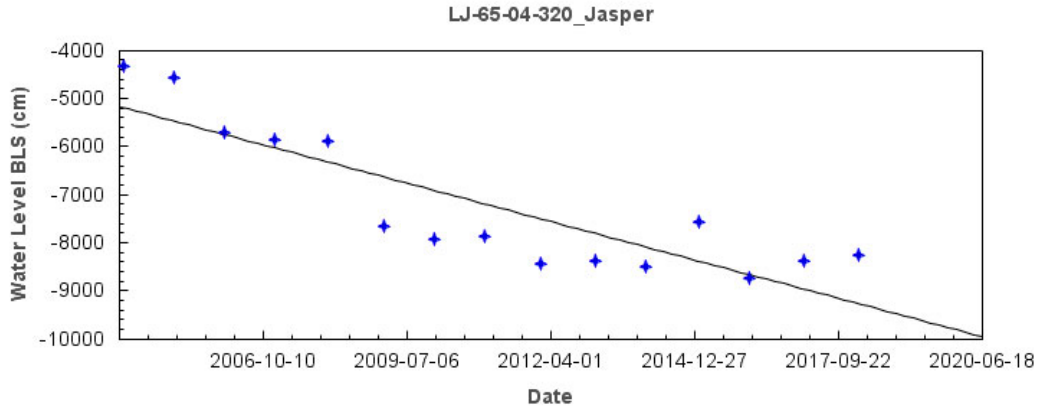
LJ-65-04-320_Jasper
Water Level BLS (cm)
-4000
-5000
-6000
-7000
-8000
-9000
-10000
2006-10-10
2009-07-06
2012-04-01
2014-12-27
2017-09-22
2020-06-18
Date

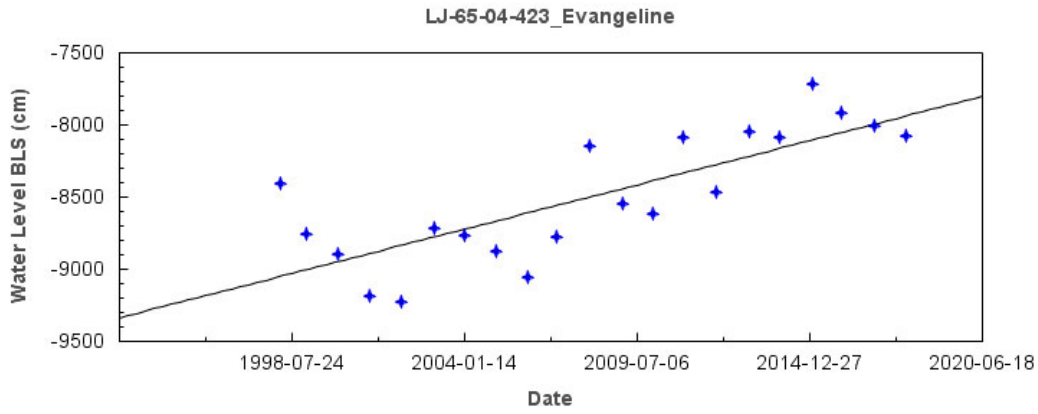
LJ-65-04-423_Evangeline
Water Level BLS (cm)
-7500
-8000
-8500
-9000
-9500
1998-07-24
2004-01-14
2009-07-06
2014-12-27
2020-06-18
Date

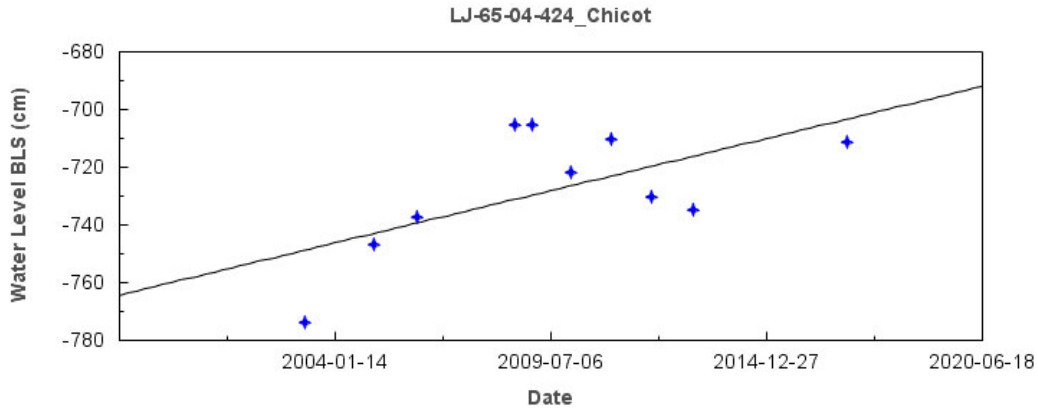
LJ-65-04-424_Chicot
Water Level BLS (cm)
-680
-700
-720
-740
-760
-780
2004-01-14
2009-07-06
2014-12-27
2020-06-18
Date

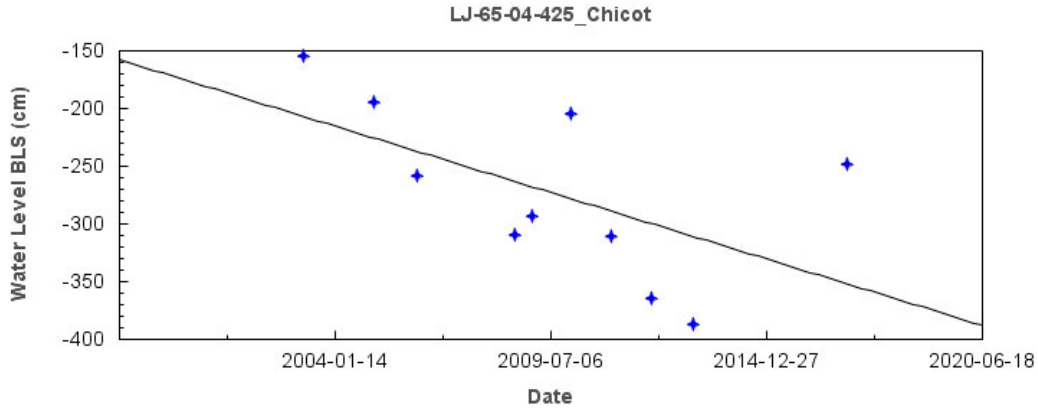
LJ-65-04-425_Chicot
Water Level BLS (cm)
-150
-200
-250
-300
-350
-400
2004-01-14
2009-07-06
2014-12-27
2020-06-18
Date

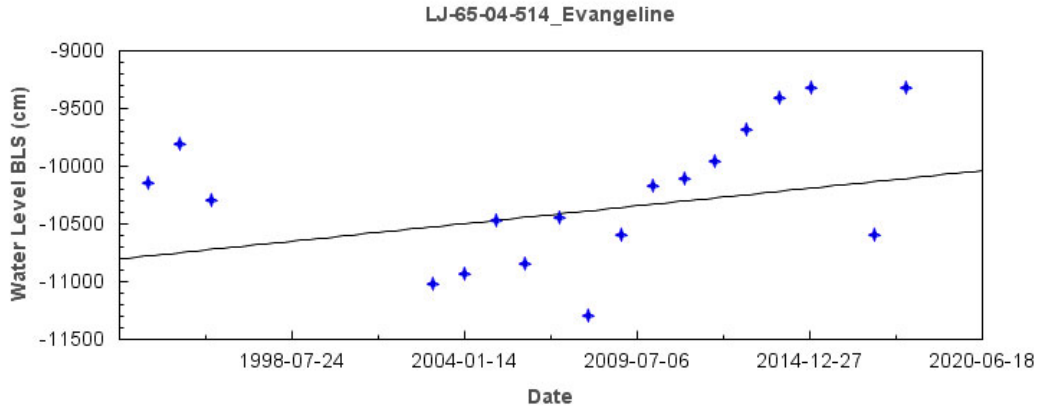
LJ-65-04-514_Evangeline
Water Level BLS (cm)
-9000
-9500
-10000
-10500
-11000
-11500
1998-07-24
2004-01-14
2009-07-06
2014-12-27
2020-06-18
Date

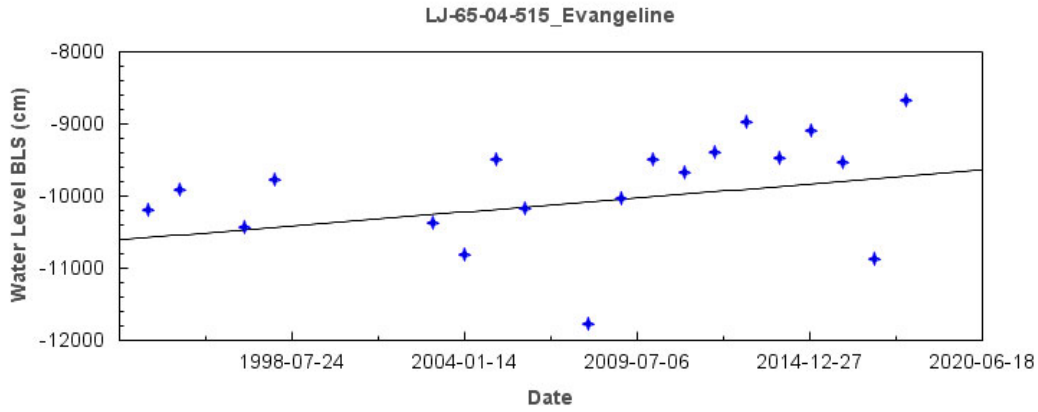
LJ-65-04-515_Evangeline
Water Level BLS (cm)
-8000
-9000
-10000
-11000
-12000
1998-07-24
2004-01-14
2009-07-06
2014-12-27
2020-06-18
Date

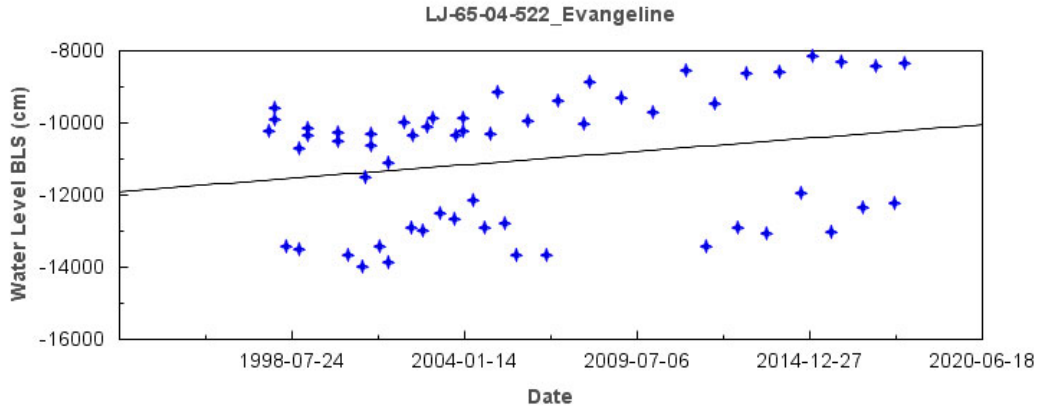
LJ-65-04-522_Evangeline
Water Level BLS (cm)
-8000
-10000
-12000
-14000
-16000
1998-07-24
2004-01-14
2009-07-06
2014-12-27
2020-06-18
Date

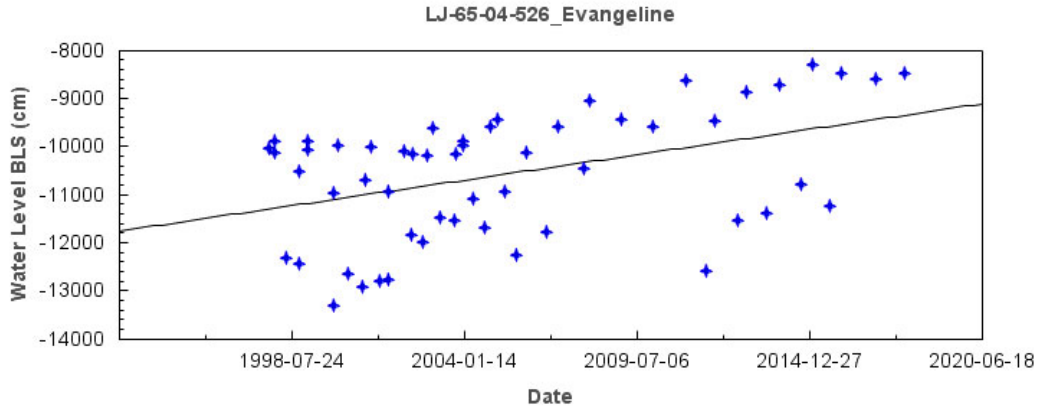
LJ-65-04-526_Evangeline
Water Level BLS (cm)
-8000
-9000
-10000
-11000
-12000
-13000
-14000
1998-07-24
2004-01-14
2009-07-06
2014-12-27
2020-06-18
Date

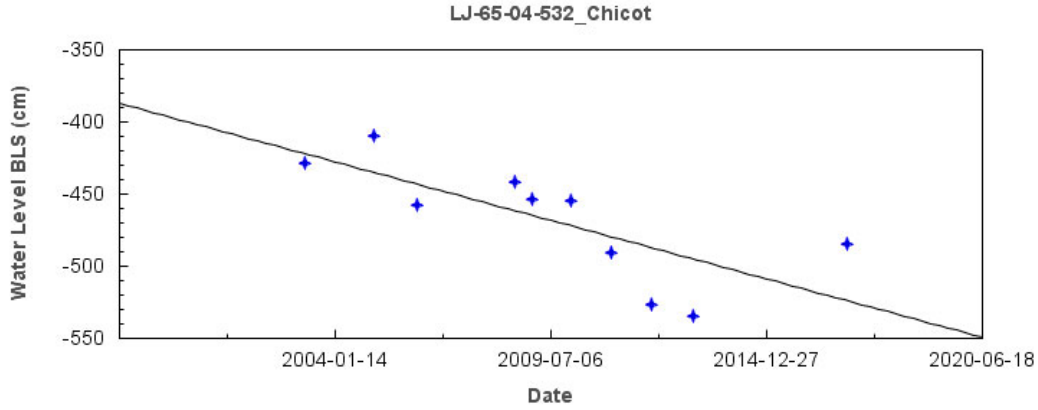
LJ-65-04-532_Chicot
Water Level BLS (cm)
-350
-400
-450
-500
-550
2004-01-14
2009-07-06
2014-12-27
2020-06-18
Date

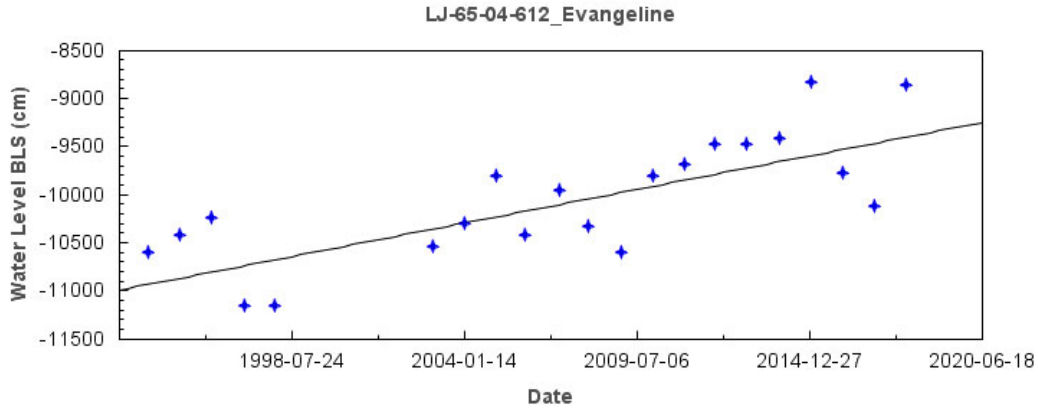
LJ-65-04-612_Evangeline
Water Level BLS (cm)
-8500
-9000
-9500
-10000
-10500
-11000
-11500
1998-07-24
2004-01-14
2009-07-06
2014-12-27
2020-06-18
Date

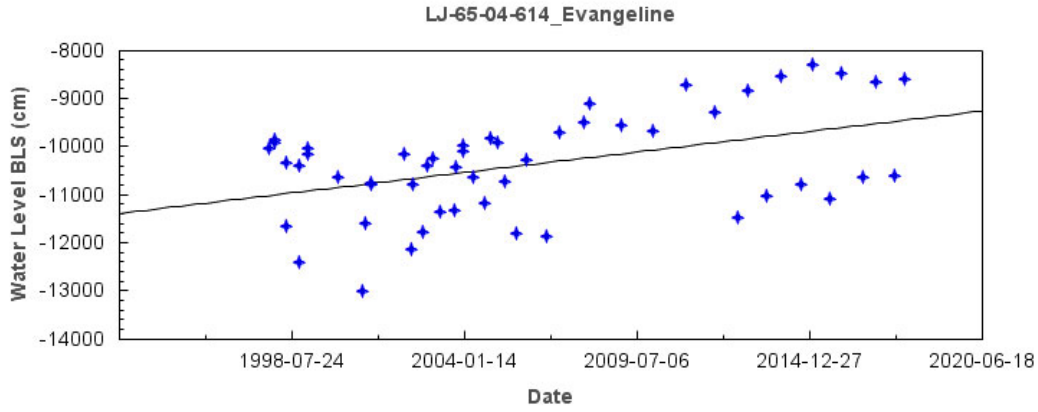
LJ-65-04-614_Evangeline
Water Level BLS (cm)
-8000
-9000
-10000
-11000
-12000
-13000
-14000
1998-07-24
2004-01-14
2009-07-06
2014-12-27
2020-06-18
Date

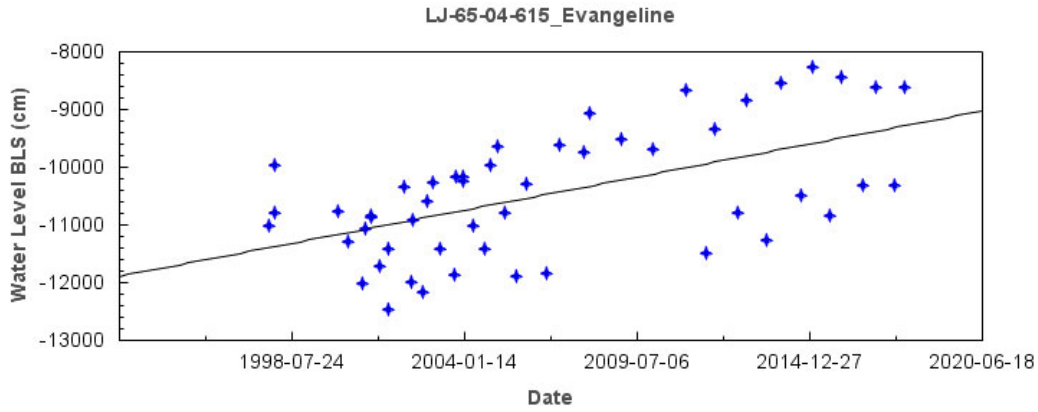
LJ-65-04-615_Evangeline
Water Level BLS (cm)
-8000
-9000
-10000
-11000
-12000
-13000
1998-07-24
2004-01-14
2009-07-06
2014-12-27
2020-06-18
Date

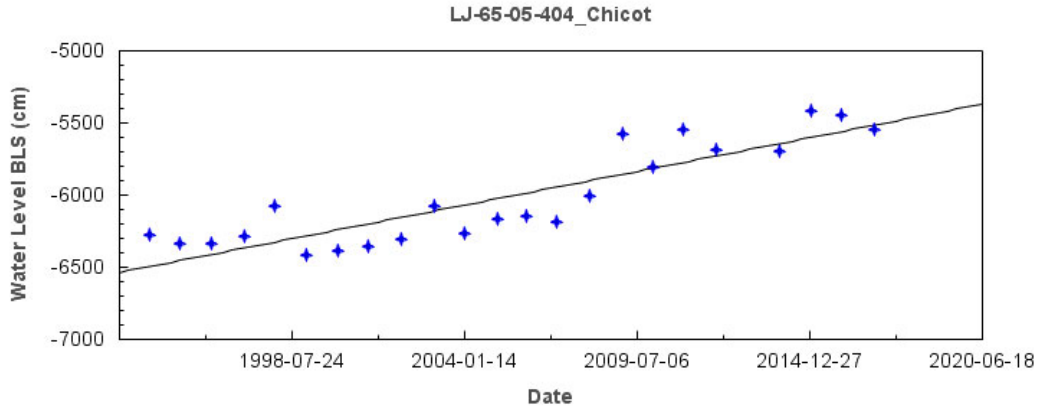
LJ-65-05-404_Chicot
Water Level BLS (cm)
-5000
-5500
-6000
-6500
-7000
1998-07-24
2004-01-14
2009-07-06
2014-12-27
2020-06-18
Date

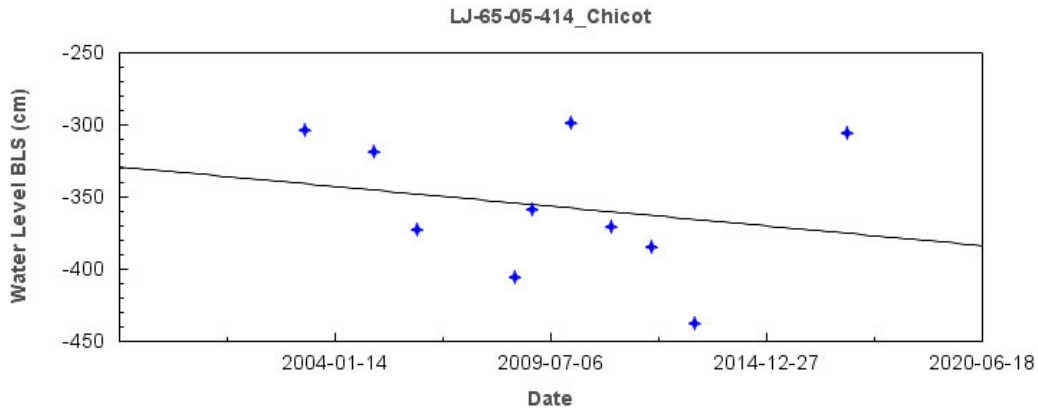
LJ-65-05-414_Chicot
Water Level BLS (cm)
-250
-300
-350
-400
-450
2004-01-14
2009-07-06
2014-12-27
2020-06-18
Date

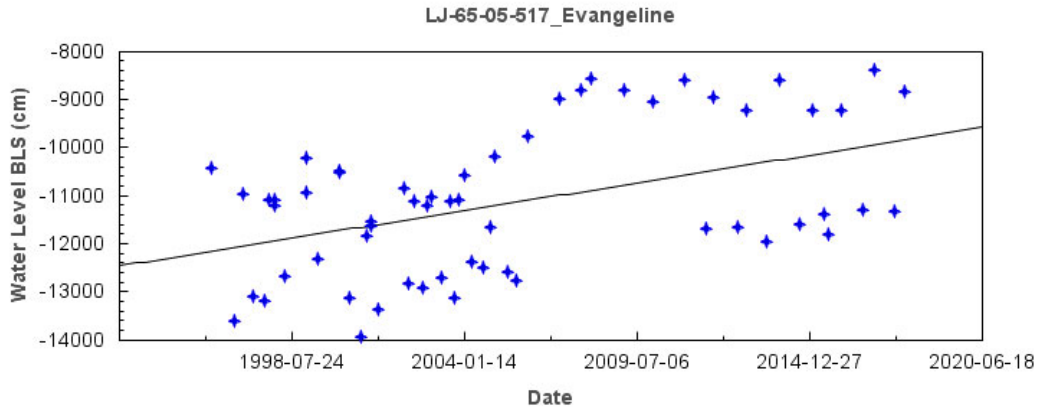
LJ-65-05-517_Evangeline
Water Level BLS (cm)
-8000
-9000
-10000
-11000
-12000
-13000
-14000
1998-07-24
2004-01-14
2009-07-06
2014-12-27
2020-06-18
Date

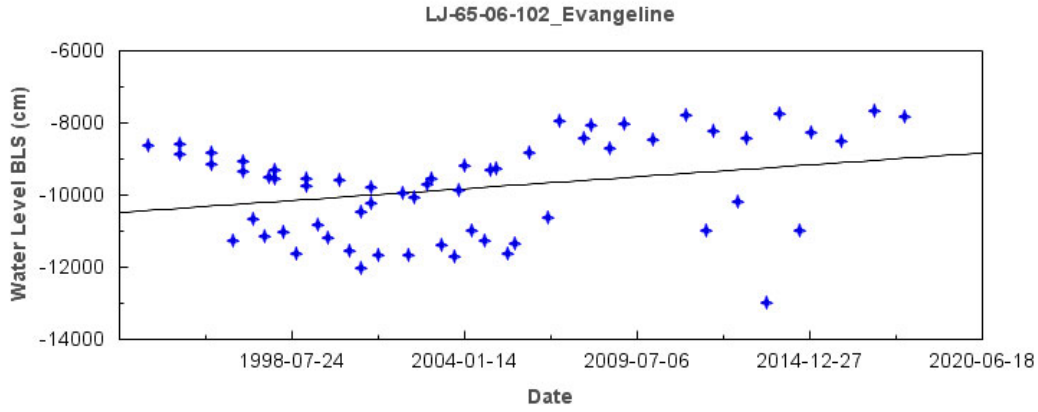
LJ-65-06-102_Evangeline
Water Level BLS (cm)
-6000
-8000
-10000
-12000
-14000
1998-07-24
2004-01-14
2009-07-06
2014-12-27
2020-06-18
Date

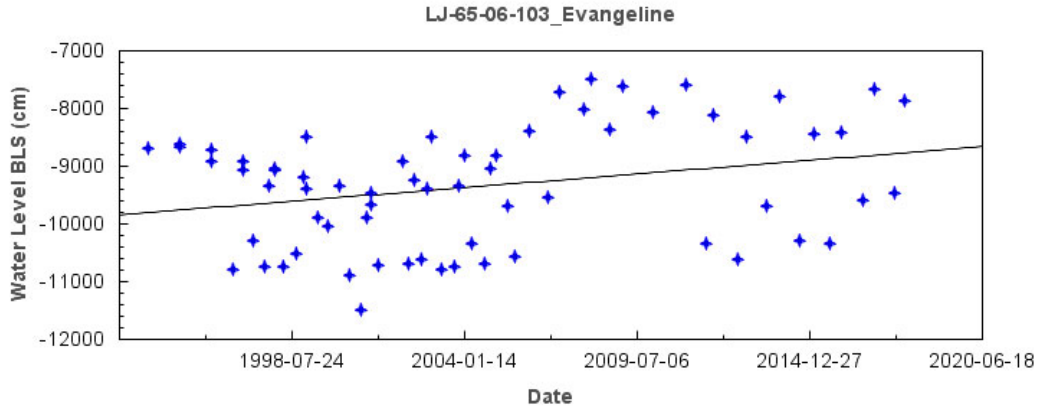
LJ-65-06-103_Evangeline
Water Level BLS (cm)
-7000
-8000
-9000
-10000
-11000
-12000
1998-07-24
2004-01-14
2009-07-06
2014-12-27
2020-06-18
Date

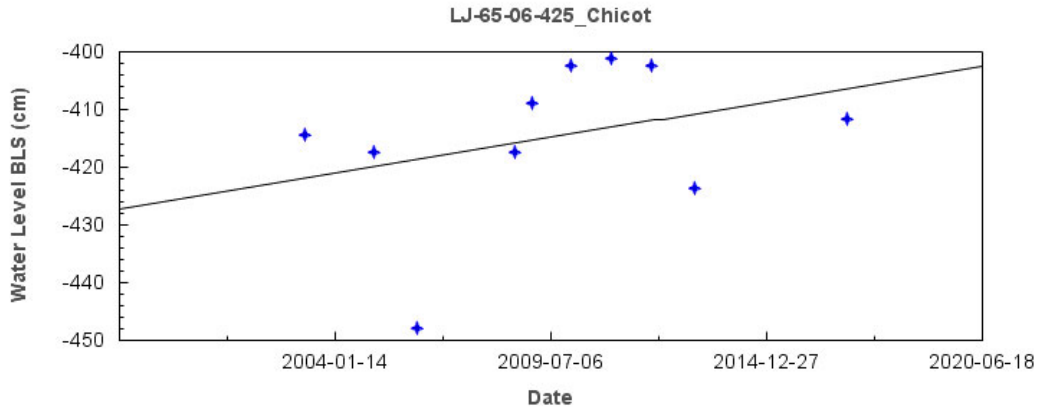
LJ-65-06-425_Chicot
Water Level BLS (cm)
-400
-410
-420
-430
-440
-450
2004-01-14
2009-07-06
2014-12-27
2020-06-18
Date

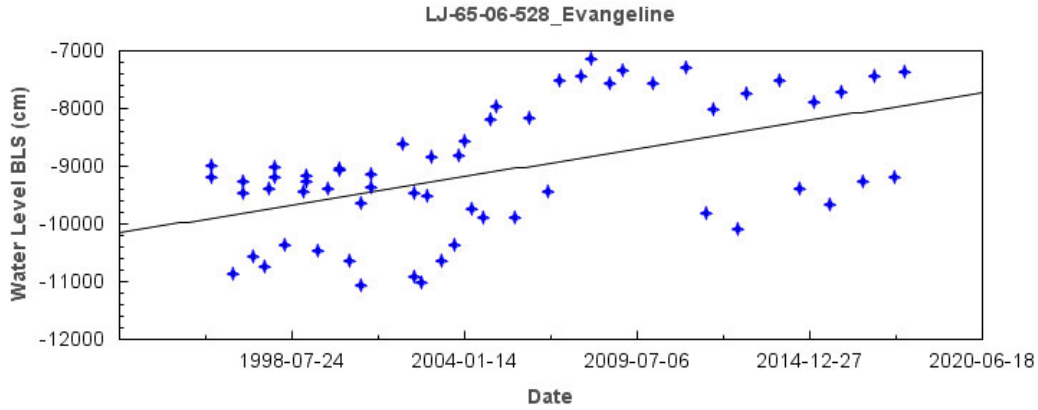
LJ-65-06-528_Evangeline
Water Level BLS (cm)
-7000
-8000
-9000
-10000
-11000
-12000
1998-07-24
2004-01-14
2009-07-06
2014-12-27
2020-06-18
Date

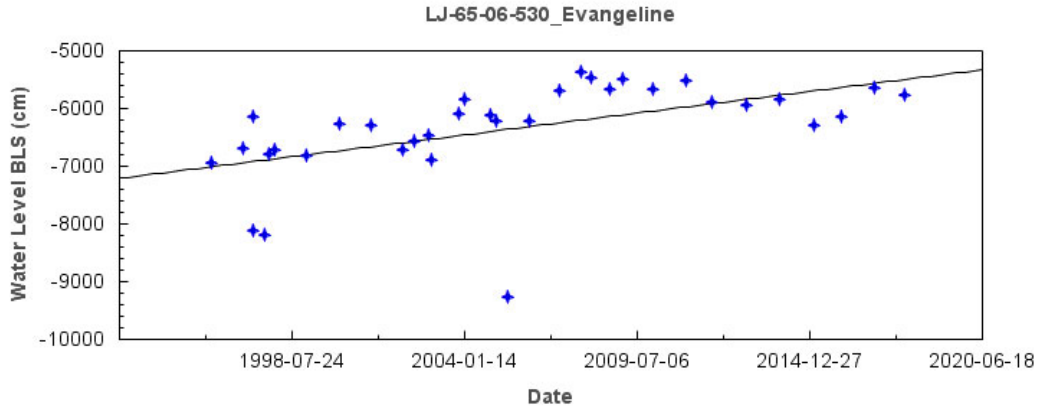
LJ-65-06-530_Evangeline
Water Level BLS (cm)
-5000
-6000
-7000
-8000
-9000
-10000
1998-07-24
2004-01-14
2009-07-06
2014-12-27
2020-06-18
Date

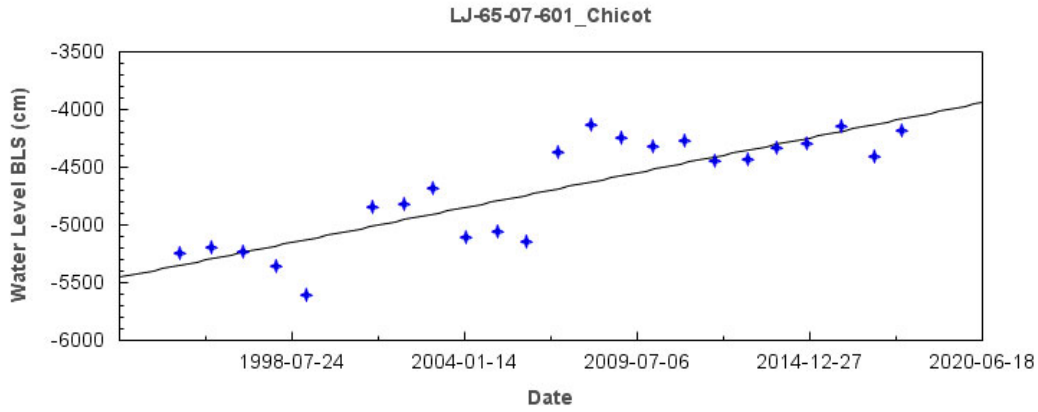
LJ-65-07-601_Chicot
Water Level BLS (cm)
-3500
-4000
-4500
-5000
-5500
-6000
1998-07-24
2004-01-14
2009-07-06
2014-12-27
2020-06-18
Date

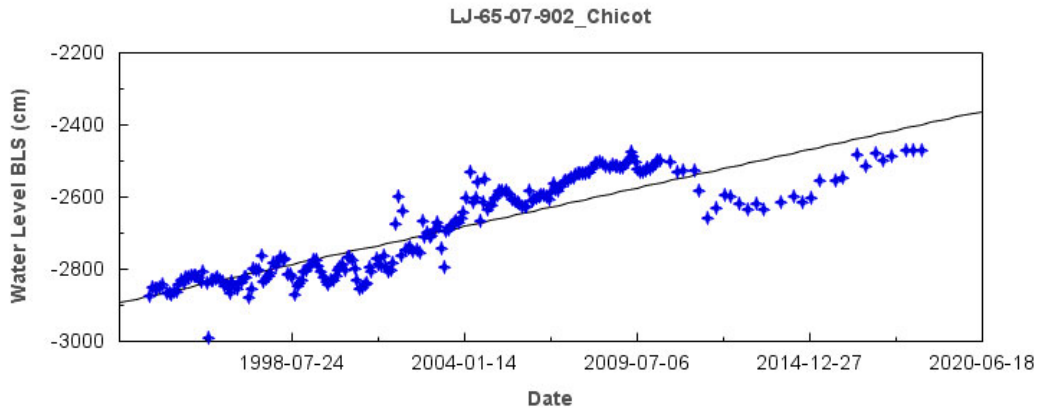
LJ-65-07-902_Chicot
Water Level BLS (cm)
-2200
-2400
-2600
-2800
-3000
1998-07-24
2004-01-14
2009-07-06
2014-12-27
2020-06-18
Date

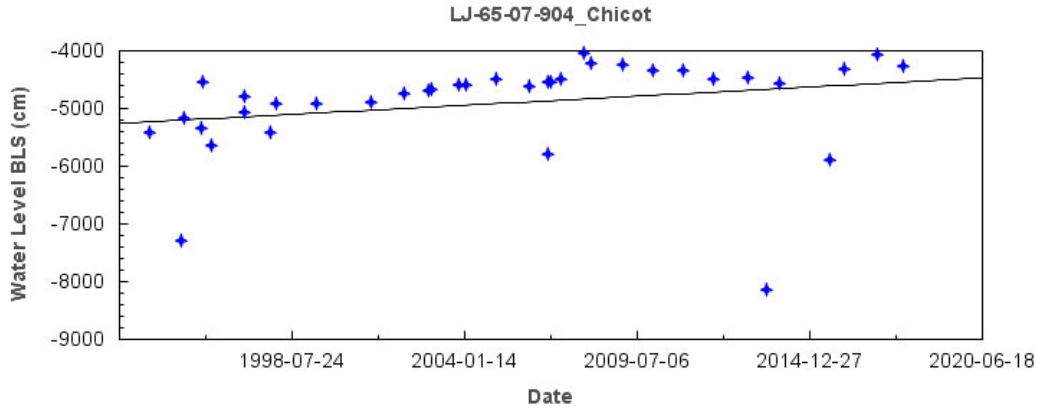
LJ-65-07-904_Chicot
Water Level BLS (cm)
-4000
-5000
-6000
-7000
-8000
-9000
1998-07-24
2004-01-14
2009-07-06
2014-12-27
2020-06-18
Date

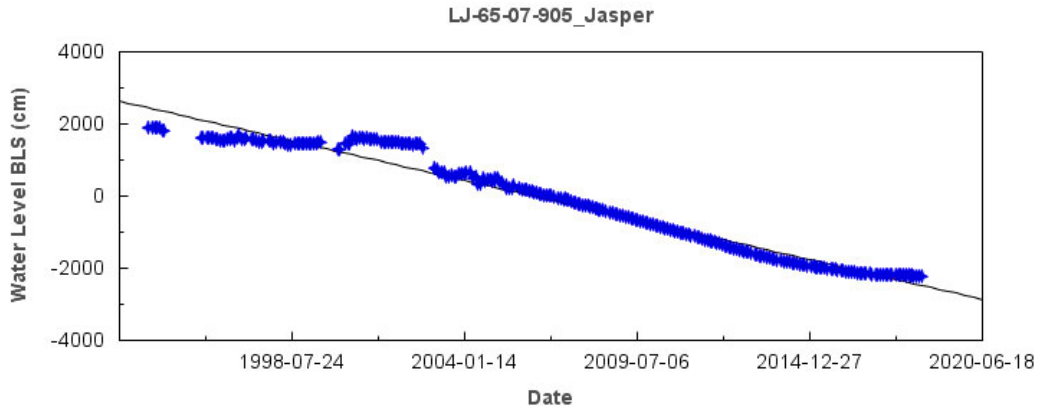
LJ-65-07-905_Jasper
Water Level BLS (cm)
4000
2000
0
-2000
-4000
1998-07-24
2004-01-14
2009-07-06
2014-12-27
2020-06-18
Date

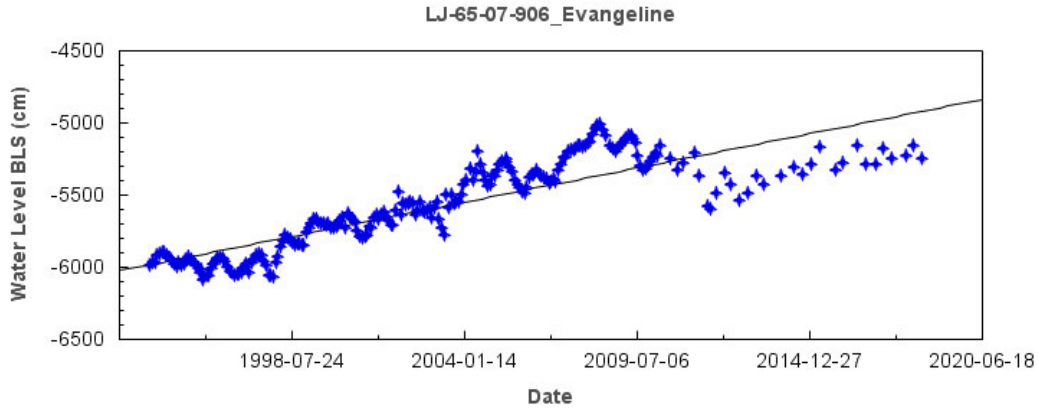
LJ-65-07-906_Evangeline
Water Level BLS (cm)
-4500
-5000
-5500
-6000
-6500
1998-07-24
2004-01-14
2009-07-06
2014-12-27
2020-06-18
Date

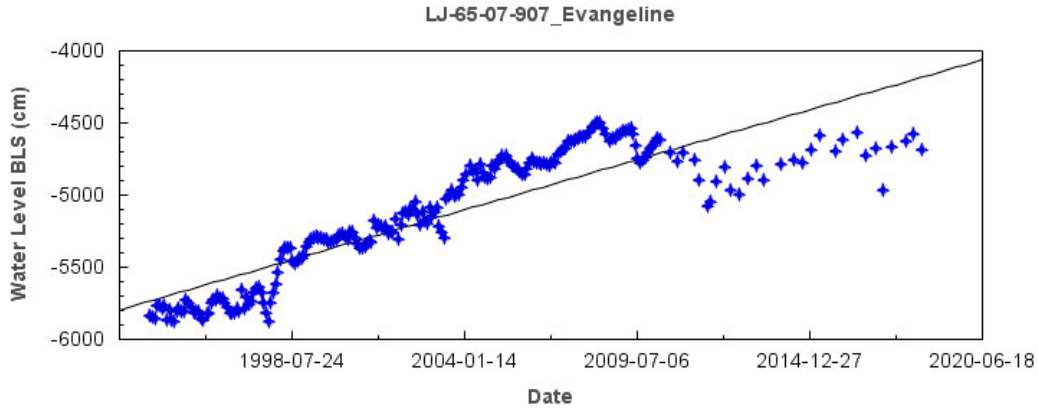
LJ-65-07-907_Evangeline
Water Level BLS (cm)
-4000
-4500
-5000
-5500
-6000
1998-07-24
2004-01-14
2009-07-06
2014-12-27
2020-06-18
Date

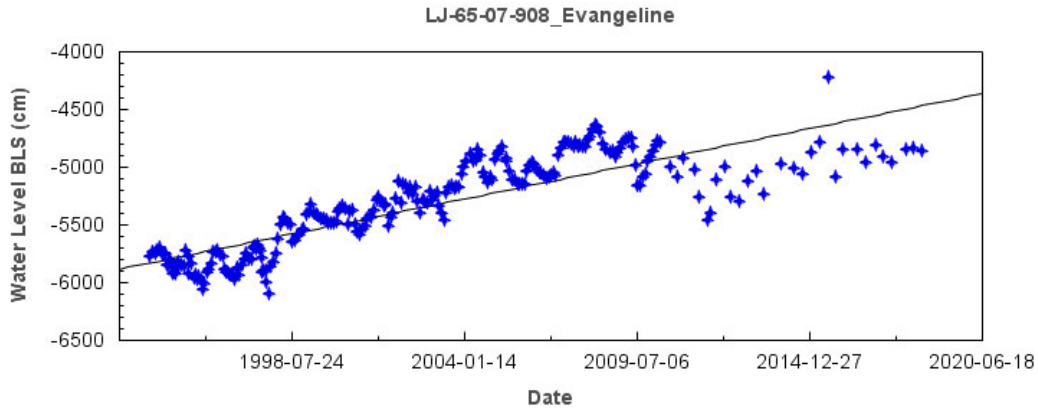
LJ-65-07-908_Evangeline
Water Level BLS (cm)
-4000
-4500
-5000
-5500
-6000
-6500
1998-07-24
2004-01-14
2009-07-06
2014-12-27
2020-06-18
Date

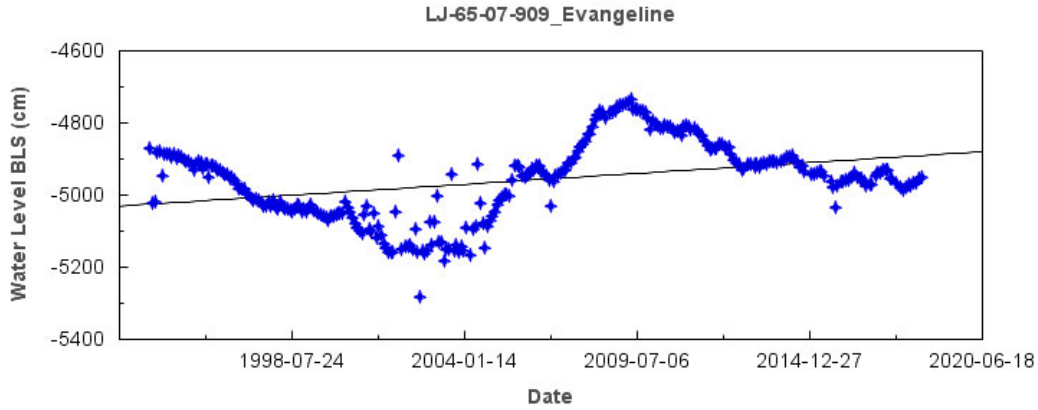
LJ-65-07-909_Evangeline
Water Level BLS (cm)
-4600
-4800
-5000
-5200
-5400
1998-07-24
2004-01-14
2009-07-06
2014-12-27
2020-06-18
Date

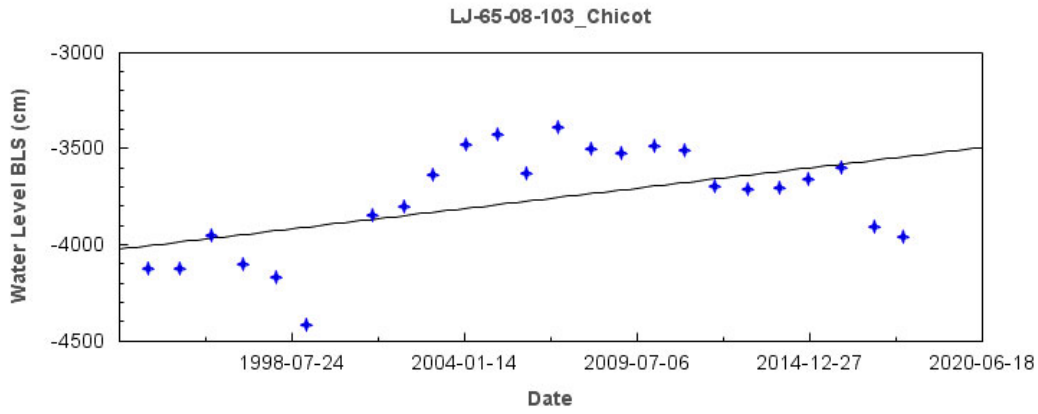
LJ-65-08-103_Chicot
Water Level BLS (cm)
-3000
-3500
-4000
-4500
1998-07-24
2004-01-14
2009-07-06
2014-12-27
2020-06-18
Date

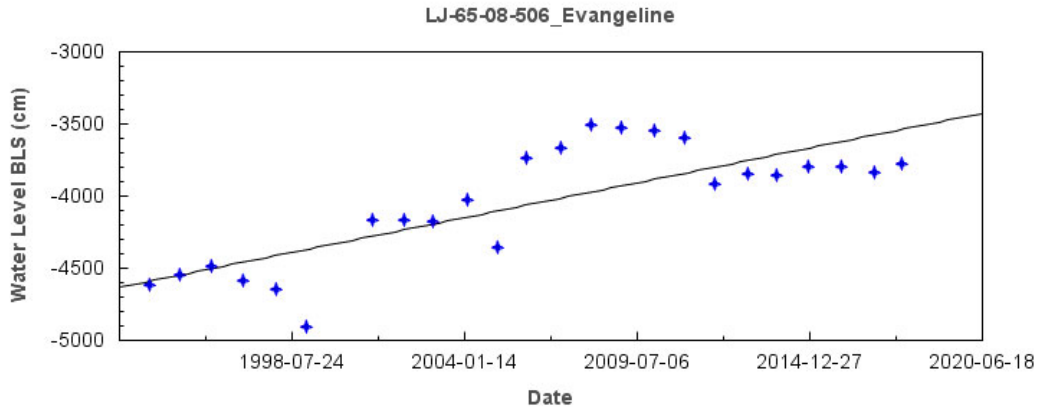
LJ-65-08-506_Evangeline
Water Level BLS (cm)
-3000
-3500
-4000
-4500
-5000
1998-07-24
2004-01-14
2009-07-06
2014-12-27
2020-06-18
Date

USGS Ground Water Monitoring Wells Liberty County

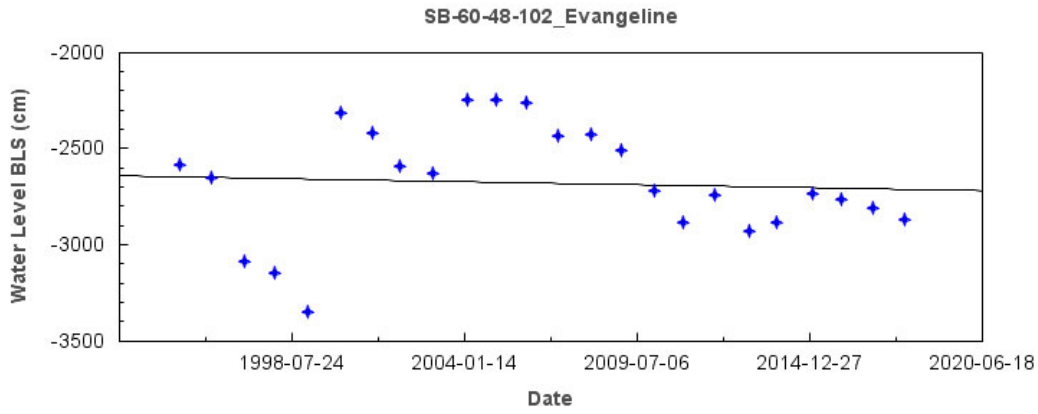

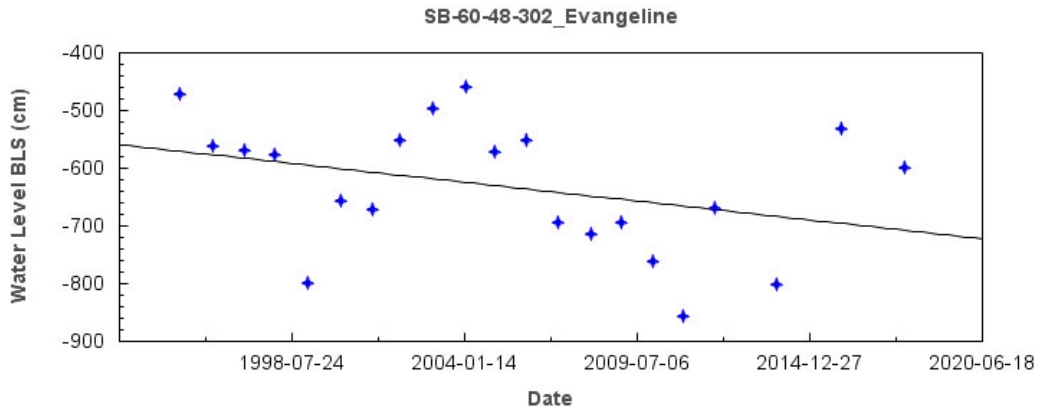

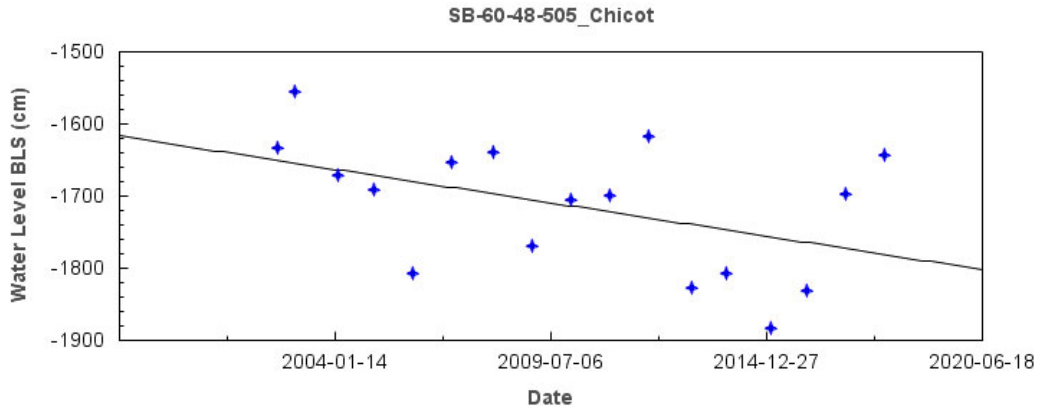

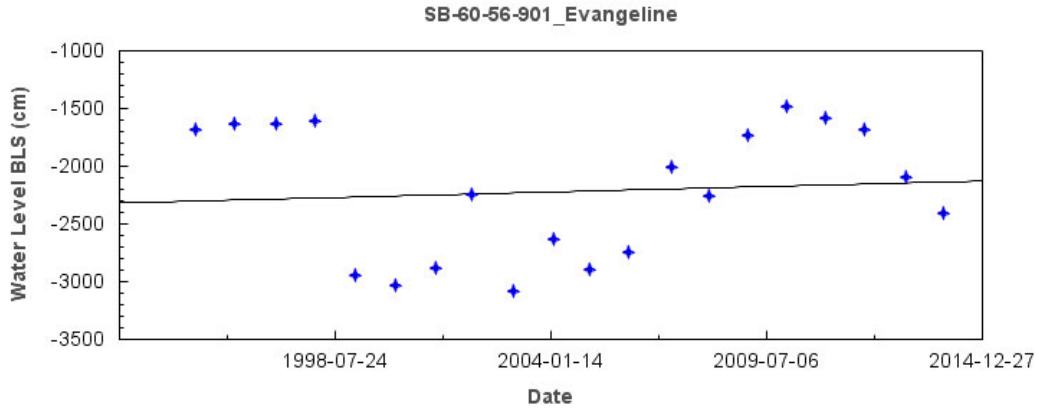
SB-60-56-901_Evangeline
Water Level BLS (cm)
-1000
-1500
-2000
-2500
-3000
-3500
1998-07-24
2004-01-14
2009-07-06
2014-12-27
Date

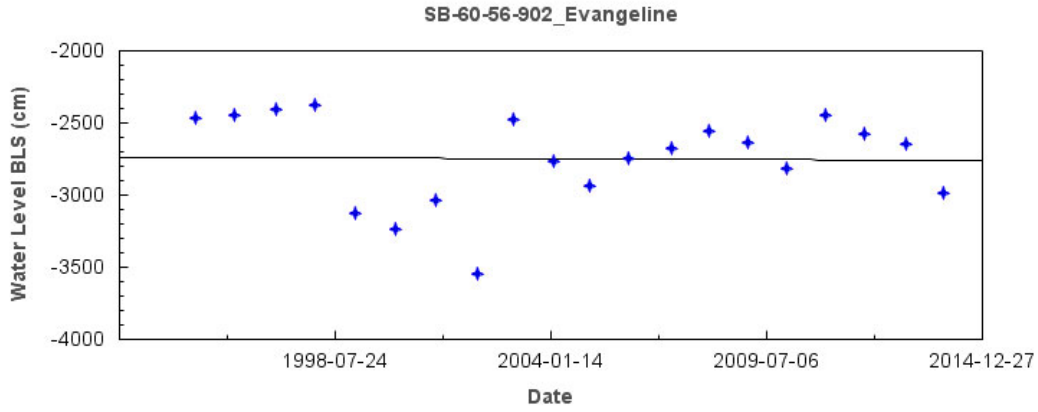
SB-60-56-902_Evangeline
Water Level BLS (cm)
-2000
-2500
-3000
-3500
-4000
1998-07-24
2004-01-14
2009-07-06
2014-12-27
Date

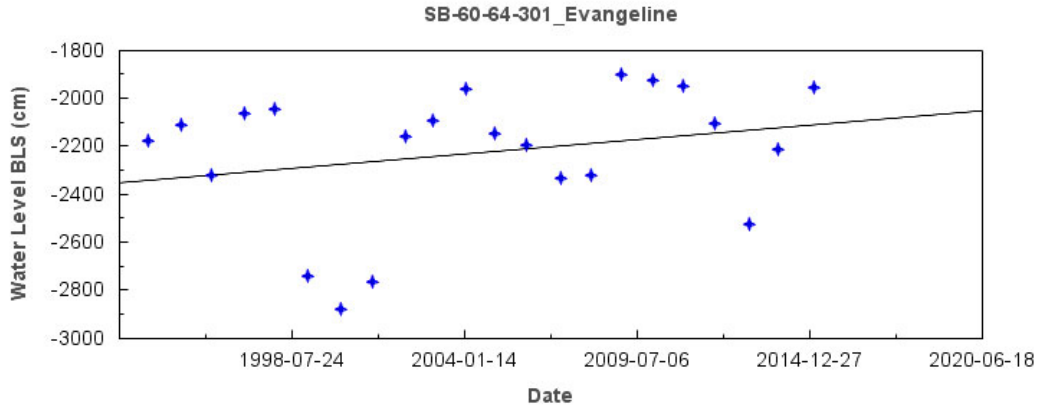
SB-60-64-301_Evangeline
Water Level BLS (cm)
-1800
-2000
-2200
-2400
-2600
-2800
-3000
1998-07-24
2004-01-14
2009-07-06
2014-12-27
2020-06-18
Date

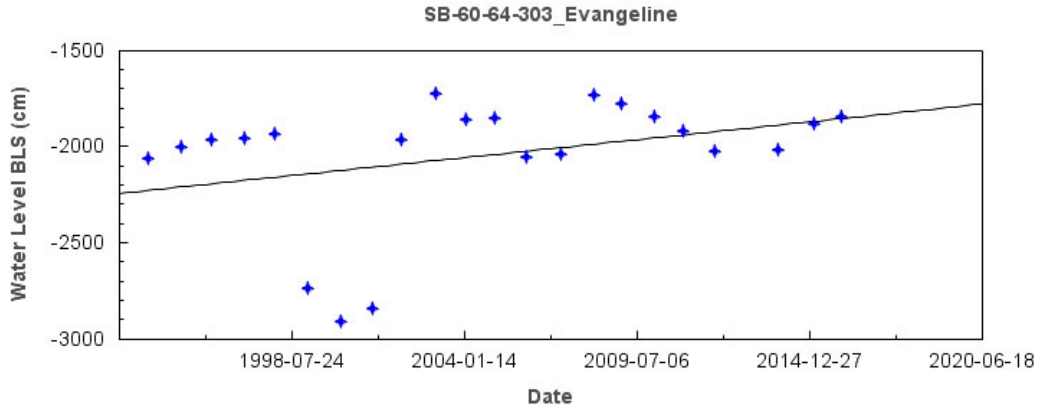
SB-60-64-303_Evangeline
Water Level BLS (cm)
-1500
-2000
-2500
-3000
1998-07-24
2004-01-14
2009-07-06
2014-12-27
2020-06-18
Date

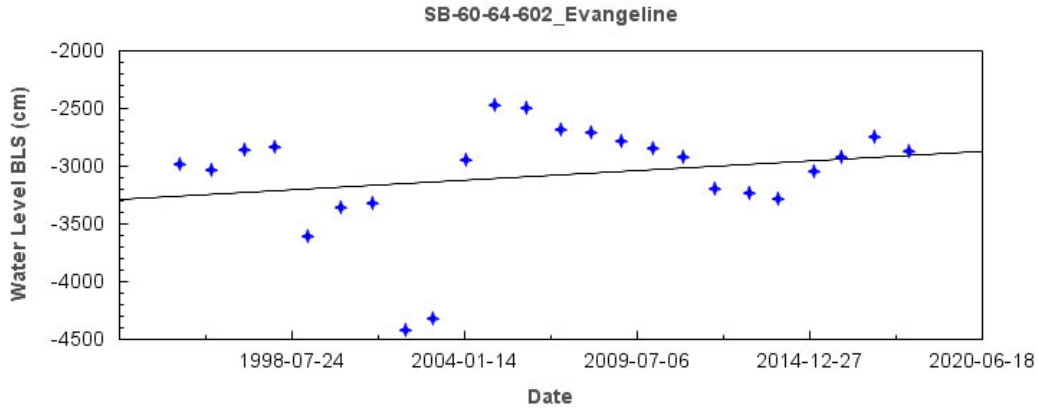
SB-60-64-602_Evangeline
Water Level BLS (cm)
-2000
-2500
-3000
-3500
-4000
-4500
1998-07-24
2004-01-14
2009-07-06
2014-12-27
2020-06-18
Date

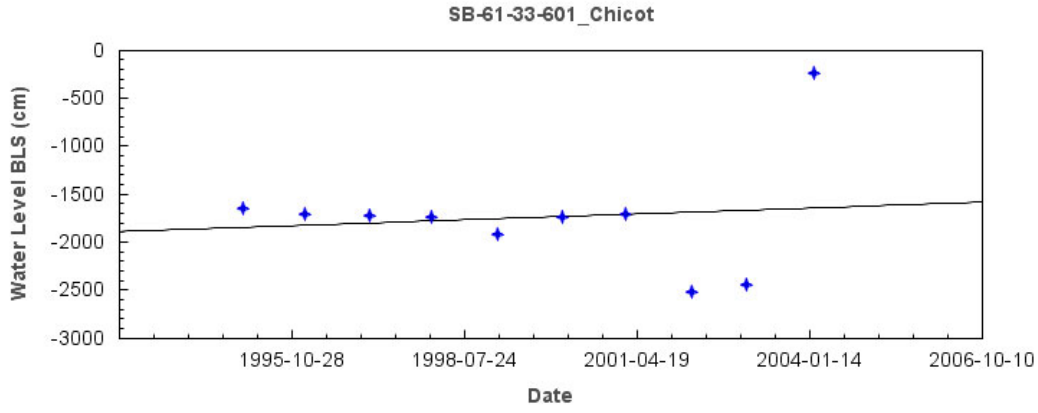
SB-61-33-601_Chicot
Water Level BLS (cm)
0
-500
-1000
-1500
-2000
-2500
-3000
1995-10-28
1998-07-24
2001-04-19
2004-01-14
2006-10-10
Date

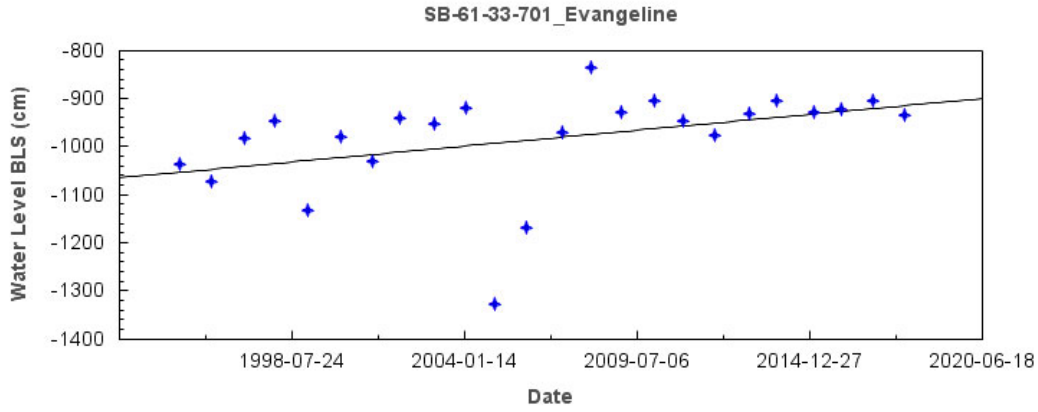
SB-61-33-701_Evangeline
Water Level BLS (cm)
-800
-900
-1000
-1100
-1200
-1300
-1400
1998-07-24
2004-01-14
2009-07-06
2014-12-27
2020-06-18
Date

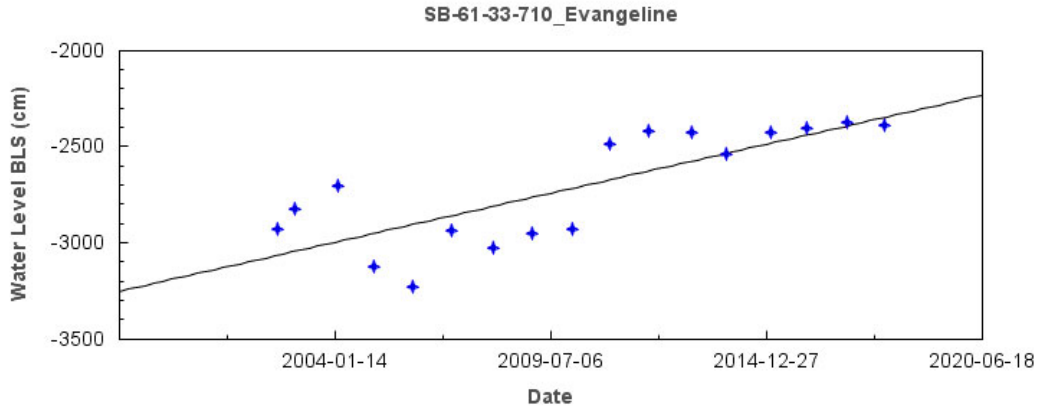
SB-61-33-710_Evangeline
Water Level BLS (cm)
-2000
-2500
-3000
-3500
2004-01-14
2009-07-06
2014-12-27
2020-06-18
Date

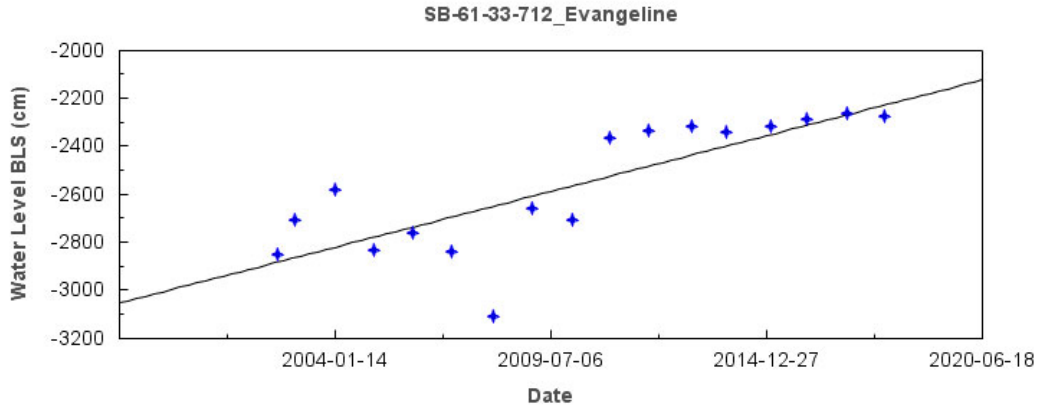
SB-61-33-712_Evangeline
Water Level BLS (cm)
-2000
-2200
-2400
-2600
-2800
-3000
-3200
2004-01-14
2009-07-06
2014-12-27
2020-06-18
Date

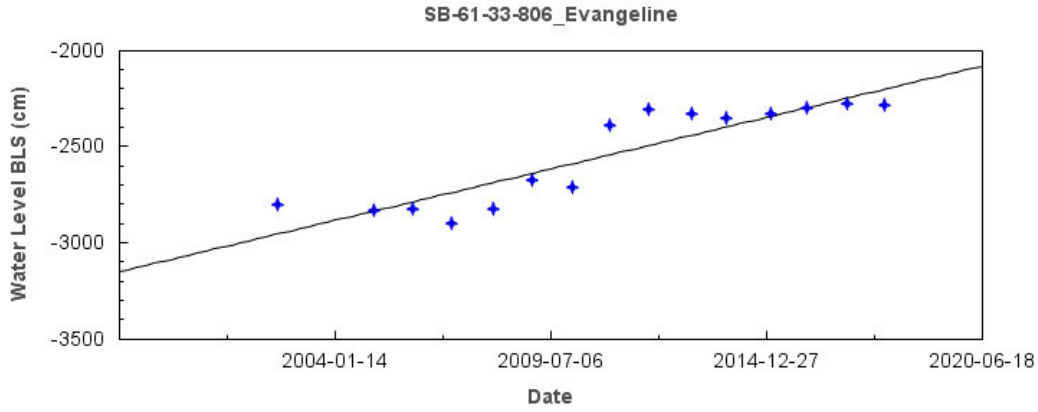
SB-61-33-806_Evangeline
Water Level BLS (cm)
-2000
-2500
-3000
-3500
2004-01-14
2009-07-06
2014-12-27
2020-06-18
Date

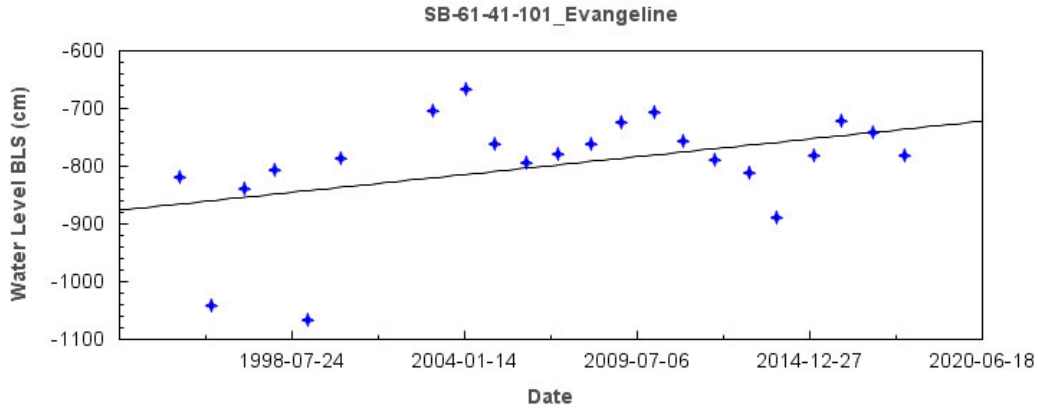
SB-61-41-101_Evangeline
Water Level BLS (cm)
-600
-700
-800
-900
-1000
-1100
1998-07-24
2004-01-14
2009-07-06
2014-12-27
2020-06-18
Date

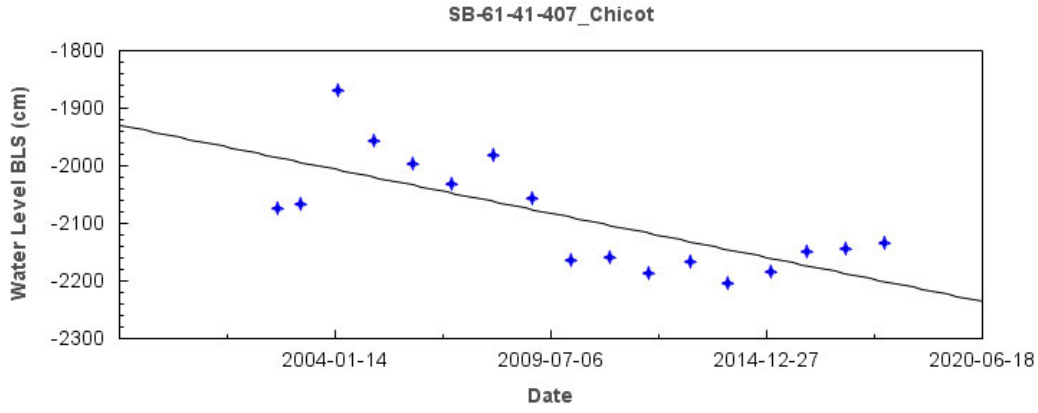
SB-61-41-407_Chicot
Water Level BLS (cm)
-1800
-1900
-2000
-2100
-2200
-2300
2004-01-14
2009-07-06
2014-12-27
2020-06-18
Date

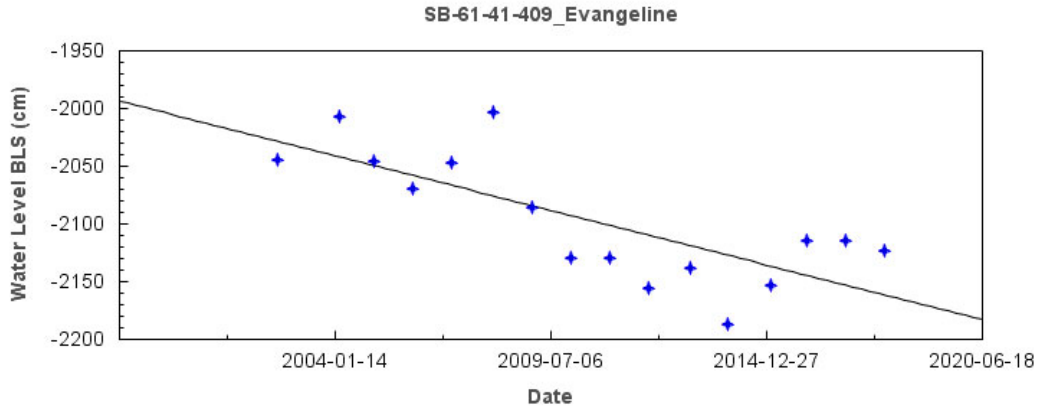
SB-61-41-409_Evangeline
Water Level BLS (cm)
-1950
-2000
-2050
-2100
-2150
-2200
2004-01-14
2009-07-06
2014-12-27
2020-06-18
Date

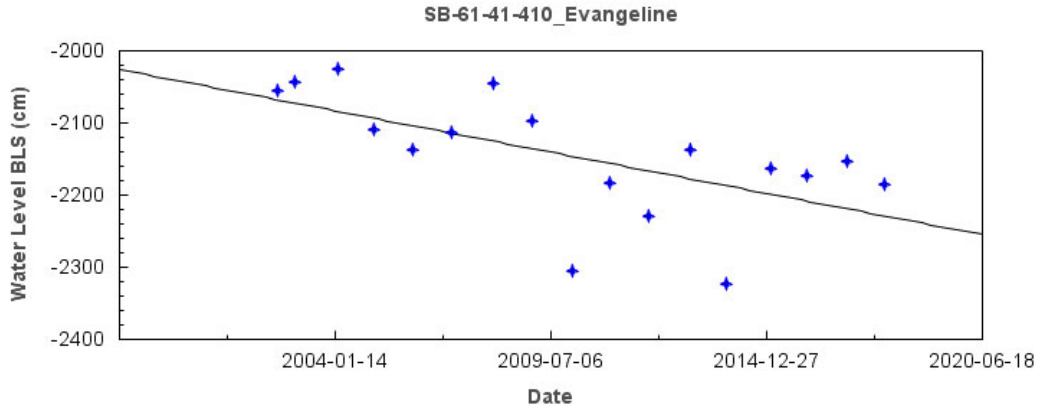
SB-61-41-410_Evangeline
Water Level BLS (cm)
-2000
-2100
-2200
-2300
-2400
2004-01-14
2009-07-06
2014-12-27
2020-06-18
Date

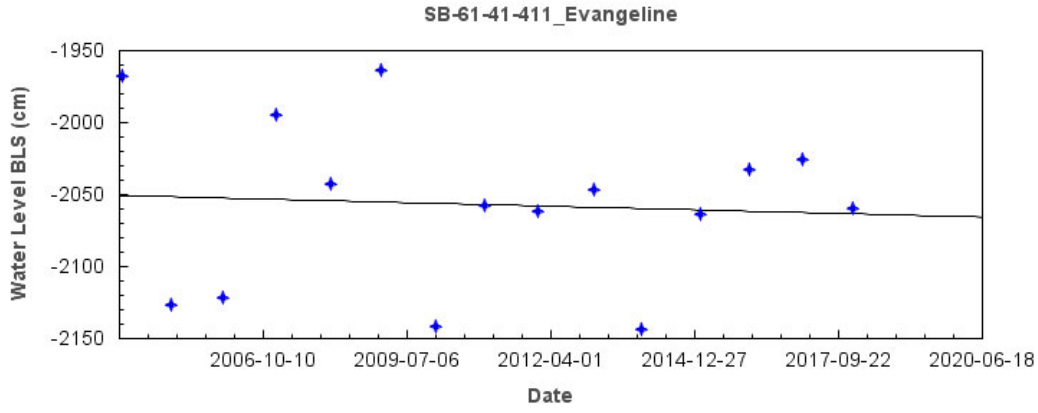
SB-61-41-411_Evangeline
Water Level BLS (cm)
-1950
-2000
-2050
-2100
-2150
2006-10-10
2009-07-06
2012-04-01
2014-12-27
2017-09-22
2020-06-18
Date

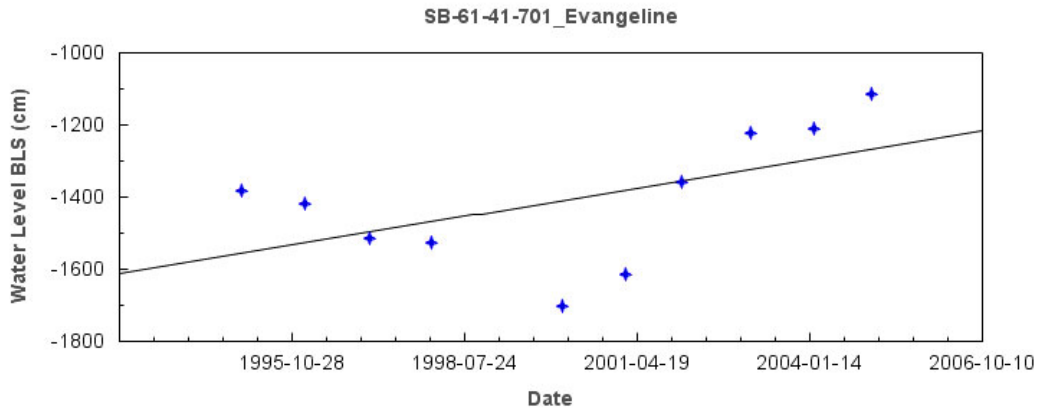
SB-61-41-701_Evangeline
Water Level BLS (cm)
-1000
-1200
-1400
-1600
-1800
1995-10-28
1998-07-24
2001-04-19
2004-01-14
2006-10-10
Date

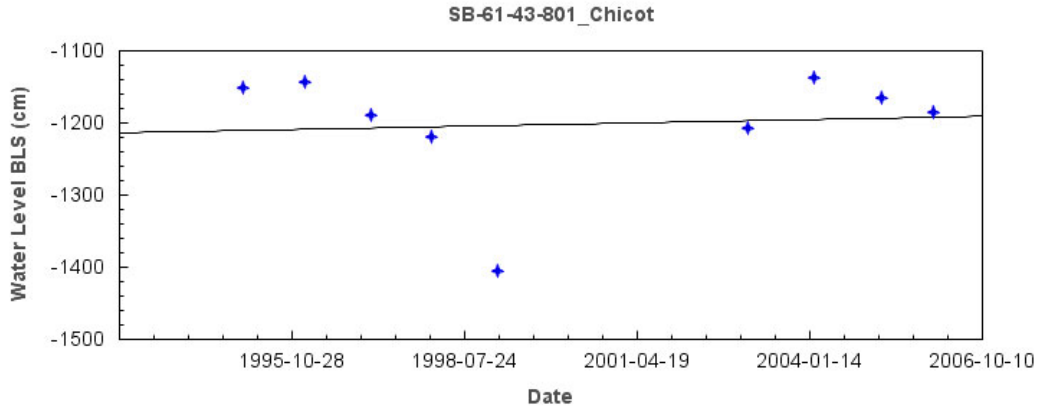
SB-61-43-801_Chicot
Water Level BLS (cm)
-1100
-1200
-1300
-1400
-1500
1995-10-28
1998-07-24
2001-04-19
2004-01-14
2006-10-10
Date

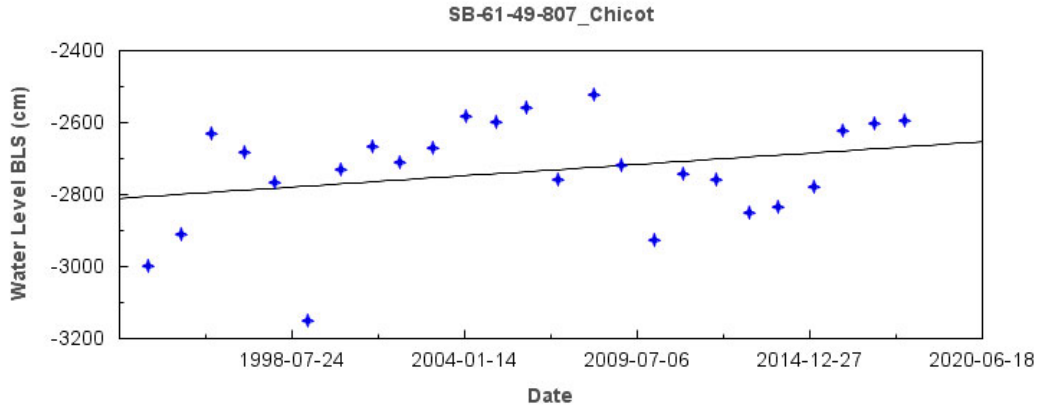
SB-61-49-807_Chicot
Water Level BLS (cm)
-2400
-2600
-2800
-3000
-3200
1998-07-24
2004-01-14
2009-07-06
2014-12-27
2020-06-18
Date

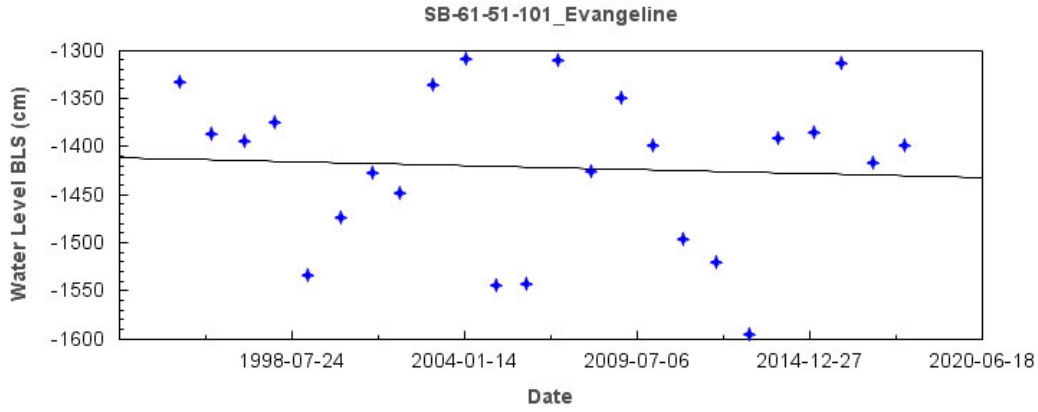
SB-61-51-101_Evangeline
Water Level BLS (cm)
-1300
-1350
-1400
-1450
-1500
-1550
-1600
1998-07-24
2004-01-14
2009-07-06
2014-12-27
2020-06-18
Date

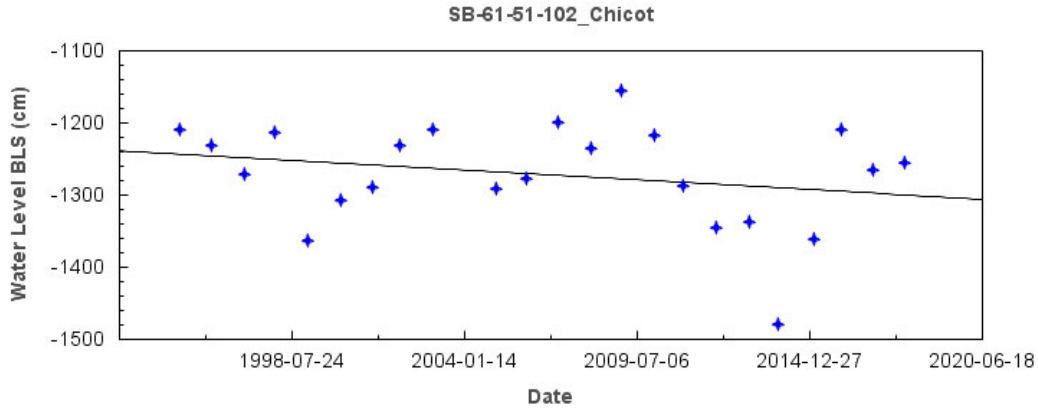
SB-61-51-102_Chicot
Water Level BLS (cm)
-1100
-1200
-1300
-1400
-1500
1998-07-24
2004-01-14
2009-07-06
2014-12-27
2020-06-18
Date

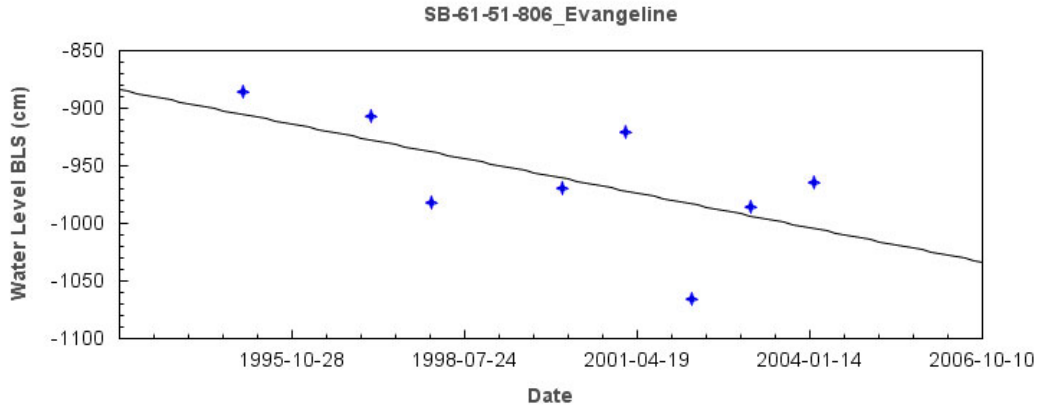
SB-61-51-806_Evangeline
Water Level BLS (cm)
-850
-900
-950
-1000
-1050
-1100
1995-10-28
1998-07-24
2001-04-19
2004-01-14
2006-10-10
Date

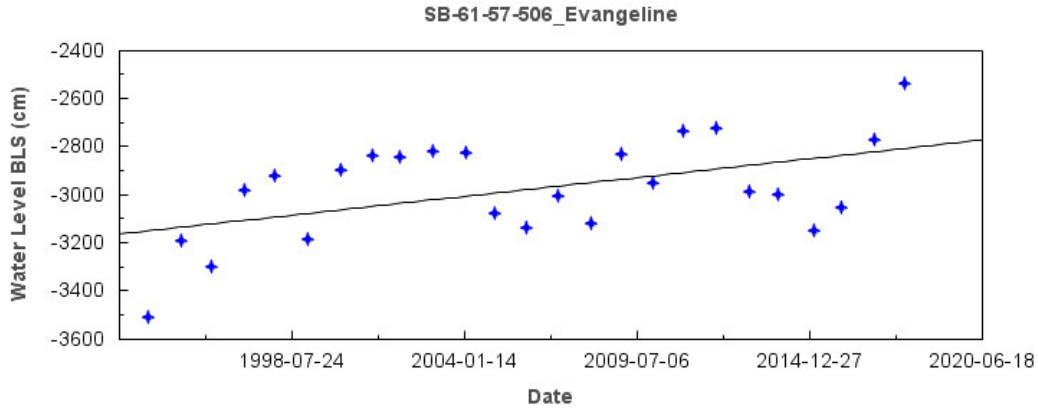
SB-61-57-506_Evangeline
Water Level BLS (cm)
-2400
-2600
-2800
-3000
-3200
-3400
-3600
1998-07-24
2004-01-14
2009-07-06
2014-12-27
2020-06-18
Date

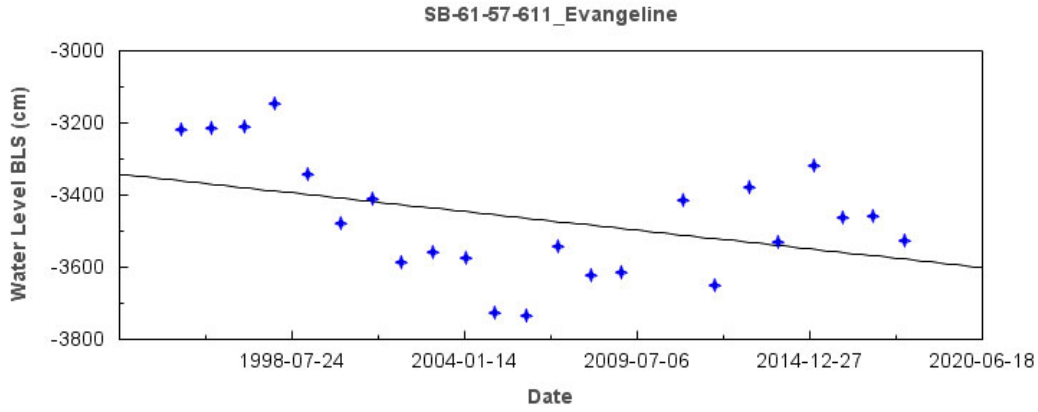
SB-61-57-611_Evangeline
Water Level BLS (cm)
-3000
-3200
-3400
-3600
-3800
1998-07-24
2004-01-14
2009-07-06
2014-12-27
2020-06-18
Date

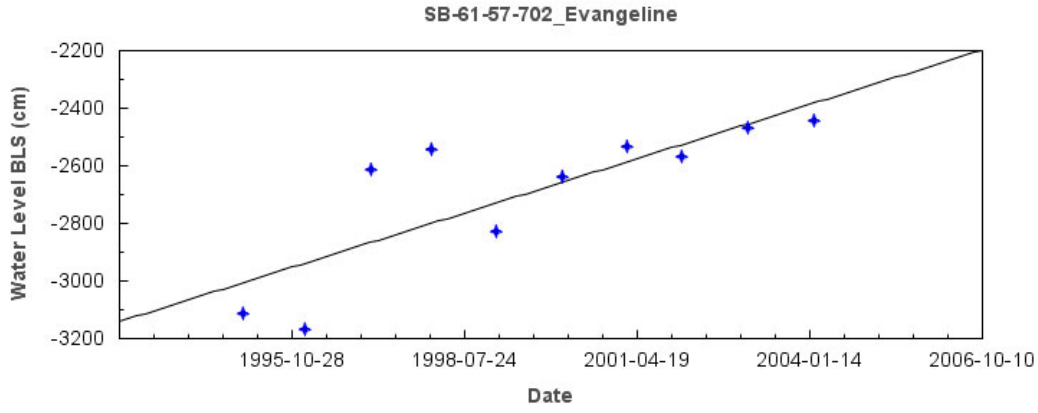
SB-61-57-702_Evangeline
Water Level BLS (cm)
-2200
-2400
-2600
-2800
-3000
-3200
1995-10-28
1998-07-24
2001-04-19
2004-01-14
2006-10-10
Date

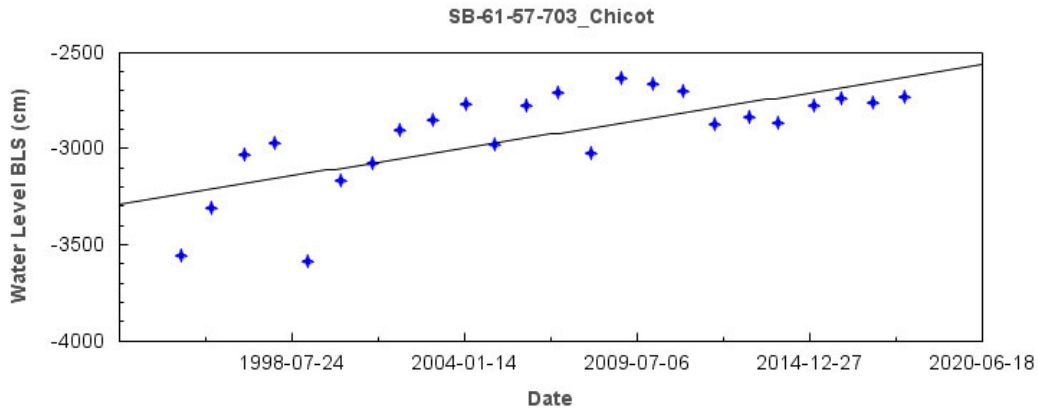
SB-61-57-703_Chicot
Water Level BLS (cm)
-2500
-3000
-3500
-4000
1998-07-24
2004-01-14
2009-07-06
2014-12-27
2020-06-18
Date

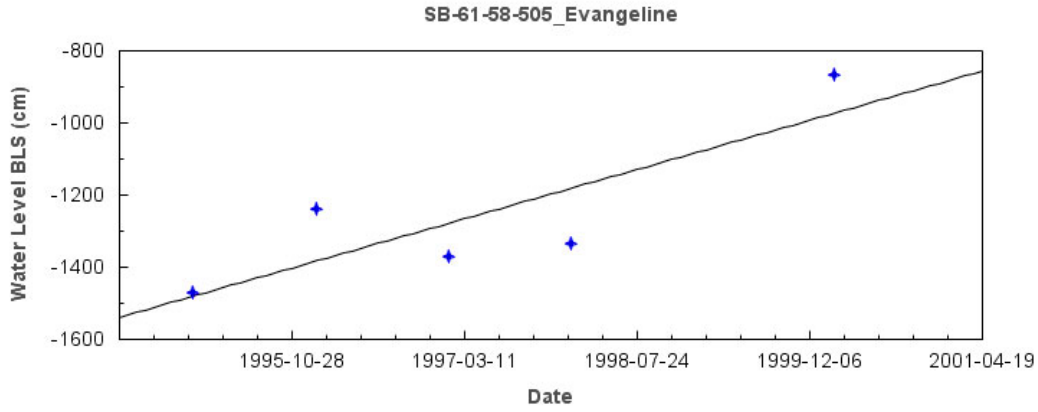
SB-61-58-505_Evangeline
Water Level BLS (cm)
-800
-1000
-1200
-1400
-1600
1995-10-28
1997-03-11
1998-07-24
1999-12-06
2001-04-19
Date

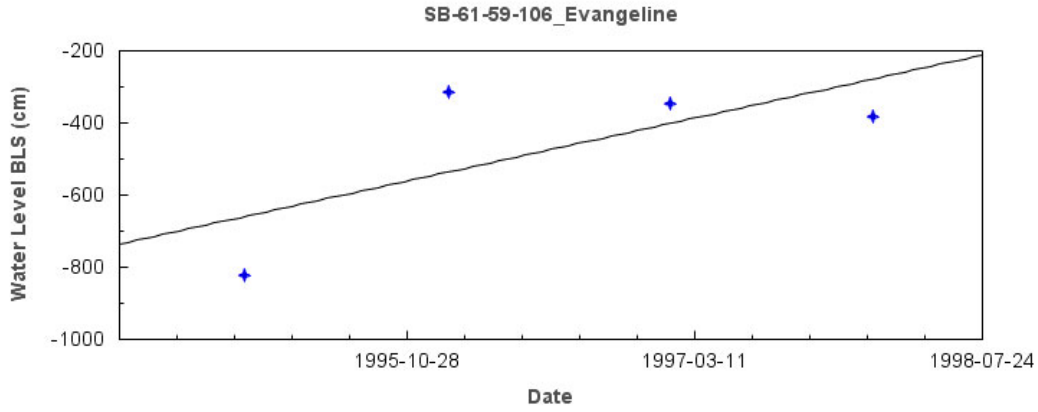
SB-61-59-106_Evangeline
Water Level BLS (cm)
-200
-400
-600
-800
-1000
1995-10-28
1997-03-11
1998-07-24
Date

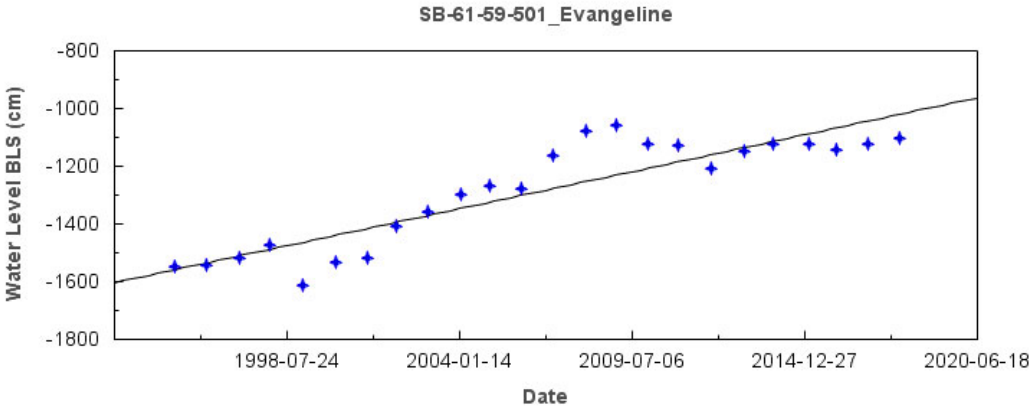
SB-61-59-501_Evangeline
Water Level BLS (cm)
-800
-1000
-1200
-1400
-1600
-1800
1998-07-24
2004-01-14
2009-07-06
2014-12-27
2020-06-18
Date

USGS Ground Water Monitoring Wells Montgomery County

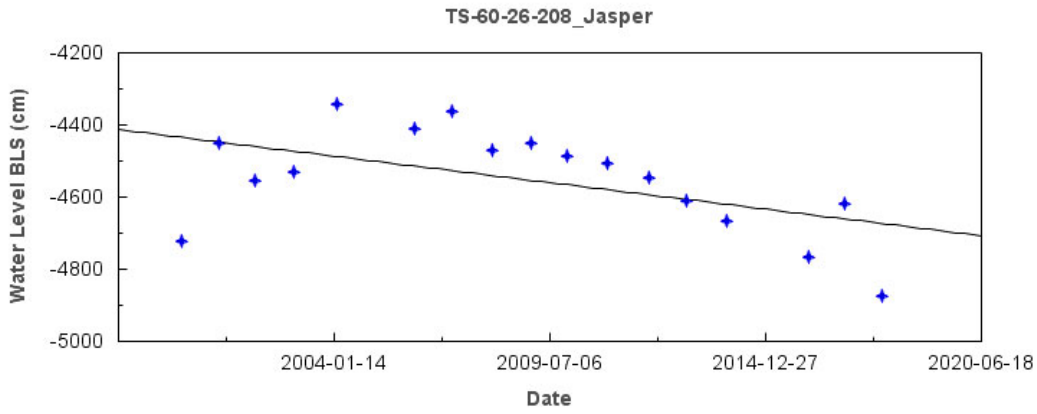

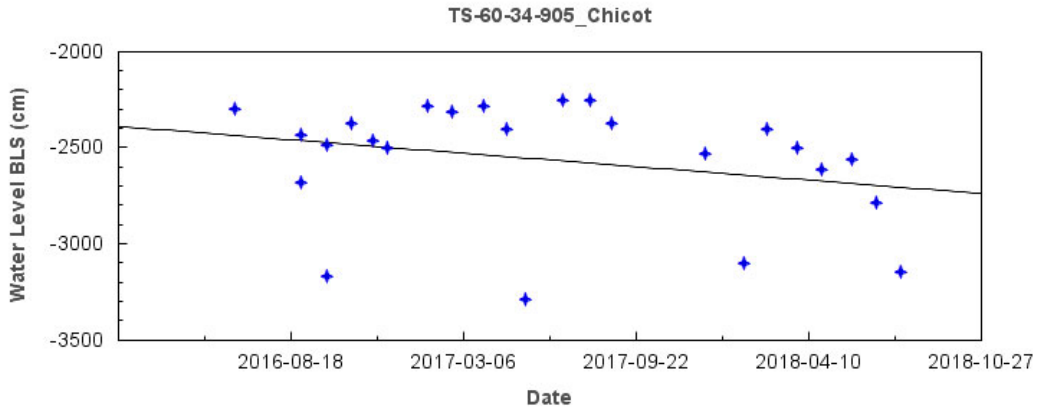

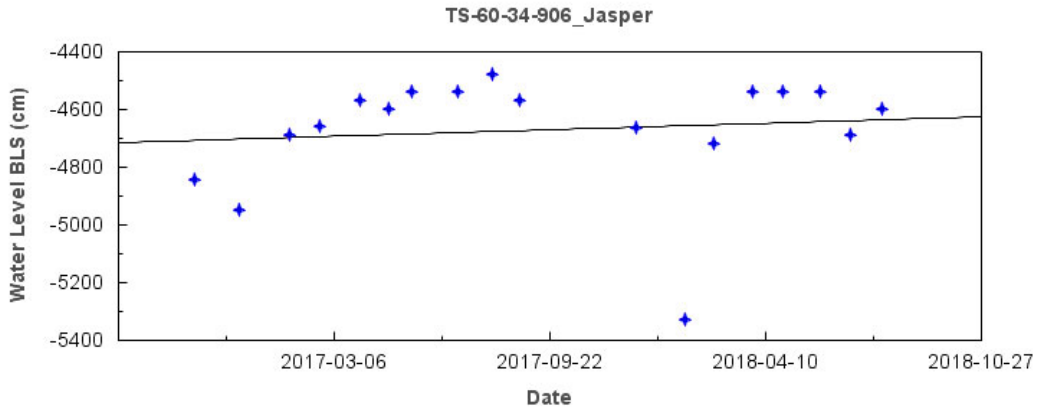

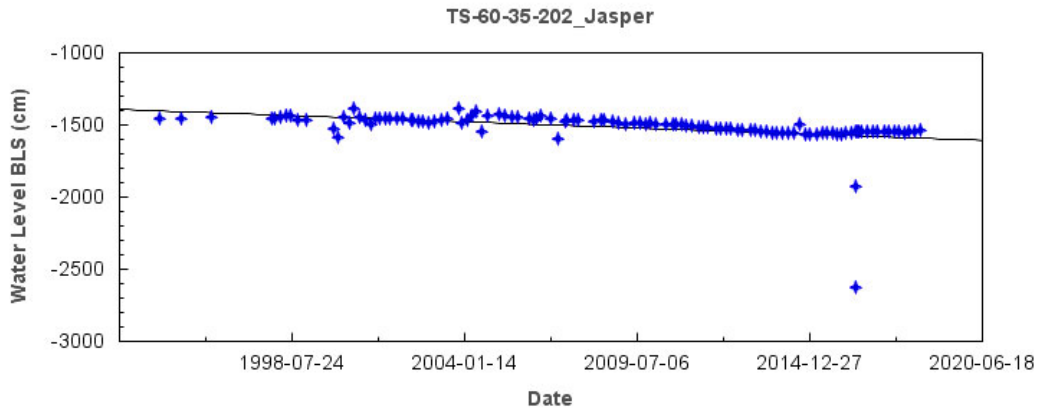
TS-60-35-202_Jasper
Water Level BLS (cm)
-1000
-1500
-2000
-2500
-3000
1998-07-24
2004-01-14
2009-07-06
2014-12-27
2020-06-18
Date

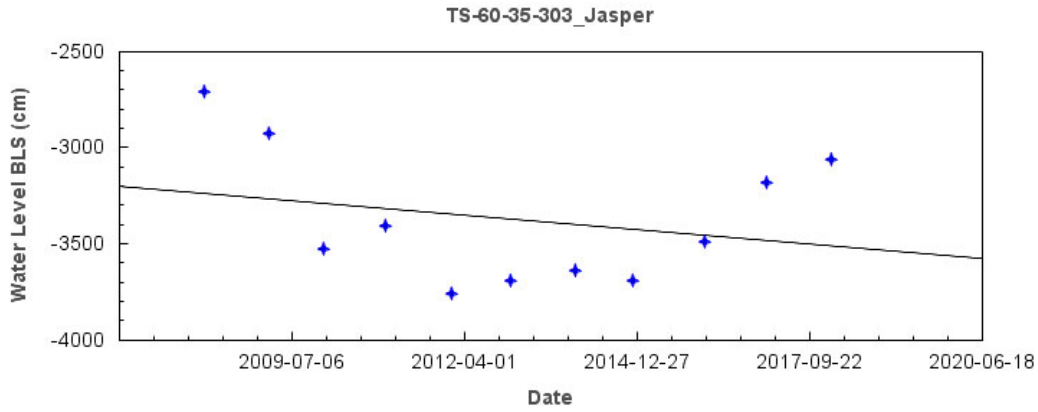
TS-60-35-303_Jasper
Water Level BLS (cm)
-2500
-3000
-3500
-4000
2009-07-06
2012-04-01
2014-12-27
2017-09-22
2020-06-18
Date

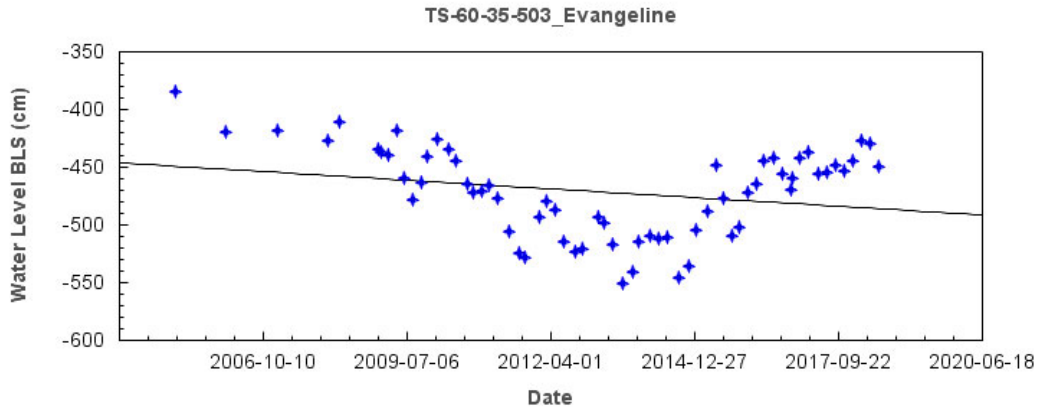
TS-60-35-503_Evangeline
Water Level BLS (cm)
-350
-400
-450
-500
-550
-600
2006-10-10
2009-07-06
2012-04-01
2014-12-27
2017-09-22
2020-06-18
Date

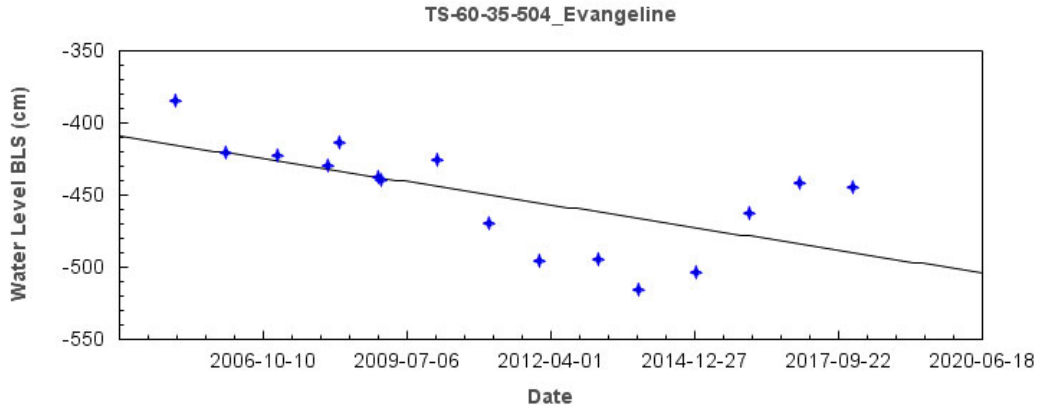
TS-60-35-504_Evangeline
Water Level BLS (cm)
-350
-400
-450
-500
-550
2006-10-10
2009-07-06
2012-04-01
2014-12-27
2017-09-22
2020-06-18
Date

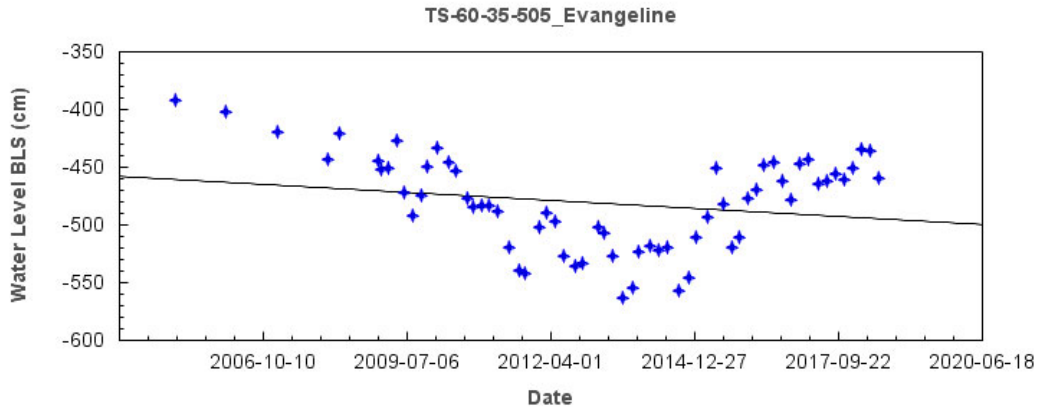
TS-60-35-505_Evangeline
Water Level BLS (cm)
-350
-400
-450
-500
-550
-600
2006-10-10
2009-07-06
2012-04-01
2014-12-27
2017-09-22
2020-06-18
Date

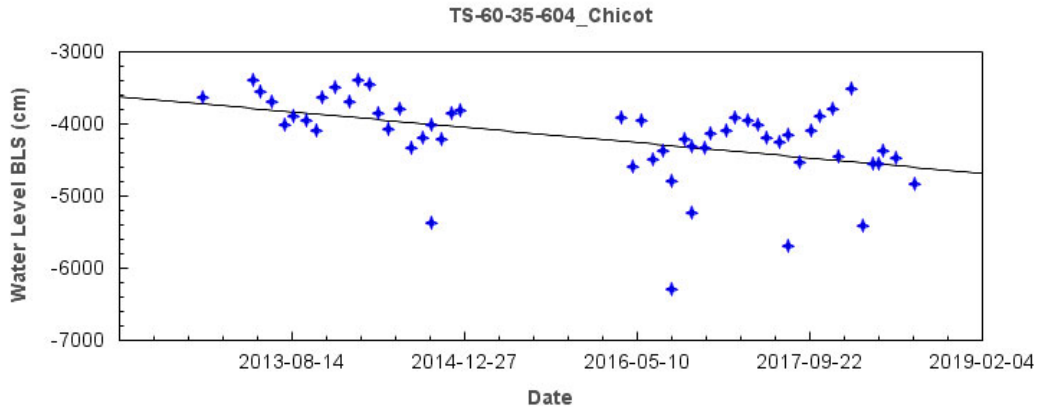
TS-60-35-604_Chicot
Water Level BLS (cm)
-3000
-4000
-5000
-6000
-7000
2013-08-14
2014-12-27
2016-05-10
2017-09-22
2019-02-04
Date

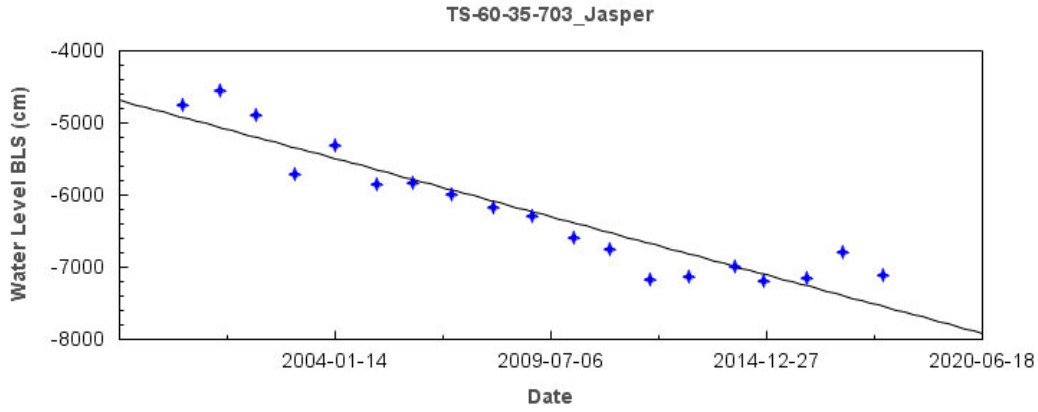
TS-60-35-703_Jasper
Water Level BLS (cm)
-4000
-5000
-6000
-7000
-8000
2004-01-14
2009-07-06
2014-12-27
2020-06-18
Date

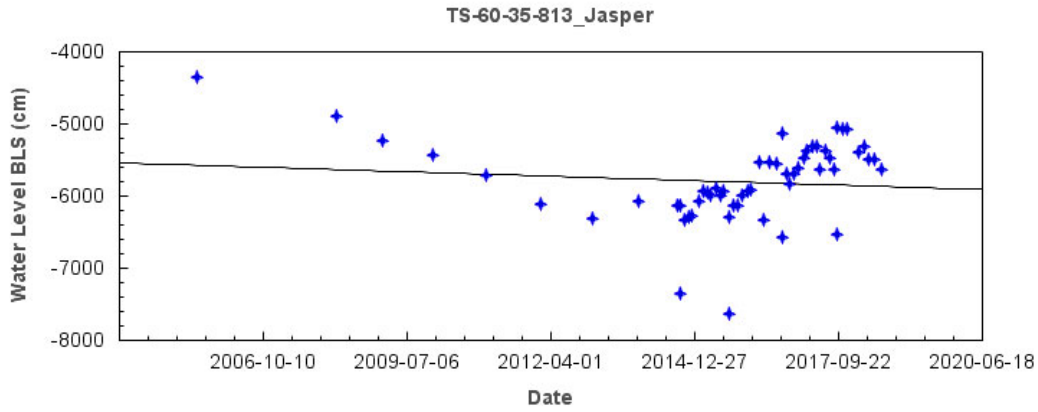
TS-60-35-813_Jasper
Water Level BLS (cm)
-4000
-5000
-6000
-7000
-8000
2006-10-10
2009-07-06
2012-04-01
2014-12-27
2017-09-22
2020-06-18
Date

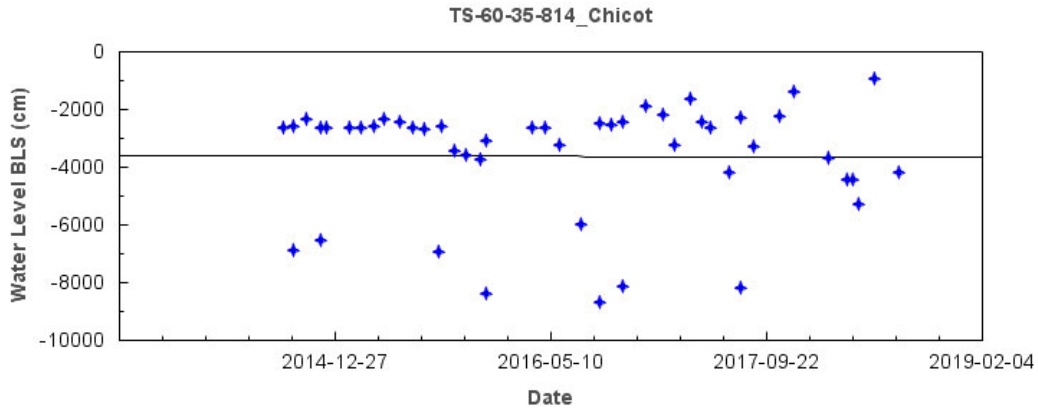
TS-60-35-814_Chicot
Water Level BLS (cm)
0
-2000
-4000
-6000
-8000
-10000
2014-12-27
2016-05-10
2017-09-22
2019-02-04
Date

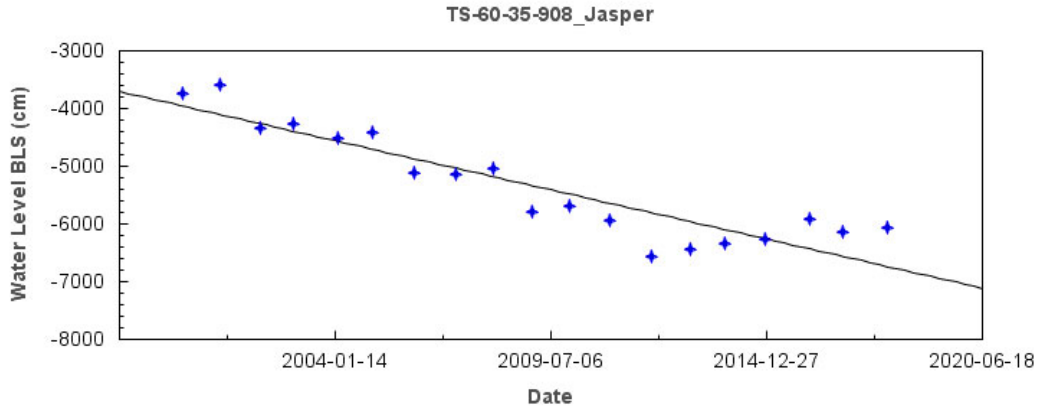
TS-60-35-908_Jasper
Water Level BLS (cm)
-3000
-4000
-5000
-6000
-7000
-8000
2004-01-14
2009-07-06
2014-12-27
2020-06-18
Date

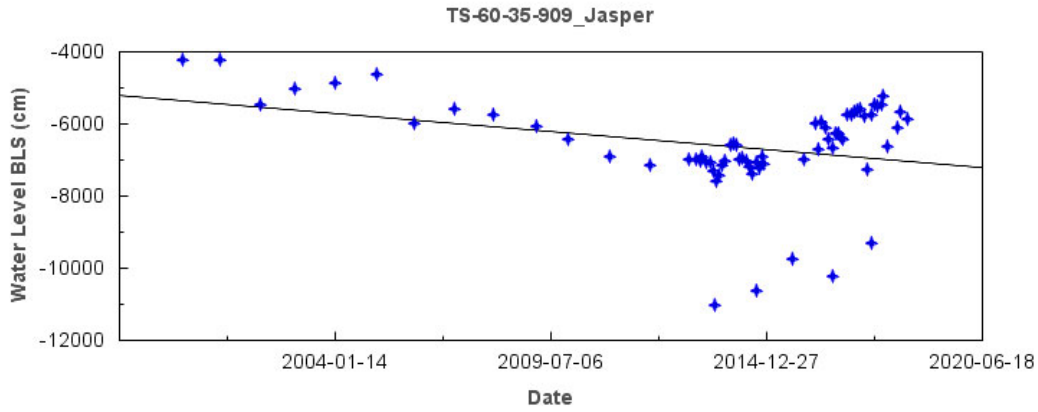
TS-60-35-909_Jasper
Water Level BLS (cm)
-4000
-6000
-8000
-10000
-12000
2004-01-14
2009-07-06
2014-12-27
2020-06-18
Date

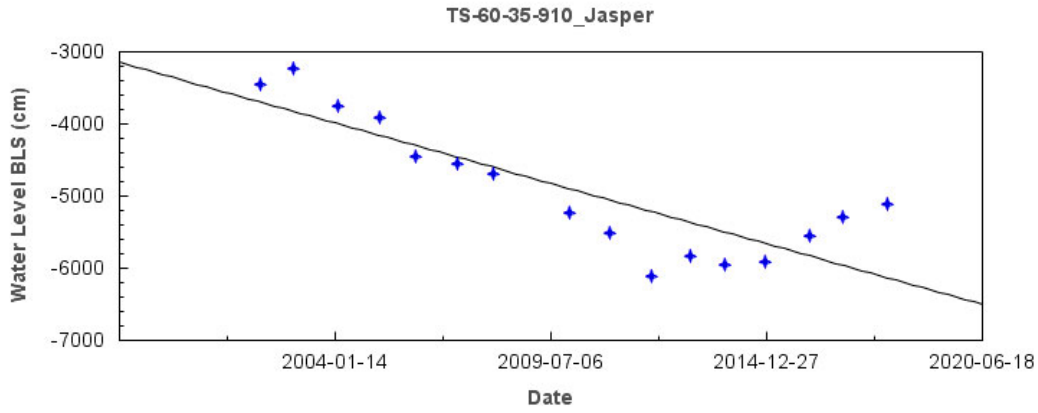
TS-60-35-910_Jasper
Water Level BLS (cm)
-3000
-4000
-5000
-6000
-7000
2004-01-14
2009-07-06
2014-12-27
2020-06-18
Date

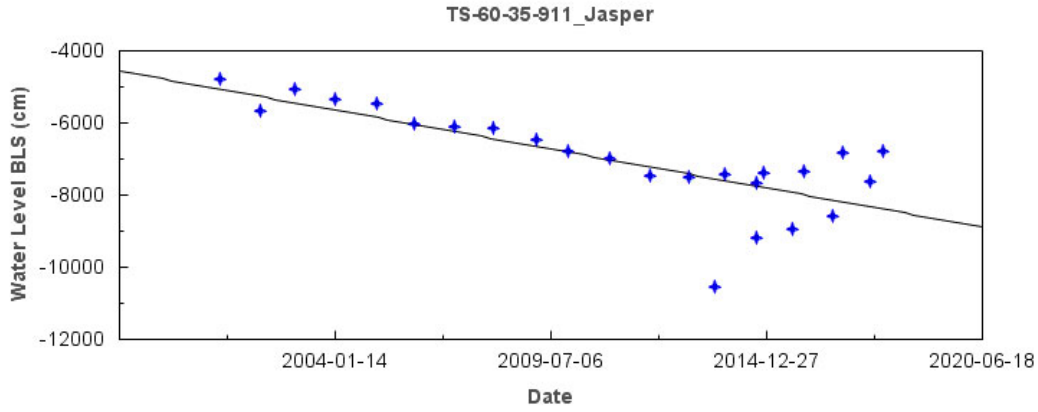
TS-60-35-911_Jasper
Water Level BLS (cm)
-4000
-6000
-8000
-10000
-12000
2004-01-14
2009-07-06
2014-12-27
2020-06-18
Date

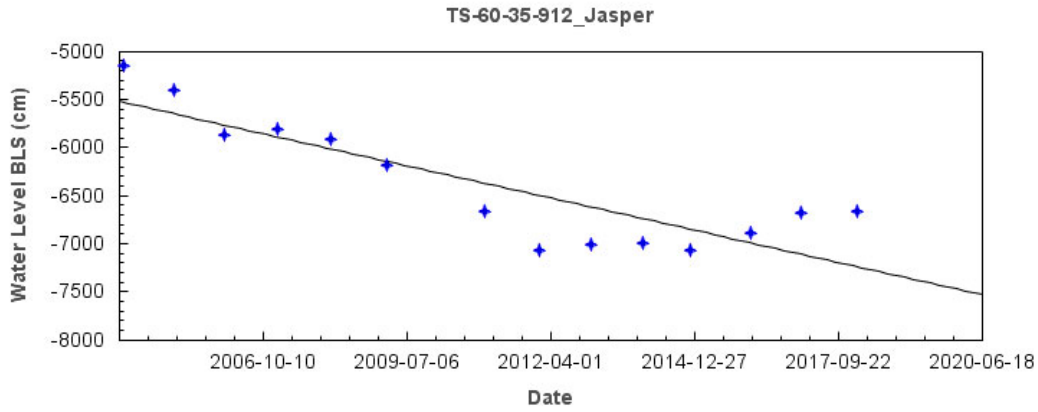
TS-60-35-912_Jasper
Water Level BLS (cm)
-5000
-5500
-6000
-6500
-7000
-7500
-8000
2006-10-10
2009-07-06
2012-04-01
2014-12-27
2017-09-22
2020-06-18
Date

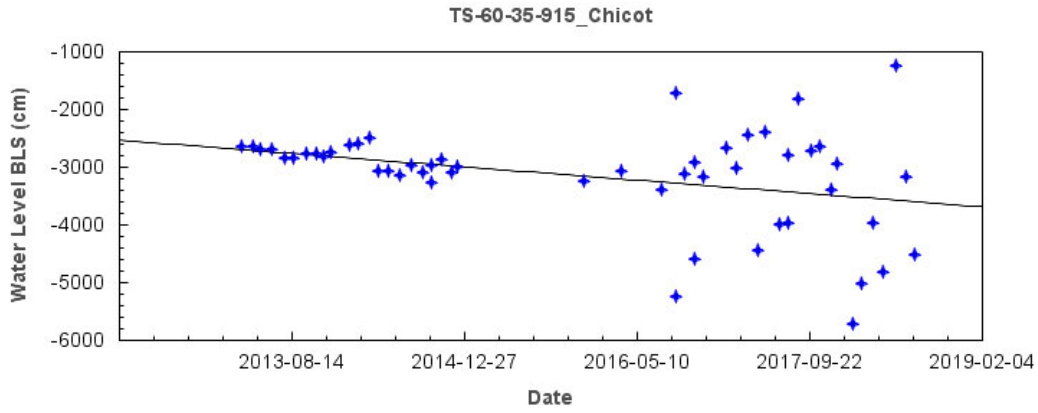
TS-60-35-915_Chicot
Water Level BLS (cm)
-1000
-2000
-3000
-4000
-5000
-6000
2013-08-14
2014-12-27
2016-05-10
2017-09-22
2019-02-04
Date

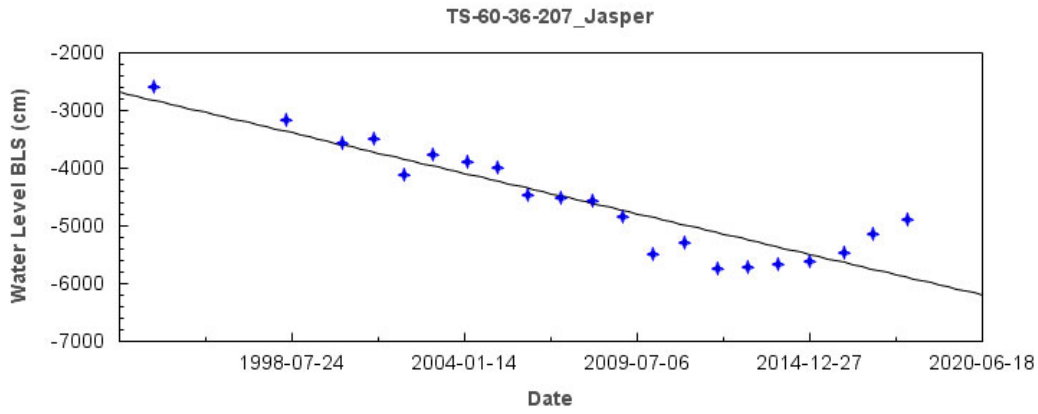
TS-60-36-207_Jasper
Water Level BLS (cm)
-2000
-3000
-4000
-5000
-6000
-7000
1998-07-24
2004-01-14
2009-07-06
2014-12-27
2020-06-18
Date

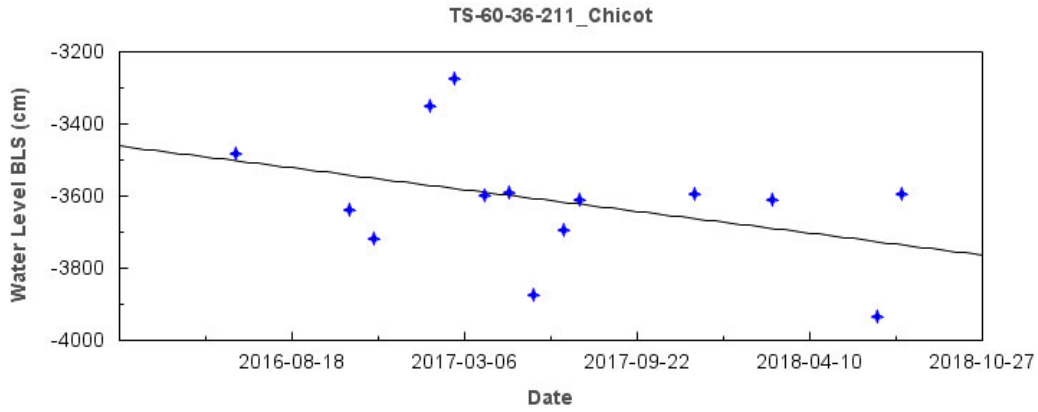
TS-60-36-211_Chicot
Water Level BLS (cm)
-3200
-3400
-3600
-3800
-4000
2016-08-18
2017-03-06
2017-09-22
2018-04-10
2018-10-27
Date

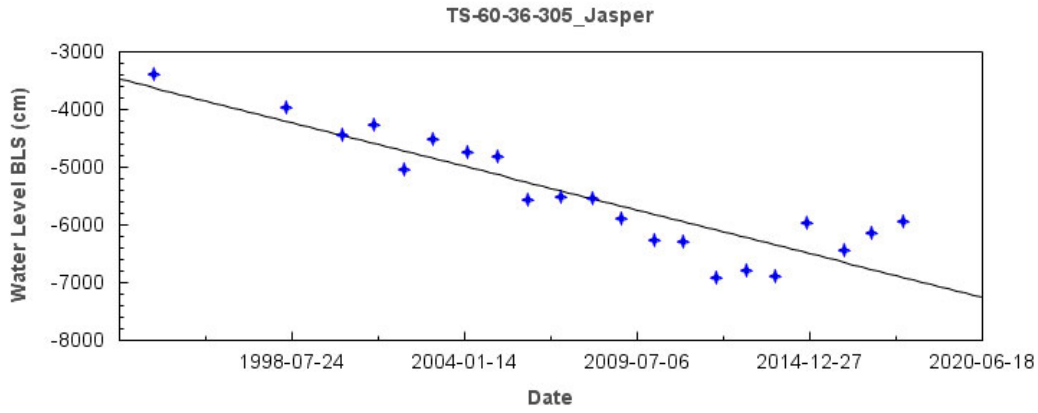
TS-60-36-305_Jasper
Water Level BLS (cm)
-3000
-4000
-5000
-6000
-7000
-8000
1998-07-24
2004-01-14
2009-07-06
2014-12-27
2020-06-18
Date

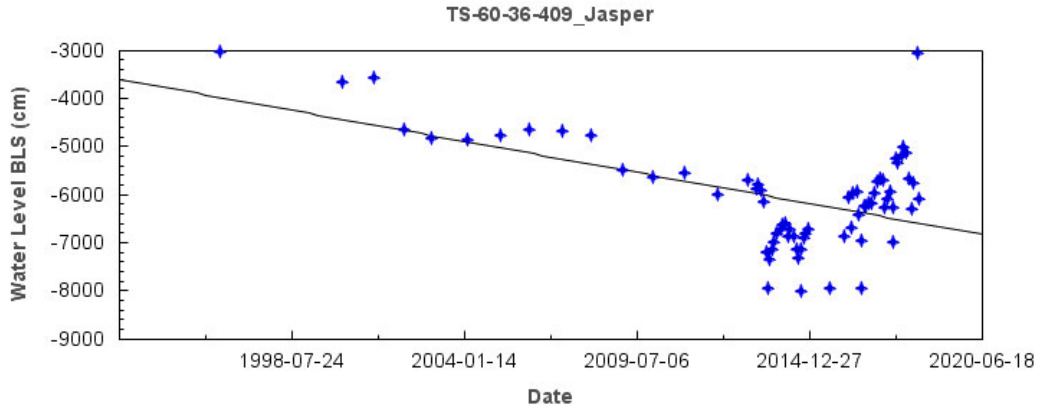
TS-60-36-409_Jasper
Water Level BLS (cm)
-3000
-4000
-5000
-6000
-7000
-8000
-9000
1998-07-24
2004-01-14
2009-07-06
2014-12-27
2020-06-18
Date

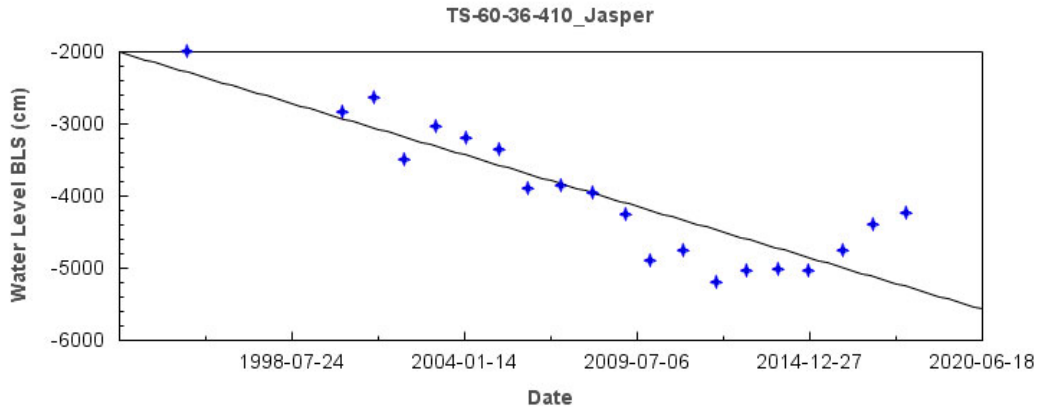
TS-60-36-410_Jasper
Water Level BLS (cm)
-2000
-3000
-4000
-5000
-6000
1998-07-24
2004-01-14
2009-07-06
2014-12-27
2020-06-18
Date

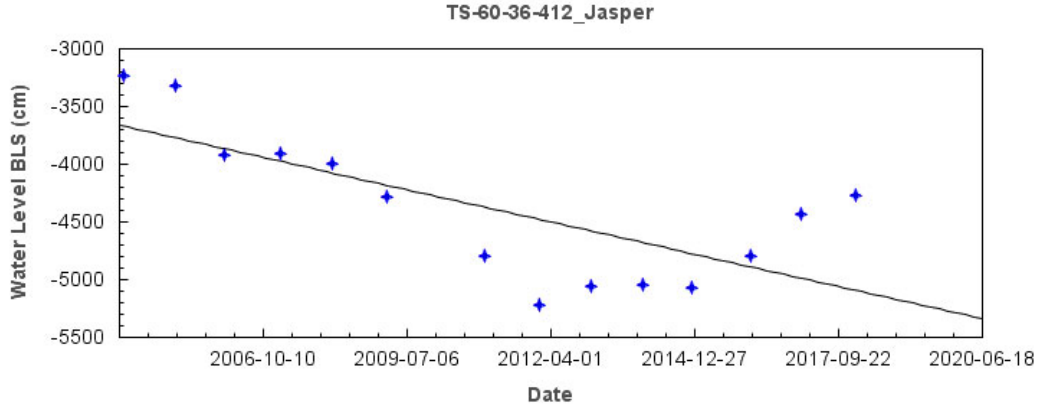
TS-60-36-412_Jasper
Water Level BLS (cm)
-3000
-3500
-4000
-4500
-5000
-5500
2006-10-10
2009-07-06
2012-04-01
2014-12-27
2017-09-22
2020-06-18
Date

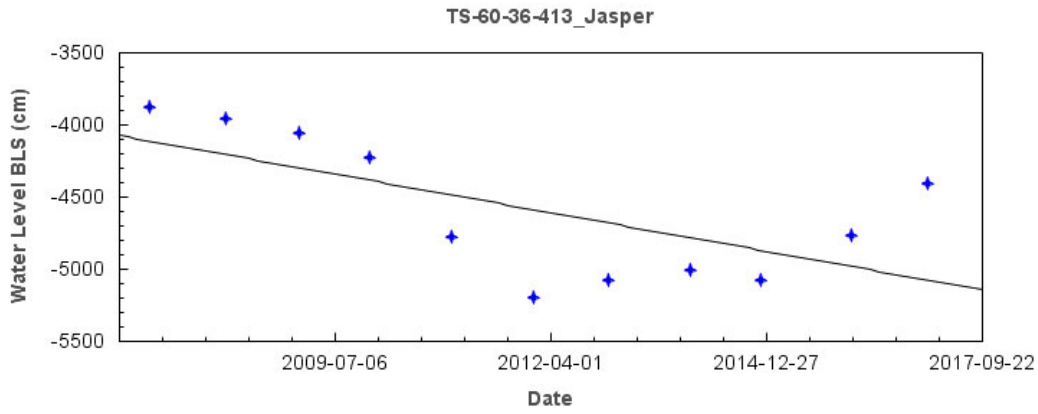
TS-60-36-413_Jasper
Water Level BLS (cm)
-3500
-4000
-4500
-5000
-5500
2009-07-06
2012-04-01
2014-12-27
2017-09-22
Date

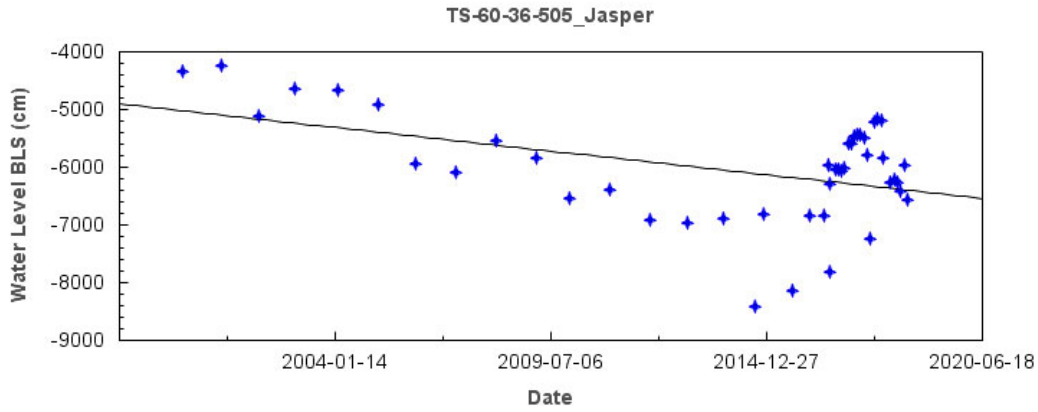
TS-60-36-505_Jasper
Water Level BLS (cm)
-4000
-5000
-6000
-7000
-8000
-9000
2004-01-14
2009-07-06
2014-12-27
2020-06-18
Date

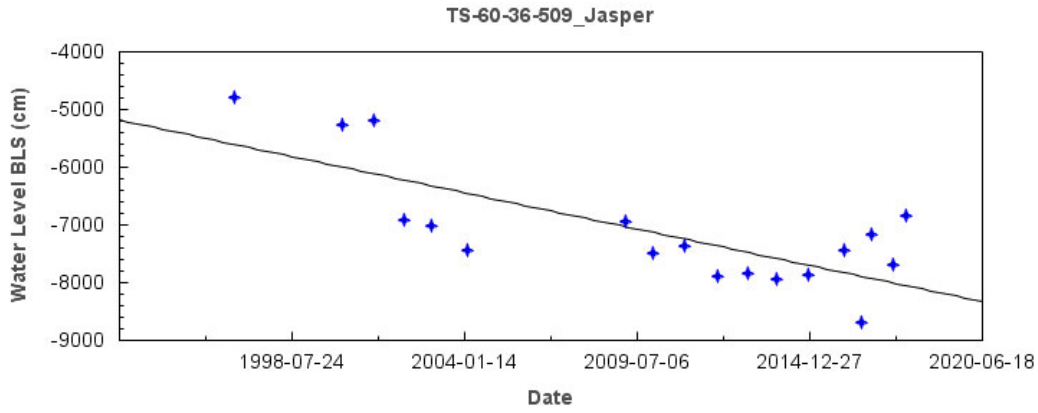
TS-60-36-509_Jasper
Water Level BLS (cm)
-4000
-5000
-6000
-7000
-8000
-9000
1998-07-24
2004-01-14
2009-07-06
2014-12-27
2020-06-18
Date

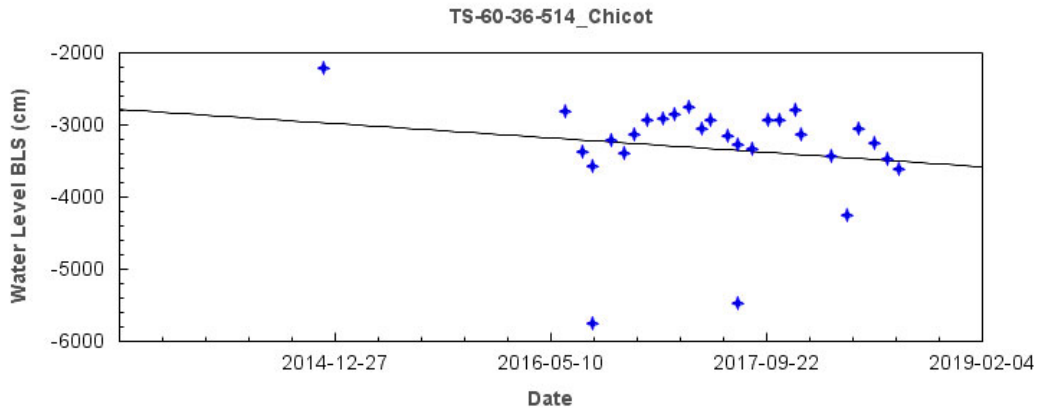
TS-60-36-514_Chicot
Water Level BLS (cm)
-2000
-3000
-4000
-5000
-6000
2014-12-27
2016-05-10
2017-09-22
2019-02-04
Date

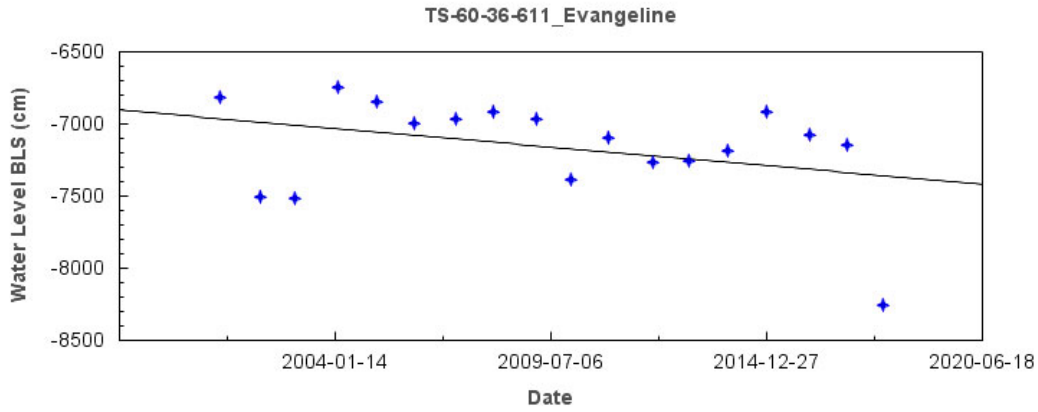
TS-60-36-611_Evangeline
Water Level BLS (cm)
-6500
-7000
-7500
-8000
-8500
2004-01-14
2009-07-06
2014-12-27
2020-06-18
Date

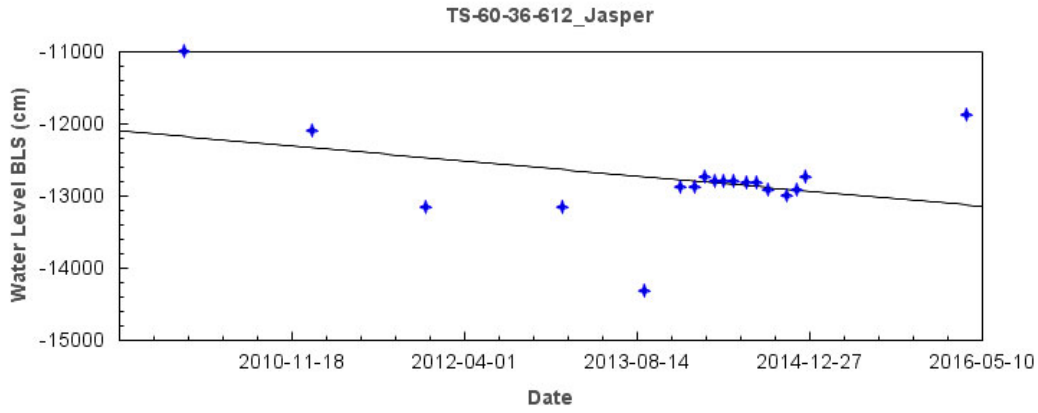
TS-60-36-612_Jasper
Water Level BLS (cm)
-11000
-12000
-13000
-14000
-15000
2010-11-18
2012-04-01
2013-08-14
2014-12-27
2016-05-10
Date

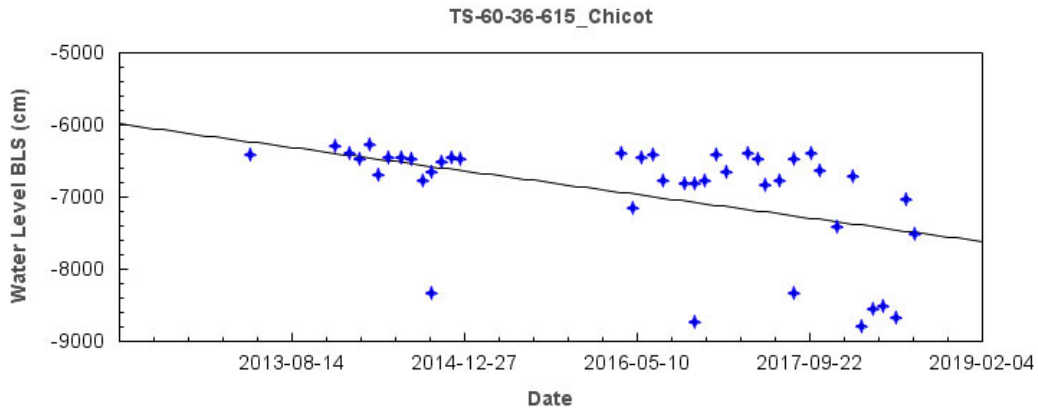
TS-60-36-615_Chicot
Water Level BLS (cm)
-5000
-6000
-7000
-8000
-9000
2013-08-14
2014-12-27
2016-05-10
2017-09-22
2019-02-04
Date

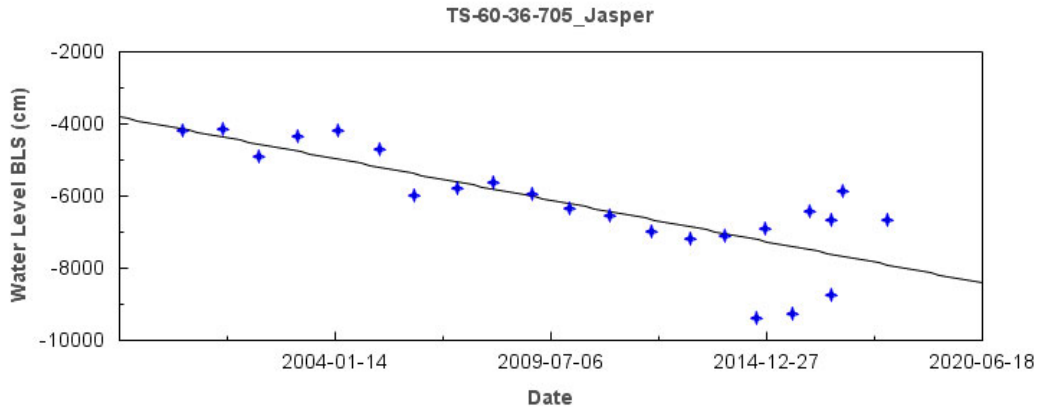
TS-60-36-705_Jasper
Water Level BLS (cm)
-2000
-4000
-6000
-8000
-10000
2004-01-14
2009-07-06
2014-12-27
2020-06-18
Date

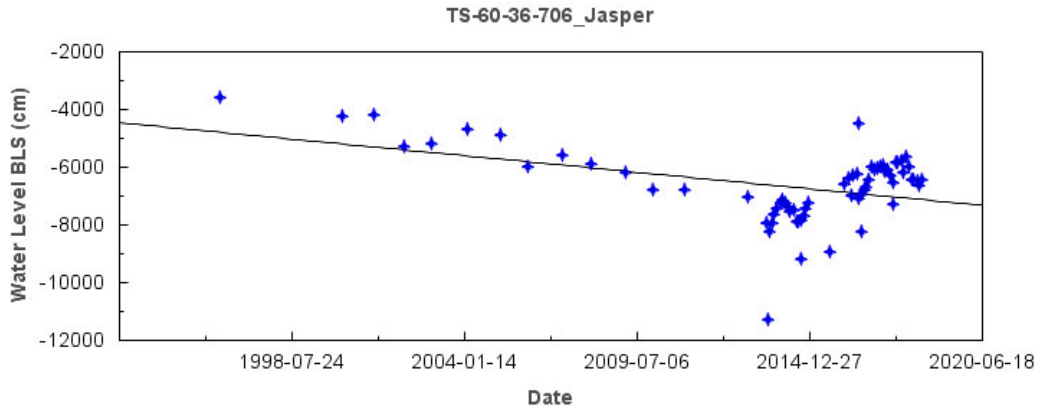
TS-60-36-706_Jasper
Water Level BLS (cm)
-2000
-4000
-6000
-8000
-10000
-12000
1998-07-24
2004-01-14
2009-07-06
2014-12-27
2020-06-18
Date

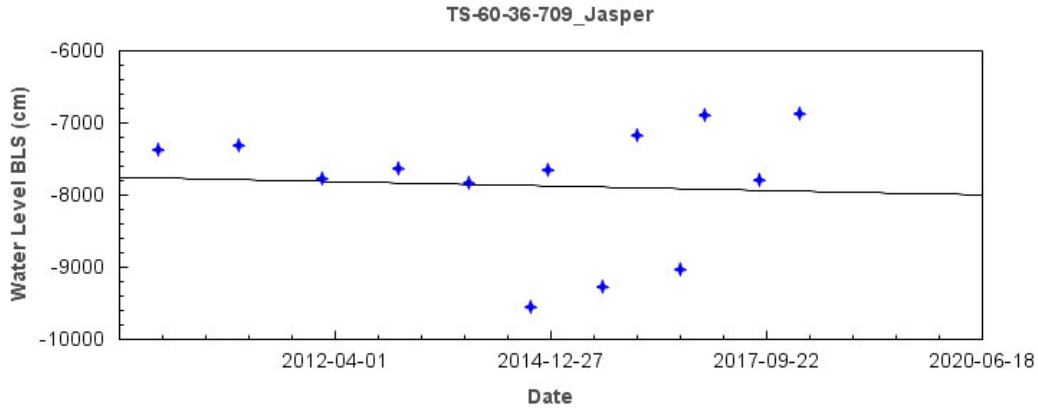
TS-60-36-709_Jasper
Water Level BLS (cm)
-6000
-7000
-8000
-9000
-10000
2012-04-01
2014-12-27
2017-09-22
2020-06-18
Date

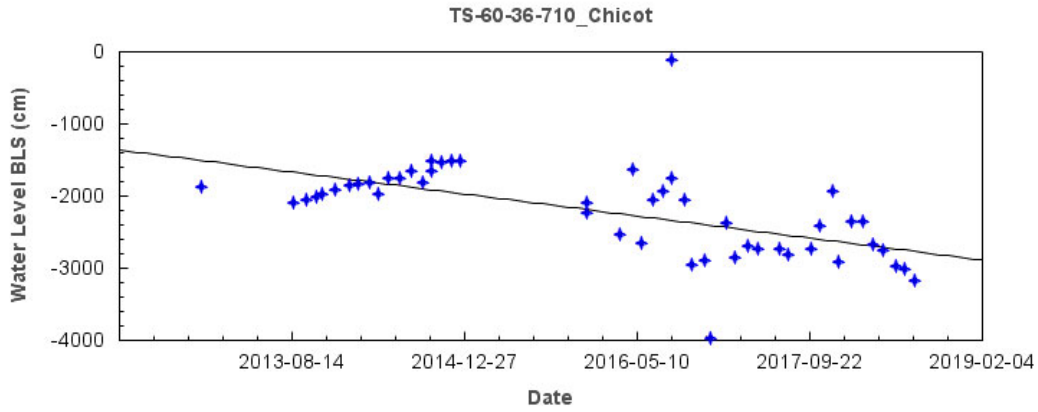
TS-60-36-710_Chicot
Water Level BLS (cm)
0
-1000
-2000
-3000
-4000
2013-08-14
2014-12-27
2016-05-10
2017-09-22
2019-02-04
Date

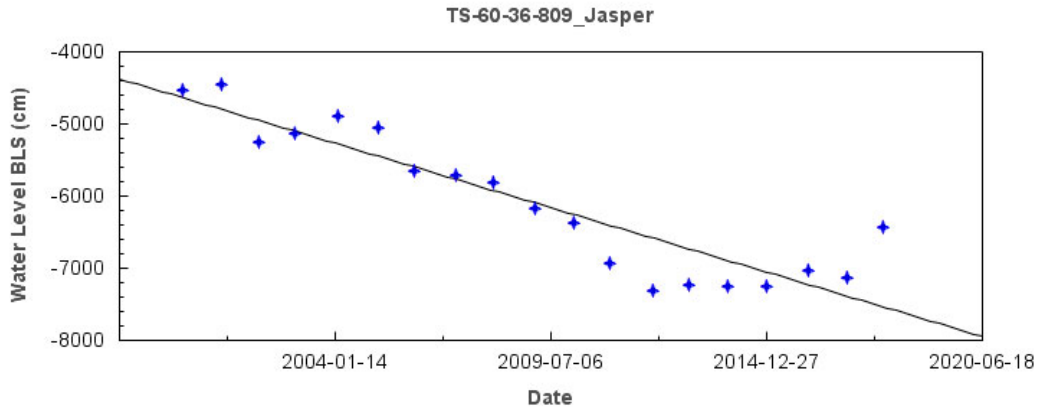
TS-60-36-809_Jasper
Water Level BLS (cm)
-4000
-5000
-6000
-7000
-8000
2004-01-14
2009-07-06
2014-12-27
2020-06-18
Date

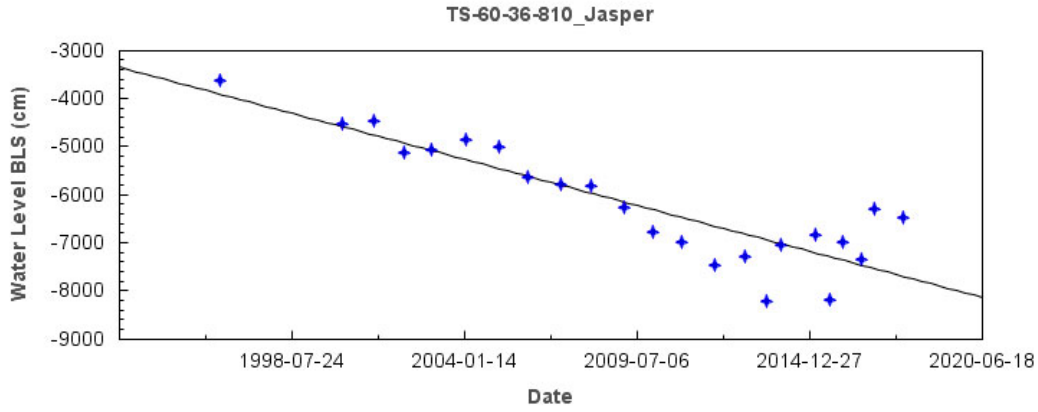
TS-60-36-810_Jasper
Water Level BLS (cm)
-3000
-4000
-5000
-6000
-7000
-8000
-9000
1998-07-24
2004-01-14
2009-07-06
2014-12-27
2020-06-18
Date

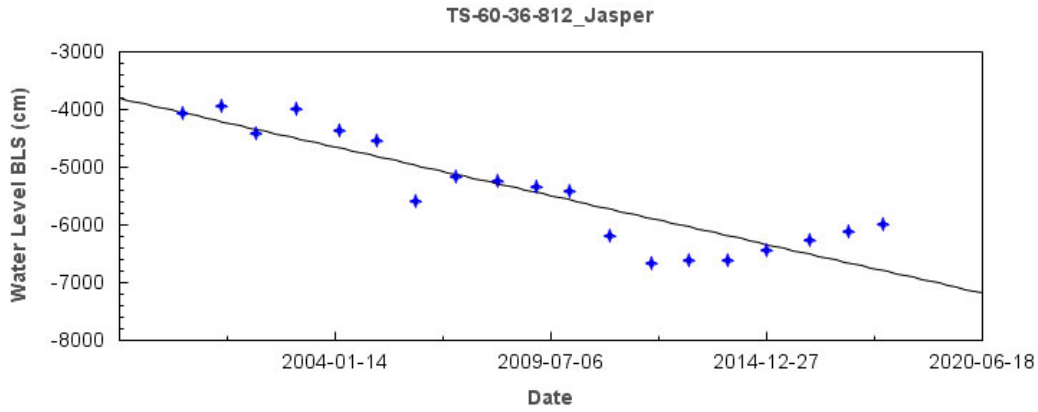
TS-60-36-812_Jasper
Water Level BLS (cm)
-3000
-4000
-5000
-6000
-7000
-8000
2004-01-14
2009-07-06
2014-12-27
2020-06-18
Date

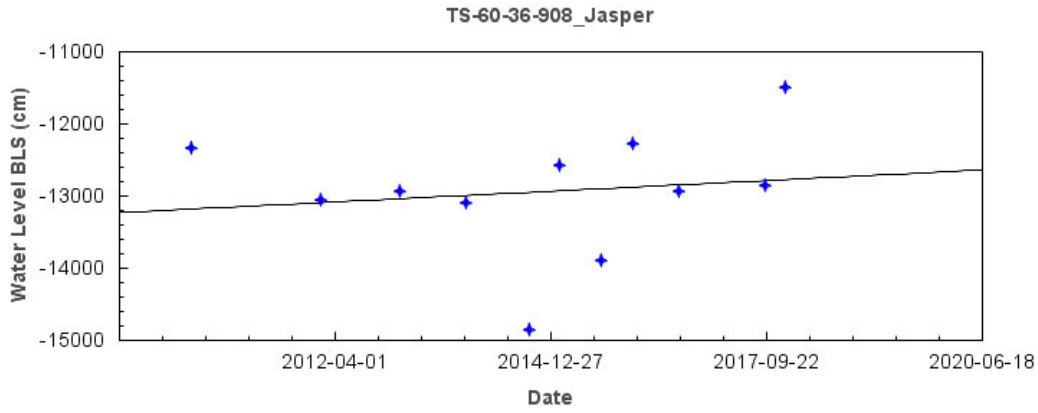
TS-60-36-908_Jasper
Water Level BLS (cm)
-11000
-12000
-13000
-14000
-15000
2012-04-01
2014-12-27
2017-09-22
2020-06-18
Date

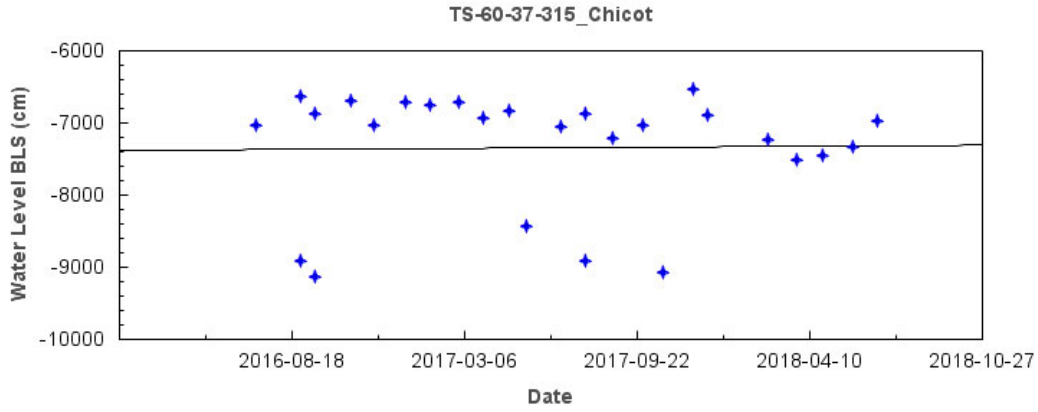
TS-60-37-315_Chicot
Water Level BLS (cm)
-6000
-7000
-8000
-9000
-10000
2016-08-18
2017-03-06
2017-09-22
2018-04-10
2018-10-27
Date

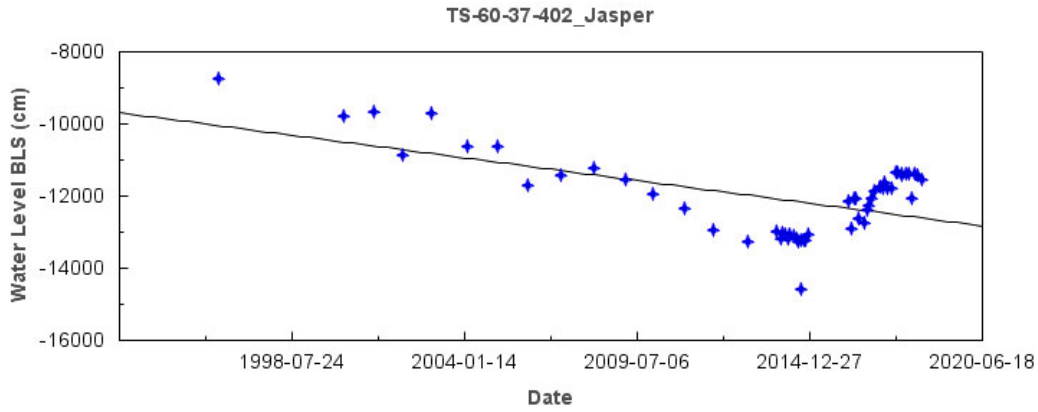
TS-60-37-402_Jasper
Water Level BLS (cm)
-8000
-10000
-12000
-14000
-16000
1998-07-24
2004-01-14
2009-07-06
2014-12-27
2020-06-18
Date

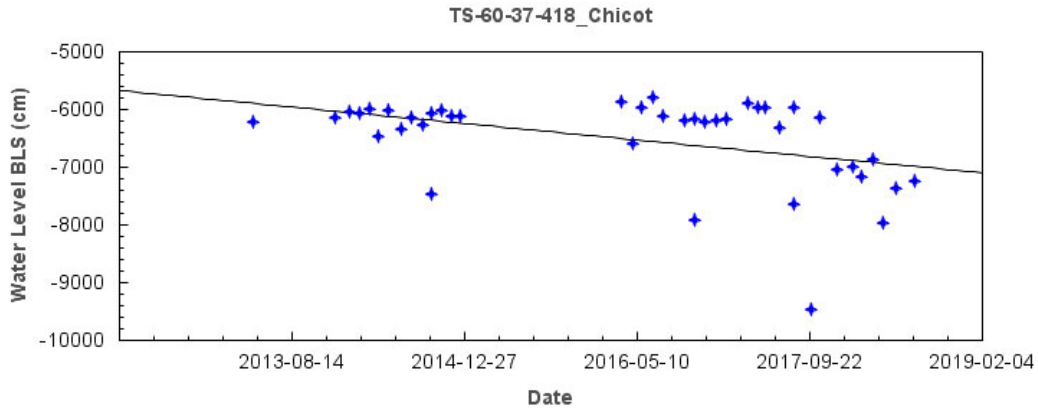
TS-60-37-418_Chicot
Water Level BLS (cm)
-5000
-6000
-7000
-8000
-9000
-10000
2013-08-14
2014-12-27
2016-05-10
2017-09-22
2019-02-04
Date

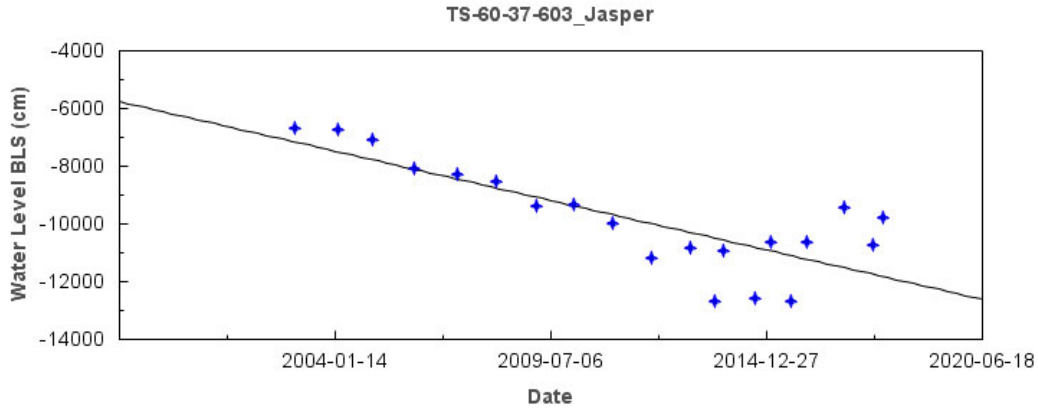
TS-60-37-603_Jasper
Water Level BLS (cm)
-4000
-6000
-8000
-10000
-12000
-14000
2004-01-14
2009-07-06
2014-12-27
2020-06-18
Date

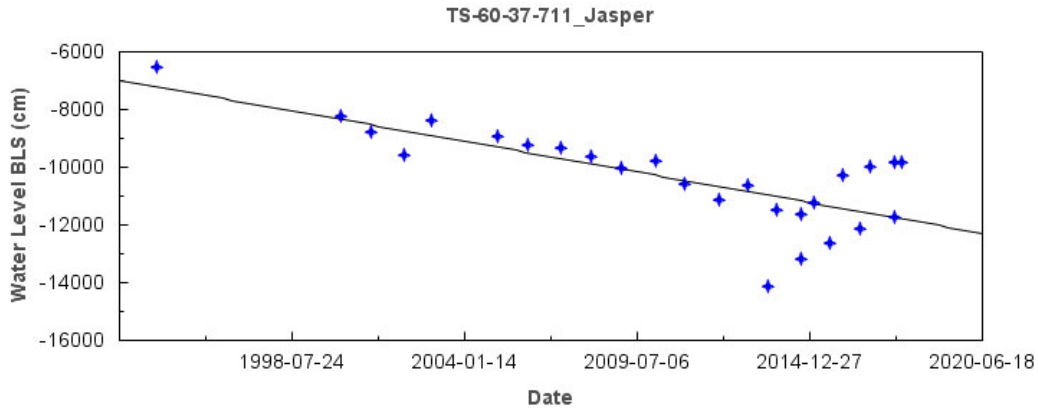
TS-60-37-711_Jasper
Water Level BLS (cm)
-6000
-8000
-10000
-12000
-14000
-16000
1998-07-24
2004-01-14
2009-07-06
2014-12-27
2020-06-18
Date

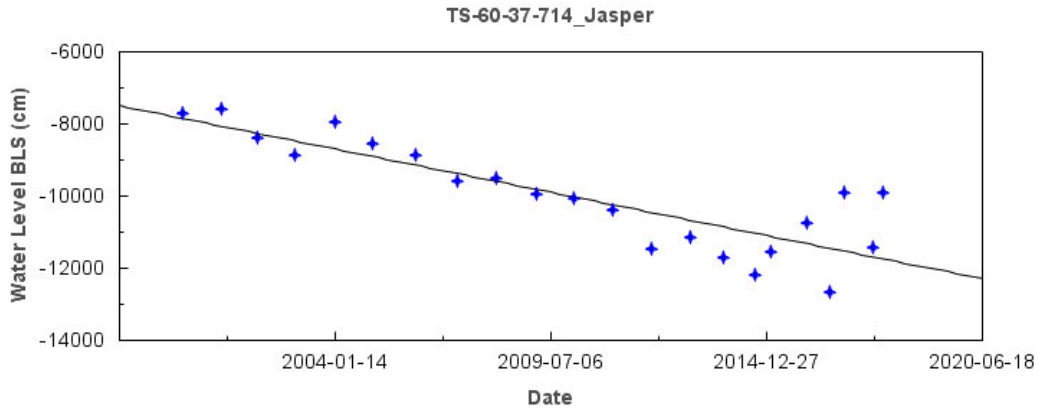
TS-60-37-714_Jasper
Water Level BLS (cm)
-6000
-8000
-10000
-12000
-14000
2004-01-14
2009-07-06
2014-12-27
2020-06-18
Date

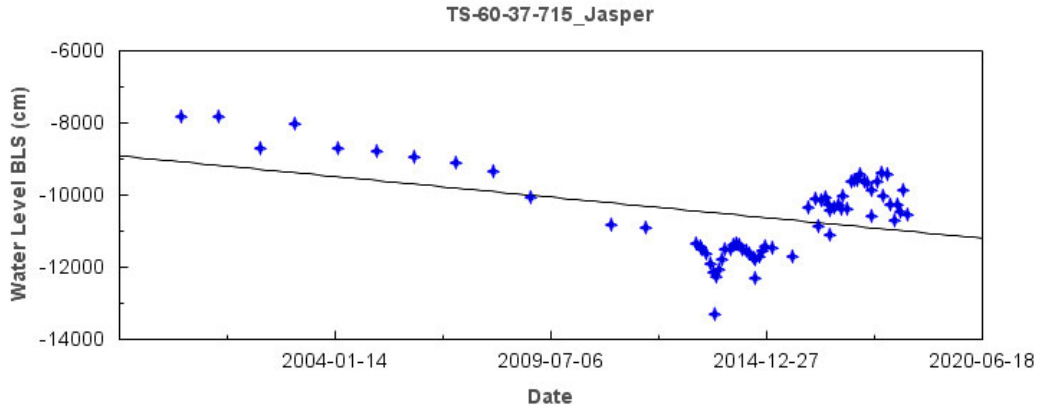
TS-60-37-715_Jasper
Water Level BLS (cm)
-6000
-8000
-10000
-12000
-14000
2004-01-14
2009-07-06
2014-12-27
2020-06-18
Date

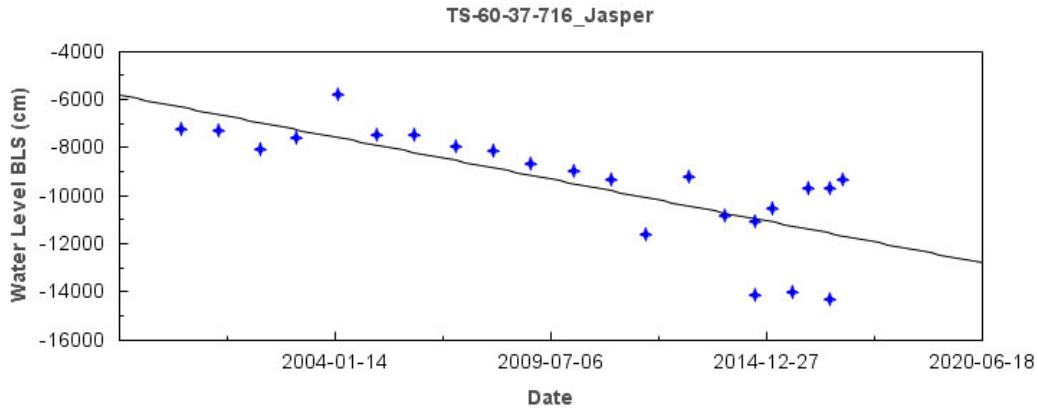
TS-60-37-716_Jasper
Water Level BLS (cm)
-4000
-6000
-8000
-10000
-12000
-14000
-16000
2004-01-14
2009-07-06
2014-12-27
2020-06-18
Date

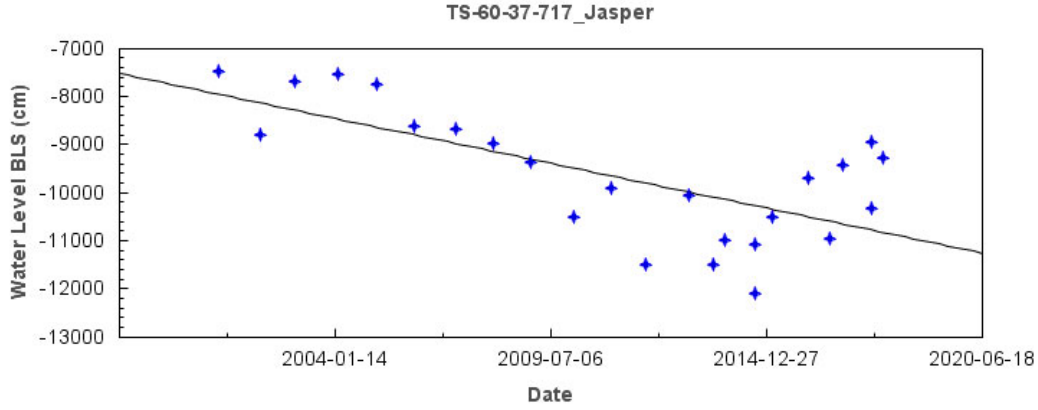
TS-60-37-717_Jasper
Water Level BLS (cm)
-7000
-8000
-9000
-10000
-11000
-12000
-13000
2004-01-14
2009-07-06
2014-12-27
2020-06-18
Date

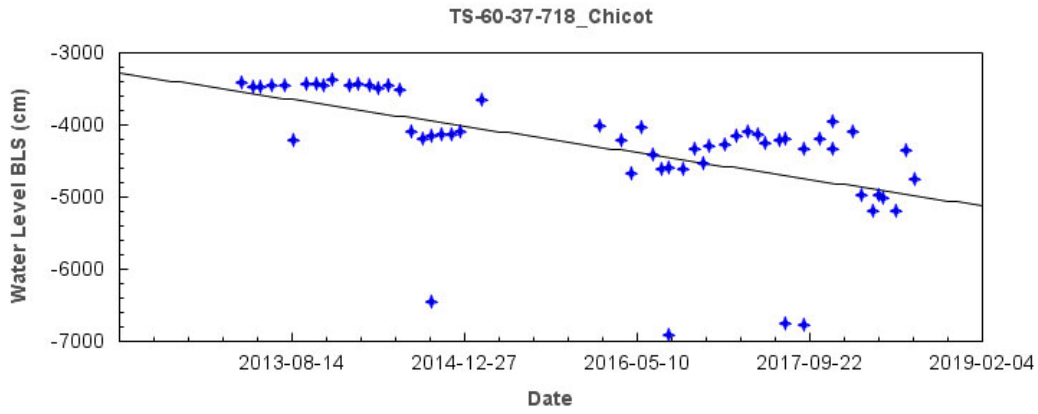
TS-60-37-718_Chicot
Water Level BLS (cm)
-3000
-4000
-5000
-6000
-7000
2013-08-14
2014-12-27
2016-05-10
2017-09-22
2019-02-04
Date

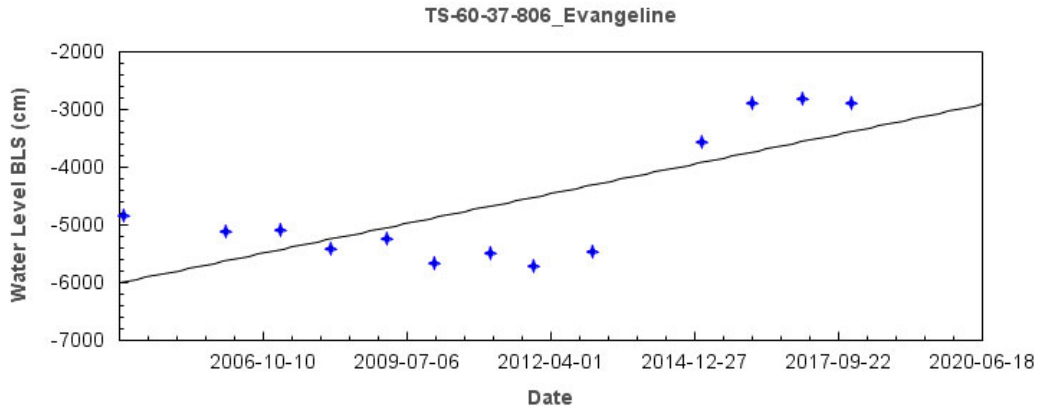
TS-60-37-806_Evangeline
Water Level BLS (cm)
-2000
-3000
-4000
-5000
-6000
-7000
2006-10-10
2009-07-06
2012-04-01
2014-12-27
2017-09-22
2020-06-18
Date

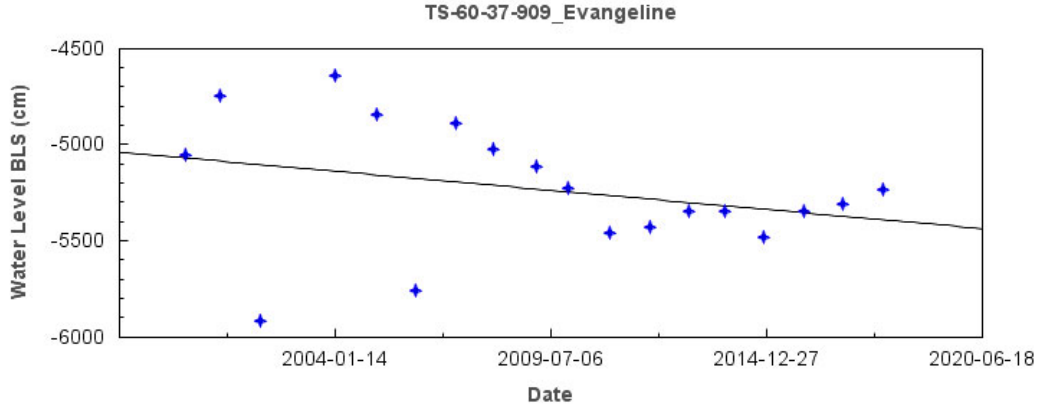
TS-60-37-909_Evangeline
Water Level BLS (cm)
-4500
-5000
-5500
-6000
2004-01-14
2009-07-06
2014-12-27
2020-06-18
Date

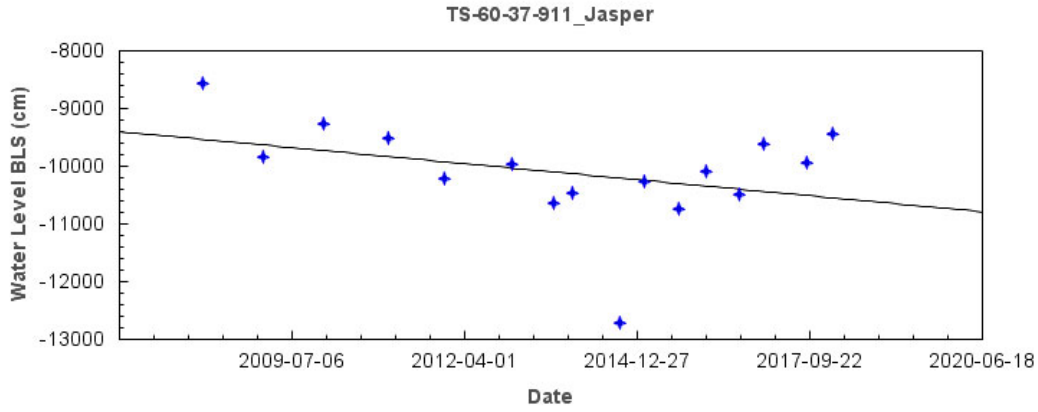
TS-60-37-911_Jasper
Water Level BLS (cm)
-8000
-9000
-10000
-11000
-12000
-13000
2009-07-06
2012-04-01
2014-12-27
2017-09-22
2020-06-18
Date

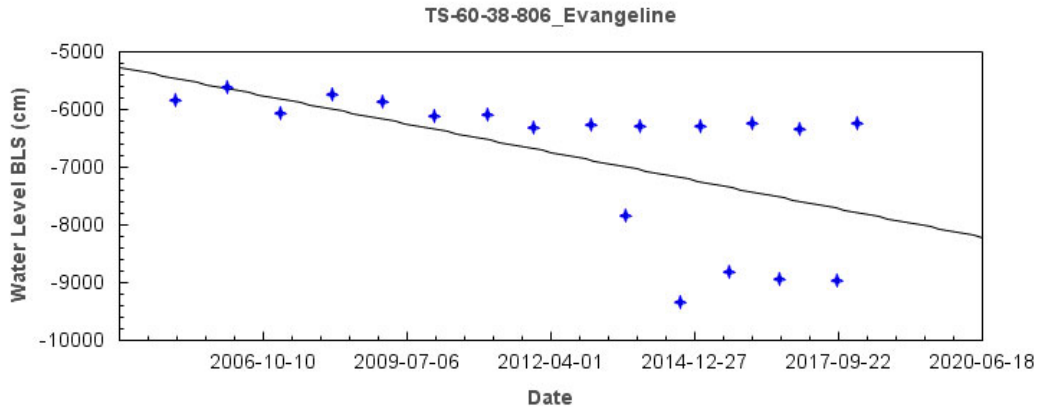
TS-60-38-806_Evangeline
Water Level BLS (cm)
-5000
-6000
-7000
-8000
-9000
-10000
2006-10-10
2009-07-06
2012-04-01
2014-12-27
2017-09-22
2020-06-18
Date

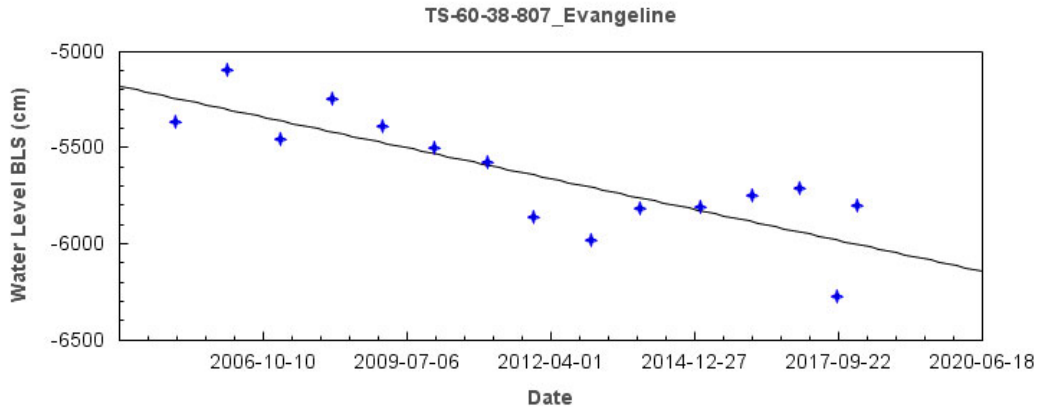
TS-60-38-807_Evangeline
Water Level BLS (cm)
-5000
-5500
-6000
-6500
2006-10-10
2009-07-06
2012-04-01
2014-12-27
2017-09-22
2020-06-18
Date

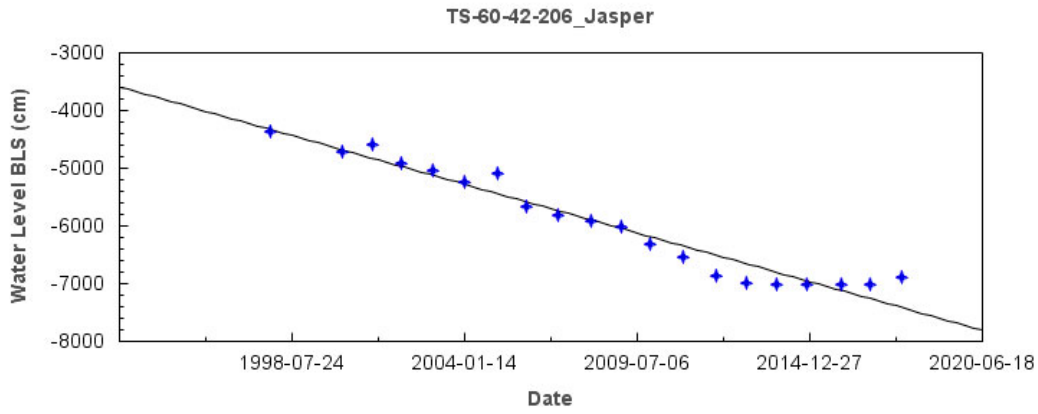
TS-60-42-206_Jasper
Water Level BLS (cm)
-3000
-4000
-5000
-6000
-7000
-8000
1998-07-24
2004-01-14
2009-07-06
2014-12-27
2020-06-18
Date

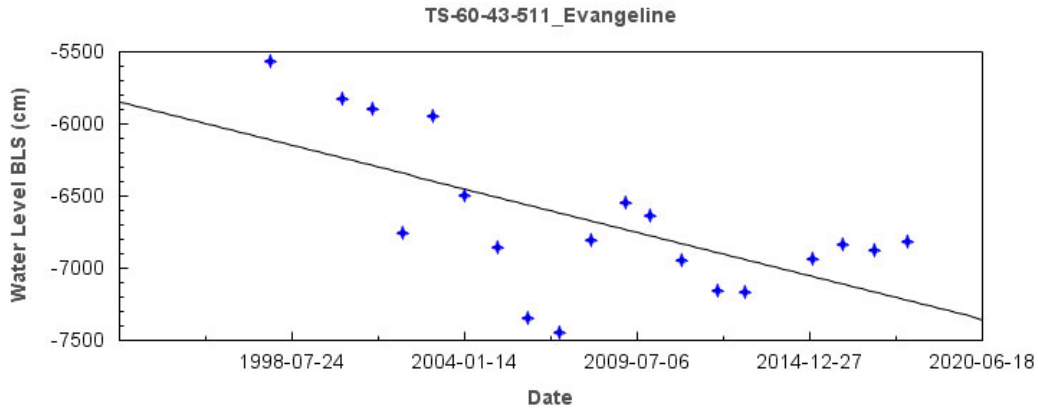
TS-60-43-511_Evangeline
Water Level BLS (cm)
-5500
-6000
-6500
-7000
-7500
1998-07-24
2004-01-14
2009-07-06
2014-12-27
2020-06-18
Date

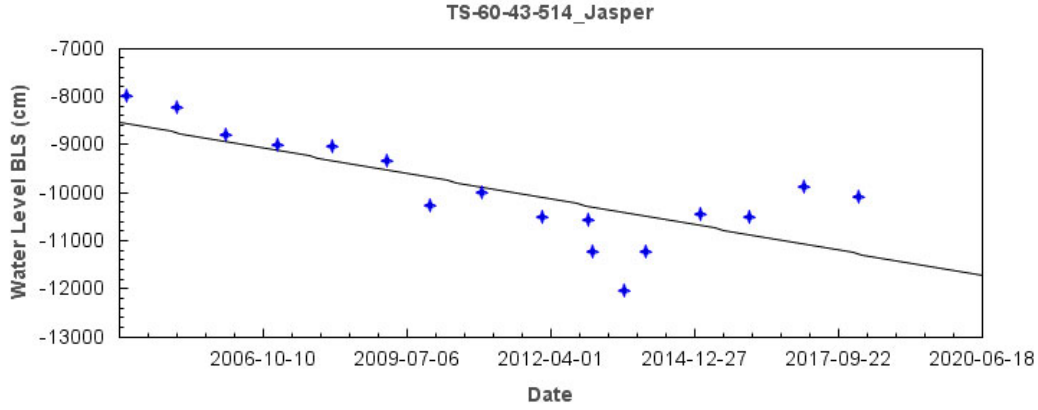
TS-60-43-514_Jasper
Water Level BLS (cm)
-7000
-8000
-9000
-10000
-11000
-12000
-13000
2006-10-10
2009-07-06
2012-04-01
2014-12-27
2017-09-22
2020-06-18
Date

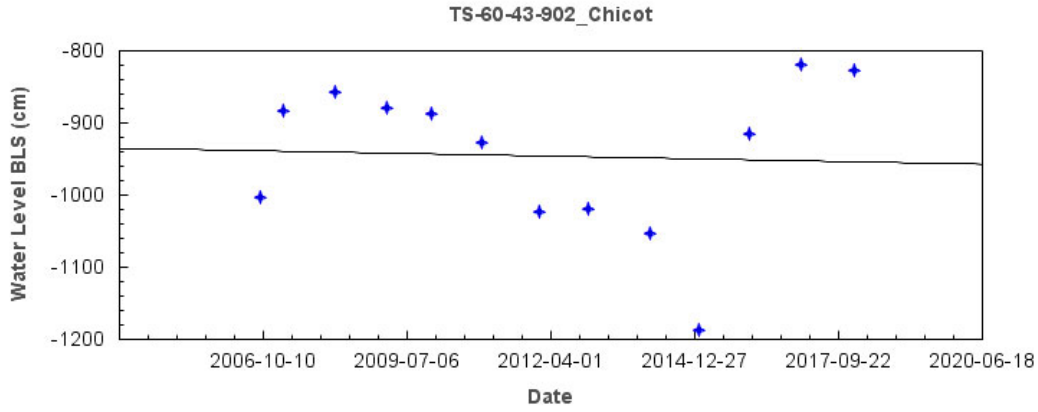
TS-60-43-902_Chicot
Water Level BLS (cm)
-800
-900
-1000
-1100
-1200
2006-10-10
2009-07-06
2012-04-01
2014-12-27
2017-09-22
2020-06-18
Date

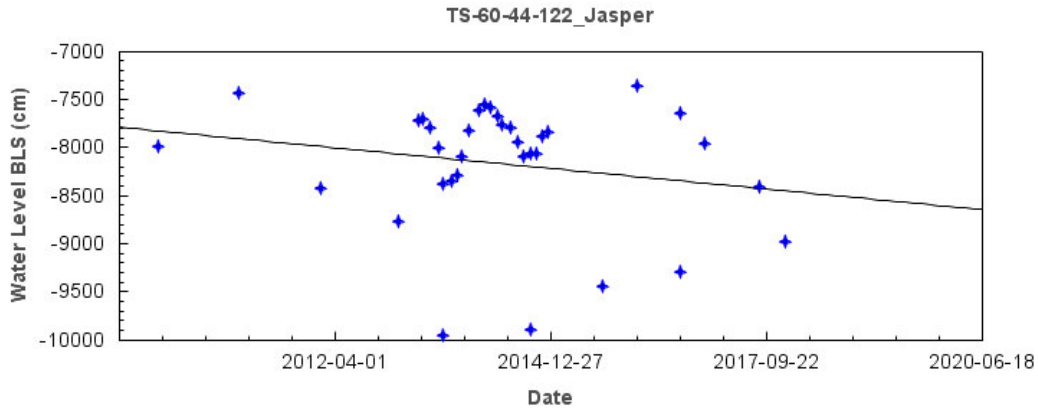
TS-60-44-122_Jasper
Water Level BLS (cm)
-7000
-7500
-8000
-8500
-9000
-9500
-10000
2012-04-01
2014-12-27
2017-09-22
2020-06-18
Date

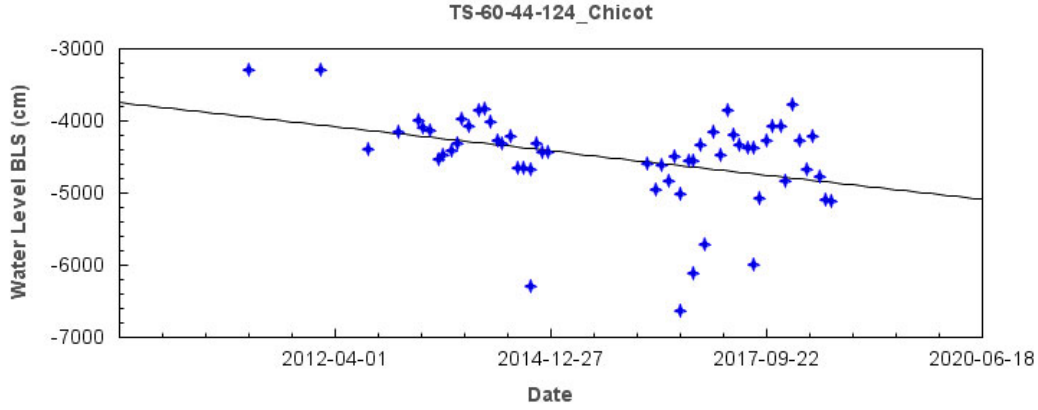
TS-60-44-124_Chicot
Water Level BLS (cm)
-3000
-4000
-5000
-6000
-7000
2012-04-01
2014-12-27
2017-09-22
2020-06-18
Date

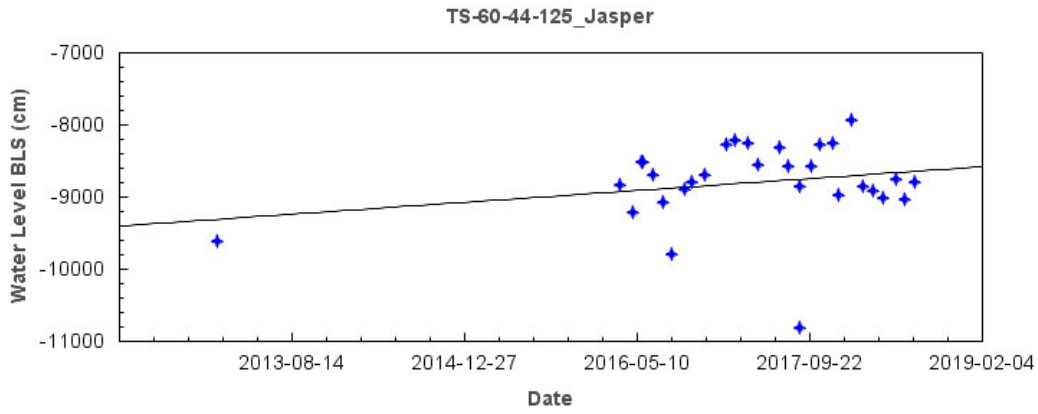
TS-60-44-125_Jasper
Water Level BLS (cm)
-7000
-8000
-9000
-10000
-11000
2013-08-14
2014-12-27
2016-05-10
2017-09-22
2019-02-04
Date

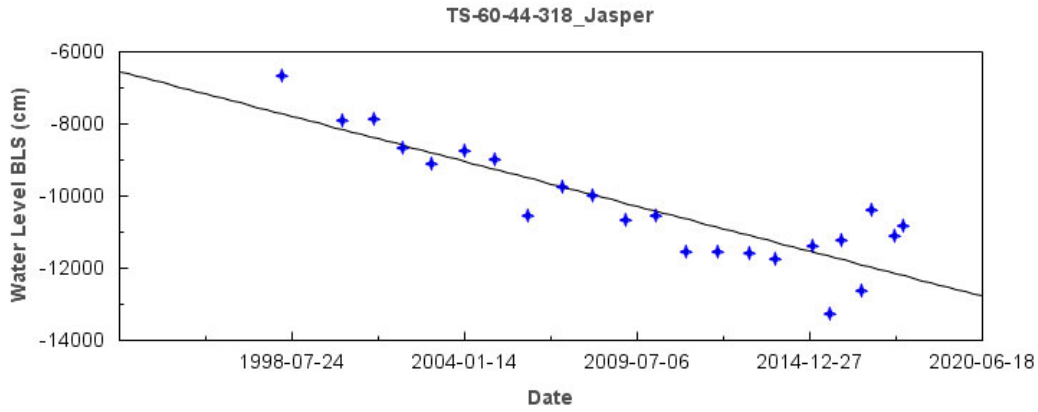
TS-60-44-318_Jasper
Water Level BLS (cm)
-6000
-8000
-10000
-12000
-14000
1998-07-24
2004-01-14
2009-07-06
2014-12-27
2020-06-18
Date

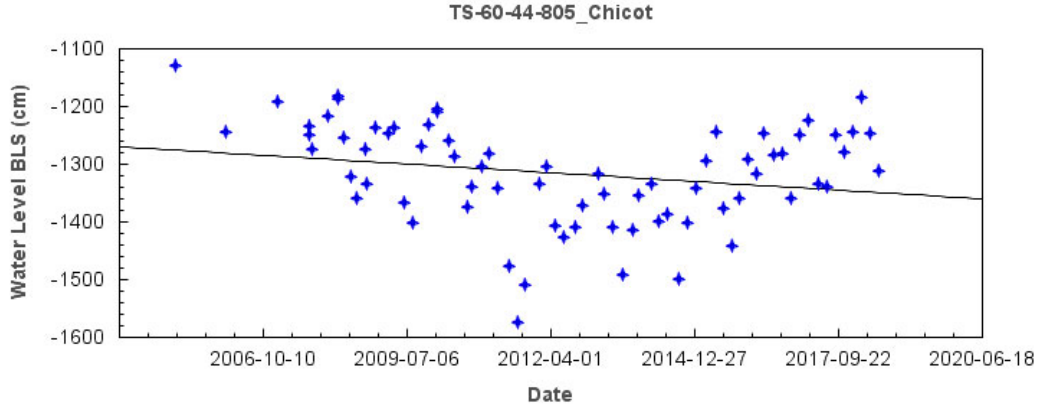
TS-60-44-805_Chicot
Water Level BLS (cm)
-1100
-1200
-1300
-1400
-1500
-1600
2006-10-10
2009-07-06
2012-04-01
2014-12-27
2017-09-22
2020-06-18
Date

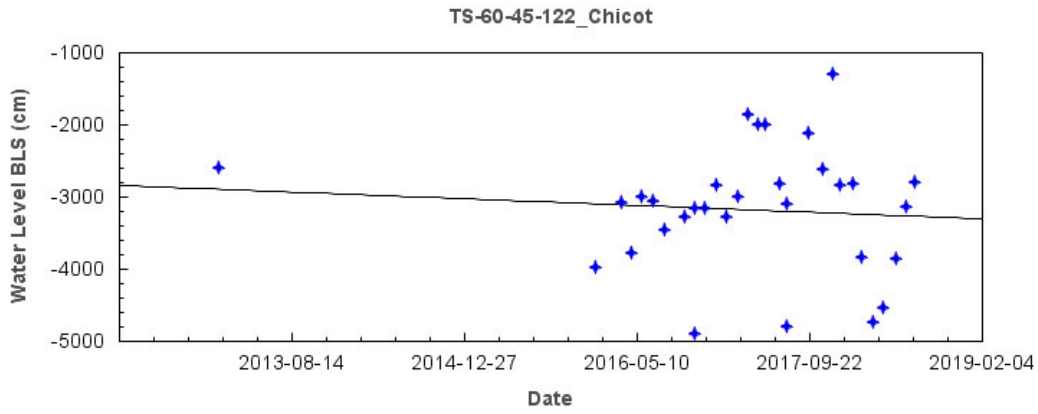
TS-60-45-122_Chicot
Water Level BLS (cm)
-1000
-2000
-3000
-4000
-5000
2013-08-14
2014-12-27
2016-05-10
2017-09-22
2019-02-04
Date

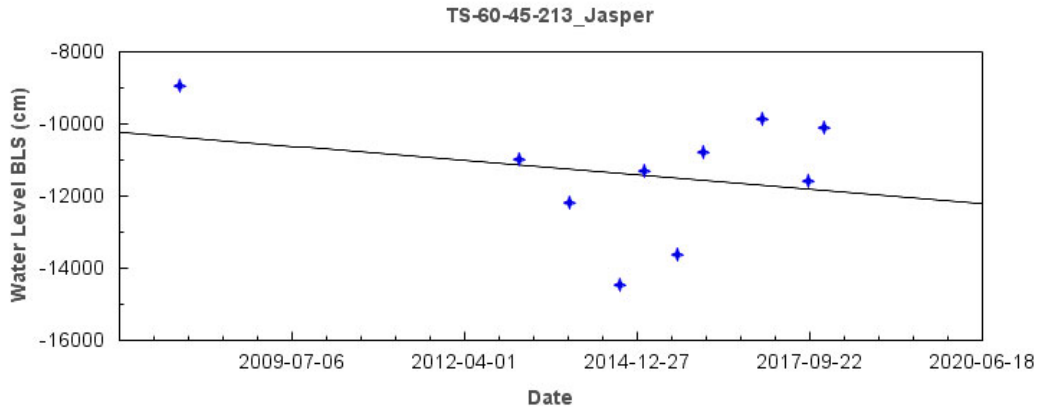
TS-60-45-213_Jasper
Water Level BLS (cm)
-8000
-10000
-12000
-14000
-16000
2009-07-06
2012-04-01
2014-12-27
2017-09-22
2020-06-18
Date

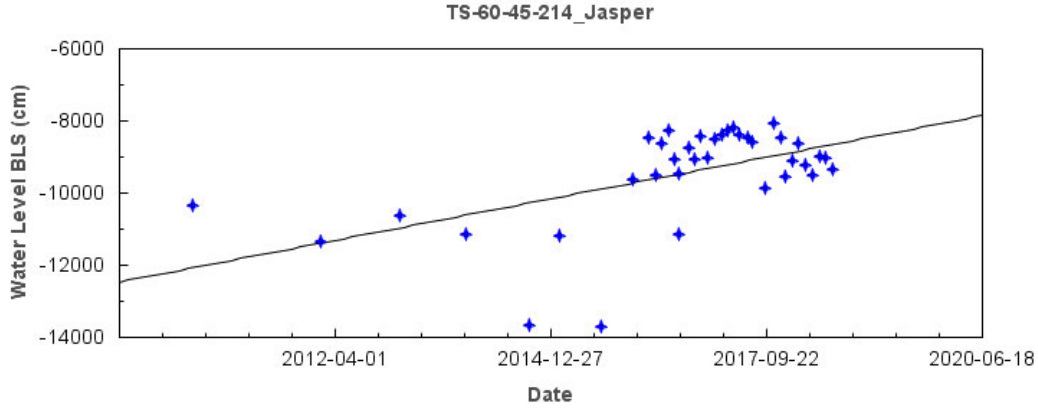
TS-60-45-214_Jasper
Water Level BLS (cm)
-6000
-8000
-10000
-12000
-14000
2012-04-01
2014-12-27
2017-09-22
2020-06-18
Date

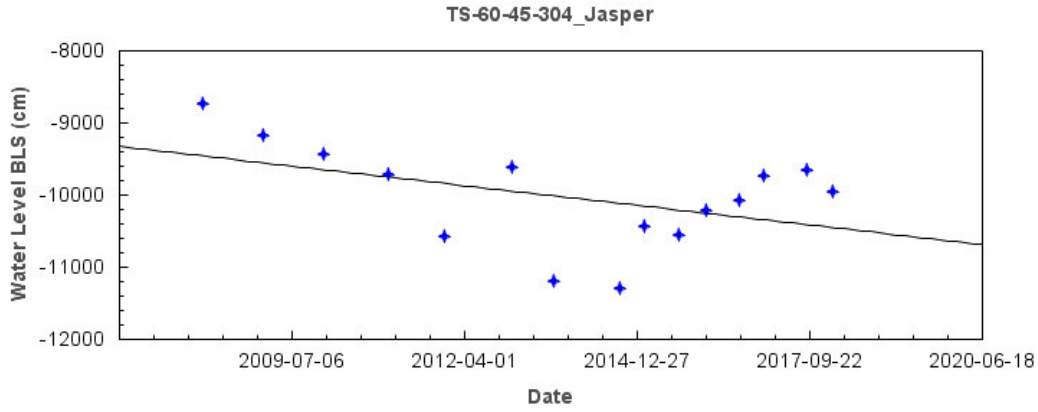
TS-60-45-304_Jasper
Water Level BLS (cm)
-8000
-9000
-10000
-11000
-12000
2009-07-06
2012-04-01
2014-12-27
2017-09-22
2020-06-18
Date

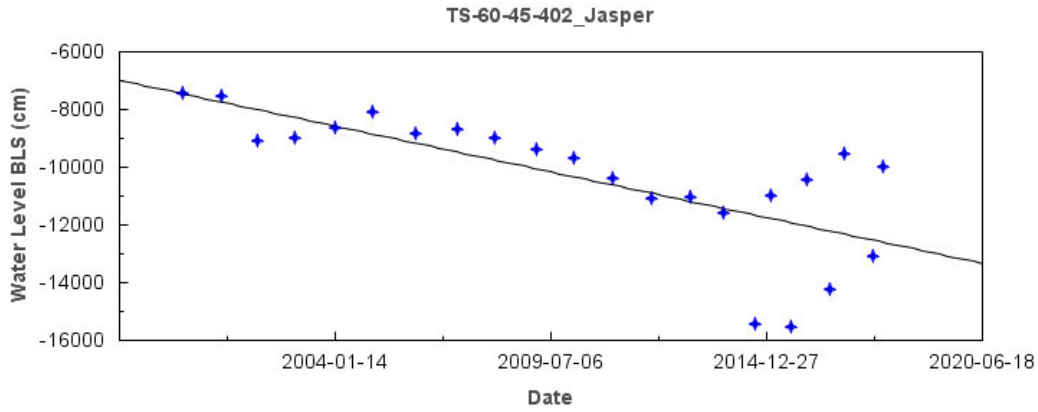
TS-60-45-402_Jasper
Water Level BLS (cm)
-6000
-8000
-10000
-12000
-14000
-16000
2004-01-14
2009-07-06
2014-12-27
2020-06-18
Date

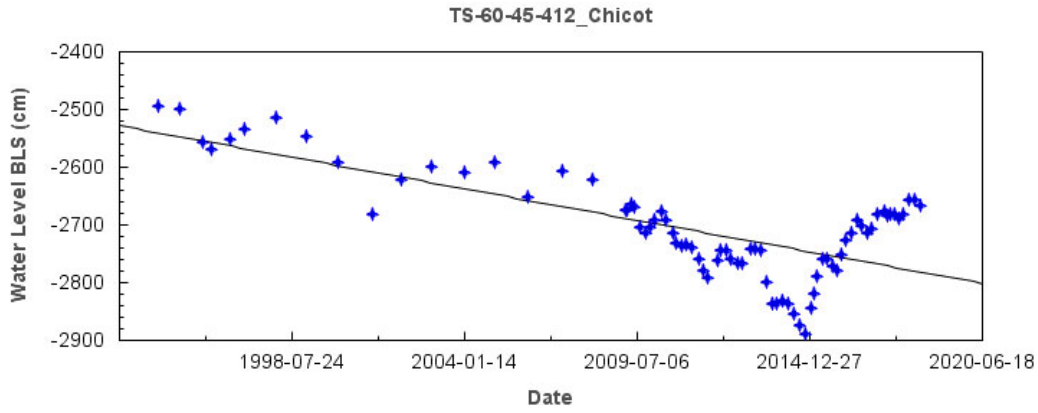
TS-60-45-412_Chicot
Water Level BLS (cm)
-2400
-2500
-2600
-2700
-2800
-2900
1998-07-24
2004-01-14
2009-07-06
2014-12-27
2020-06-18
Date

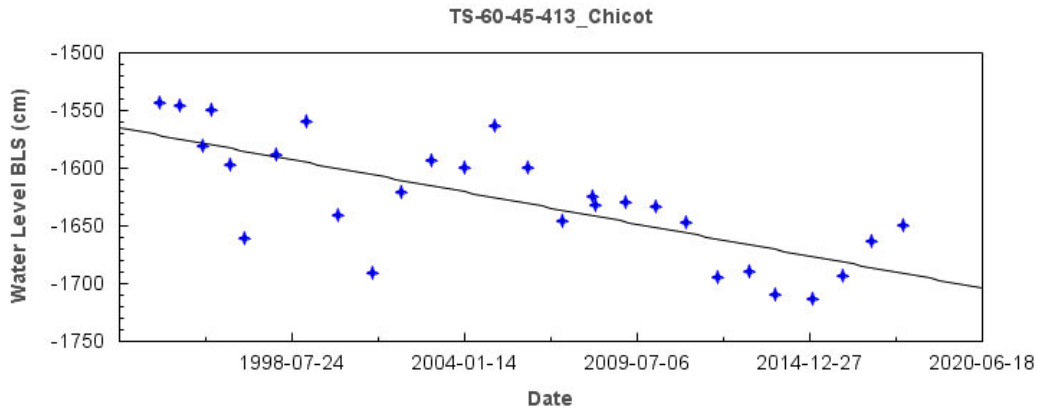
TS-60-45-413_Chicot
Water Level BLS (cm)
-1500
-1550
-1600
-1650
-1700
-1750
1998-07-24
2004-01-14
2009-07-06
2014-12-27
2020-06-18
Date

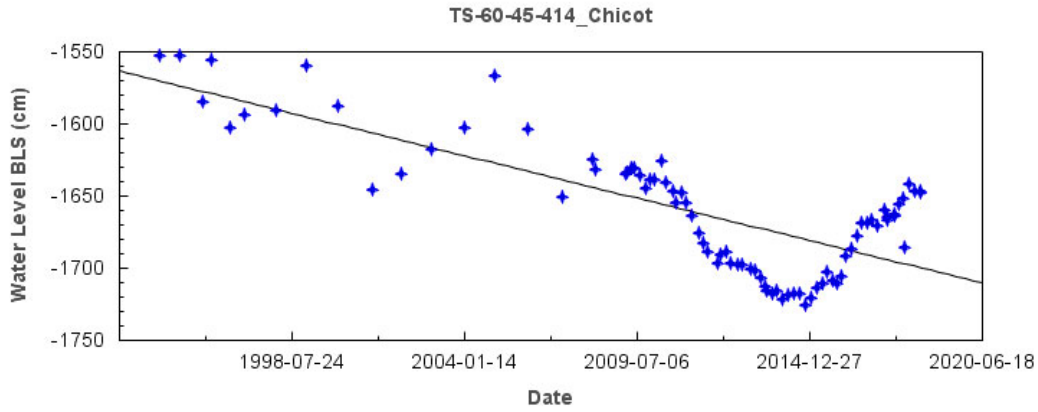
TS-60-45-414_Chicot
Water Level BLS (cm)
-1550
-1600
-1650
-1700
-1750
1998-07-24
2004-01-14
2009-07-06
2014-12-27
2020-06-18
Date

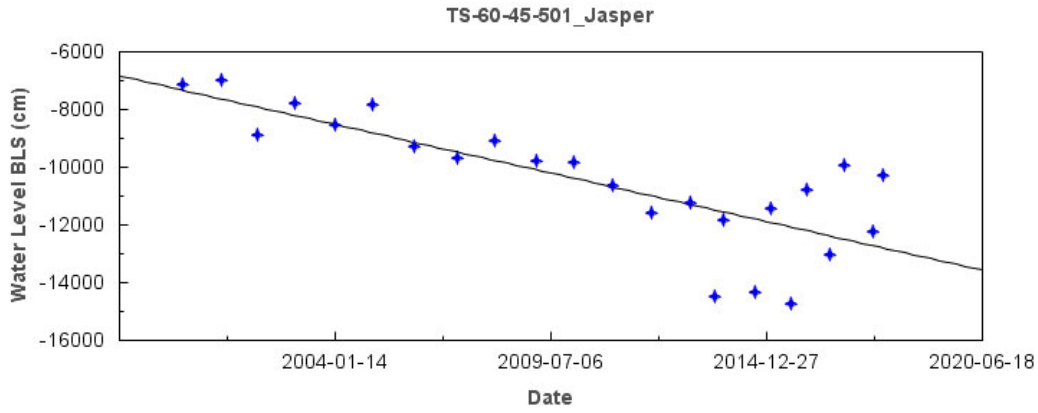
TS-60-45-501_Jasper
Water Level BLS (cm)
-6000
-8000
-10000
-12000
-14000
-16000
2004-01-14
2009-07-06
2014-12-27
2020-06-18
Date

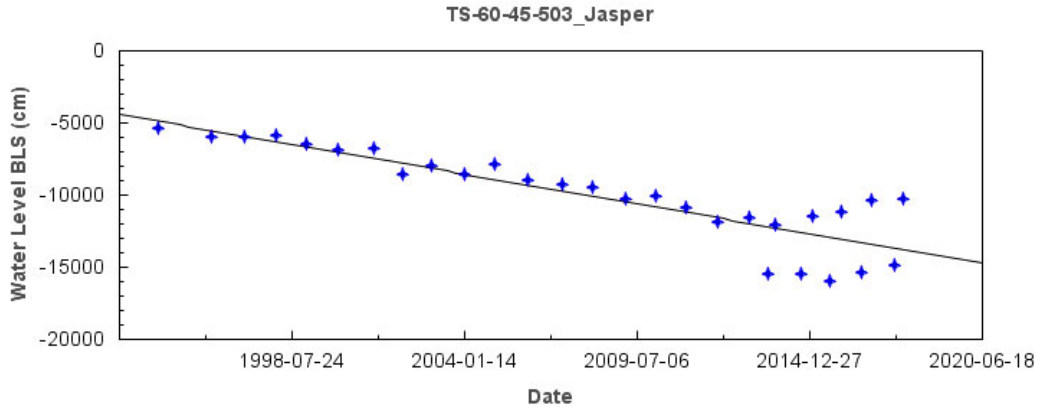
TS-60-45-503_Jasper
Water Level BLS (cm)
0
-5000
-10000
-15000
-20000
1998-07-24
2004-01-14
2009-07-06
2014-12-27
2020-06-18
Date

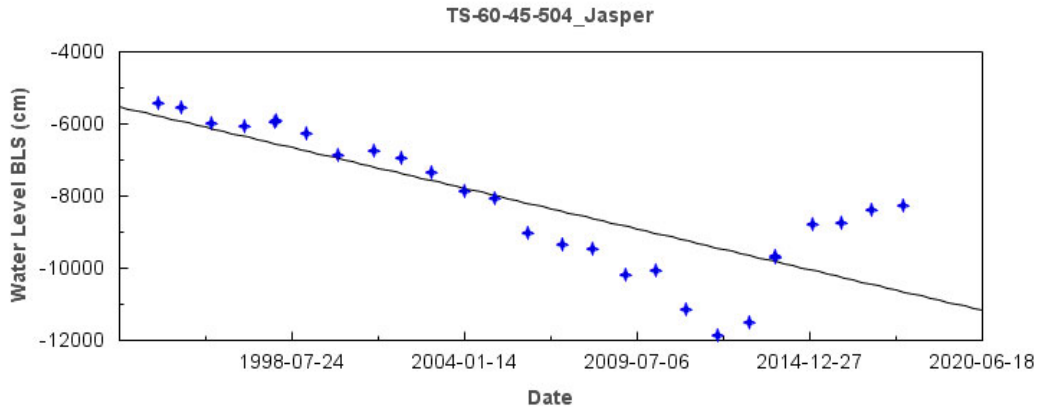
TS-60-45-504_Jasper
Water Level BLS (cm)
-4000
-6000
-8000
-10000
-12000
1998-07-24
2004-01-14
2009-07-06
2014-12-27
2020-06-18
Date

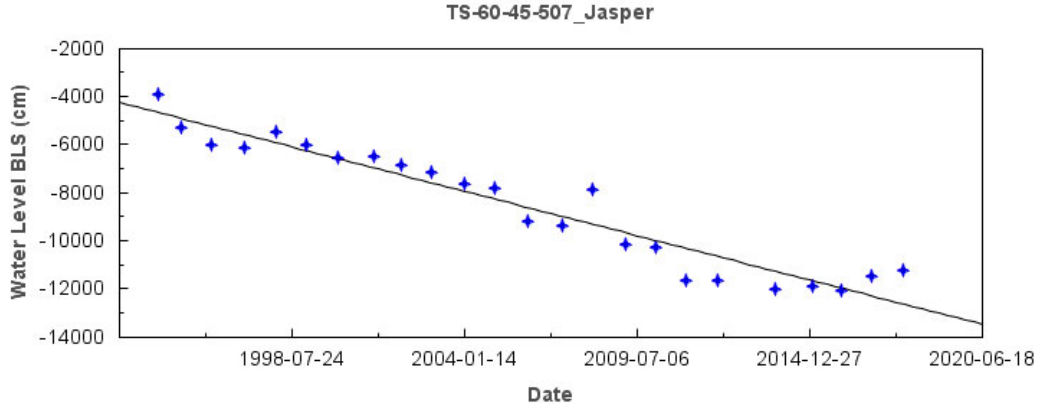
TS-60-45-507_Jasper
Water Level BLS (cm)
-2000
-4000
-6000
-8000
-10000
-12000
-14000
1998-07-24
2004-01-14
2009-07-06
2014-12-27
2020-06-18
Date

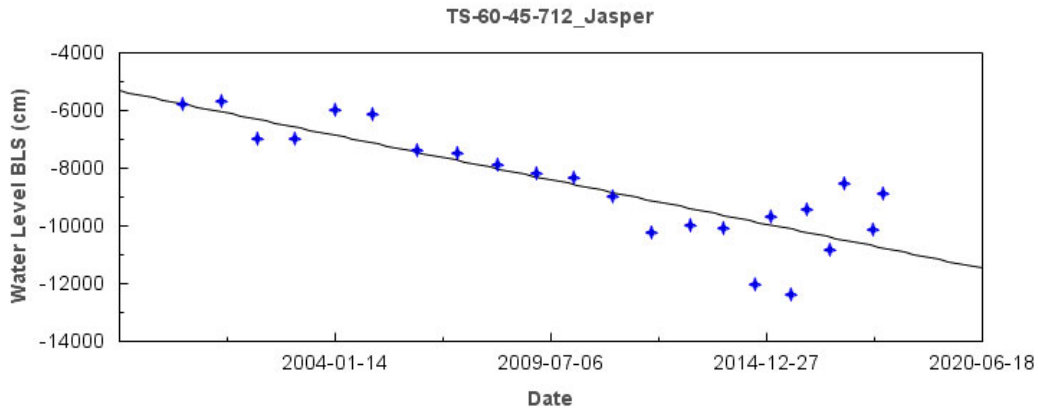
TS-60-45-712_Jasper
Water Level BLS (cm)
-4000
-6000
-8000
-10000
-12000
-14000
2004-01-14
2009-07-06
2014-12-27
2020-06-18
Date

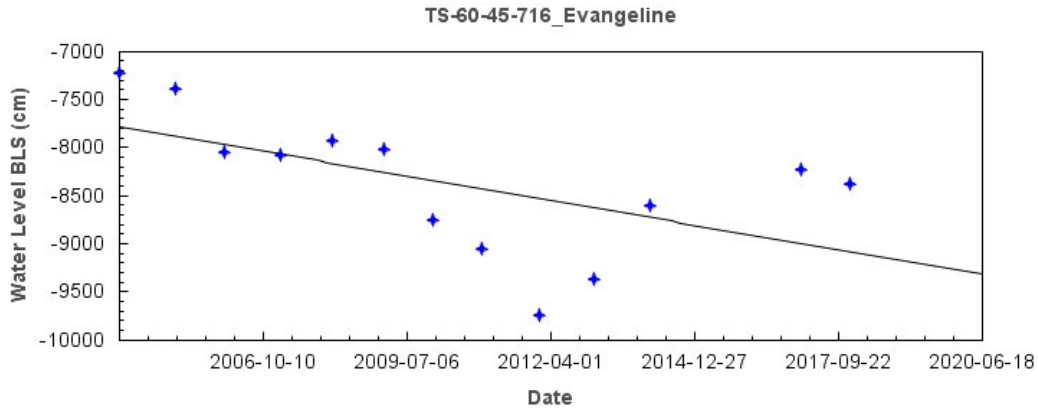
TS-60-45-716_Evangeline
Water Level BLS (cm)
-7000
-7500
-8000
-8500
-9000
-9500
-10000
2006-10-10
2009-07-06
2012-04-01
2014-12-27
2017-09-22
2020-06-18
Date

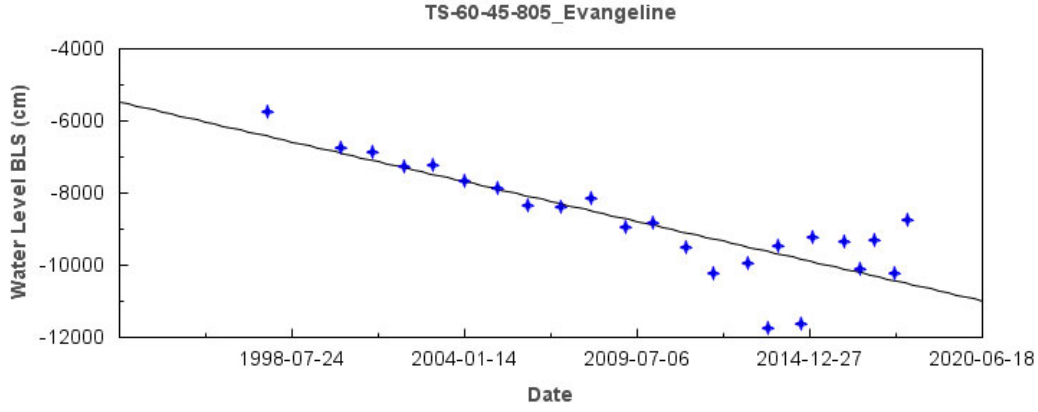
TS-60-45-805_Evangeline
Water Level BLS (cm)
-4000
-6000
-8000
-10000
-12000
1998-07-24
2004-01-14
2009-07-06
2014-12-27
2020-06-18
Date

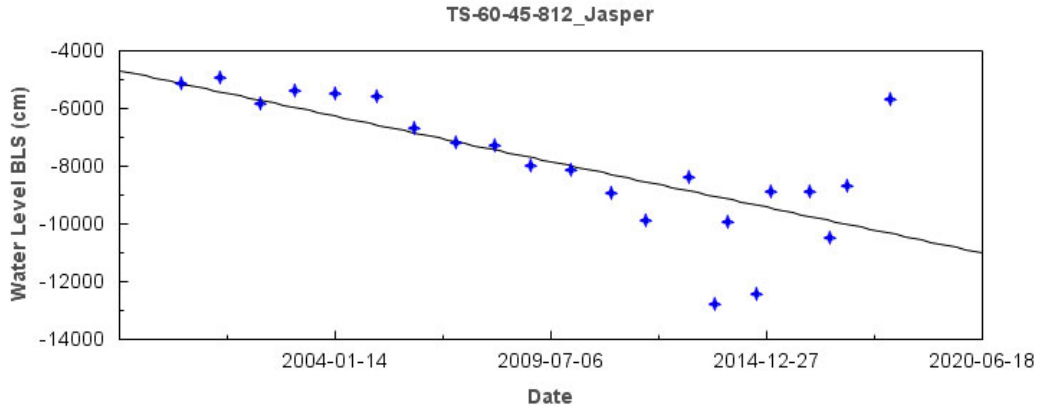
TS-60-45-812_Jasper
Water Level BLS (cm)
-4000
-6000
-8000
-10000
-12000
-14000
2004-01-14
2009-07-06
2014-12-27
2020-06-18
Date

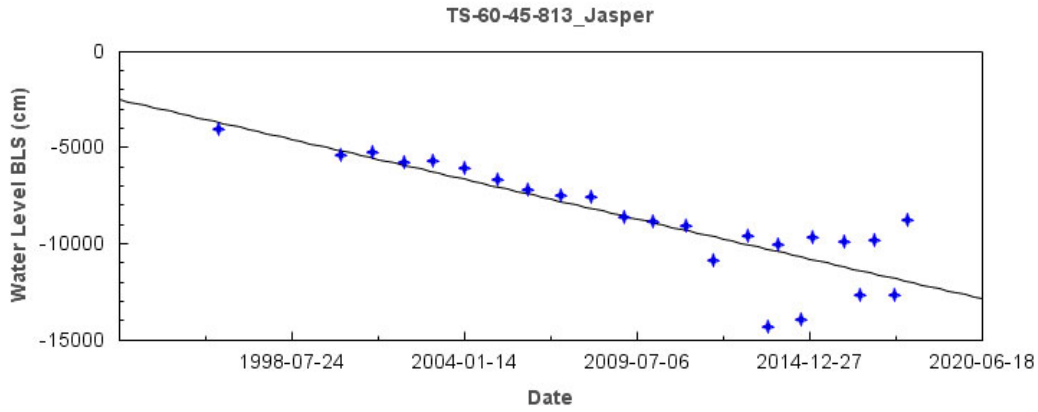
TS-60-45-813_Jasper
Water Level BLS (cm)
0
-5000
-10000
-15000
1998-07-24
2004-01-14
2009-07-06
2014-12-27
2020-06-18
Date

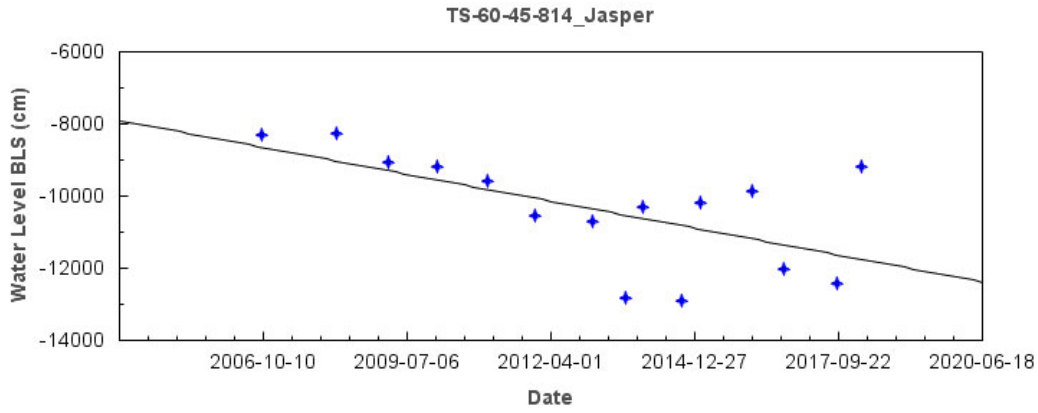
TS-60-45-814_Jasper
Water Level BLS (cm)
-6000
-8000
-10000
-12000
-14000
2006-10-10
2009-07-06
2012-04-01
2014-12-27
2017-09-22
2020-06-18
Date

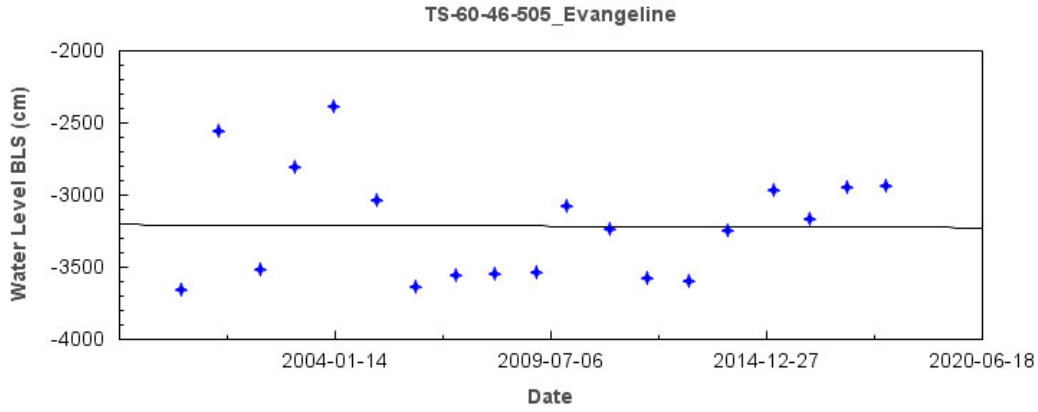
TS-60-46-505_Evangeline
Water Level BLS (cm)
-2000
-2500
-3000
-3500
-4000
2004-01-14
2009-07-06
2014-12-27
2020-06-18
Date

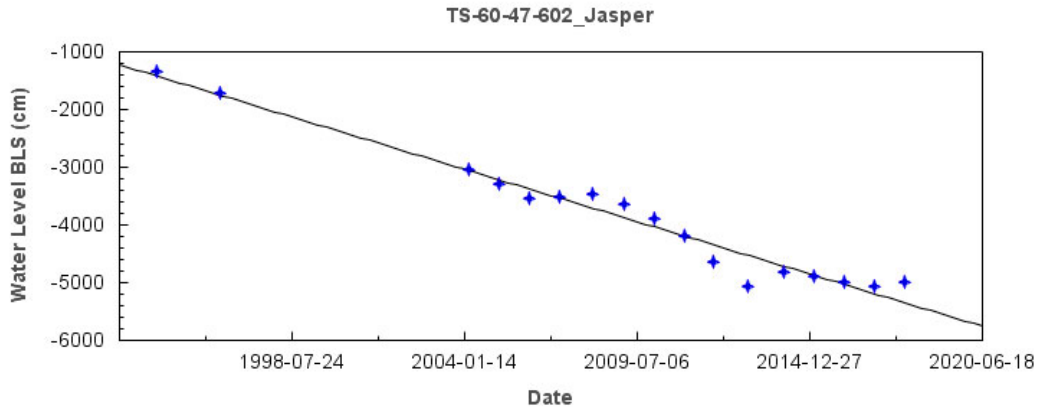
TS-60-47-602_Jasper
Water Level BLS (cm)
-1000
-2000
-3000
-4000
-5000
-6000
1998-07-24
2004-01-14
2009-07-06
2014-12-27
2020-06-18
Date

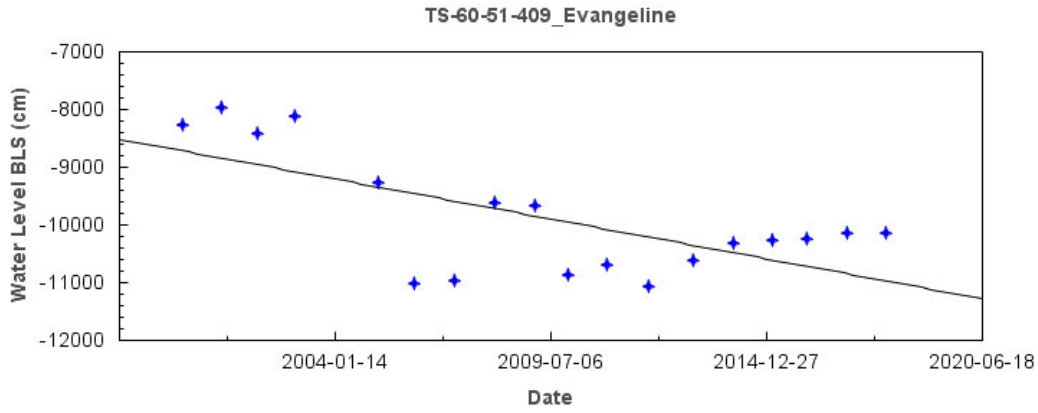
TS-60-51-409_Evangeline
Water Level BLS (cm)
-7000
-8000
-9000
-10000
-11000
-12000
2004-01-14
2009-07-06
2014-12-27
2020-06-18
Date

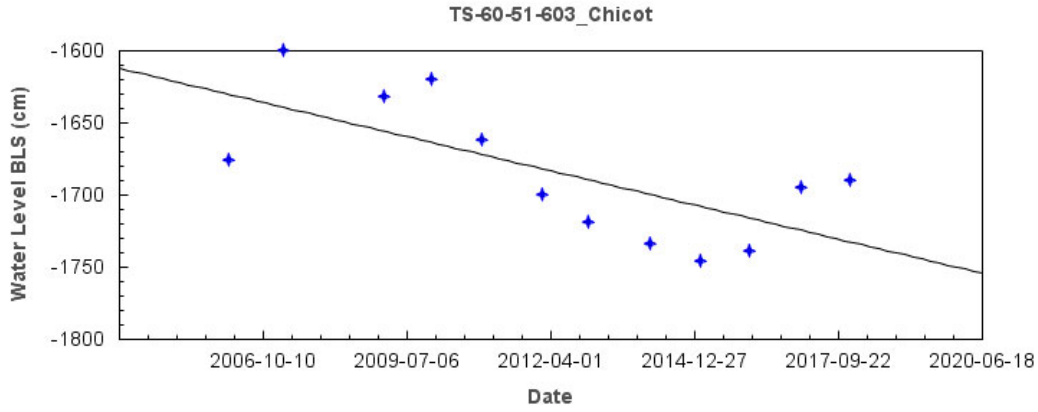
TS-60-51-603_Chicot
Water Level BLS (cm)
-1600
-1650
-1700
-1750
-1800
2006-10-10
2009-07-06
2012-04-01
2014-12-27
2017-09-22
2020-06-18
Date

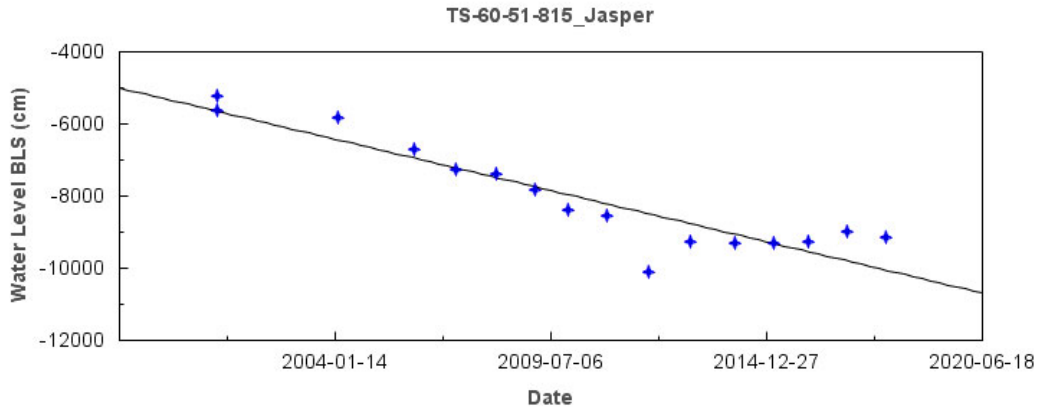
TS-60-51-815_Jasper
Water Level BLS (cm)
-4000
-6000
-8000
-10000
-12000
2004-01-14
2009-07-06
2014-12-27
2020-06-18
Date

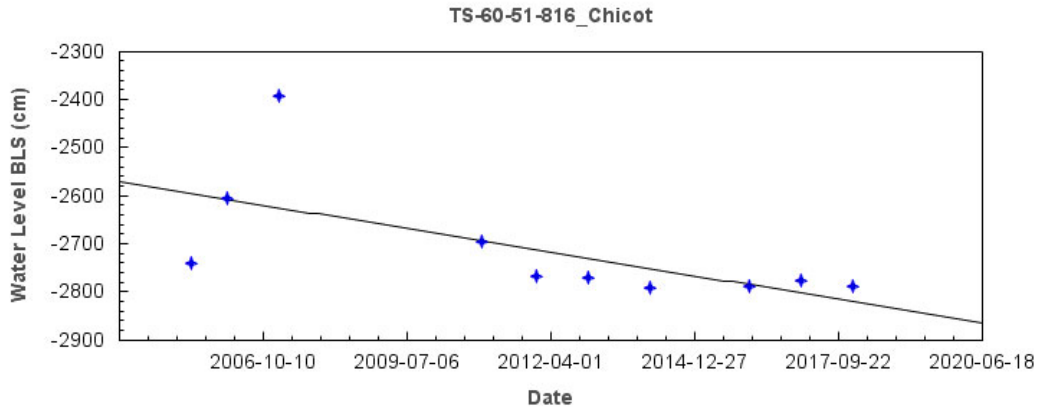
TS-60-51-816_Chicot
Water Level BLS (cm)
-2300
-2400
-2500
-2600
-2700
-2800
-2900
2006-10-10
2009-07-06
2012-04-01
2014-12-27
2017-09-22
2020-06-18
Date

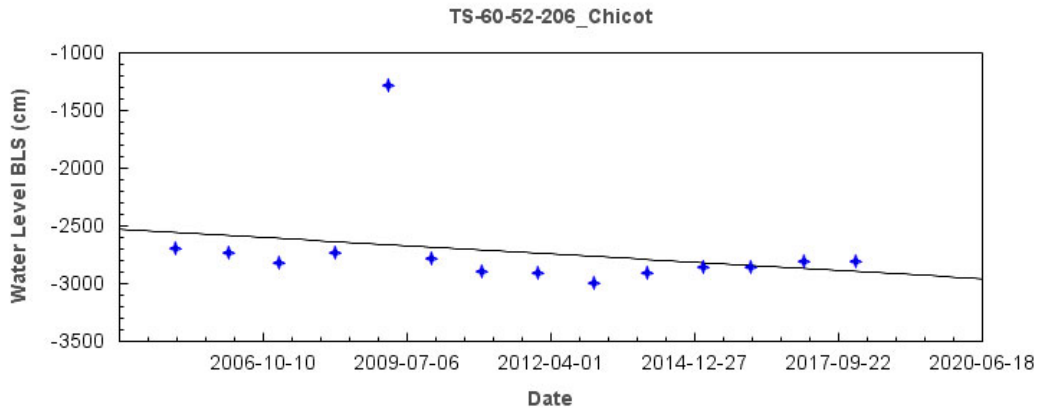
TS-60-52-206_Chicot
Water Level BLS (cm)
-1000
-1500
-2000
-2500
-3000
-3500
2006-10-10
2009-07-06
2012-04-01
2014-12-27
2017-09-22
2020-06-18
Date

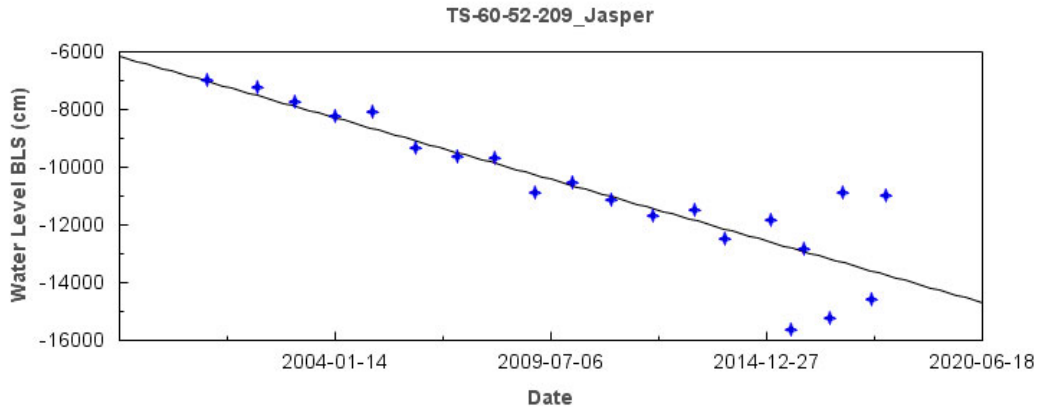
TS-60-52-209_Jasper
Water Level BLS (cm)
-6000
-8000
-10000
-12000
-14000
-16000
2004-01-14
2009-07-06
2014-12-27
2020-06-18
Date

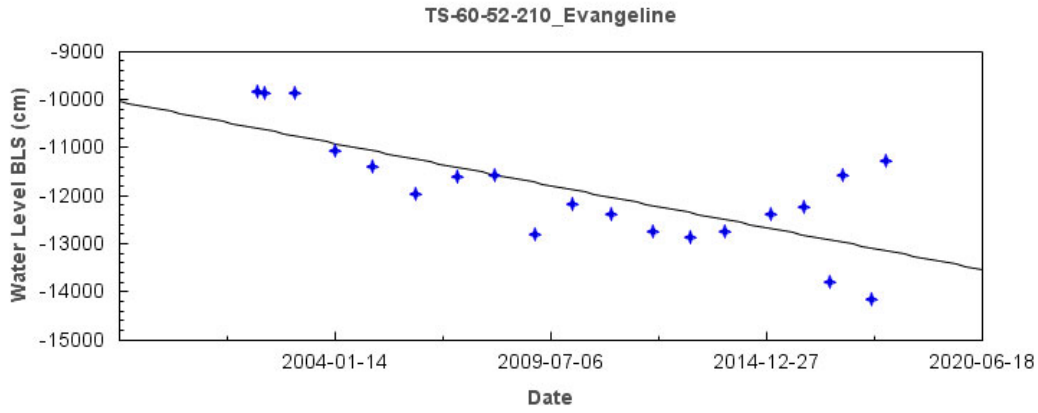
TS-60-52-210_Evangeline
Water Level BLS (cm)
-9000
-10000
-11000
-12000
-13000
-14000
-15000
2004-01-14
2009-07-06
2014-12-27
2020-06-18
Date

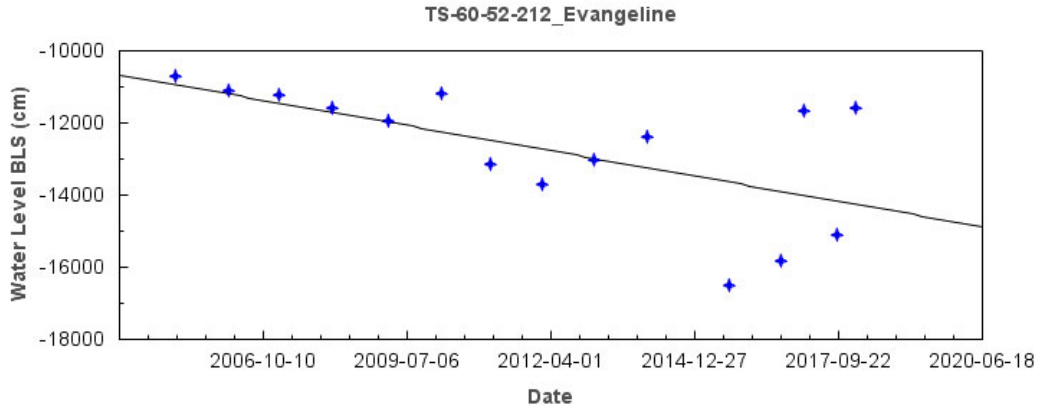
TS-60-52-212_Evangeline
Water Level BLS (cm)
-10000
-12000
-14000
-16000
-18000
2006-10-10
2009-07-06
2012-04-01
2014-12-27
2017-09-22
2020-06-18
Date

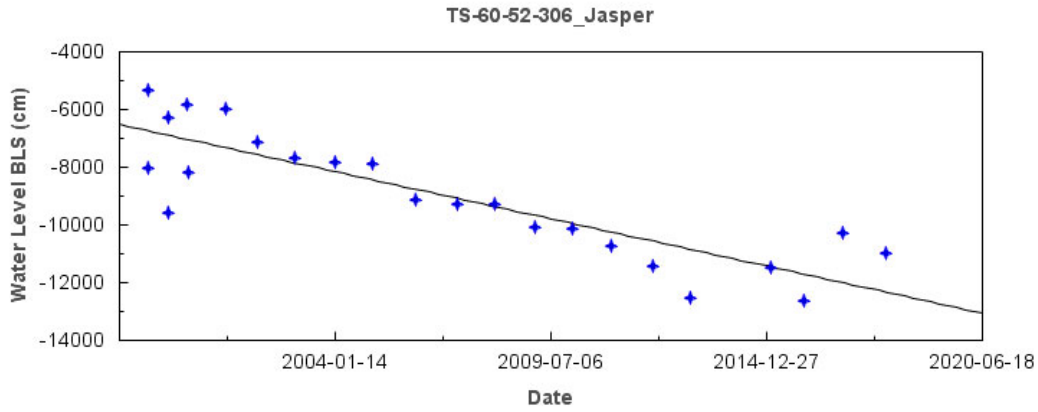
TS-60-52-306_Jasper
Water Level BLS (cm)
-4000
-6000
-8000
-10000
-12000
-14000
2004-01-14
2009-07-06
2014-12-27
2020-06-18
Date

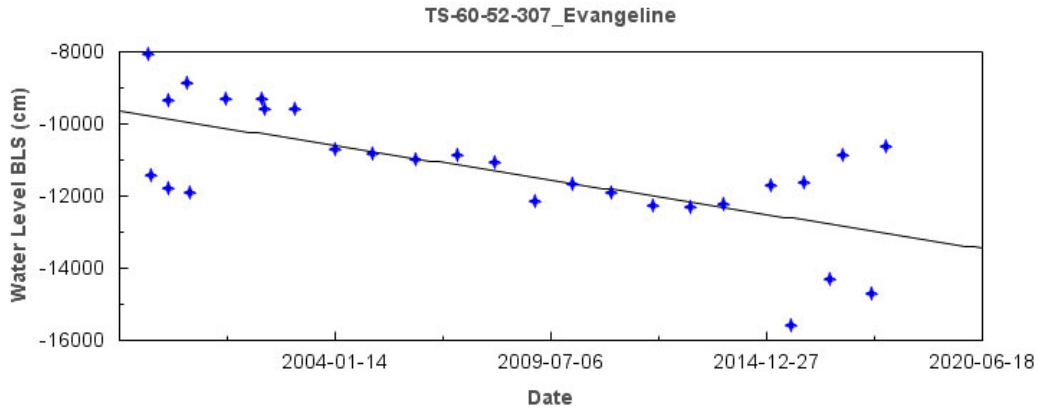
TS-60-52-307_Evangeline
Water Level BLS (cm)
-8000
-10000
-12000
-14000
-16000
2004-01-14
2009-07-06
2014-12-27
2020-06-18
Date

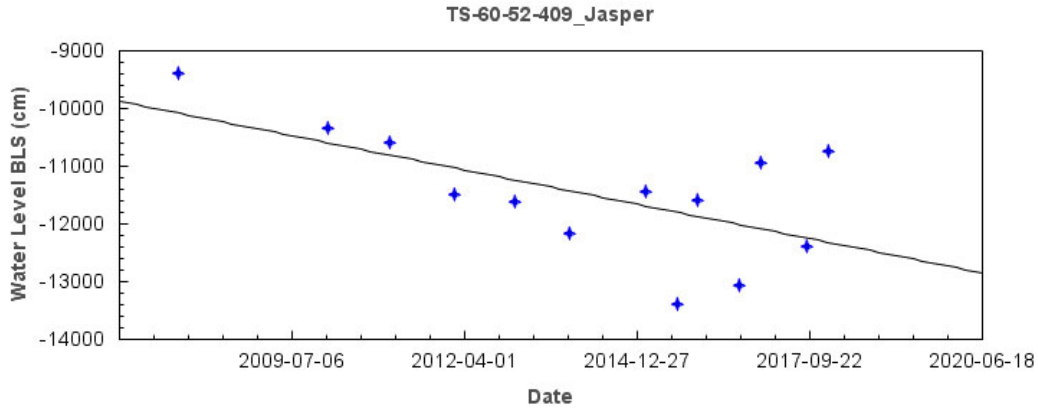
TS-60-52-409_Jasper
Water Level BLS (cm)
-9000
-10000
-11000
-12000
-13000
-14000
2009-07-06
2012-04-01
2014-12-27
2017-09-22
2020-06-18
Date

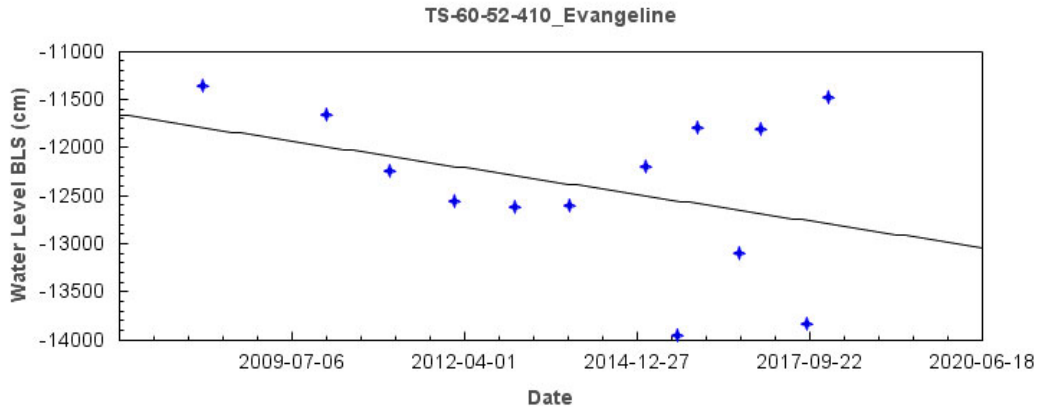
TS-60-52-410_Evangeline
Water Level BLS (cm)
-11000
-11500
-12000
-12500
-13000
-13500
-14000
2009-07-06
2012-04-01
2014-12-27
2017-09-22
2020-06-18
Date

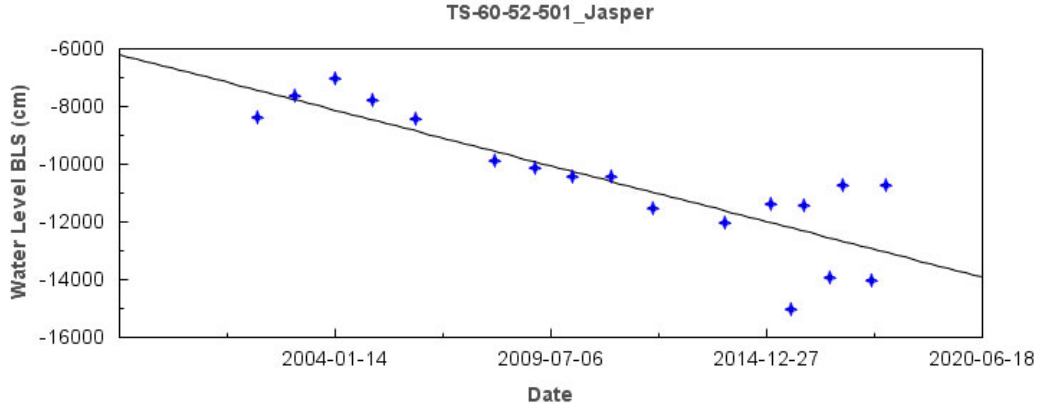
TS-60-52-501_Jasper
Water Level BLS (cm)
-6000
-8000
-10000
-12000
-14000
-16000
2004-01-14
2009-07-06
2014-12-27
2020-06-18
Date

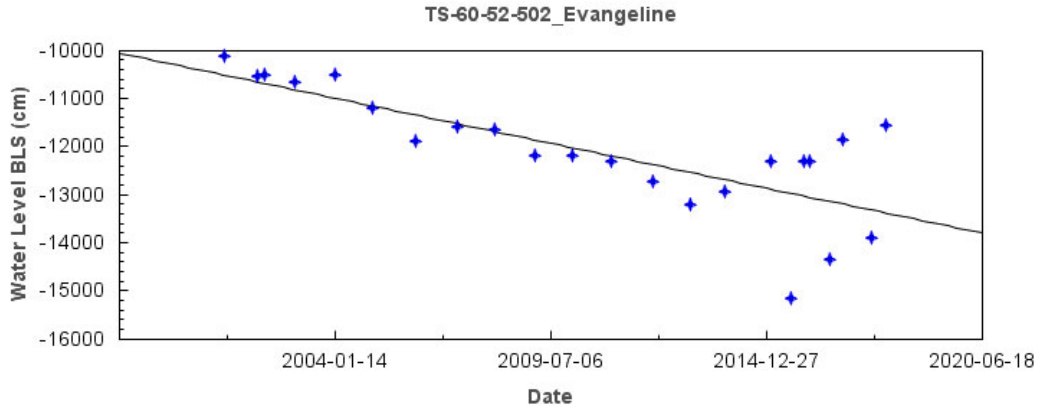
TS-60-52-502_Evangeline
Water Level BLS (cm)
-10000
-11000
-12000
-13000
-14000
-15000
-16000
2004-01-14
2009-07-06
2014-12-27
2020-06-18
Date

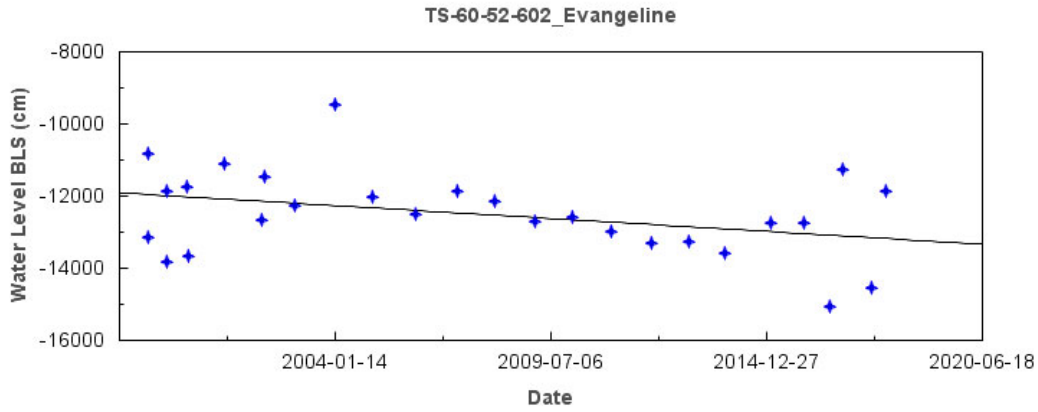
TS-60-52-602_Evangeline
Water Level BLS (cm)
-8000
-10000
-12000
-14000
-16000
2004-01-14
2009-07-06
2014-12-27
2020-06-18
Date

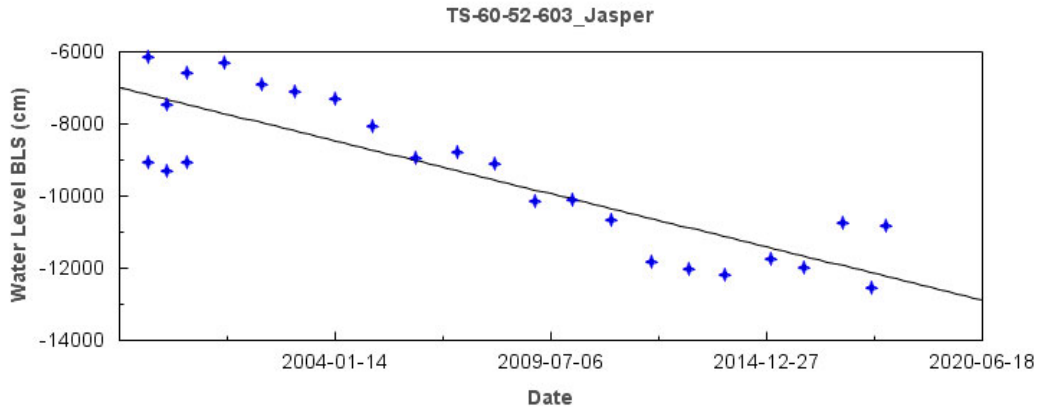
TS-60-52-603_Jasper
Water Level BLS (cm)
-6000
-8000
-10000
-12000
-14000
2004-01-14
2009-07-06
2014-12-27
2020-06-18
Date

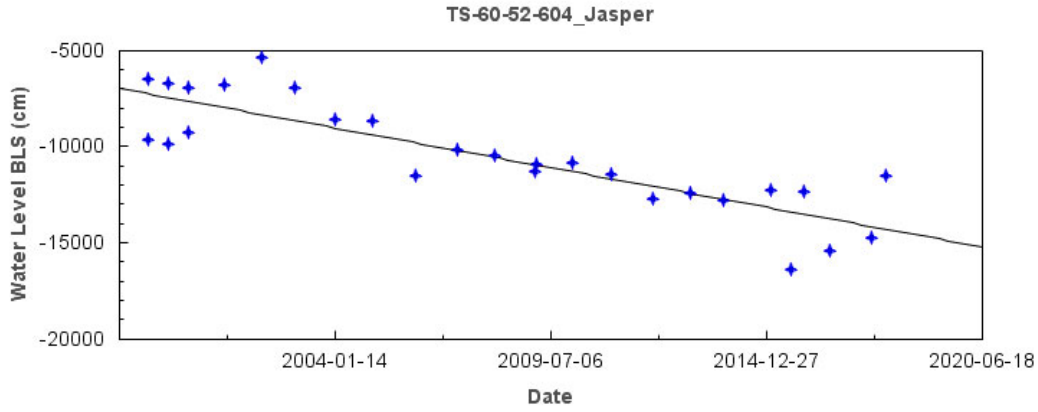
TS-60-52-604_Jasper
Water Level BLS (cm)
-5000
-10000
-15000
-20000
2004-01-14
2009-07-06
2014-12-27
2020-06-18
Date

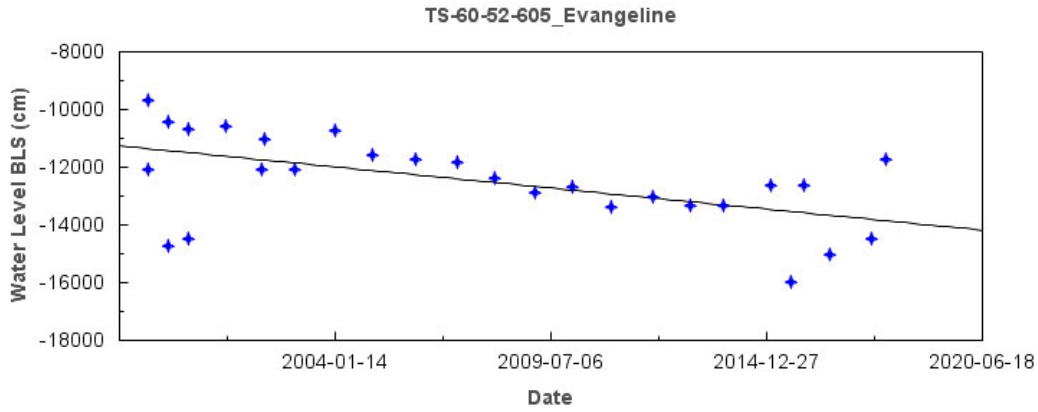
TS-60-52-605_Evangeline
Water Level BLS (cm)
-8000
-10000
-12000
-14000
-16000
-18000
2004-01-14
2009-07-06
2014-12-27
2020-06-18
Date

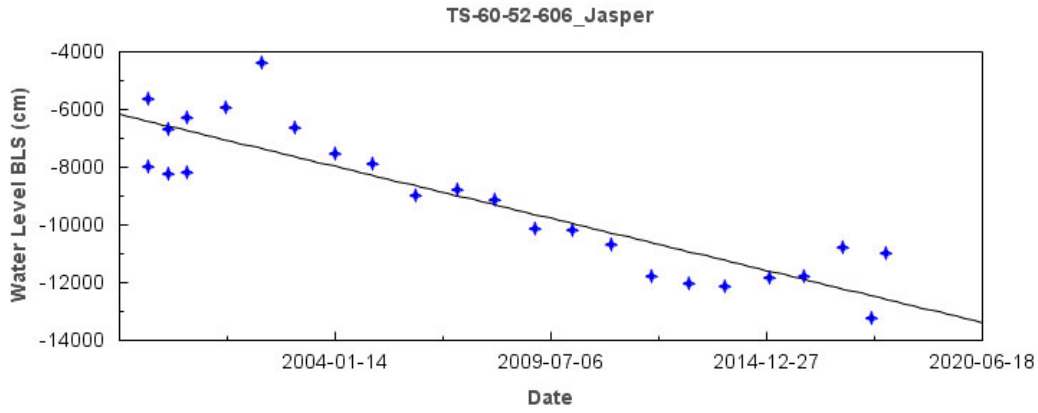
TS-60-52-606_Jasper
Water Level BLS (cm)
-4000
-6000
-8000
-10000
-12000
-14000
2004-01-14
2009-07-06
2014-12-27
2020-06-18
Date

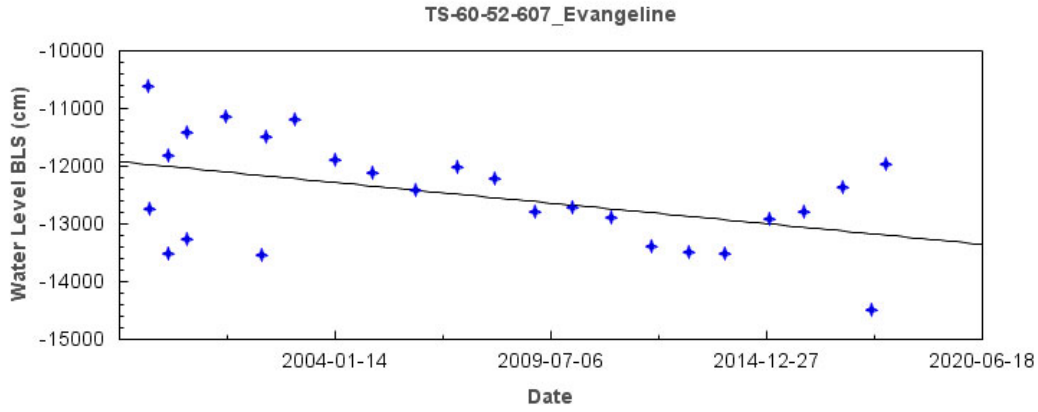
TS-60-52-607_Evangeline
Water Level BLS (cm)
-10000
-11000
-12000
-13000
-14000
-15000
2004-01-14
2009-07-06
2014-12-27
2020-06-18
Date

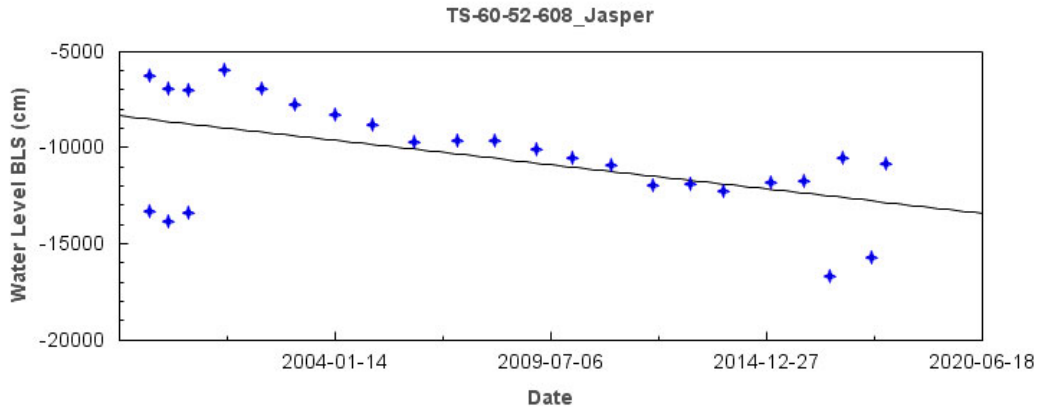
TS-60-52-608_Jasper
Water Level BLS (cm)
-5000
-10000
-15000
-20000
2004-01-14
2009-07-06
2014-12-27
2020-06-18
Date

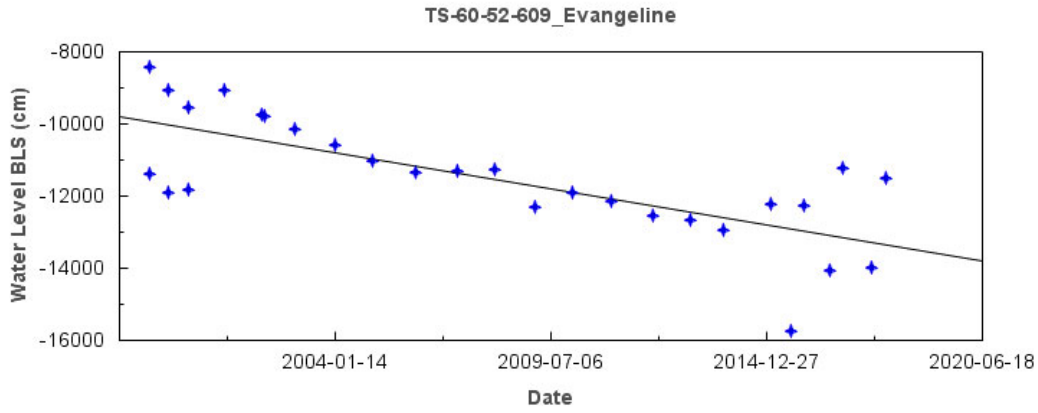
TS-60-52-609_Evangeline
Water Level BLS (cm)
-8000
-10000
-12000
-14000
-16000
2004-01-14
2009-07-06
2014-12-27
2020-06-18
Date

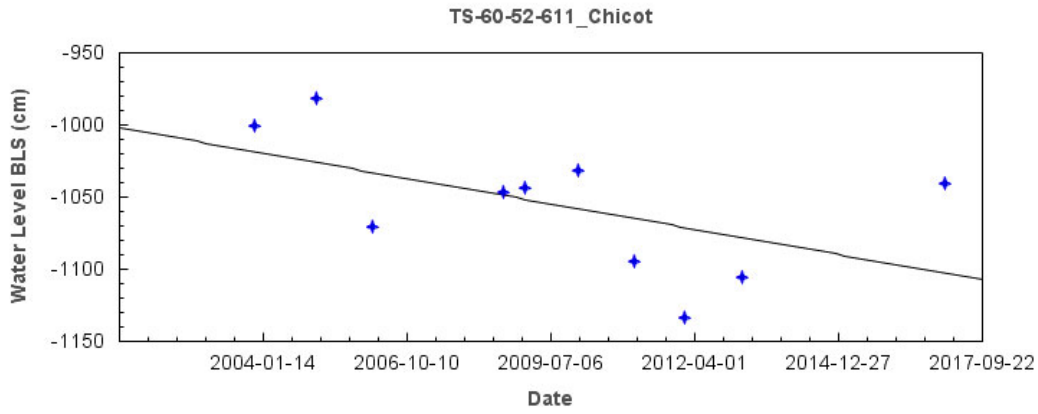
TS-60-52-611_Chicot
Water Level BLS (cm)
-950
-1000
-1050
-1100
-1150
2004-01-14
2006-10-10
2009-07-06
2012-04-01
2014-12-27
2017-09-22
Date

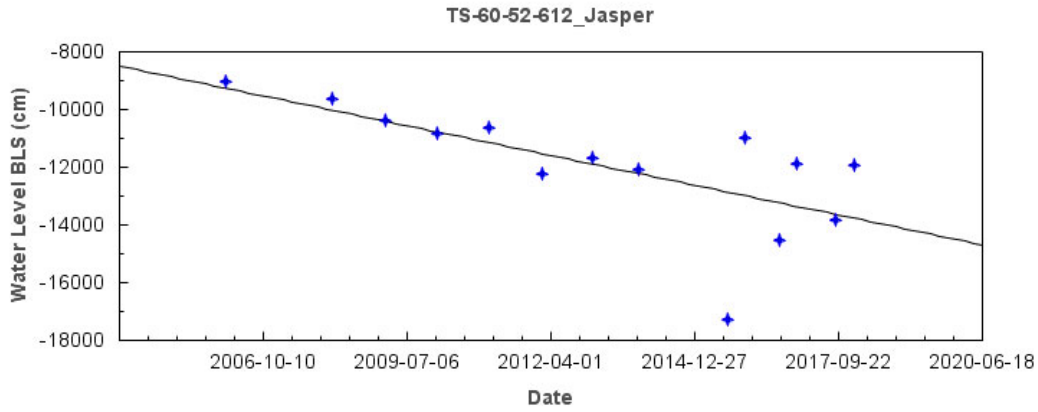
TS-60-52-612_Jasper
Water Level BLS (cm)
-8000
-10000
-12000
-14000
-16000
-18000
2006-10-10
2009-07-06
2012-04-01
2014-12-27
2017-09-22
2020-06-18
Date

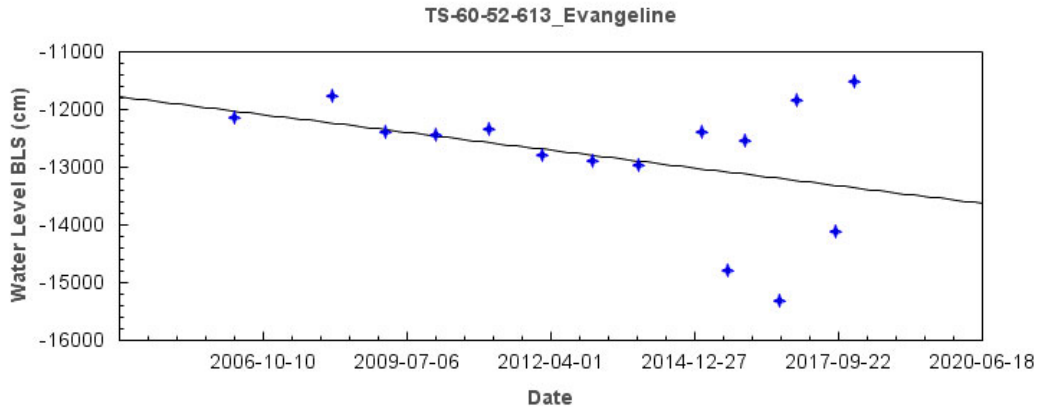
TS-60-52-613_Evangeline
Water Level BLS (cm)
-11000
-12000
-13000
-14000
-15000
-16000
2006-10-10
2009-07-06
2012-04-01
2014-12-27
2017-09-22
2020-06-18
Date

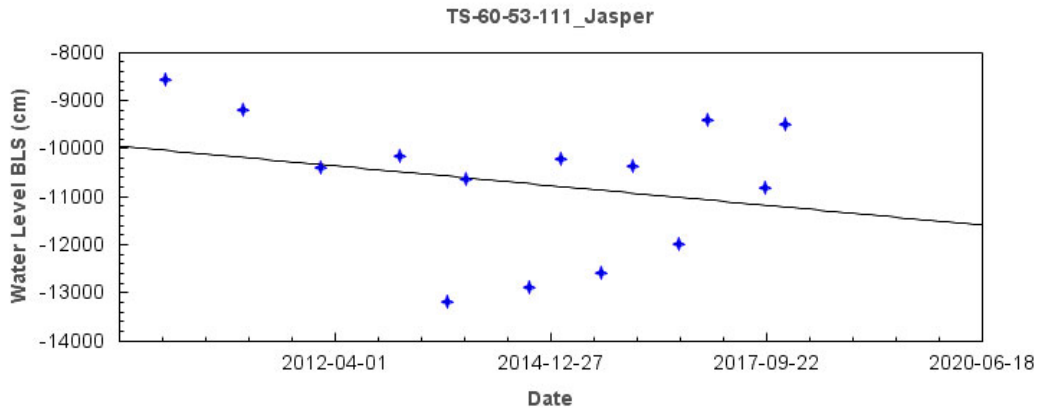
TS-60-53-111_Jasper
Water Level BLS (cm)
-8000
-9000
-10000
-11000
-12000
-13000
-14000
2012-04-01
2014-12-27
2017-09-22
2020-06-18
Date

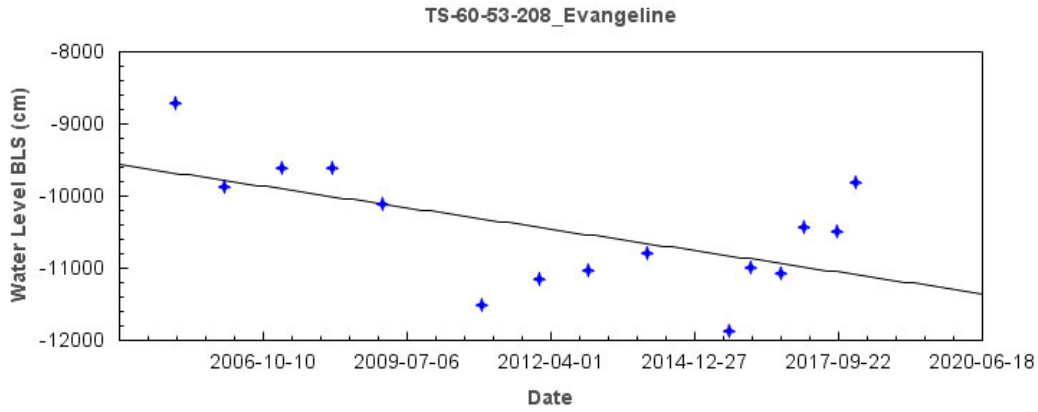
TS-60-53-208_Evangeline
Water Level BLS (cm)
-8000
-9000
-10000
-11000
-12000
2006-10-10
2009-07-06
2012-04-01
2014-12-27
2017-09-22
2020-06-18
Date

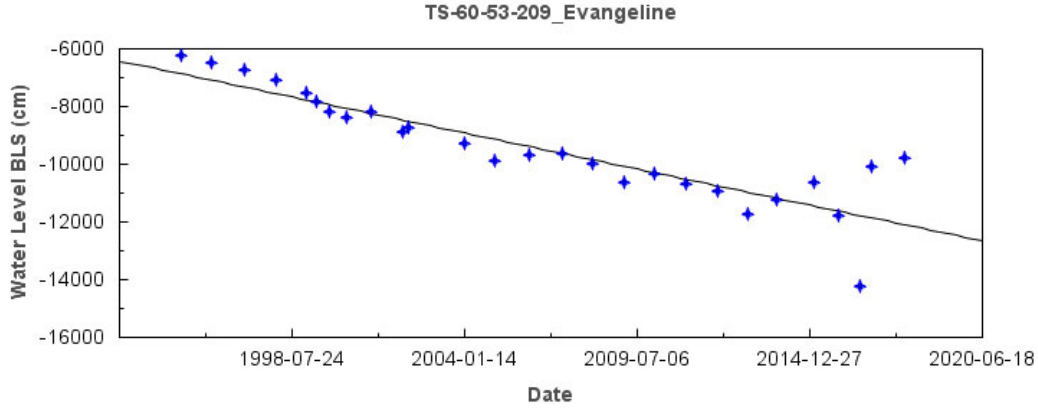
TS-60-53-209_Evangeline
Water Level BLS (cm)
-6000
-8000
-10000
-12000
-14000
-16000
1998-07-24
2004-01-14
2009-07-06
2014-12-27
2020-06-18
Date

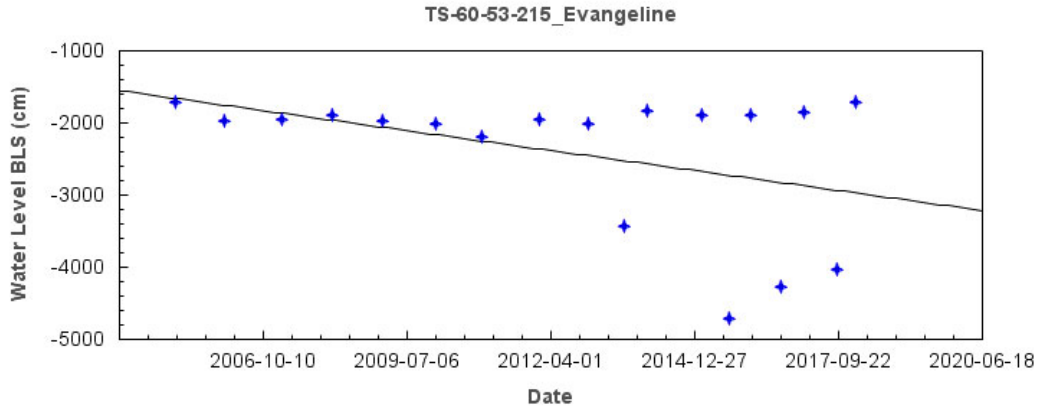
TS-60-53-215_Evangeline
Water Level BLS (cm)
-1000
-2000
-3000
-4000
-5000
2006-10-10
2009-07-06
2012-04-01
2014-12-27
2017-09-22
2020-06-18
Date

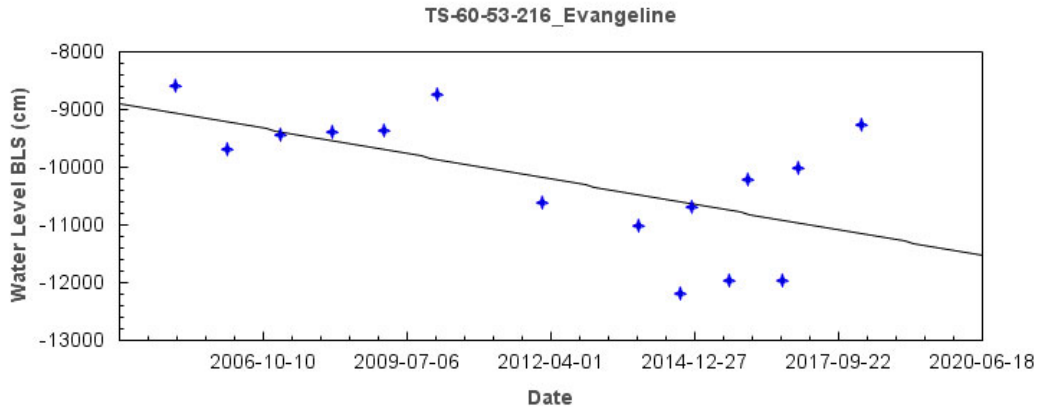
TS-60-53-216_Evangeline
Water Level BLS (cm)
-8000
-9000
-10000
-11000
-12000
-13000
2006-10-10
2009-07-06
2012-04-01
2014-12-27
2017-09-22
2020-06-18
Date

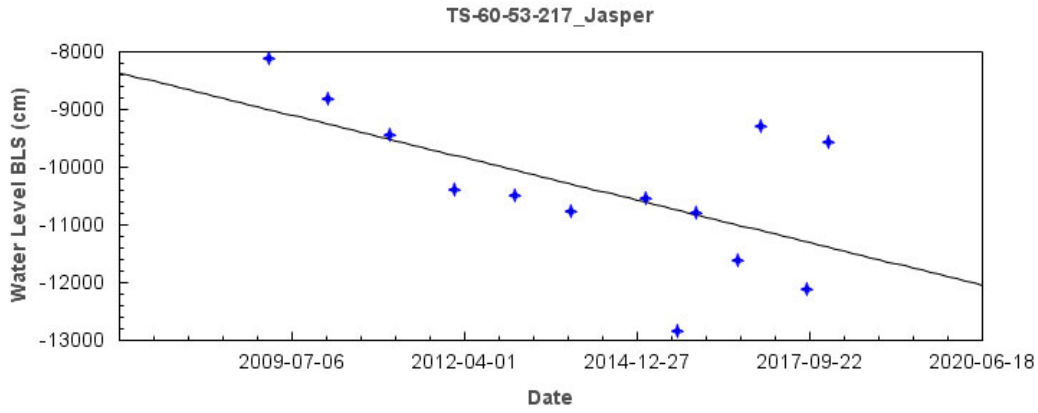
TS-60-53-217_Jasper
Water Level BLS (cm)
-8000
-9000
-10000
-11000
-12000
-13000
2009-07-06
2012-04-01
2014-12-27
2017-09-22
2020-06-18
Date

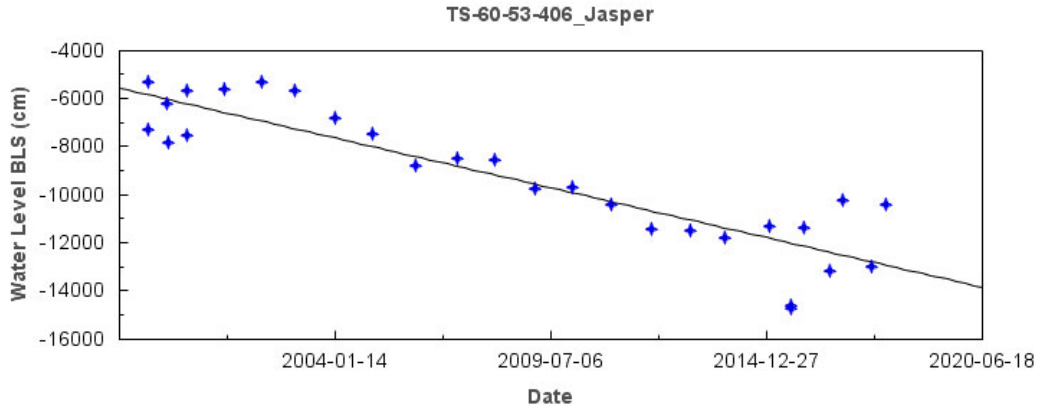
TS-60-53-406_Jasper
Water Level BLS (cm)
-4000
-6000
-8000
-10000
-12000
-14000
-16000
2004-01-14
2009-07-06
2014-12-27
2020-06-18
Date

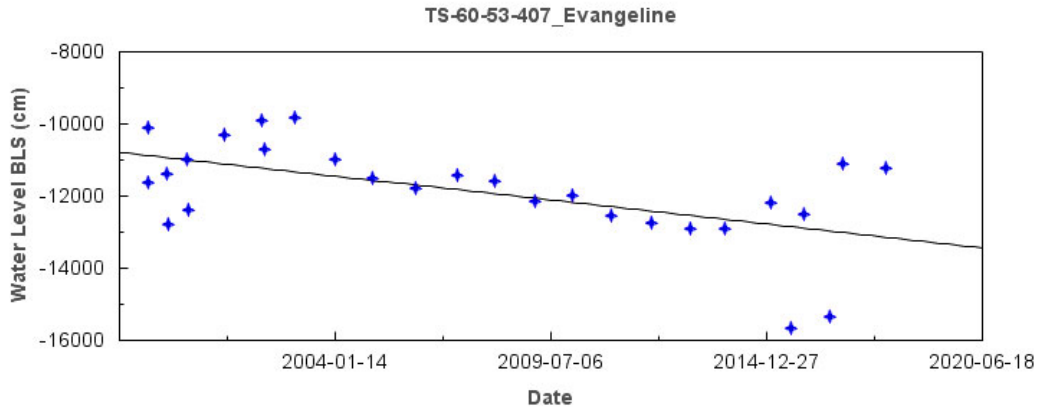
TS-60-53-407_Evangeline
Water Level BLS (cm)
-8000
-10000
-12000
-14000
-16000
2004-01-14
2009-07-06
2014-12-27
2020-06-18
Date

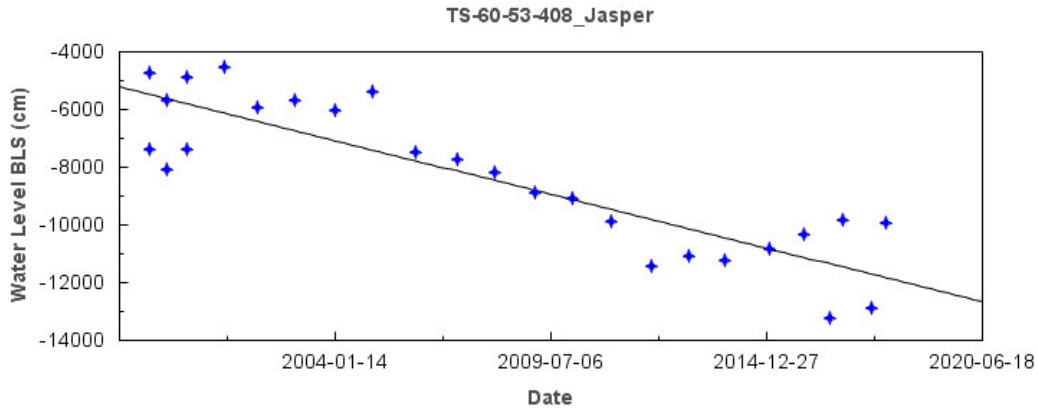
TS-60-53-408_Jasper
Water Level BLS (cm)
-4000
-6000
-8000
-10000
-12000
-14000
2004-01-14
2009-07-06
2014-12-27
2020-06-18
Date

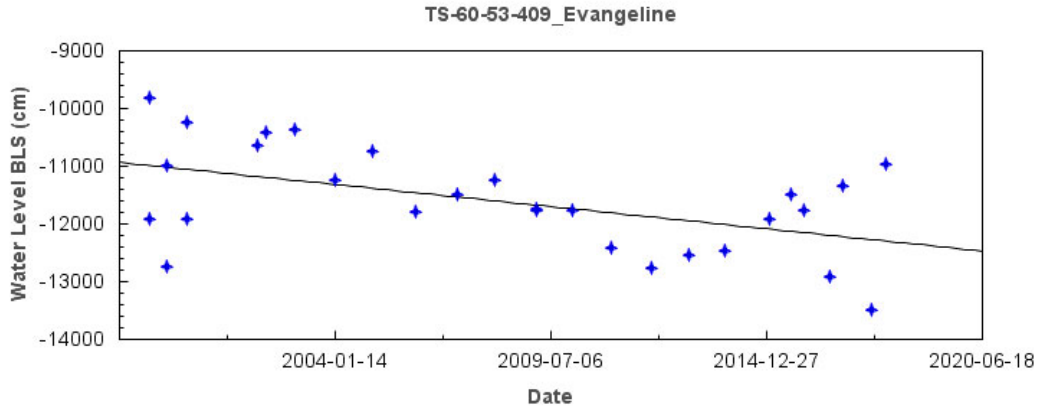
TS-60-53-409_Evangeline
Water Level BLS (cm)
-9000
-10000
-11000
-12000
-13000
-14000
2004-01-14
2009-07-06
2014-12-27
2020-06-18
Date

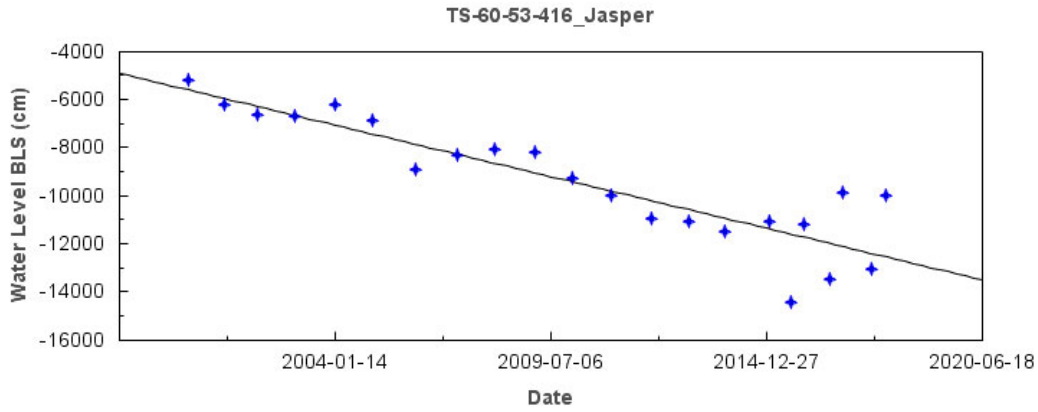
TS-60-53-416_Jasper
Water Level BLS (cm)
-4000
-6000
-8000
-10000
-12000
-14000
-16000
2004-01-14
2009-07-06
2014-12-27
2020-06-18
Date

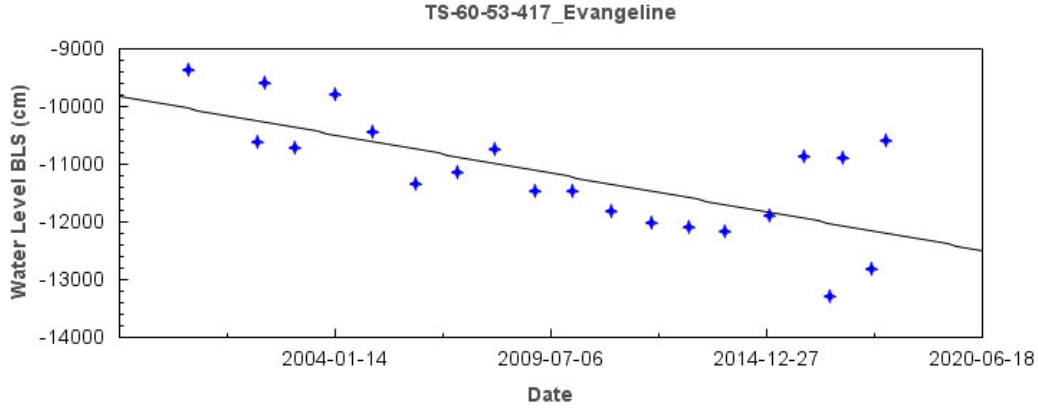
TS-60-53-417_Evangeline
Water Level BLS (cm)
-9000
-10000
-11000
-12000
-13000
-14000
2004-01-14
2009-07-06
2014-12-27
2020-06-18
Date

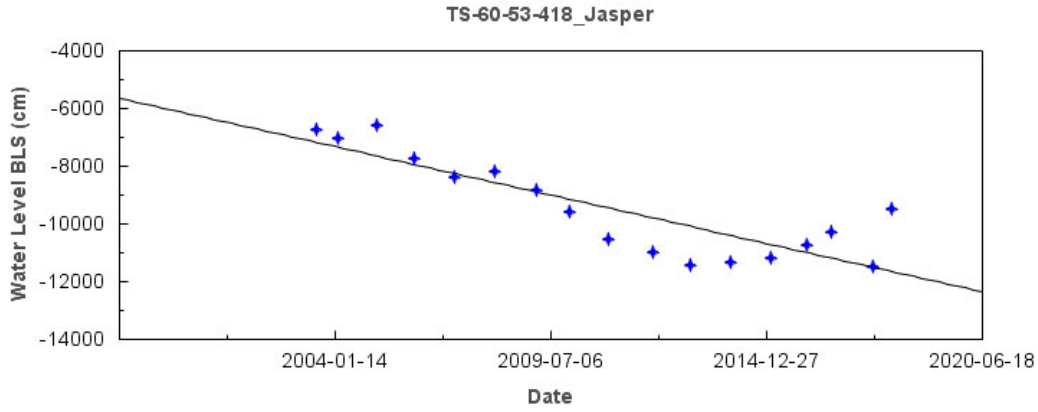
TS-60-53-418_Jasper
Water Level BLS (cm)
-4000
-6000
-8000
-10000
-12000
-14000
2004-01-14
2009-07-06
2014-12-27
2020-06-18
Date

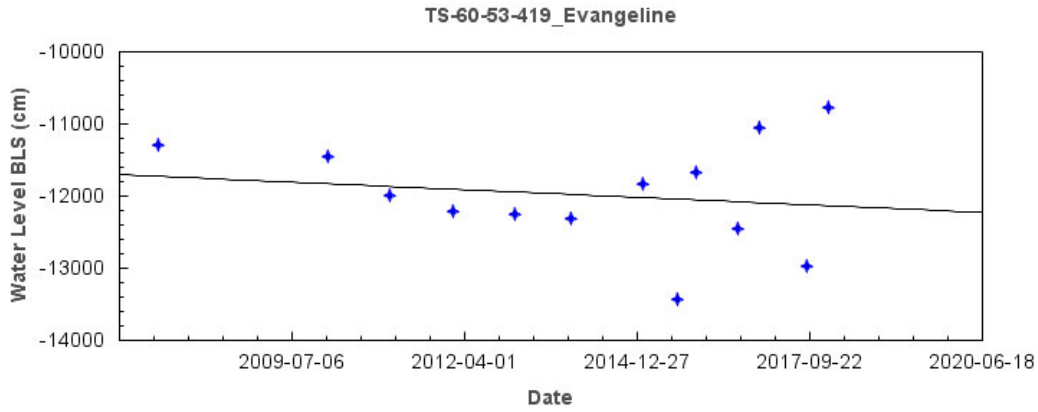
TS-60-53-419_Evangeline
Water Level BLS (cm)
-10000
-11000
-12000
-13000
-14000
2009-07-06
2012-04-01
2014-12-27
2017-09-22
2020-06-18
Date

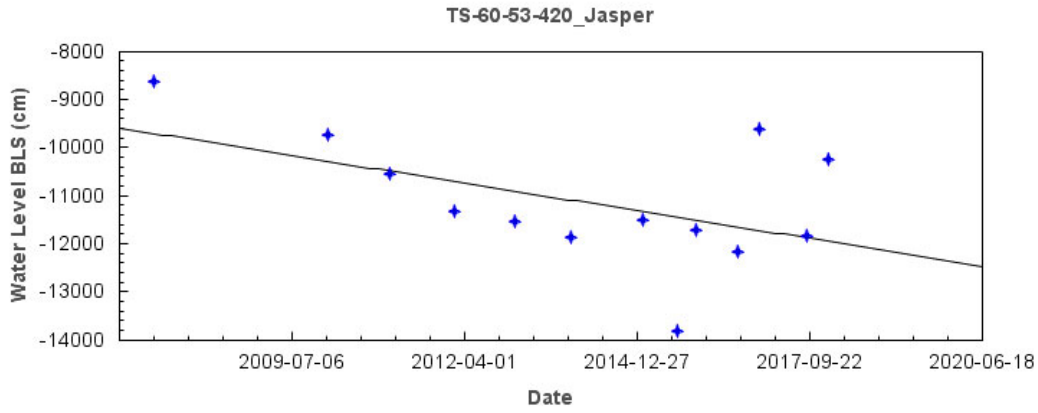
TS-60-53-420_Jasper
Water Level BLS (cm)
-8000
-9000
-10000
-11000
-12000
-13000
-14000
2009-07-06
2012-04-01
2014-12-27
2017-09-22
2020-06-18
Date

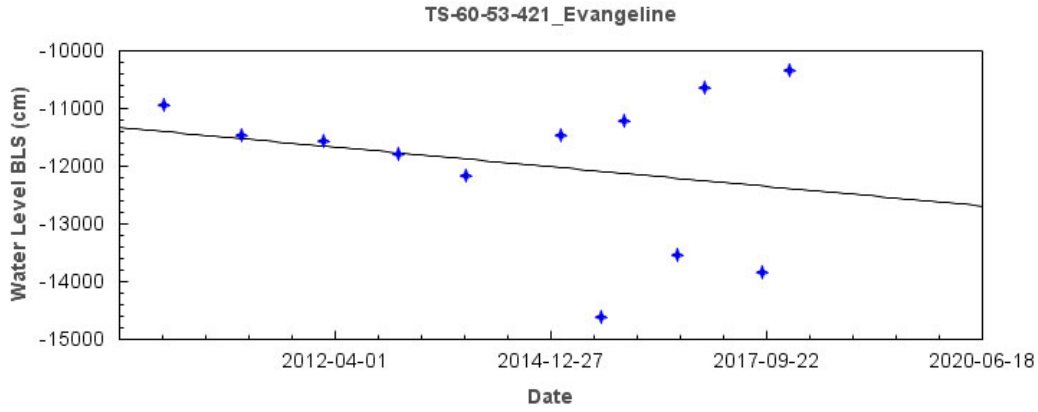
TS-60-53-421_Evangeline
Water Level BLS (cm)
-10000
-11000
-12000
-13000
-14000
-15000
2012-04-01
2014-12-27
2017-09-22
2020-06-18
Date

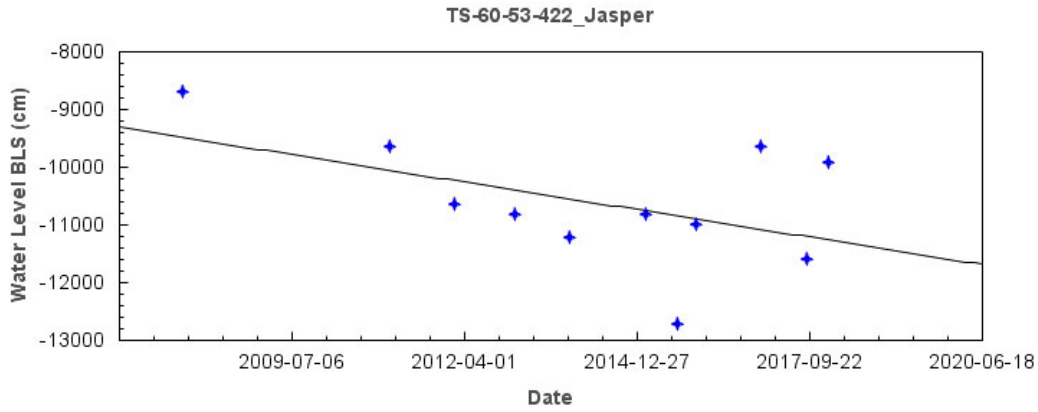
TS-60-53-422_Jasper
Water Level BLS (cm)
-8000
-9000
-10000
-11000
-12000
-13000
2009-07-06
2012-04-01
2014-12-27
2017-09-22
2020-06-18
Date

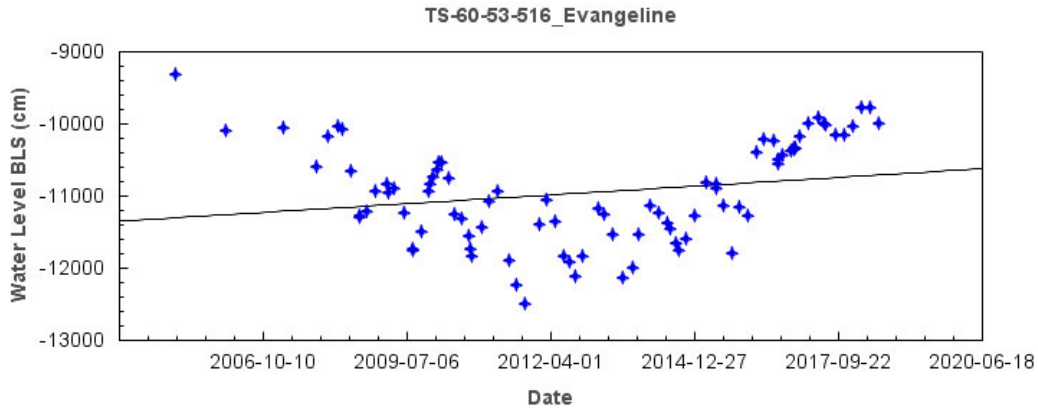
TS-60-53-516_Evangeline
Water Level BLS (cm)
-9000
-10000
-11000
-12000
-13000
2006-10-10
2009-07-06
2012-04-01
2014-12-27
2017-09-22
2020-06-18
Date

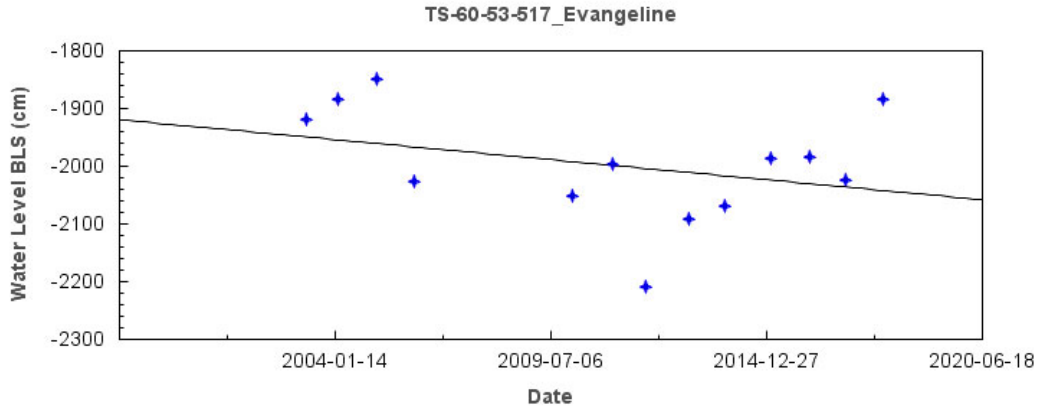
TS-60-53-517_Evangeline
Water Level BLS (cm)
-1800
-1900
-2000
-2100
-2200
-2300
2004-01-14
2009-07-06
2014-12-27
2020-06-18
Date

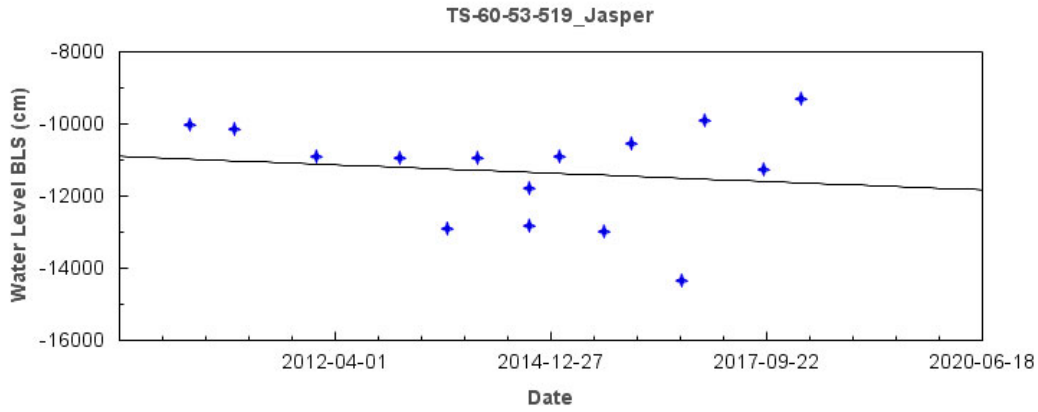
TS-60-53-519_Jasper
Water Level BLS (cm)
-8000
-10000
-12000
-14000
-16000
2012-04-01
2014-12-27
2017-09-22
2020-06-18
Date

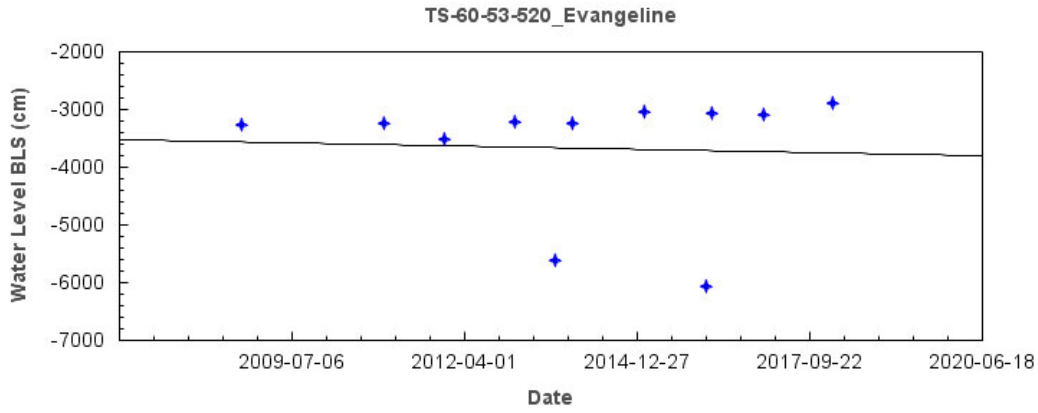
TS-60-53-520_Evangeline
Water Level BLS (cm)
-2000
-3000
-4000
-5000
-6000
-7000
2009-07-06
2012-04-01
2014-12-27
2017-09-22
2020-06-18
Date

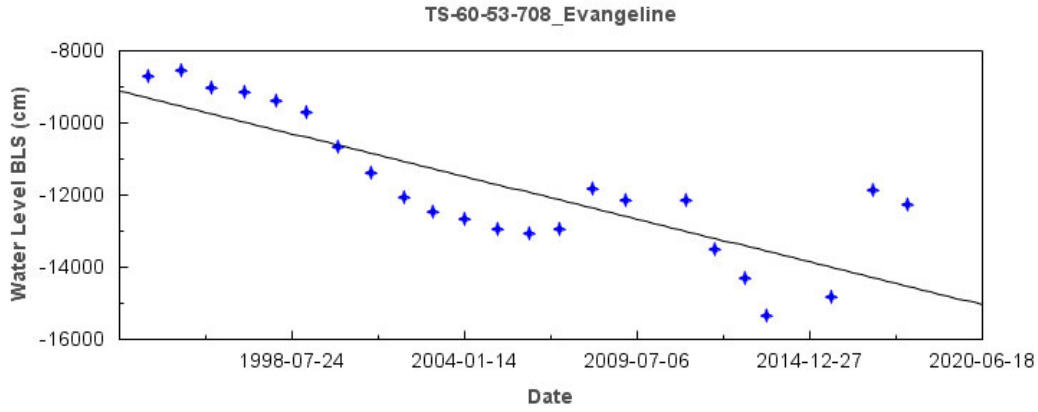
TS-60-53-708_Evangeline
Water Level BLS (cm)
-8000
-10000
-12000
-14000
-16000
1998-07-24
2004-01-14
2009-07-06
2014-12-27
2020-06-18
Date

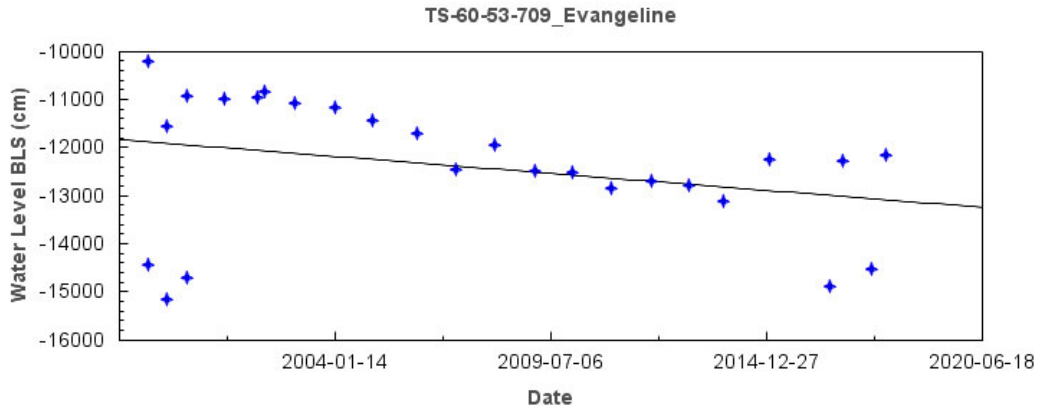
TS-60-53-709_Evangeline
Water Level BLS (cm)
-10000
-11000
-12000
-13000
-14000
-15000
-16000
2004-01-14
2009-07-06
2014-12-27
2020-06-18
Date

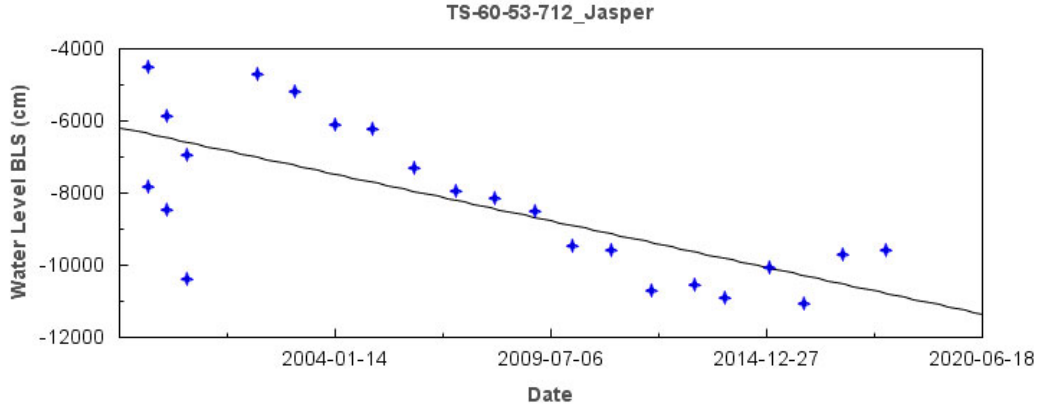
TS-60-53-712_Jasper
Water Level BLS (cm)
-4000
-6000
-8000
-10000
-12000
2004-01-14
2009-07-06
2014-12-27
2020-06-18
Date

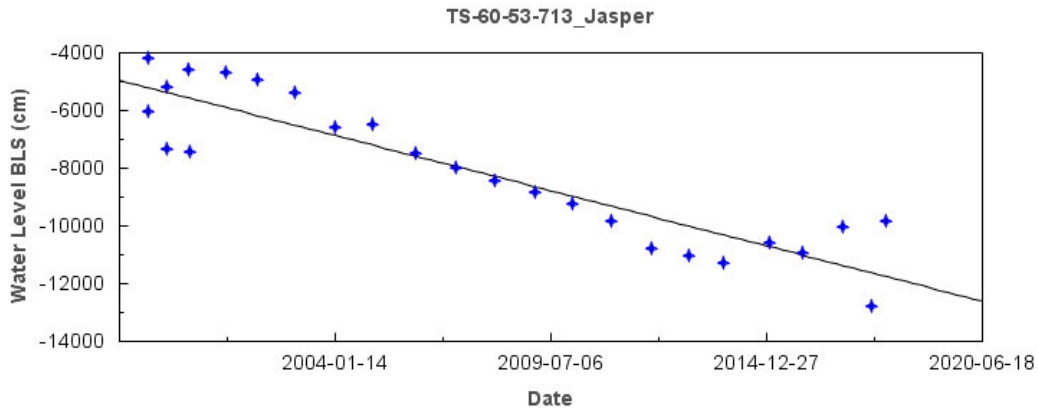
TS-60-53-713_Jasper
Water Level BLS (cm)
-4000
-6000
-8000
-10000
-12000
-14000
2004-01-14
2009-07-06
2014-12-27
2020-06-18
Date

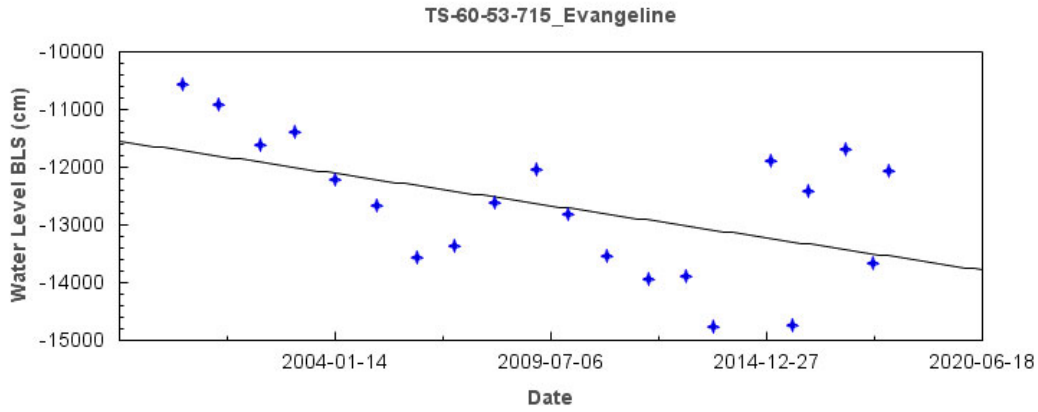
TS-60-53-715_Evangeline
Water Level BLS (cm)
-10000
-11000
-12000
-13000
-14000
-15000
2004-01-14
2009-07-06
2014-12-27
2020-06-18
Date

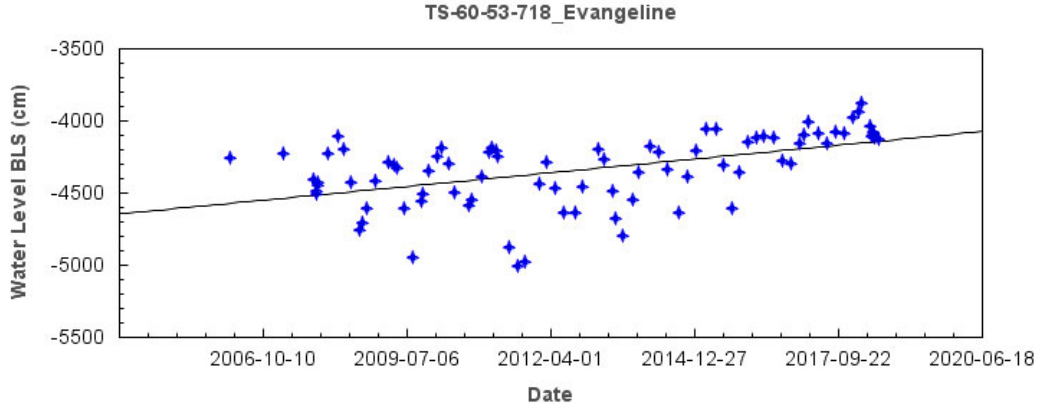
TS-60-53-718_Evangeline
Water Level BLS (cm)
-3500
-4000
-4500
-5000
-5500
2006-10-10
2009-07-06
2012-04-01
2014-12-27
2017-09-22
2020-06-18
Date

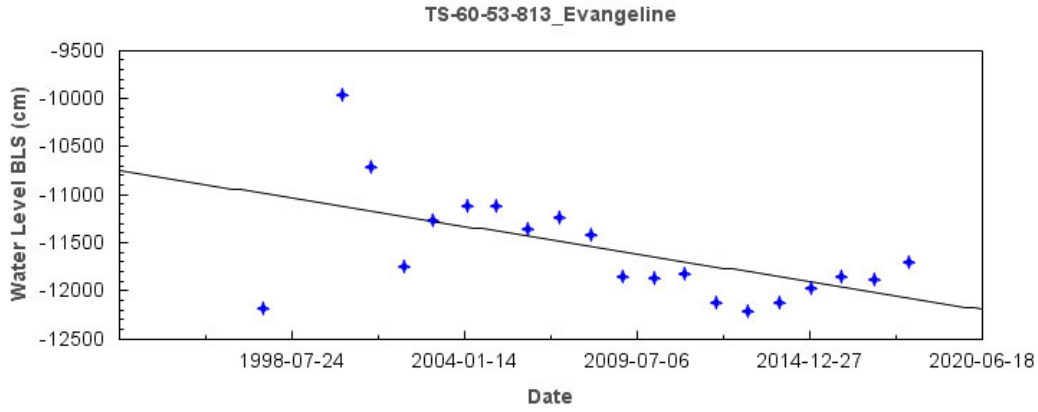
TS-60-53-813_Evangeline
Water Level BLS (cm)
-9500
-10000
-10500
-11000
-11500
-12000
-12500
1998-07-24
2004-01-14
2009-07-06
2014-12-27
2020-06-18
Date

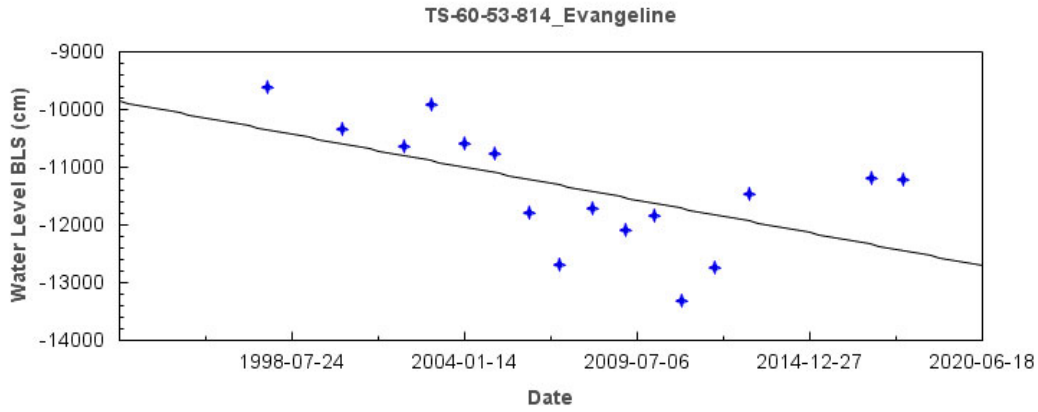
TS-60-53-814_Evangeline
Water Level BLS (cm)
-9000
-10000
-11000
-12000
-13000
-14000
1998-07-24
2004-01-14
2009-07-06
2014-12-27
2020-06-18
Date

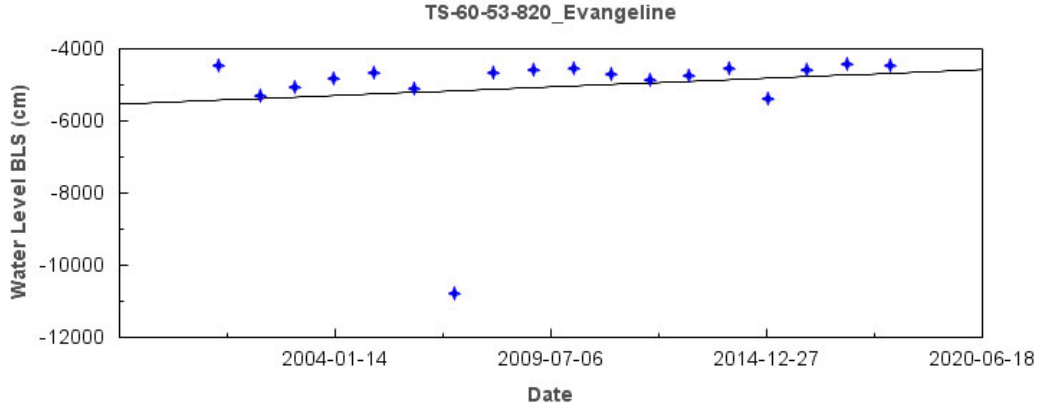
TS-60-53-820_Evangeline
Water Level BLS (cm)
-4000
-6000
-8000
-10000
-12000
2004-01-14
2009-07-06
2014-12-27
2020-06-18
Date

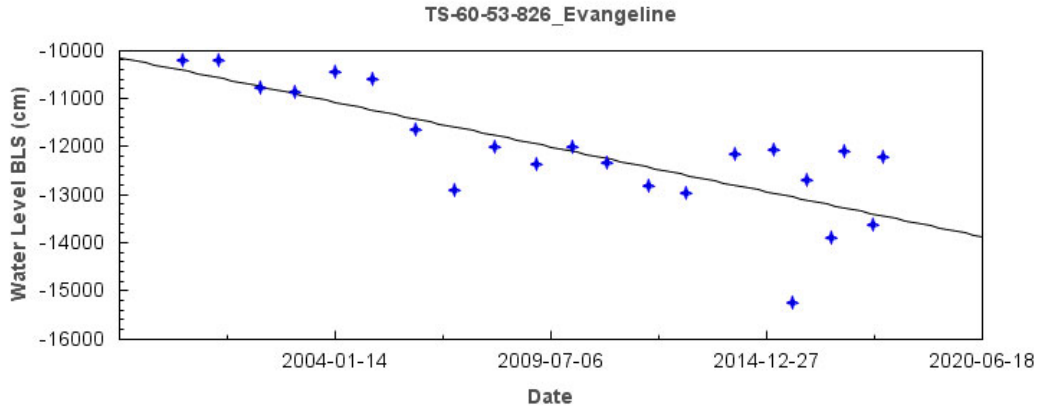
TS-60-53-826_Evangeline
Water Level BLS (cm)
-10000
-11000
-12000
-13000
-14000
-15000
-16000
2004-01-14
2009-07-06
2014-12-27
2020-06-18
Date

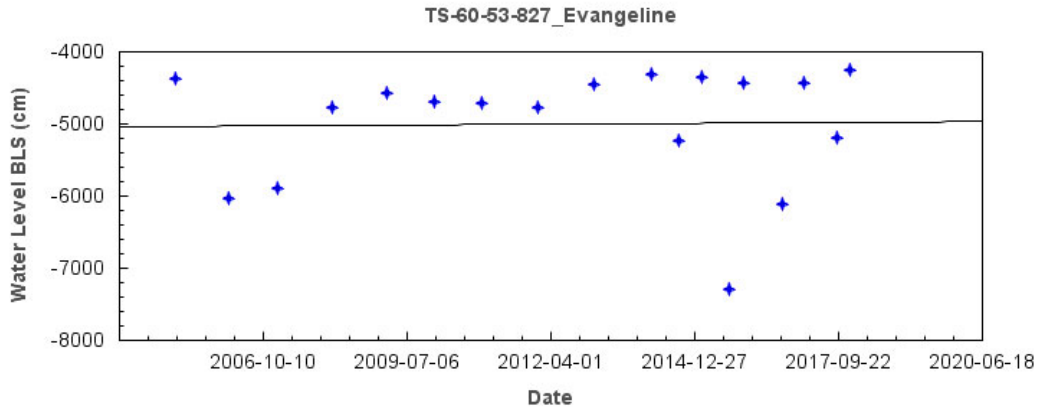
TS-60-53-827_Evangeline
Water Level BLS (cm)
-4000
-5000
-6000
-7000
-8000
2006-10-10
2009-07-06
2012-04-01
2014-12-27
2017-09-22
2020-06-18
Date

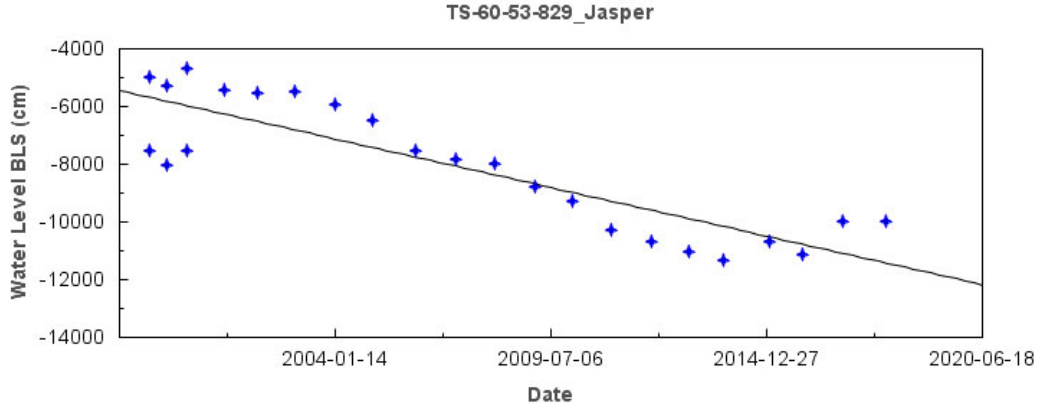
TS-60-53-829_Jasper
Water Level BLS (cm)
-4000
-6000
-8000
-10000
-12000
-14000
2004-01-14
2009-07-06
2014-12-27
2020-06-18
Date

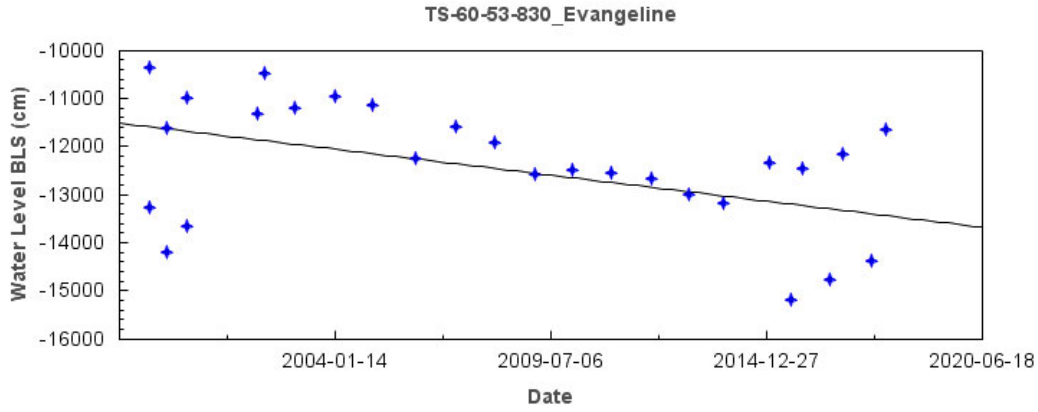
TS-60-53-830_Evangeline
Water Level BLS (cm)
-10000
-11000
-12000
-13000
-14000
-15000
-16000
2004-01-14
2009-07-06
2014-12-27
2020-06-18
Date

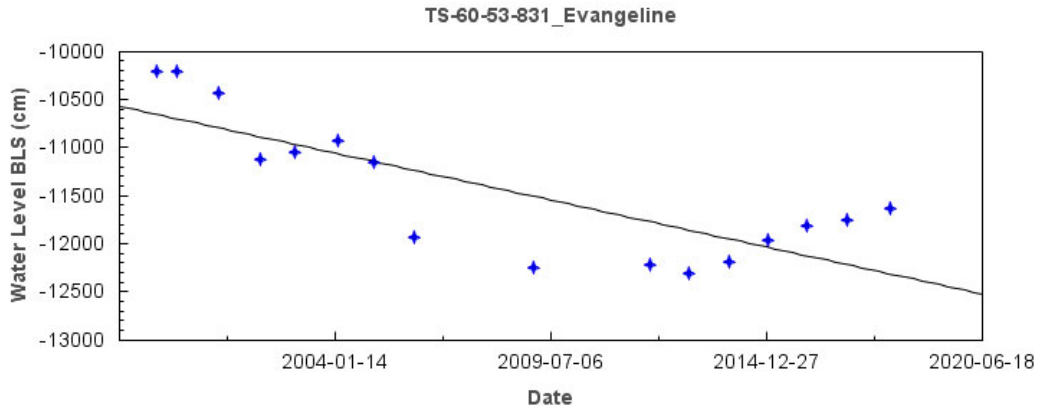
TS-60-53-831_Evangeline
Water Level BLS (cm)
-10000
-10500
-11000
-11500
-12000
-12500
-13000
2004-01-14
2009-07-06
2014-12-27
2020-06-18
Date

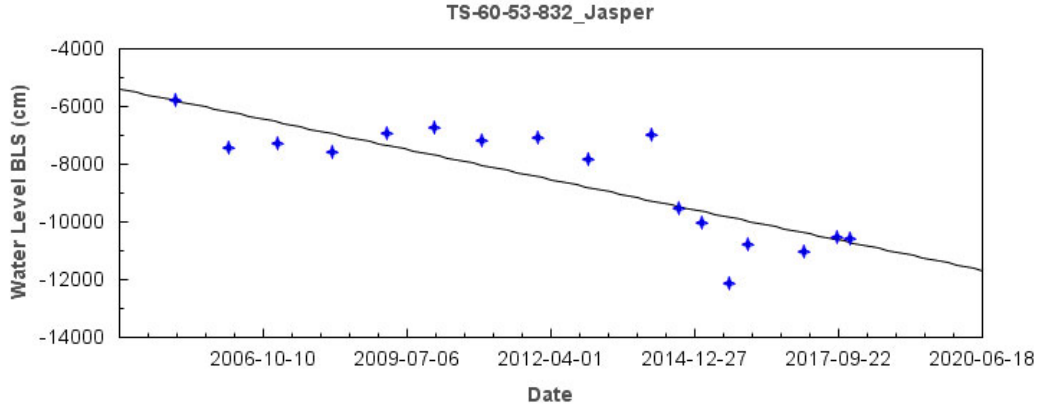
TS-60-53-832_Jasper
Water Level BLS (cm)
-4000
-6000
-8000
-10000
-12000
-14000
2006-10-10
2009-07-06
2012-04-01
2014-12-27
2017-09-22
2020-06-18
Date

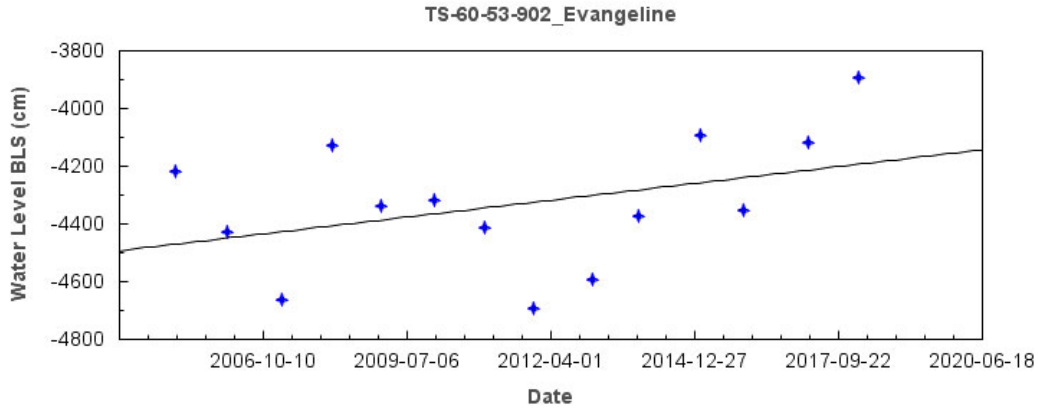
TS-60-53-902_Evangeline
Water Level BLS (cm)
-3800
-4000
-4200
-4400
-4600
-4800
2006-10-10
2009-07-06
2012-04-01
2014-12-27
2017-09-22
2020-06-18
Date

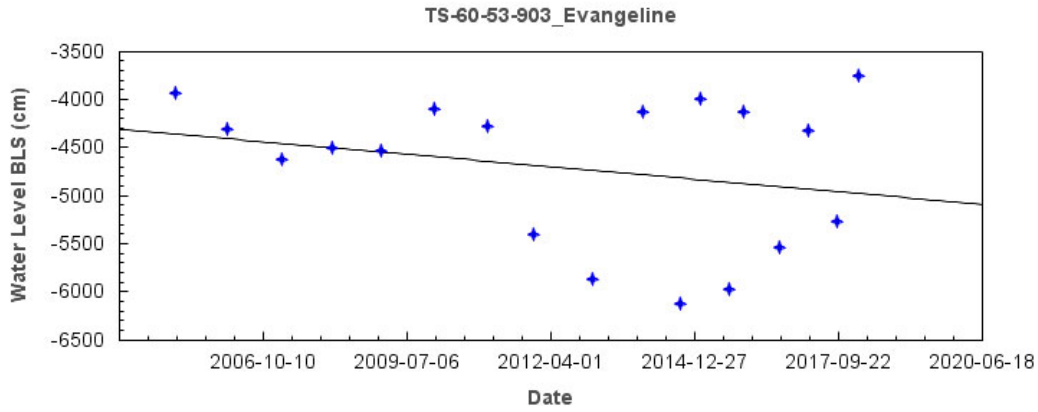
TS-60-53-903_Evangeline
Water Level BLS (cm)
-3500
-4000
-4500
-5000
-5500
-6000
-6500
2006-10-10
2009-07-06
2012-04-01
2014-12-27
2017-09-22
2020-06-18
Date

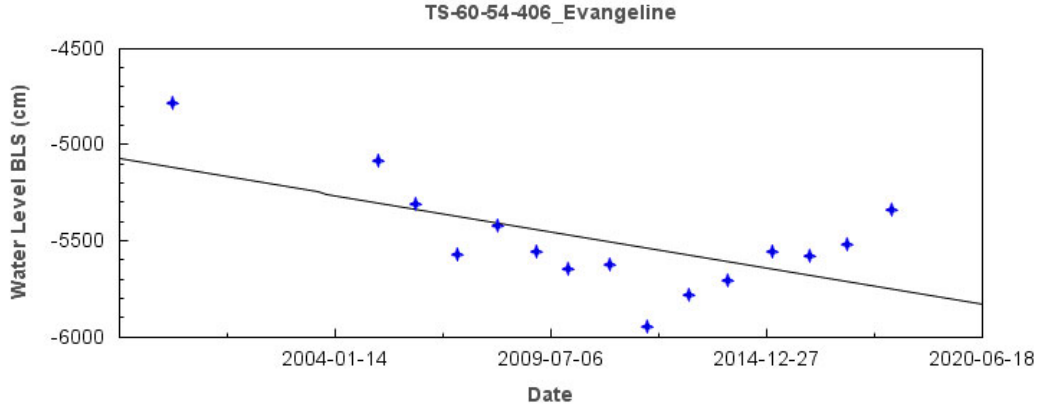
TS-60-54-406_Evangeline
Water Level BLS (cm)
-4500
-5000
-5500
-6000
2004-01-14
2009-07-06
2014-12-27
2020-06-18
Date

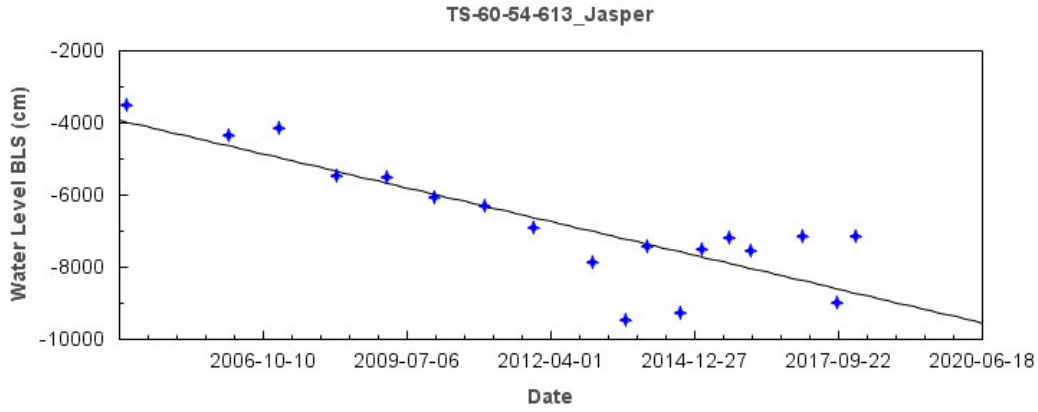
TS-60-54-613_Jasper
Water Level BLS (cm)
-2000
-4000
-6000
-8000
-10000
2006-10-10
2009-07-06
2012-04-01
2014-12-27
2017-09-22
2020-06-18
Date

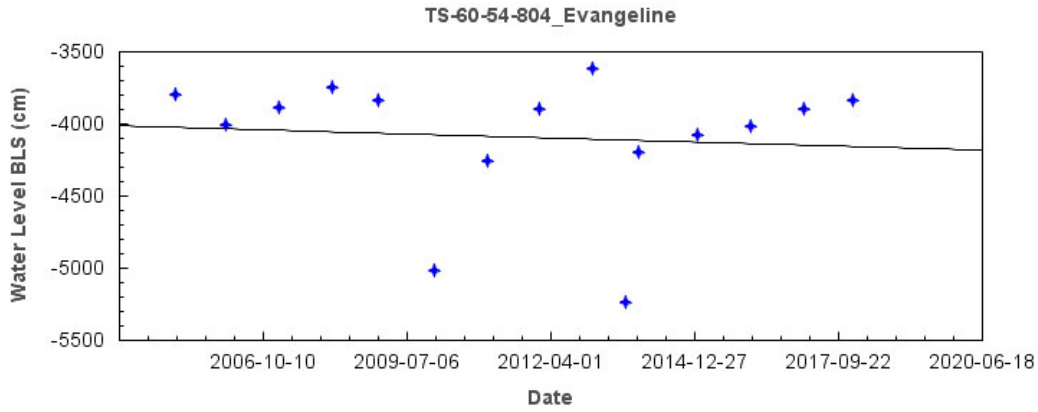
TS-60-54-804_Evangeline
Water Level BLS (cm)
-3500
-4000
-4500
-5000
-5500
2006-10-10
2009-07-06
2012-04-01
2014-12-27
2017-09-22
2020-06-18
Date

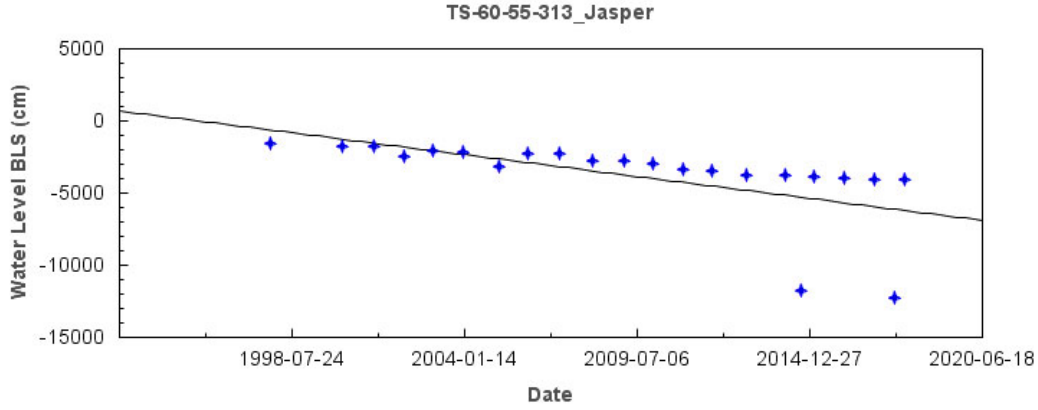
TS-60-55-313_Jasper
Water Level BLS (cm)
5000
0
-5000
-10000
-15000
1998-07-24
2004-01-14
2009-07-06
2014-12-27
2020-06-18
Date

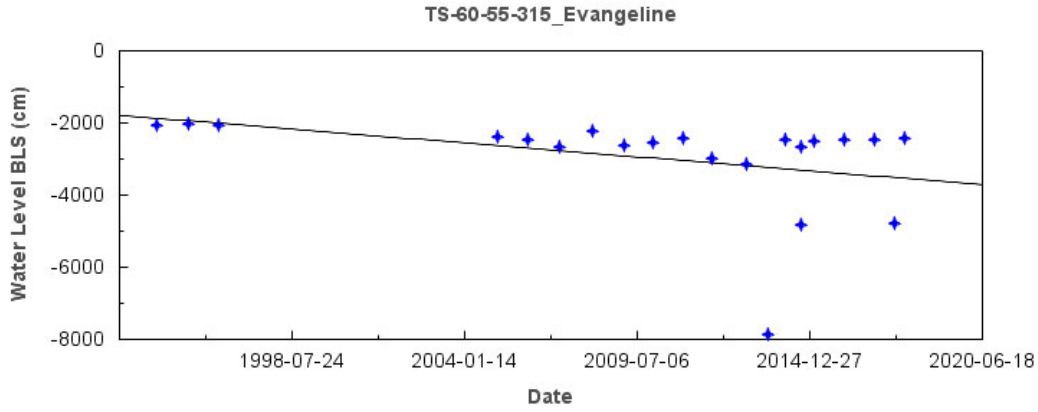
TS-60-55-315_Evangeline
Water Level BLS (cm)
0
-2000
-4000
-6000
-8000
1998-07-24
2004-01-14
2009-07-06
2014-12-27
2020-06-18
Date

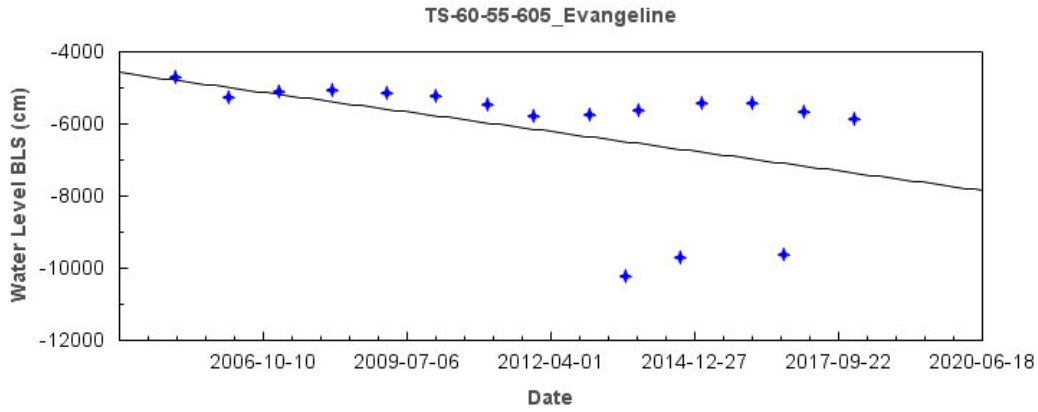
TS-60-55-605_Evangeline
Water Level BLS (cm)
-4000
-6000
-8000
-10000
-12000
2006-10-10
2009-07-06
2012-04-01
2014-12-27
2017-09-22
2020-06-18
Date

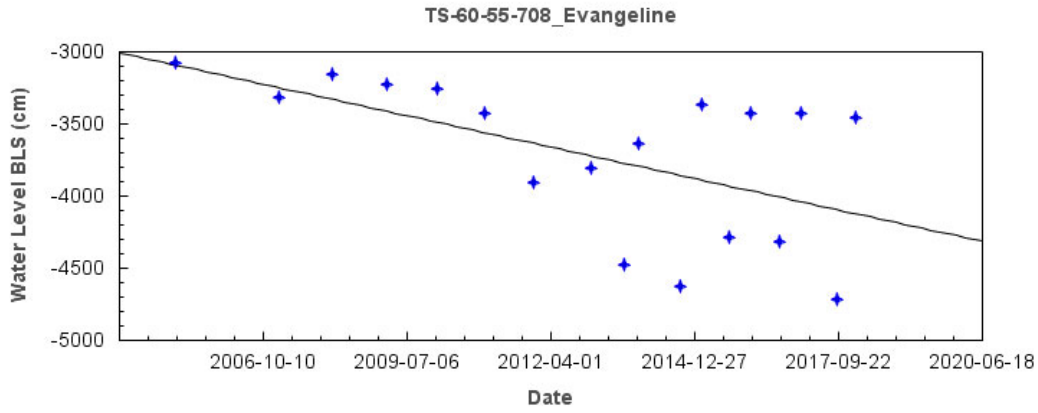
TS-60-55-708_Evangeline
Water Level BLS (cm)
-3000
-3500
-4000
-4500
-5000
2006-10-10
2009-07-06
2012-04-01
2014-12-27
2017-09-22
2020-06-18
Date

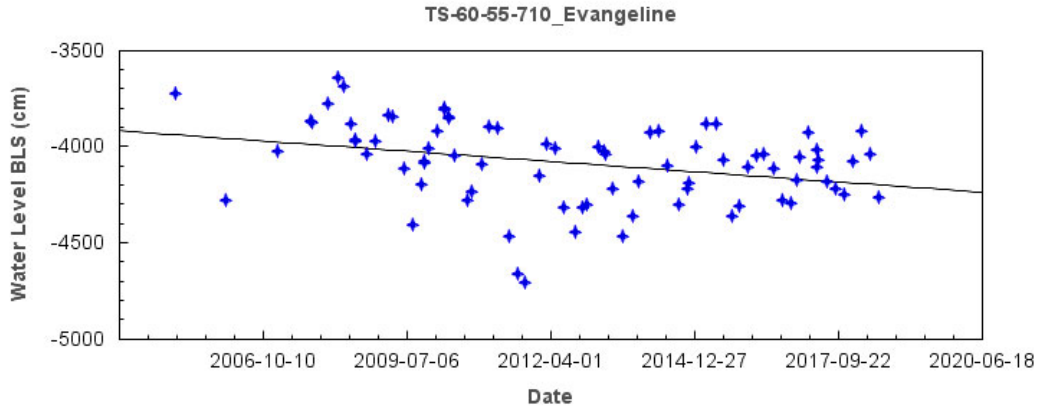
TS-60-55-710_Evangeline
Water Level BLS (cm)
-3500
-4000
-4500
-5000
2006-10-10
2009-07-06
2012-04-01
2014-12-27
2017-09-22
2020-06-18
Date

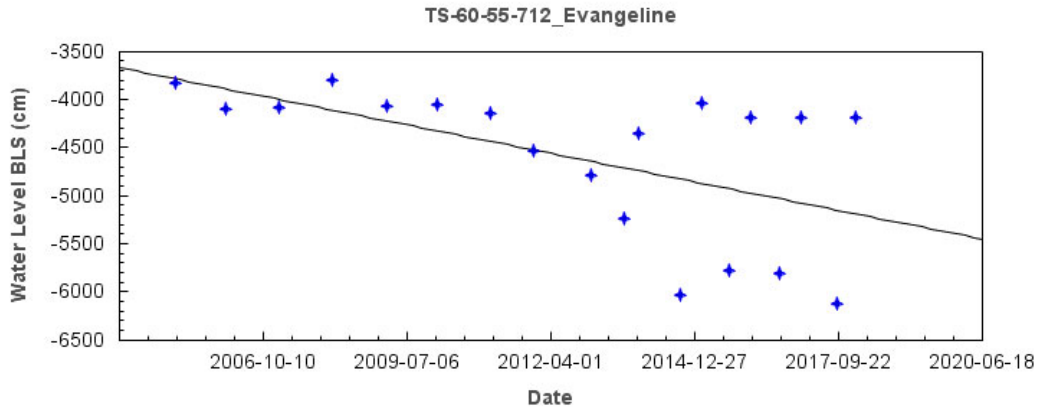
TS-60-55-712_Evangeline
Water Level BLS (cm)
-3500
-4000
-4500
-5000
-5500
-6000
-6500
2006-10-10
2009-07-06
2012-04-01
2014-12-27
2017-09-22
2020-06-18
Date

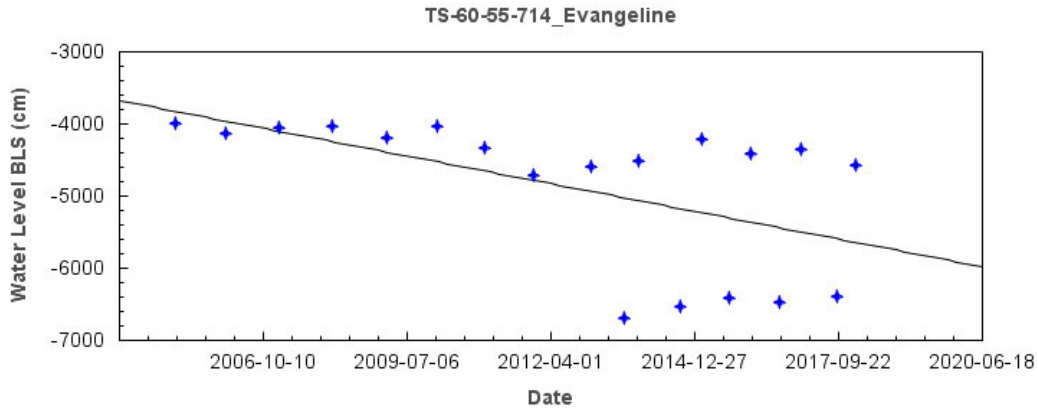
TS-60-55-714_Evangeline
Water Level BLS (cm)
-3000
-4000
-5000
-6000
-7000
2006-10-10
2009-07-06
2012-04-01
2014-12-27
2017-09-22
2020-06-18
Date

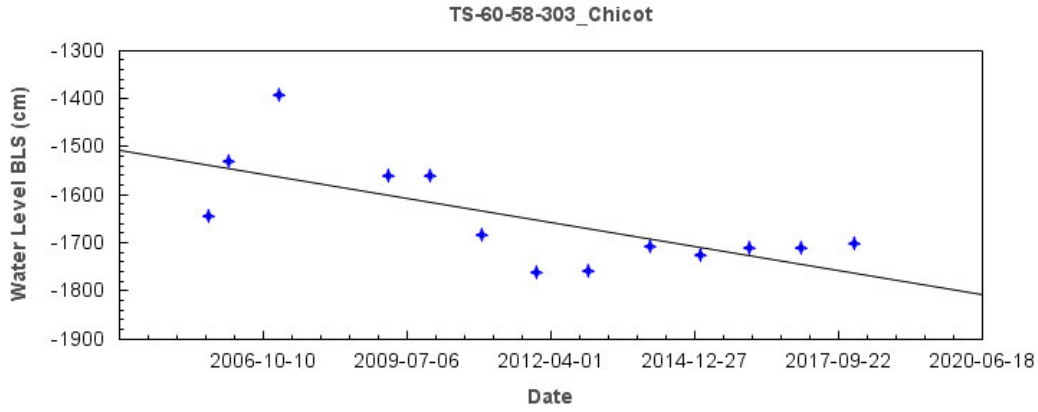
TS-60-58-303_Chicot
Water Level BLS (cm)
-1300
-1400
-1500
-1600
-1700
-1800
-1900
2006-10-10
2009-07-06
2012-04-01
2014-12-27
2017-09-22
2020-06-18
Date

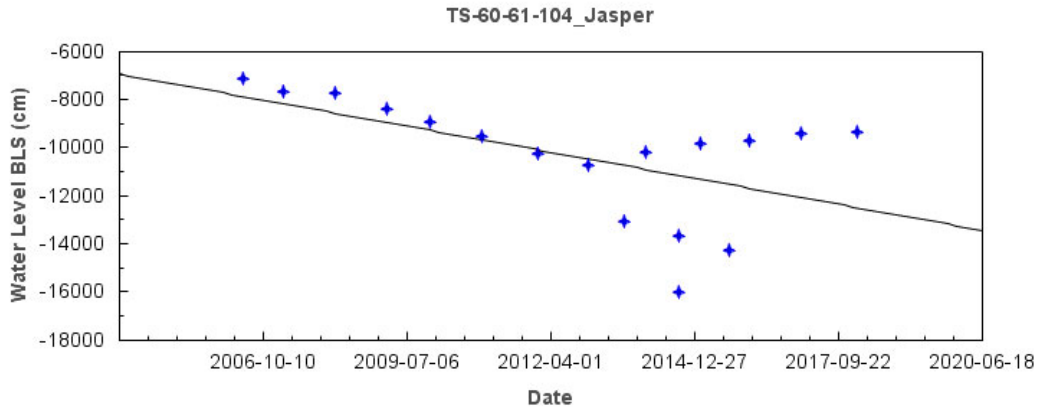
TS-60-61-104_Jasper
Water Level BLS (cm)
-6000
-8000
-10000
-12000
-14000
-16000
-18000
2006-10-10
2009-07-06
2012-04-01
2014-12-27
2017-09-22
2020-06-18
Date

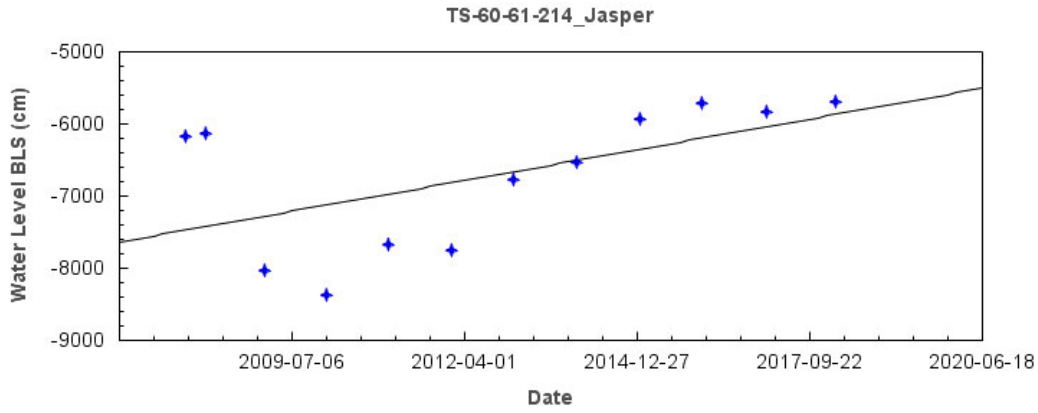
TS-60-61-214_Jasper
Water Level BLS (cm)
-5000
-6000
-7000
-8000
-9000
2009-07-06
2012-04-01
2014-12-27
2017-09-22
2020-06-18
Date

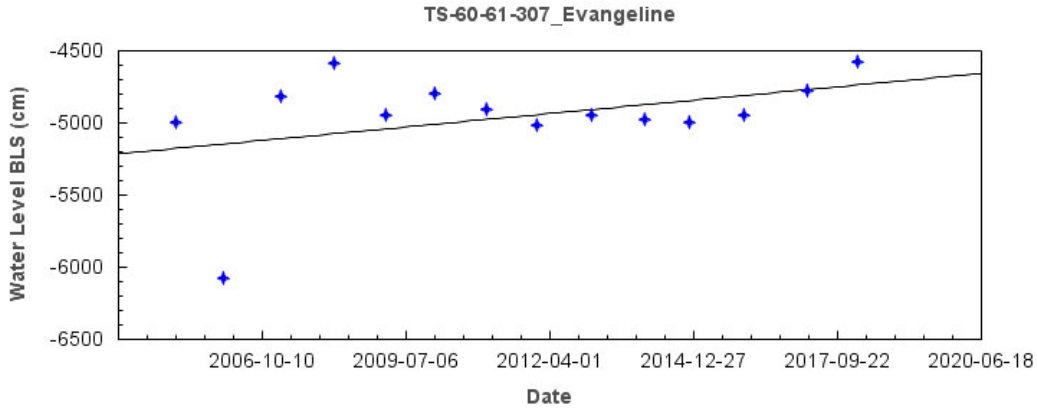
TS-60-61-307_Evangeline
Water Level BLS (cm)
-4500
-5000
-5500
-6000
-6500
2006-10-10
2009-07-06
2012-04-01
2014-12-27
2017-09-22
2020-06-18
Date

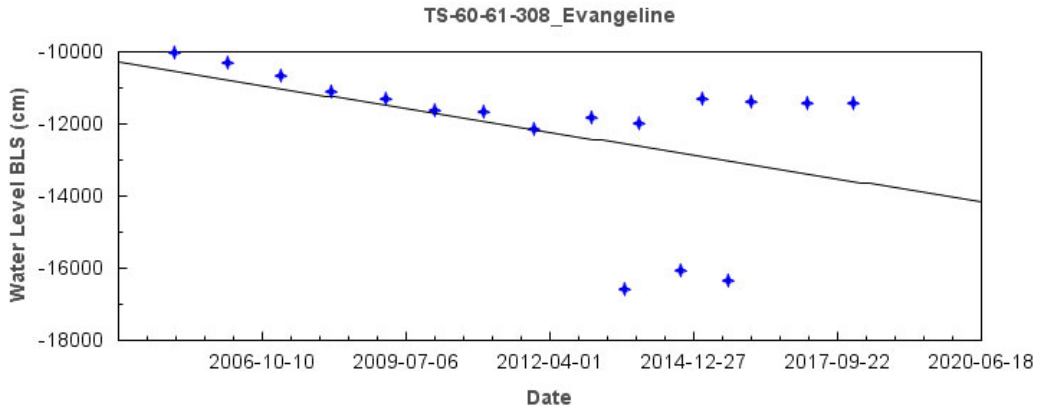
TS-60-61-308_Evangeline
Water Level BLS (cm)
-10000
-12000
-14000
-16000
-18000
2006-10-10
2009-07-06
2012-04-01
2014-12-27
2017-09-22
2020-06-18
Date

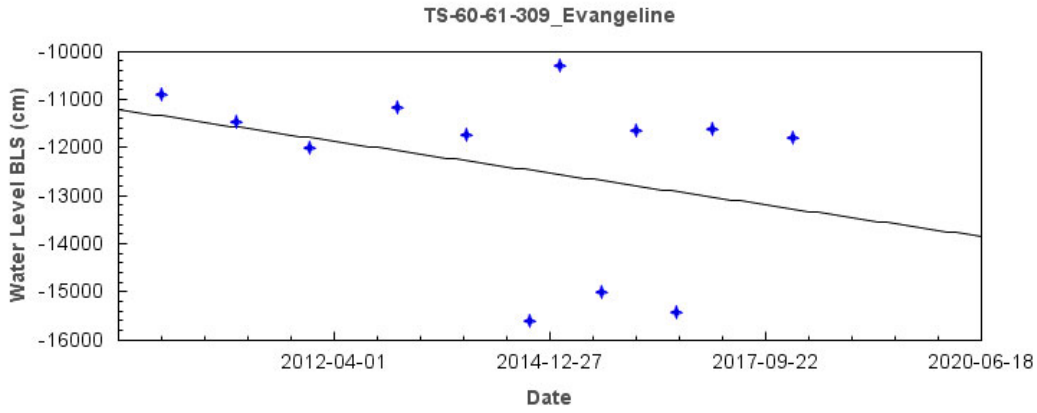
TS-60-61-309_Evangeline
Water Level BLS (cm)
-10000
-11000
-12000
-13000
-14000
-15000
-16000
2012-04-01
2014-12-27
2017-09-22
2020-06-18
Date

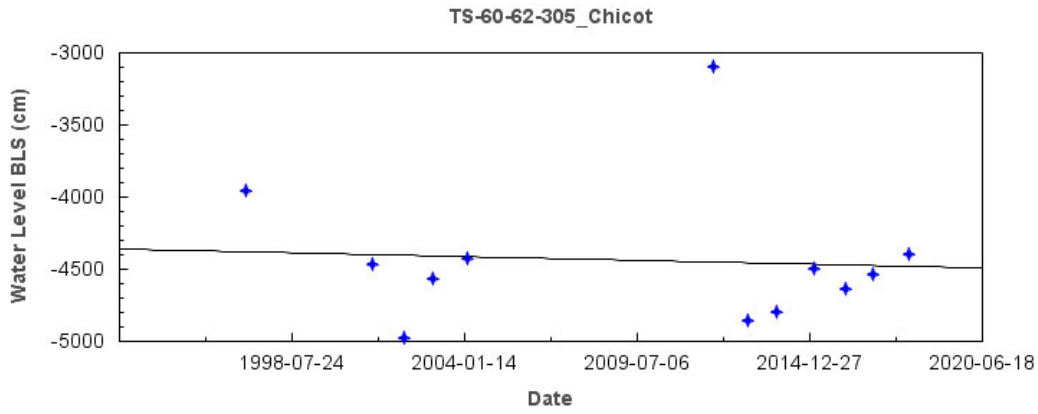
TS-60-62-305_Chicot
Water Level BLS (cm)
-3000
-3500
-4000
-4500
-5000
1998-07-24
2004-01-14
2009-07-06
2014-12-27
2020-06-18
Date

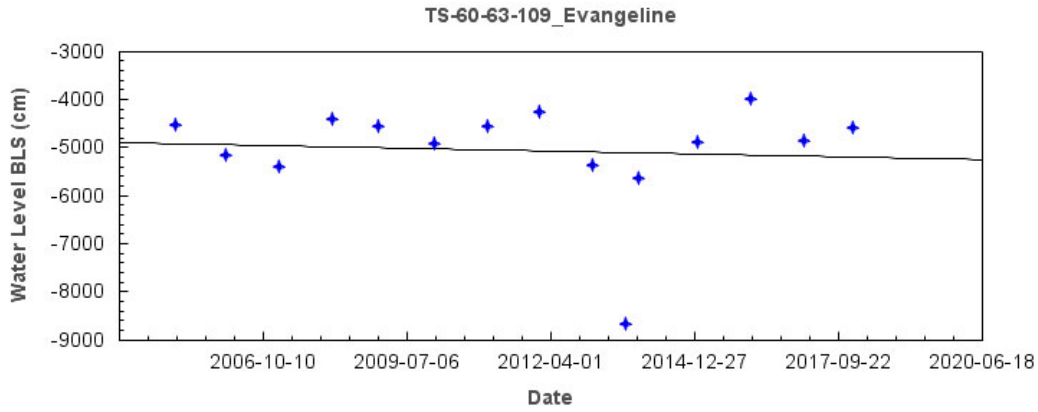
TS-60-63-109_Evangeline
Water Level BLS (cm)
-3000
-4000
-5000
-6000
-7000
-8000
-9000
2006-10-10
2009-07-06
2012-04-01
2014-12-27
2017-09-22
2020-06-18
Date

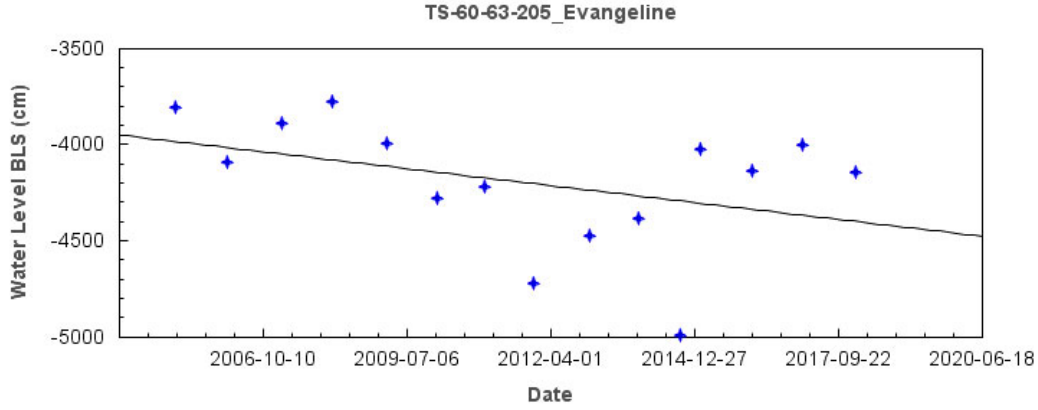
TS-60-63-205_Evangeline
Water Level BLS (cm)
-3500
-4000
-4500
-5000
2006-10-10
2009-07-06
2012-04-01
2014-12-27
2017-09-22
2020-06-18
Date

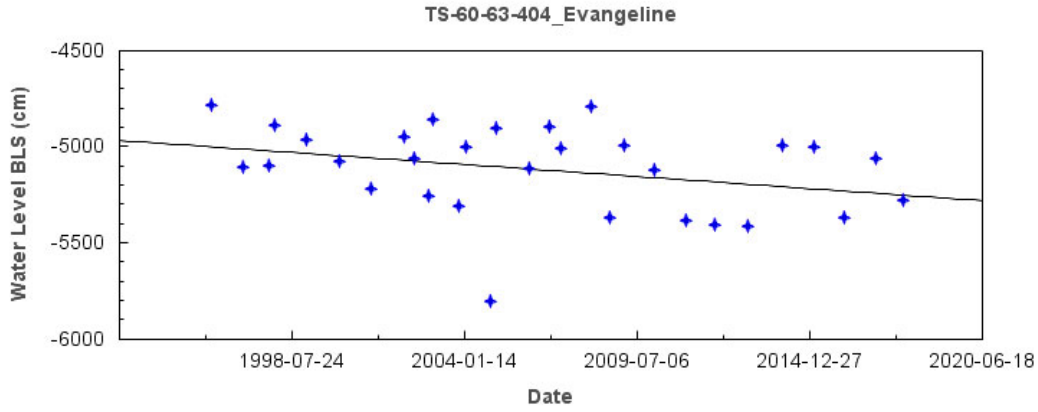
TS-60-63-404_Evangeline
Water Level BLS (cm)
-4500
-5000
-5500
-6000
1998-07-24
2004-01-14
2009-07-06
2014-12-27
2020-06-18
Date

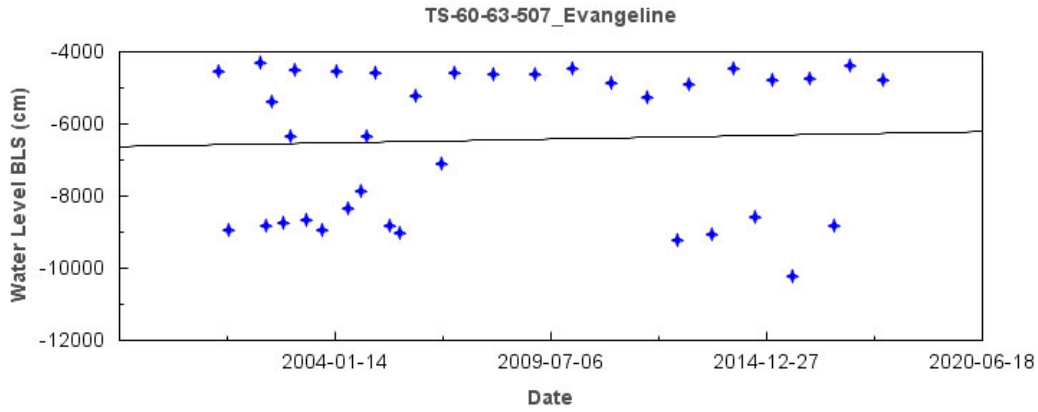
TS-60-63-507_Evangeline
Water Level BLS (cm)
-4000
-6000
-8000
-10000
-12000
2004-01-14
2009-07-06
2014-12-27
2020-06-18
Date

9 Appendix II: GPS Timeseries

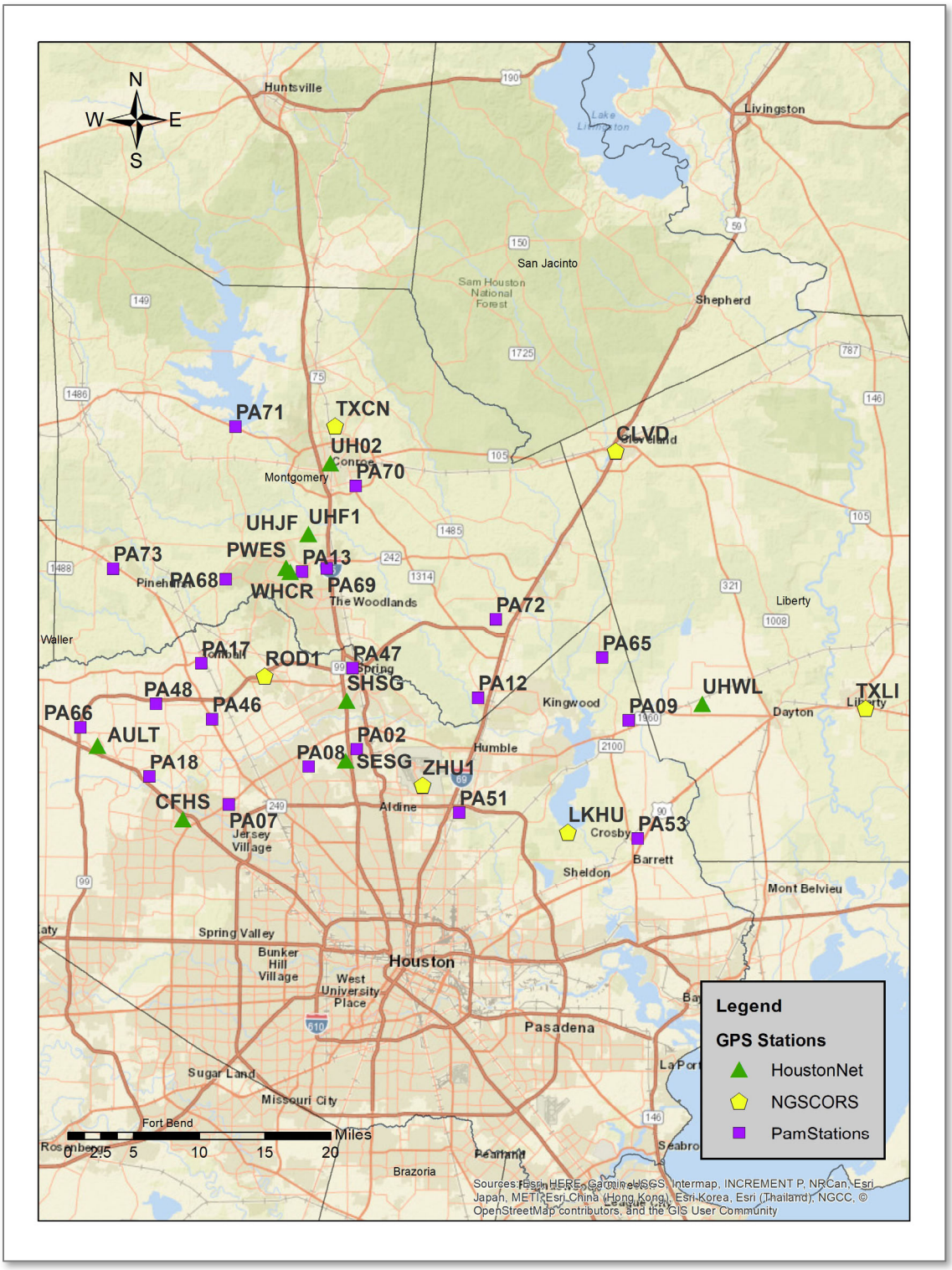

GPS Station List (Page 1 of 1)

Station	StationType	Latitude	Longitude	RefFrame	FirstReadDate	LastReadDate	Subsidence Rate (cm/year)
AULT	HoustonNet	29.9981	-95.7447	HRF16	2015.5565	2018.4120	-0.974301916
CFHS	HoustonNet	29.9188	-95.6344	HRF16	2015.5948	2018.4586	-1.432937909
CLVD	NGSCORS	30.3350	-95.0940	HRF16	2012.6653	2017.1472	-0.320659070
LKHU	NGSCORS	29.9135	-95.1457	HRF16	1996.3395	2018.5708	0.014665315
PA02	PamStations	30.0006	-95.4159	HRF16	1994.3151	2018.5562	-2.664713110
PA07	PamStations	29.9363	-95.5766	HRF16	1999.1123	2018.4959	-2.739174416
PA08	PamStations	29.9797	-95.4763	HRF16	1999.6082	2018.5781	-2.245242555
PA09	PamStations	30.0381	-95.0715	HRF16	1999.3425	2018.5397	-0.482542152
PA12	PamStations	30.0597	-95.2631	HRF16	2000.8907	2018.5616	-0.586084203
PA13	PamStations	30.1948	-95.4900	HRF16	2000.9098	2018.5425	-1.676469083
PA17	PamStations	30.0912	-95.6153	HRF16	2000.8907	2018.5397	-1.731556178
PA18	PamStations	29.9649	-95.6782	HRF16	2000.8579	2018.5205	-1.999763205
PA46	PamStations	30.0300	-95.6000	HRF16	2007.3178	2018.5397	-2.052986916
PA47	PamStations	30.0895	-95.4235	HRF16	2007.3342	2018.5589	-1.969514250
PA48	PamStations	30.0454	-95.6717	HRF16	2007.3178	2018.5589	-1.536493222
PA51	PamStations	29.9325	-95.2842	HRF16	2007.3370	2018.5973	-0.555754404
PA53	PamStations	29.9080	-95.0573	HRF16	2007.3370	2018.5151	-0.219759918
PA65	PamStations	30.1064	-95.1067	HRF16	2012.4290	2018.5397	-1.185078932
PA66	PamStations	30.0178	-95.7673	HRF16	2011.1644	2018.5589	-1.460716696
PA68	PamStations	30.1848	-95.5868	HRF16	2011.7973	2018.6027	-1.187467448
PA69	PamStations	30.1990	-95.4590	HRF16	2011.7452	2018.5425	-1.308166750
PA70	PamStations	30.2911	-95.4244	HRF16	2011.7589	2018.5753	-0.751747084
PA71	PamStations	30.3531	-95.5789	HRF16	2011.7808	2018.5808	-0.678375231
PA72	PamStations	30.1470	-95.2425	HRF16	2011.9918	2018.4685	-0.246068620
PA73	PamStations	30.1934	-95.7302	HRF16	2012.0492	2018.5973	-0.976358513
PWES	HoustonNet	30.1990	-95.5106	HRF16	2015.2225	2018.5708	-0.728322205
ROD1	NGSCORS	30.0786	-95.5344	HRF16	2007.0034	2018.5708	-1.212753807
SESG	HoustonNet	29.9875	-95.4296	HRF16	2014.6776	2018.5708	-0.899265592
SHSG	HoustonNet	30.0536	-95.4301	HRF16	2014.7214	2018.4394	-1.094723290
TXCN	NGSCORS	30.3563	-95.4520	HRF16	2005.5797	2018.5708	-1.246774610
TXLI	NGSCORS	30.0558	-94.7708	HRF16	2005.5797	2018.5708	0.082179585
UH02	HoustonNet	30.3152	-95.4571	HRF16	2015.0034	2018.5708	-0.546801884
UHF1	HoustonNet	30.2363	-95.4831	HRF16	2014.3901	2018.3792	-0.556084221
UHJF	HoustonNet	30.2363	-95.4831	HRF16	2014.3901	2018.3792	-0.277575675
UHWL	HoustonNet	30.0577	-94.9784	HRF16	2014.3573	2018.5708	-0.048341634
WHCR	HoustonNet	30.1943	-95.5054	HRF16	2014.7789	2018.5708	-0.406261937
ZHU1	NGSCORS	29.9619	-95.3314	HRF16	2003.0418	2018.5708	-0.792238004

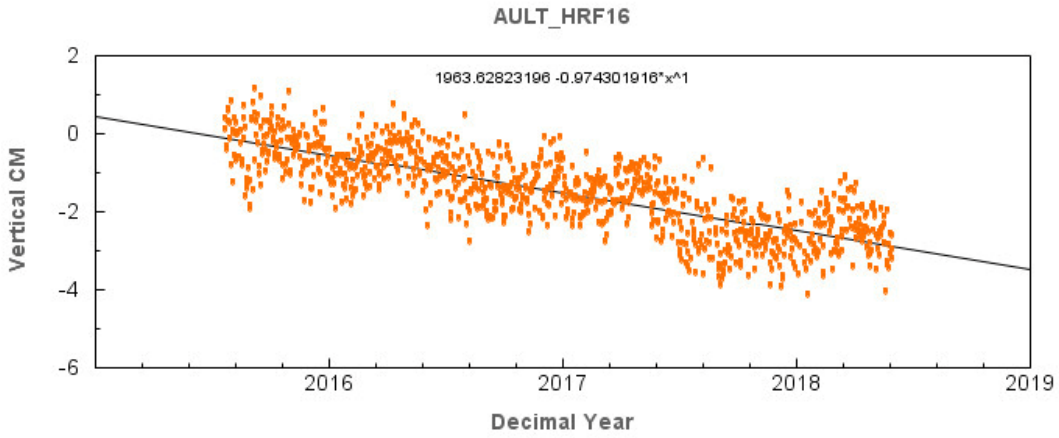
AULT_HRF16
1963.62823196 -0.974301916*x^1
Vertical CM
Decimal Year
2
0
-2
-4
-6
2016
2017
2018
2019

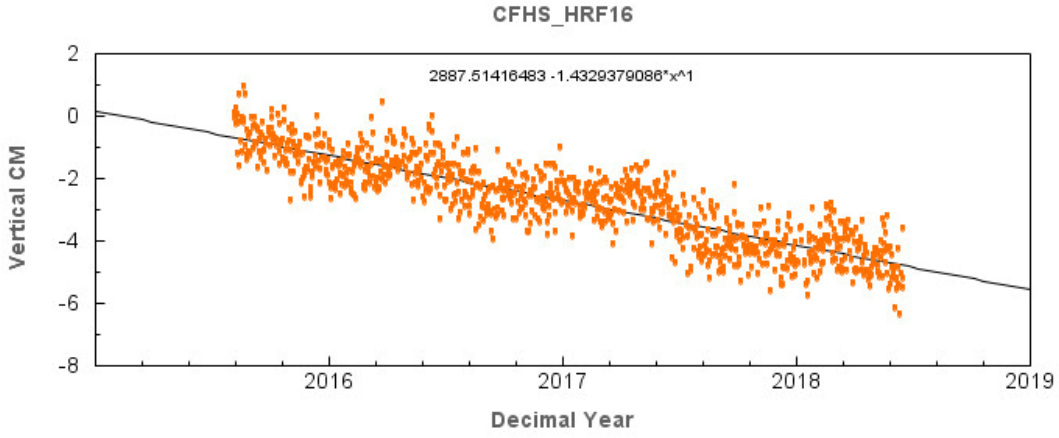
CFHS_HRF16
2887.51416483 -1.4329379086*x^1
Vertical CM
Decimal Year
2
0
-2
-4
-6
-8
2016
2017
2018
2019

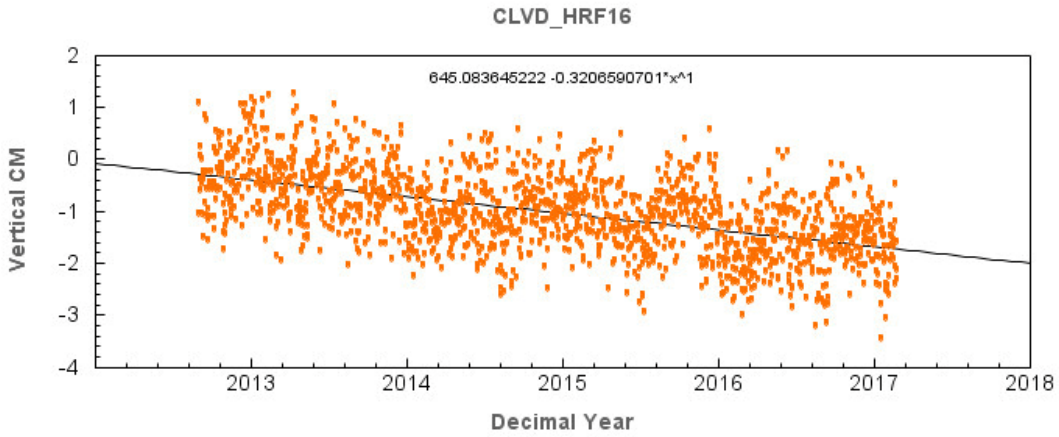
CLVD_HRF16
645.083645222 -0.3206590701*x^1
Vertical CM
Decimal Year
2
1
0
-1
-2
-3
-4
2013
2014
2015
2016
2017
2018

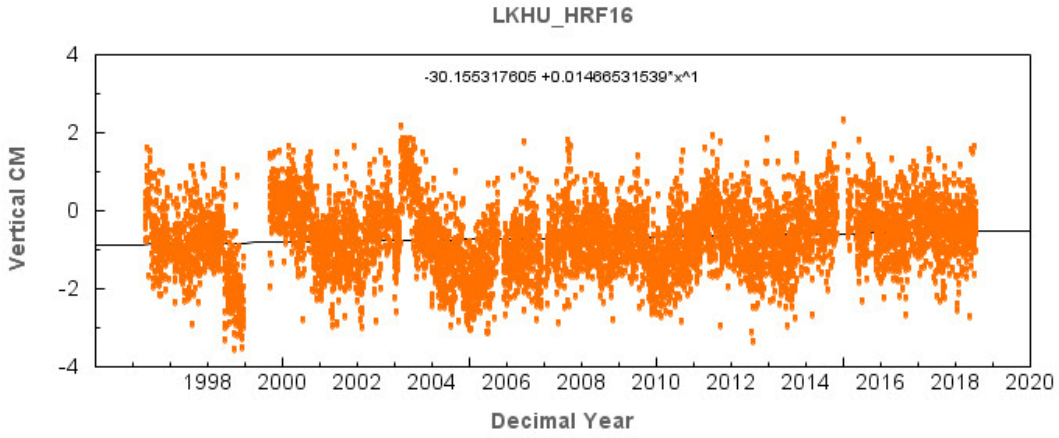
LKHU_HRF16
-30.155317605 +0.01466531539*x^1
Vertical CM
4
2
0
-2
-4
1998
2000
2002
2004
2006
2008
2010
2012
2014
2016
2018
2020
Decimal Year

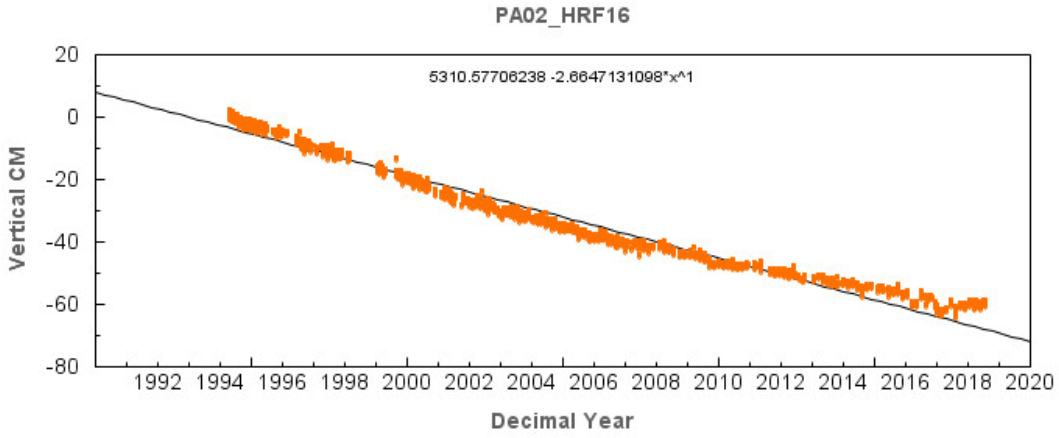
PA02_HRF16
5310.57706238 -2.6647131098*x^1
Vertical CM
20
0
-20
-40
-60
-80
1992
1994
1996
1998
2000
2002
2004
2006
2008
2010
2012
2014
2016
2018
2020
Decimal Year

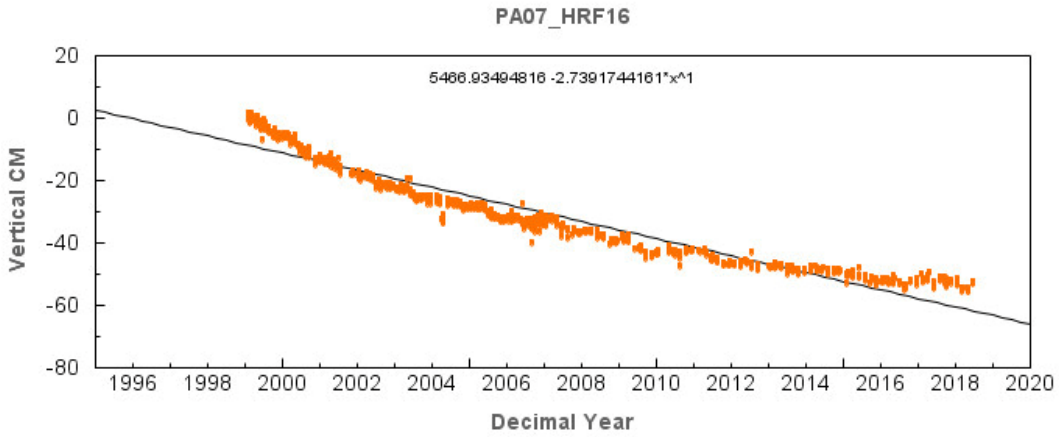
PA07_HRF16
5466.93494816 -2.7391744161*x^1
Vertical CM
20
0
-20
-40
-60
-80
1996
1998
2000
2002
2004
2006
2008
2010
2012
2014
2016
2018
2020
Decimal Year

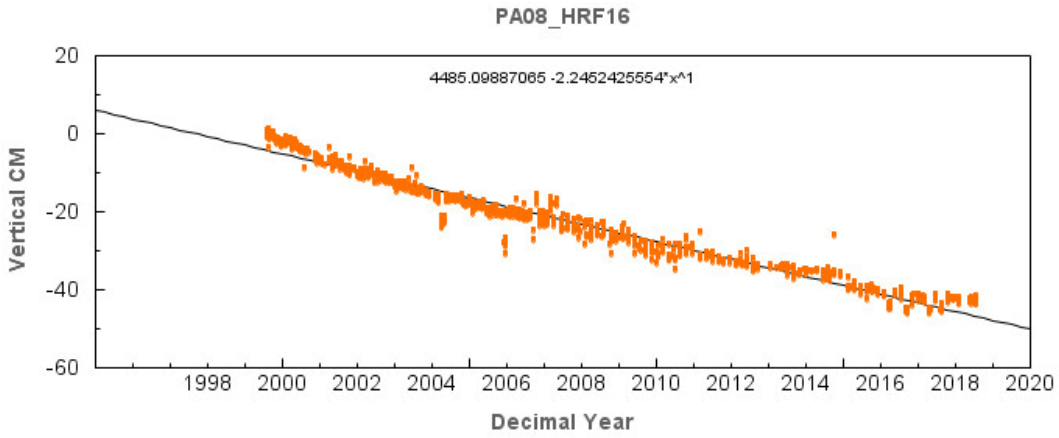
PA08_HRF16
4485.09887065 -2.2452425554*x^1
Vertical CM
Decimal Year
20
0
-20
-40
-60
1998
2000
2002
2004
2006
2008
2010
2012
2014
2016
2018
2020

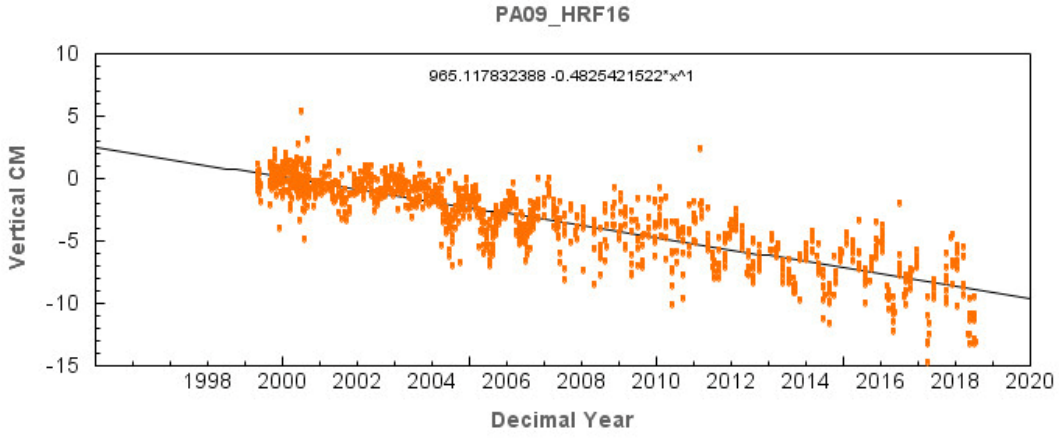
PA09_HRF16
965.117832388 -0.4825421522*x^1
Vertical CM
Decimal Year
10
5
0
-5
-10
-15
1998
2000
2002
2004
2006
2008
2010
2012
2014
2016
2018
2020

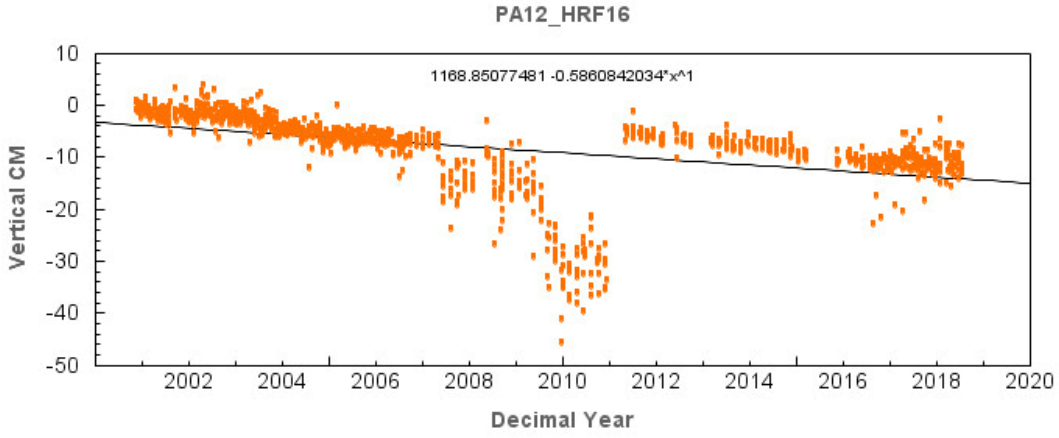
PA12_HRF16
1168.85077481 -0.5860842034*x^1
Vertical CM
Decimal Year
10
0
-10
-20
-30
-40
-50
2002
2004
2006
2008
2010
2012
2014
2016
2018
2020

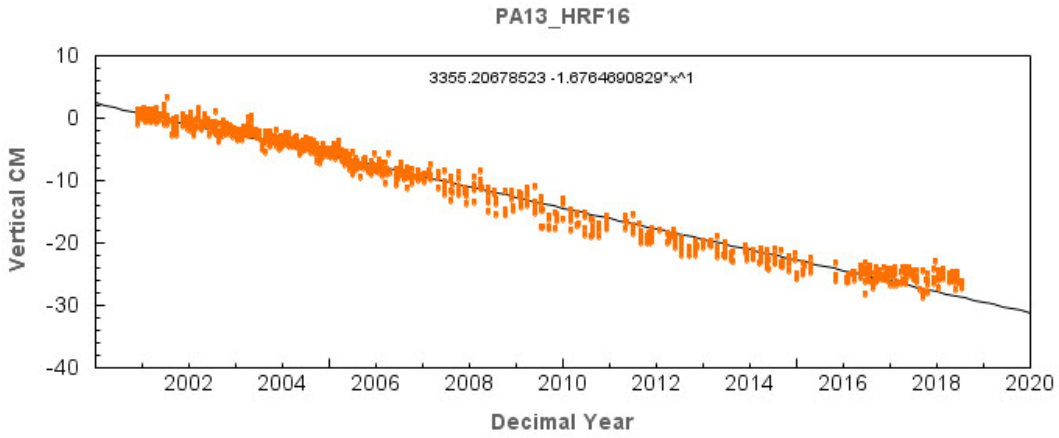
PA13_HRF16
3355.20678523 -1.6764690829*x^1
Vertical CM
Decimal Year
10
0
-10
-20
-30
-40
2002
2004
2006
2008
2010
2012
2014
2016
2018
2020

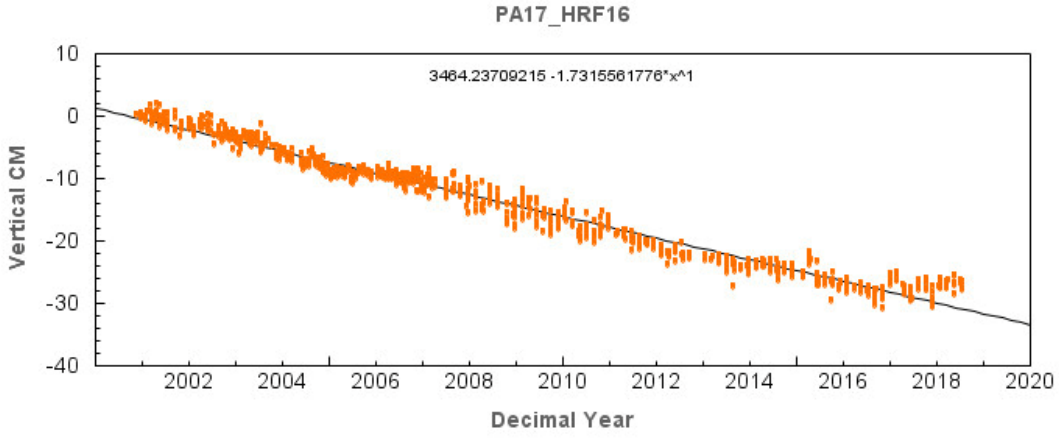
PA17_HRF16
3464.23709215 -1.7315561776*x^1
Vertical CM
Decimal Year
10
0
-10
-20
-30
-40
2002
2004
2006
2008
2010
2012
2014
2016
2018
2020

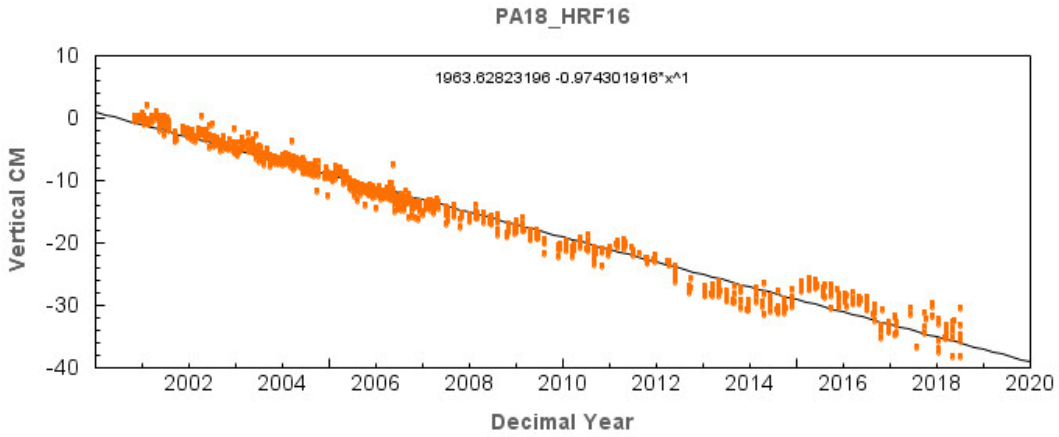
PA18_HRF16
1963.62823196 -0.974301916*x^1
Vertical CM
Decimal Year
10
0
-10
-20
-30
-40
2002
2004
2006
2008
2010
2012
2014
2016
2018
2020

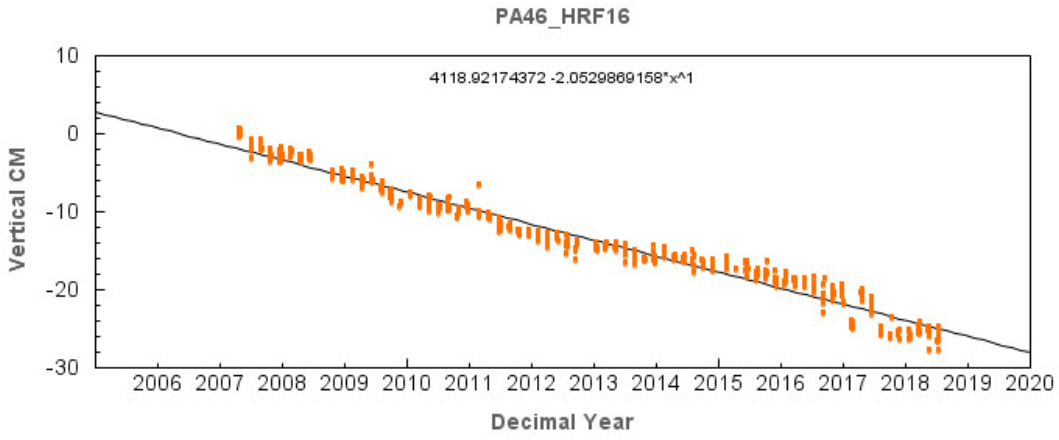
PA46_HRF16
4118.92174372 -2.0529869158*x^1
Vertical CM
10
0
-10
-20
-30
2006 2007 2008 2009 2010 2011 2012 2013 2014 2015 2016 2017 2018 2019 2020
Decimal Year

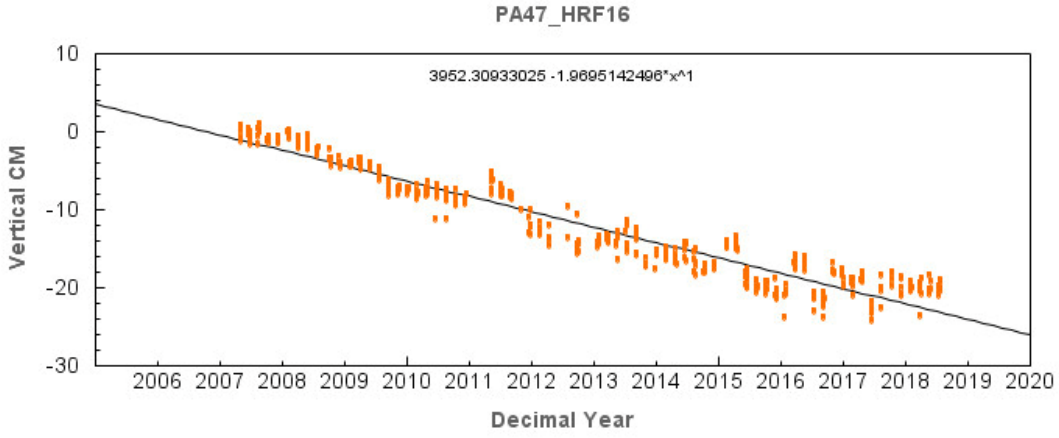
PA47_HRF16
3952.30933025 -1.9695142496*x^1
Vertical CM
10
0
-10
-20
-30
2006 2007 2008 2009 2010 2011 2012 2013 2014 2015 2016 2017 2018 2019 2020
Decimal Year

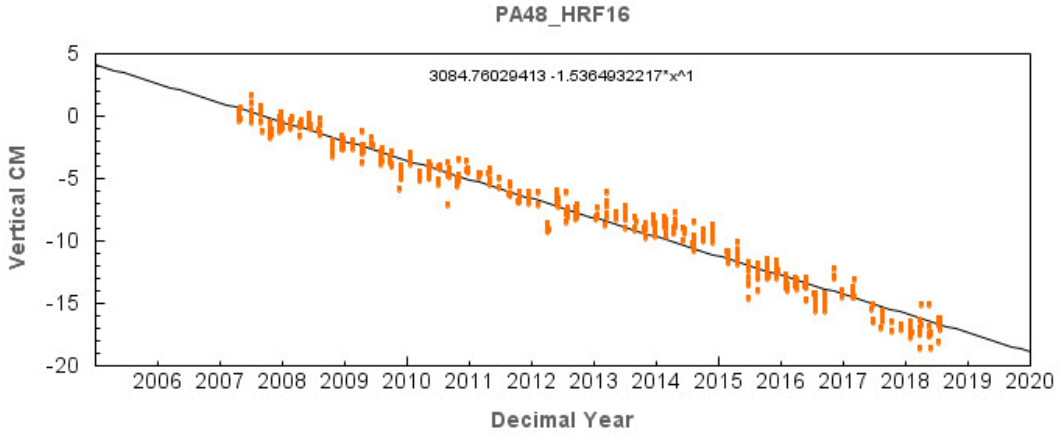
PA48_HRF16
3084.76029413 -1.5364932217*x^1
Vertical CM
5
0
-5
-10
-15
-20
2006 2007 2008 2009 2010 2011 2012 2013 2014 2015 2016 2017 2018 2019 2020
Decimal Year

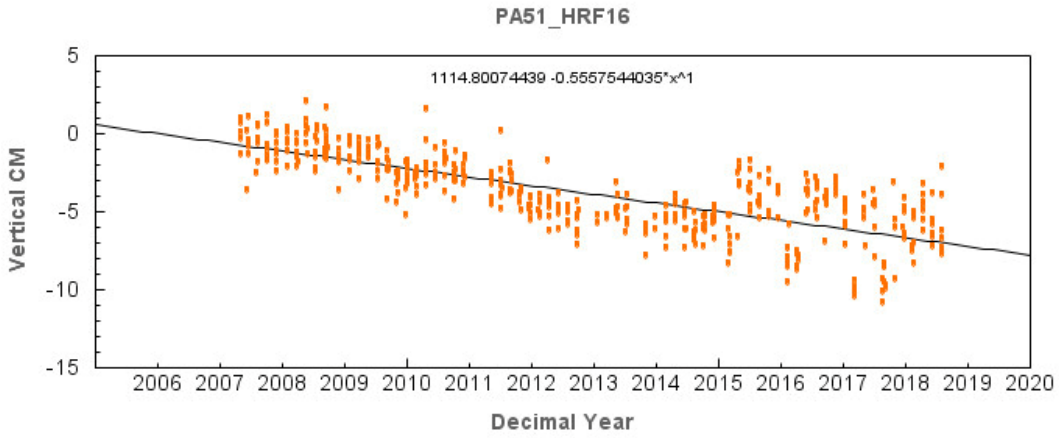
PA51_HRF16
1114.80074439 -0.5557544035*x^1
Vertical CM
5
0
-5
-10
-15
2006 2007 2008 2009 2010 2011 2012 2013 2014 2015 2016 2017 2018 2019 2020
Decimal Year

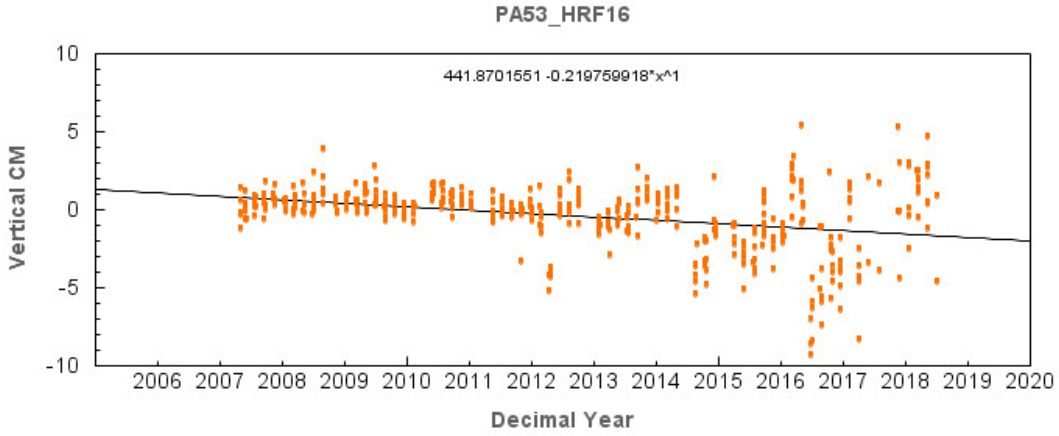
PA53_HRF16
441.8701551 -0.219759918*x^1
Vertical CM
10
5
0
-5
-10
2006 2007 2008 2009 2010 2011 2012 2013 2014 2015 2016 2017 2018 2019 2020
Decimal Year

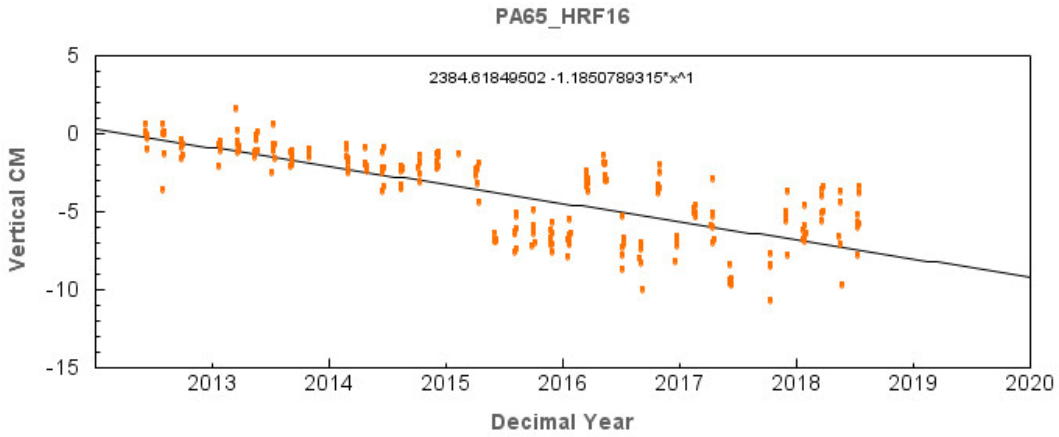
PA65_HRF16
2384.61849502 -1.1850789315*x^1
Vertical CM
5
0
-5
-10
-15
2013 2014 2015 2016 2017 2018 2019 2020
Decimal Year

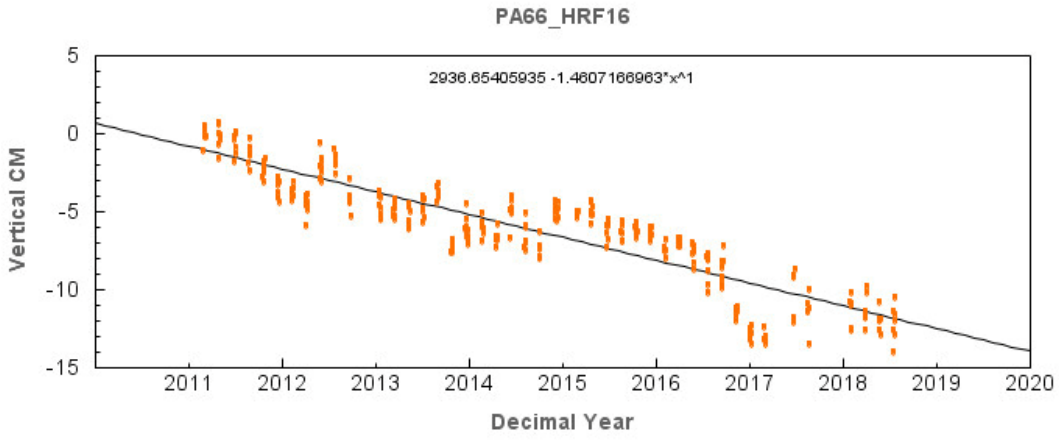
PA66_HRF16
2936.65405935 -1.4607166963*x^1
Vertical CM
Decimal Year
5
0
-5
-10
-15
2011
2012
2013
2014
2015
2016
2017
2018
2019
2020

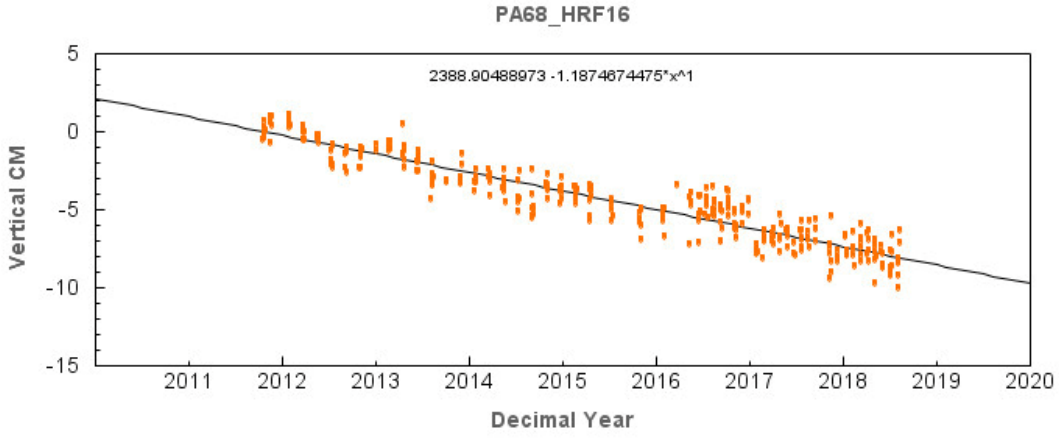
PA68_HRF16
2388.90488973 -1.1874674475*x^1
Vertical CM
Decimal Year
5
0
-5
-10
-15
2011
2012
2013
2014
2015
2016
2017
2018
2019
2020

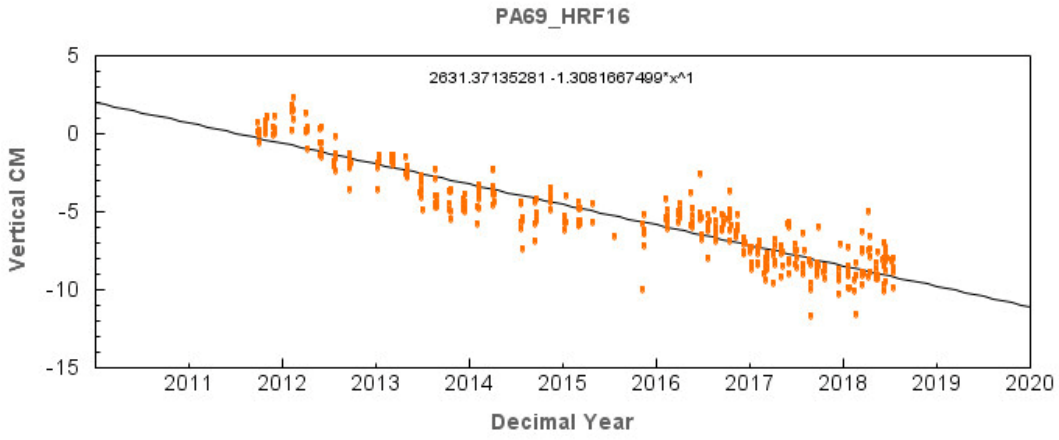
PA69_HRF16
2631.37135281 -1.3081667499*x^1
Vertical CM
Decimal Year
5
0
-5
-10
-15
2011
2012
2013
2014
2015
2016
2017
2018
2019
2020

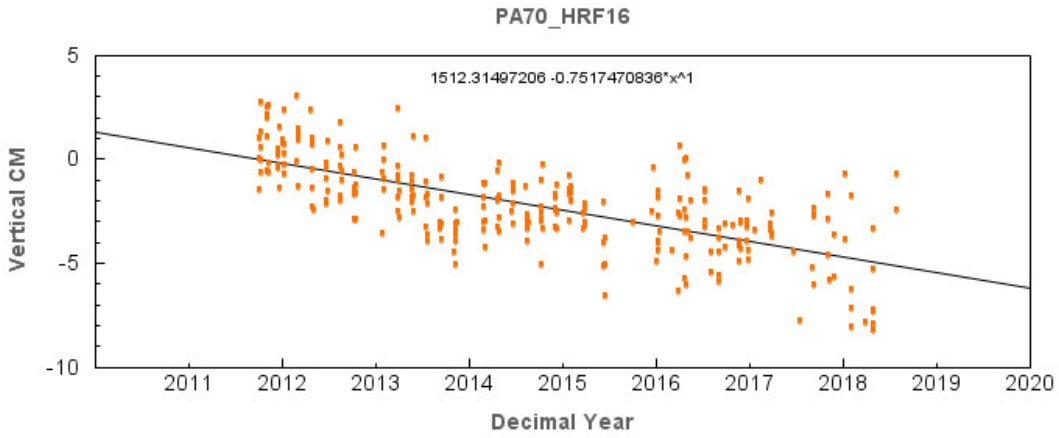
PA70_HRF16
1512.31497206 -0.7517470836*x^1
Vertical CM
Decimal Year
5
0
-5
-10
2011
2012
2013
2014
2015
2016
2017
2018
2019
2020

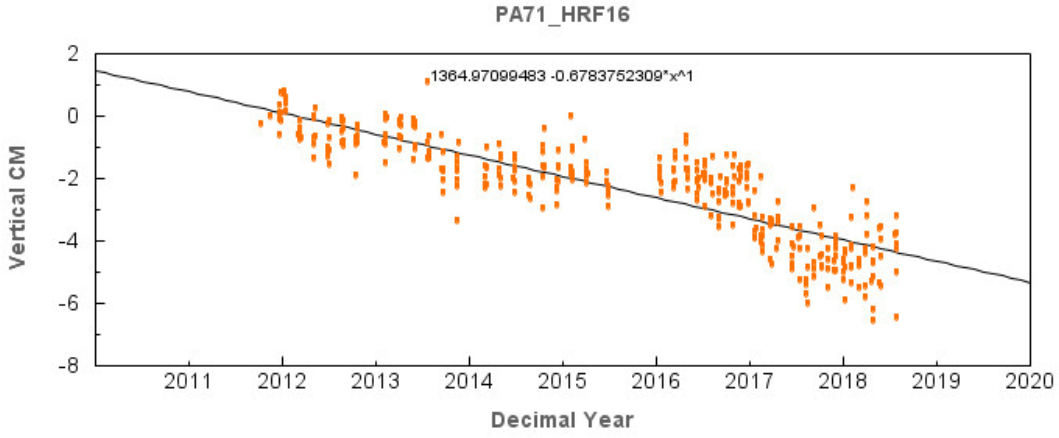
PA71_HRF16
1364.97099483 -0.6783752309*x^1
Vertical CM
Decimal Year
2
0
-2
-4
-6
-8
2011
2012
2013
2014
2015
2016
2017
2018
2019
2020

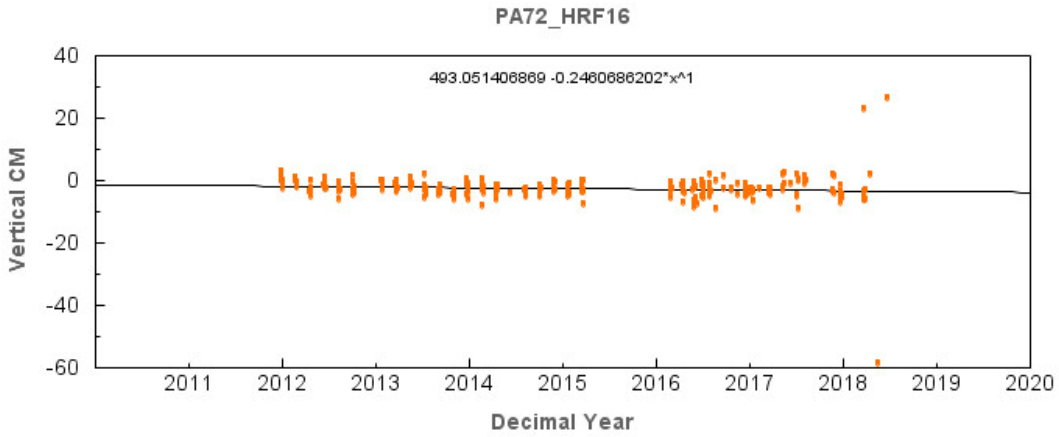
PA72_HRF16
493.051406869 -0.2460686202*x^1
Vertical CM
Decimal Year
40
20
0
-20
-40
-60
2011
2012
2013
2014
2015
2016
2017
2018
2019
2020

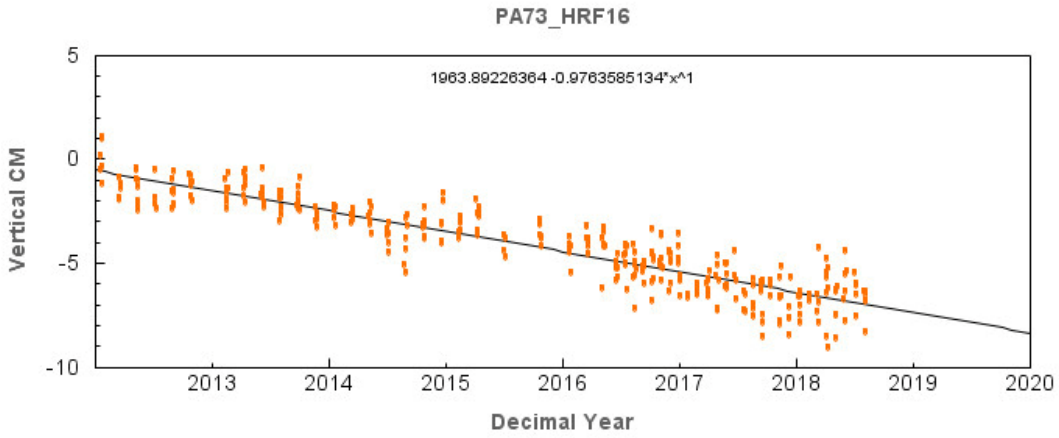
PA73_HRF16
1963.89226364 -0.9763585134*x^1
Vertical CM
5
0
-5
-10
2013
2014
2015
2016
2017
2018
2019
2020
Decimal Year

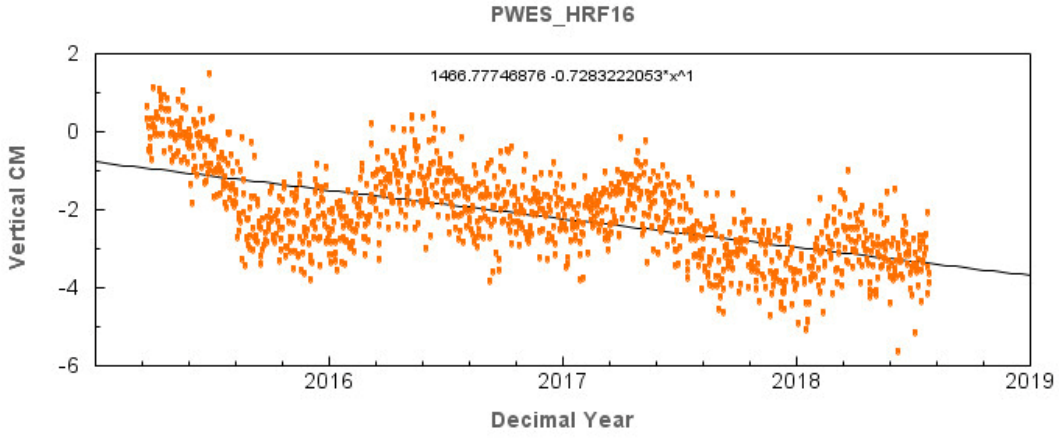
PWES_HRF16
1466.77746876 -0.7283222053*x^1
Vertical CM
2
0
-2
-4
-6
2016
2017
2018
2019
Decimal Year

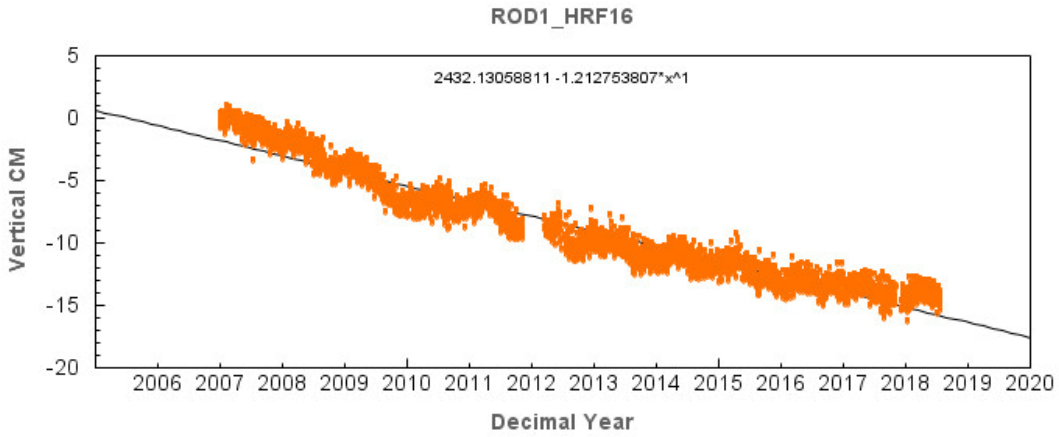
ROD1_HRF16
2432.13058811 -1.212753807*x^1
Vertical CM
5
0
-5
-10
-15
-20
2006
2007
2008
2009
2010
2011
2012
2013
2014
2015
2016
2017
2018
2019
2020
Decimal Year

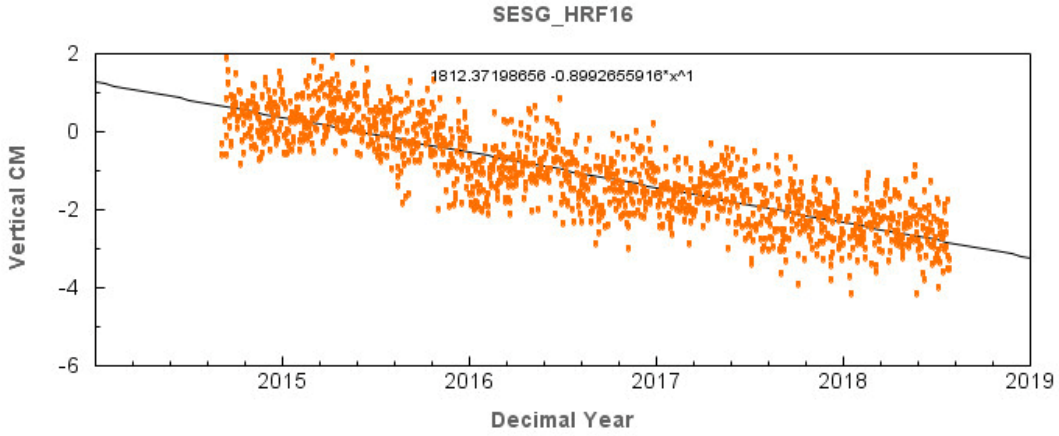
SESG_HRF16
1812.37198656 -0.8992655916*x^1
Vertical CM
Decimal Year
2
0
-2
-4
-6
2015
2016
2017
2018
2019

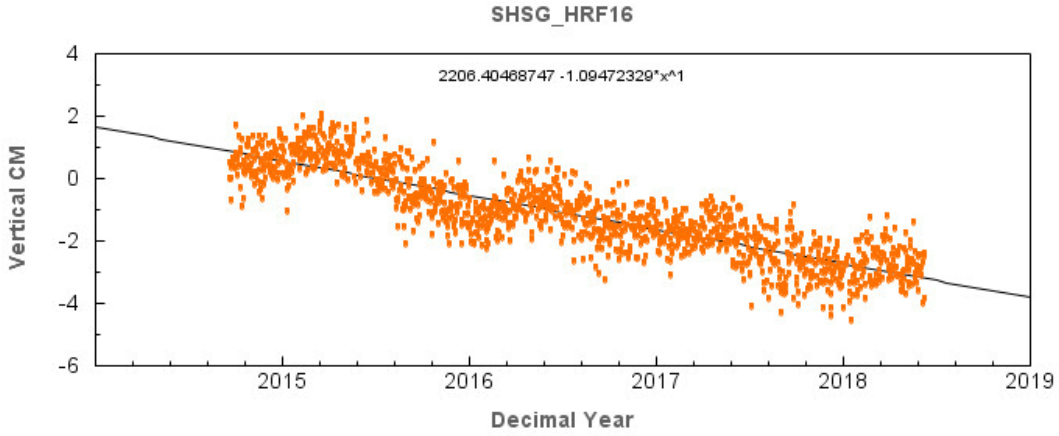
SHSG_HRF16
2206.40468747 -1.09472329*x^1
Vertical CM
Decimal Year
4
2
0
-2
-4
-6
2015
2016
2017
2018
2019

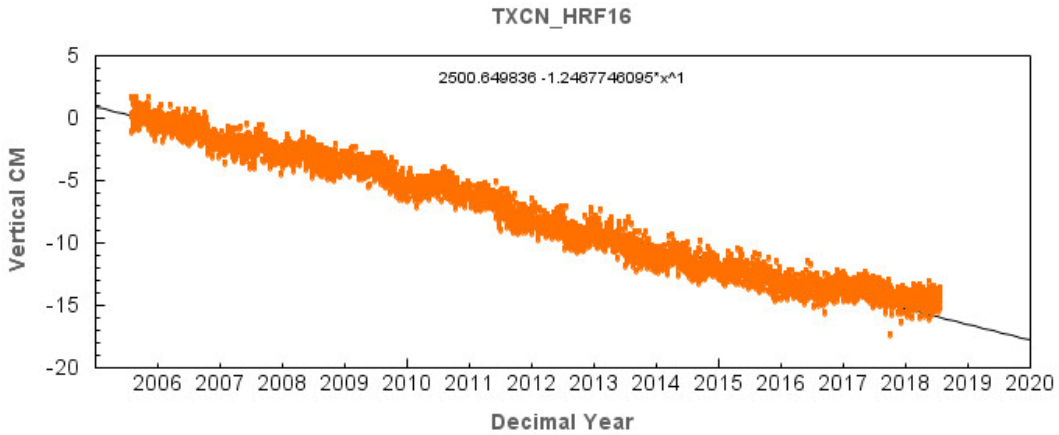
TXCN_HRF16
2500.649836 -1.2467746095*x^1
Vertical CM
Decimal Year
5
0
-5
-10
-15
-20
2006
2007
2008
2009
2010
2011
2012
2013
2014
2015
2016
2017
2018
2019
2020

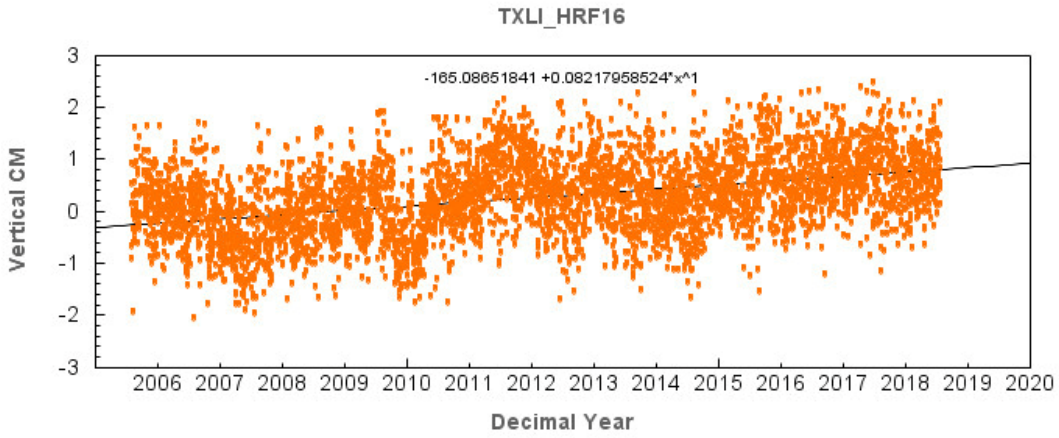
TXLI_HRF16
-165.08651841 +0.08217958524*x^1
Vertical CM
Decimal Year
3
2
1
0
-1
-2
-3
2006 2007 2008 2009 2010 2011 2012 2013 2014 2015 2016 2017 2018 2019 2020

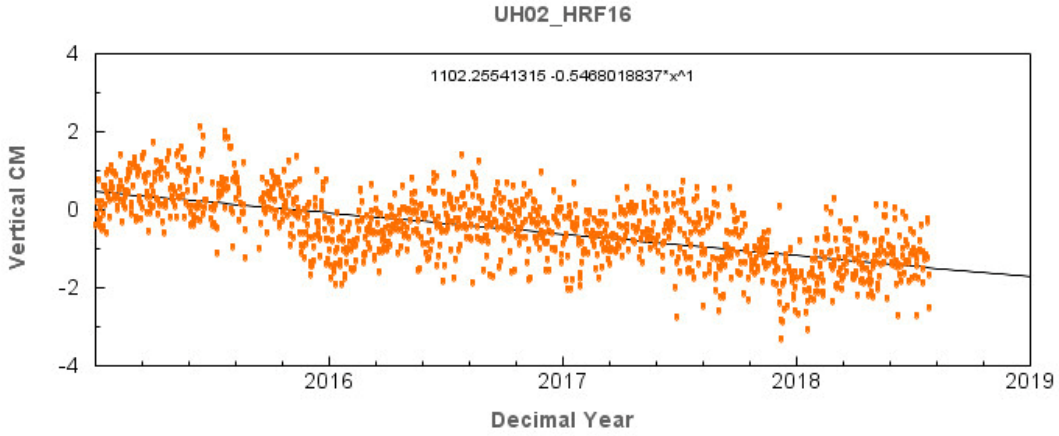
UH02_HRF16
1102.25541315 -0.5468018837*x^1
Vertical CM
Decimal Year
4
2
0
-2
-4
2016
2017
2018
2019

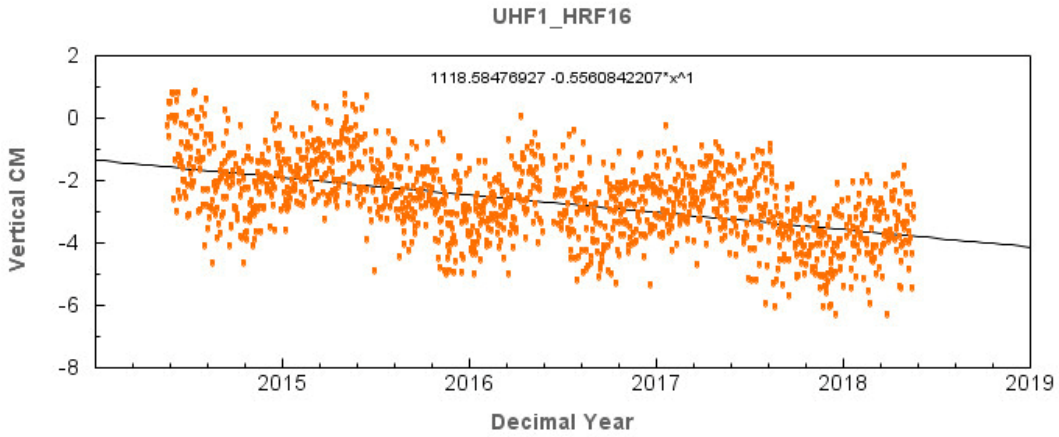
UHF1_HRF16
1118.58476927 -0.5560842207*x^1
Vertical CM
Decimal Year
2
0
-2
-4
-6
-8
2015
2016
2017
2018
2019

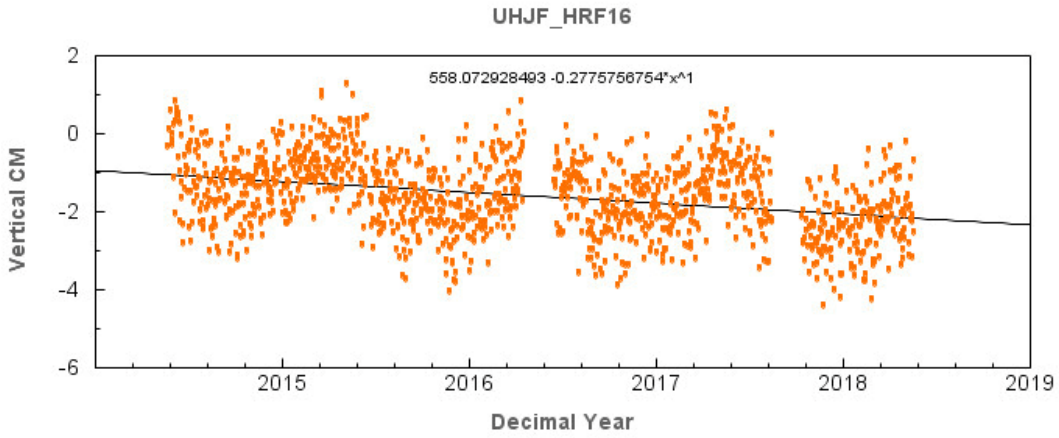
UHJF_HRF16
558.072928493 -0.2775756754*x^1
Vertical CM
Decimal Year
2
0
-2
-4
-6
2015
2016
2017
2018
2019

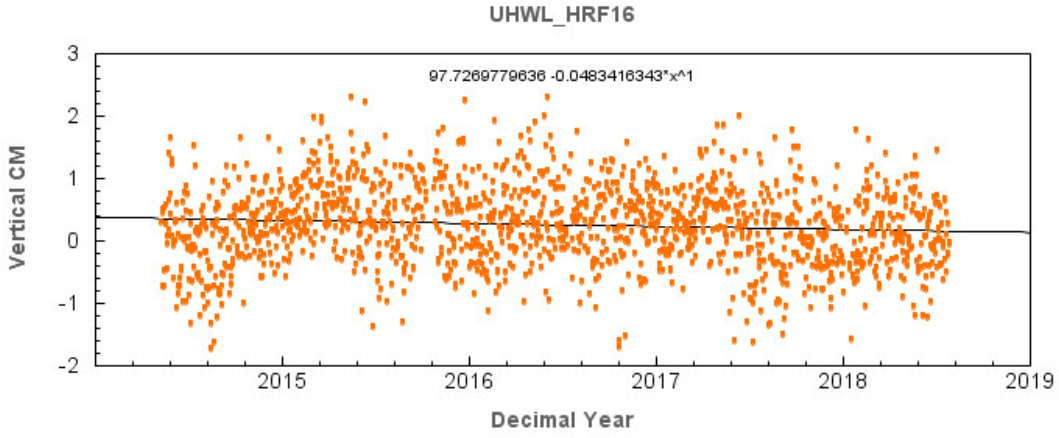
UHWL_HRF16
97.7269779636 -0.0483416343*x^1
Vertical CM
Decimal Year
3
2
1
0
-1
-2
2015
2016
2017
2018
2019

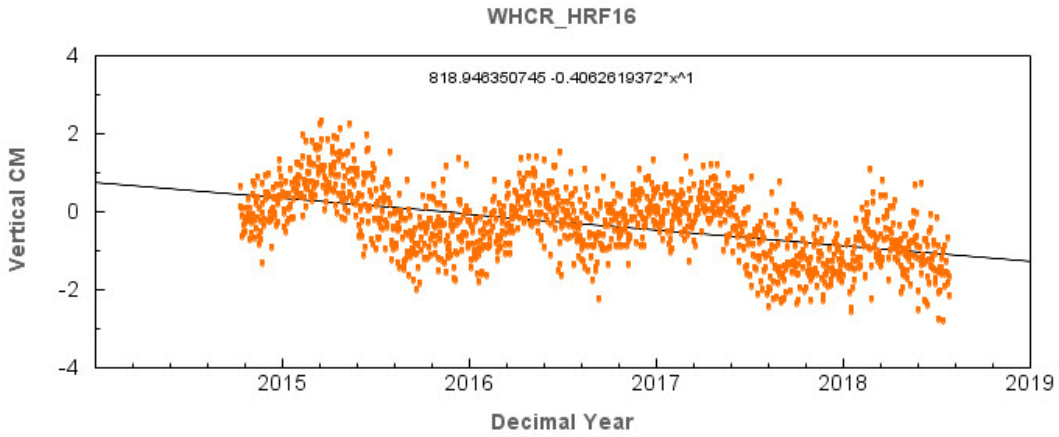
WHCR_HRF16
818.946350745 -0.4062619372*x^1
Vertical CM
Decimal Year
4
2
0
-2
-4
2015
2016
2017
2018
2019

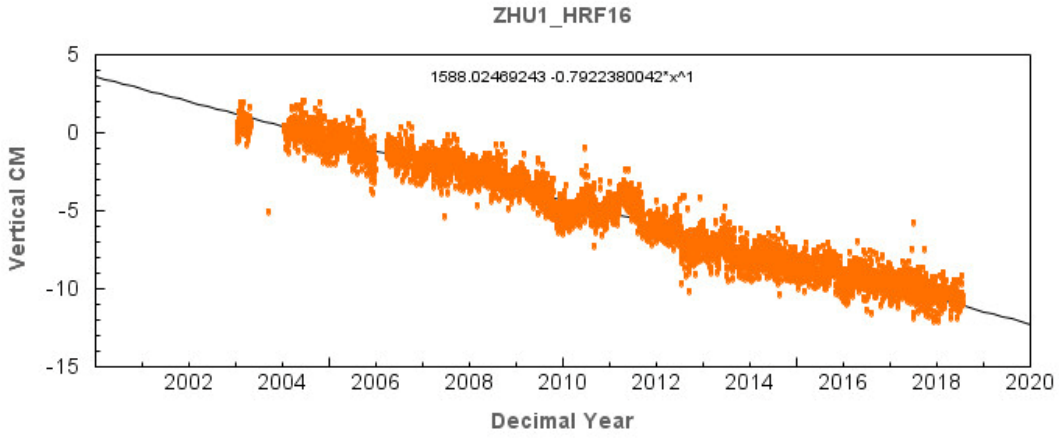
ZHU1_HRF16
1588.02469243 -0.7922380042*x^1
Vertical CM
5
0
-5
-10
-15
2002
2004
2006
2008
2010
2012
2014
2016
2018
2020
Decimal Year